Targeting cell adhesion as a method of sensitising metastatic tumour cells to TRAIL-induced apoptosis

Laura Phipps

Linacre College

A Thesis submitted to the Medical Sciences Division of the University of Oxford in partial fulfillment of the requirements for the Degree of Doctor of Philosophy

Trinity 2011

Gray Institute for Radiation Oncology & Biology

Department of Oncology

University of Oxford

Word count: 44,108
(Excl. ref, fig legends, supplementary)

Abstract

Targeting cell adhesion as a method of sensitising metastatic tumour cells to TRAIL-induced apoptosis

Submitted for Degree of Doctor of Philosophy

Laura Phipps Linacre College Trinity 2011

Due to its selectivity in killing cancer cells, Tumour necrosis factor-related apoptosis-inducing ligand (TRAIL) has provided a potential new agent for cancer treatment. However, despite promising pre-clinical results, it appears that TRAIL therapies will be most effective when used in combination with a sensitizing agent. In light of previous evidence suggesting that cell adhesion could influence sensitivity to Tumour necrosis factor family ligands, this thesis presents a study of the effects of disrupting matrix adhesion on the sensitivity of human MDA-MB-231 breast and 1205Lu melanoma cell lines to TRAIL-induced apoptosis.

This was investigated using a number of models including i) culturing cells on normal and low attachment plates; ii) disrupting the transcription of genes involved in cell attachment and spreading in MDA-MB-231 cells using shRNA to Myocardin-related transcription factors-A and B (MRTF-A/B); iii) disrupting the integrin signalling pathway using inhibitors or siRNA to β integrin subunits, talin, integrin-linked kinase (ILK), focal adhesion kinase (FAK) and SRC. With the exception of ILK depletion, disruption of cell adhesion and spreading in all models resulted in sensitisation to TRAIL-induced apoptosis. Cells under these conditions also showed alterations in death receptor signalling and amplification of intrinsic apoptosis pathway signalling through caspase-9. Both MRTF-A/B depleted cells and those treated with the SRC family kinase inhibitor PP2 showed alterations in signalling through ERK1/2. When investigated in an experimental model of metastasis in mice, FAK and SRC inhibitors increased the clearance of MDA-MB-231 cells from the mouse lung when used in combination with recombinant human TRAIL therapy.

By utilizing these models, the work in this thesis has shown that disrupting cell adhesion could provide a new combination strategy to sensitise tumour cells to TRAIL therapy.

Acknowledgments

I would like to start by thanking my supervisor, Professor Ruth Muschel, for allowing me to work on this project for the past 4 years, and for trusting me with the freedom to test my own ideas. I would also like to acknowledge Cancer Research UK for funding my project, and to Prof R. Treisman, Prof D. Critchley and Prof W. El-Deiry for providing valuable tools and reagents.

I would like to thank everyone in the lab for making it such a fun and enjoyable place to work and for becoming some of my closest friends. Particular thanks to LB, Ling, Cat, AM, Chad and Spela for giving me a social life outside work. To those with the unenviable task of reading parts of this thesis: Cat, Chad, Esther, Christine, Remko, and Thomas. To Danny for his enthusiasm and talent at creating software to analyse anything and everything. I am also grateful to Sally Hill, Karla Watson and Magda Flieger for their patience in helping me to overcome my fear of mice and for tolerating my even greater fear of spiders.

A HUGE thanks to Charlotte, Ger, Kirsten and Caroline for their unyielding friendship, and to my housemates and friends here in Oxford. To my family, particularly my parents, for believing in me even when I didn't believe in myself. Dirk, weil Du es immer schaffst, mich zum Lachen zu bringen: Du bist der Hammer!

Finally, I would like to dedicate this thesis to my Nan who, despite not being able to see me complete it, would be incredibly proud of what I have achieved.

Publications

Targeting cell spreading: a method of sensitizing metastatic tumor cells to TRAIL-induced apoptosis.

Phipps LE, Hino S, Muschel RJ.

Mol Cancer Res. 2011 Mar; 9(3):249-58. Epub 2011 Feb 4.

PMID: 21296861

(Feature article, front cover)

Contents

Figures list.....10
Abbreviations.....14

Chapter 1: Introduction.....18
1.1 Cell death.....18
1.1.1 Characteristics of apoptosis.....18
1.1.2 Caspases.....19
1.1.3 Intrinsic pathway of apoptosis.....21
1.1.3.1 B-cell lymphoma 2 (BCL-2) family.....21
1.1.3.2 The apoptosome.....24
1.1.4 Extrinsic pathway of apoptosis.....25
1.1.4.1 TNF family.....25
1.1.4.2 Death induced signalling complex (DISC).....25
1.1.4.3 Caspases 8 and 10.....26
1.1.4.4 Type I and Type II cells.....27
1.2 TNF-related apoptosis-inducing ligand (TRAIL).....27
1.2.1 TRAIL receptors.....28
1.2.2 TRAIL signalling.....29
1.2.3 Physiological roles of TRAIL.....30
1.2.4 TRAIL as a tumour suppressor.....31
1.2.5 TRAIL as a metastasis suppressor.....32
1.2.6 TRAIL resistance in cancer.....32
1.2.7 TRAIL therapies.....34
1.2.7.1 Recombinant human TRAIL.....35
1.2.7.2 DR4 and DR5 monoclonal antibodies.....36
1.2.7.3 Combination studies.....37
1.3 Metastasis.....39
1.3.1 Metastatic inefficiency and apoptosis.....40
1.3.2 Anoikis.....444
1.4 Aims.....46

Chapter 2: Materials and Methods.....47
2.1 Cell culture.....47
2.1.1 Cell lines and maintenance.....47
2.1.2 Freezing cells.....48
2.1.3 Counting cells.....48
2.2 Cell-based assay protocols.....49
2.2.1 Low attachment plates.....49
2.2.2 TNF ligands.....49

2.2.3 Integrin blocking 49
2.2.4 Inhibitor treatments 50
2.2.5 Death receptor blocking 51
2.2.6 Other reagents 51
2.2.7 Caspase 3/7 activity 51
2.2.8 Cell viability 51
2.2.9 Cell spreading measurements 52
2.3 Western blot 53
2.3.1 Preparation of cell lysates 53
2.3.2 Quantification of protein concentration 53
2.3.3 Sample preparation 54
2.3.4 Gel electrophoresis 54
2.3.5 Blotting protocol 54
2.3.6 Membrane development 55
2.3.7 Stripping of membranes 55
2.3.8 Primary antibodies 56
2.4 Osteoprotegerin ELISA 57
2.5 Human Apoptosis Array 58
2.6 Transfection protocols 58
2.6.1 siRNA transfection 58
2.6.2 shRNA expression 59
2.7 Immunofluorescence staining 60
2.7.1 TUNEL staining 60
2.7.2 Phalloidin staining 62
2.8 Flow cytometry 63
2.9 PCR 63
2.9.1 RNA Extraction 63
2.9.2 qRT-PCR reaction 64
2.10 *In vivo* work 65
2.10.1 Animals 65
2.10.2 Preparation of cells for *in vivo* injection 65
2.10.3 Recombinant human TRAIL 66
2.10.4 Lung isolation protocol 66
2.10.5 Lung imaging protocol 67
2.10.6 Lung isolation protocol for immunofluorescence 67
2.10.7 Lung sectioning and counting 67

Chapter 3: Hypothesis generation 69

3.0 Hypothesis 69
3.1 Aims 69
3.2 Results 70

3.2.1 TRAIL sensitivity in human cancer cell lines....70
3.2.2 The importance of TRAIL in the mouse lung *in vivo* 71
3.2.3 TRAIL sensitivity on low attachment plates....73
3.2.4 Increased death receptor expression in detached cells....75

3.3 Summary of findings 77

3.4 Discussion....77

Chapter 4: Disruption of transcriptional control of the cytoskeleton; TRAIL sensitisation through MRTF-A/B depletion....83

4.0 Hypothesis 83

4.1 Introduction 83

4.1.1 Myocardin-related transcription factors and Serum response factor 83
4.1.2 MRTFs and the cytoskeleton 85
4.1.3 MRTF/SRF activation 85
4.1.4 MRTFs and cancer 87

4.2 Aims 88

4.3 Methods 89

4.3.1 Cell lines 89

4.4 Results....89

4.4.1 MRTF-A and B depletion in MDA-MB-231 cells 89
4.4.2 Sensitivity of MRTF-A and B depleted clones to tumour necrosis factor family ligands. 90
4.4.3 Analysis of apoptosis-related protein changes....94
4.4.3.1 Alterations in death receptor signalling in MRTF-A/B depleted cells. 97
4.4.4 MRTF-dependent genes previously identified using microarray....101
4.4.4.1 OPG and TRAIL expression 103
4.4.5 Caspase activation 106
4.4.6 NFκB, AKT and ERK1/2 activity....108

4.5 Summary of findings 110

4.6 Discussion.... 110

Chapter 5: Targeting the integrin signalling pathway as a method of TRAIL sensitisation....119

5.0 Hypothesis.... 119

5.1 Introduction.... 119

5.1.1 Integrins 119
5.1.2 Talin....122
5.1.3 SRC and FAK 123
5.1.4 Integrin-linked kinase (ILK) 125

5.2 Aims 127

5.3 Results **127**
5.3.1 Beta integrin blocking 127
5.3.2 Knockdown of talin 1 using siRNA 131
5.3.3 Knockdown of ILK using siRNA 134
5.3.4 FAK inhibition using PF-573,228 135
5.3.5 SRC inhibition using PP2 and AZD0530 138
5.3.6 SRC knockdown using shRNA 143
5.3.7 ERK1/2 and AKT activity is affected by SRC inhibitors and correlates with TRAIL sensitivity 145
5.3.8 ERK1/2 and PI3K/AKT inhibitors 149
5.3.9 PP2 enhances caspase-9 activation 153
5.4 Summary of findings **155**
5.5 Discussion **155**

Chapter 6: PF-573228, PP2 and β1 integrin blocking in combination with a TRAIL therapy *in vivo* **163**
6.0 Hypothesis **163**
6.1 Introduction **163**
6.2 Aims **164**
6.3 Method development **165**
6.3.1 An assay to quantify tumour cells present in the lung 165
6.3.1.1 Lung removal 165
6.3.1.2 Lung cell counts 166
6.3.2 An assay to measure cell shape within the pulmonary vasculature of a mouse 167
6.3.2.1 Obtaining z-stacks 167
6.3.2.2 Analysing z-stacks 167
6.3.3 Validation of *in vivo* methodology using MRTF-A/B depleted cells 168
6.4 Results **171**
6.4.1 Recombinant human TRAIL (rhTRAIL) 171
6.4.2 β1-blocking antibodies, PP2 and PF-573,228 in combination with rhTRAIL *in vivo* 173
6.4.2.1 PF-573,228 in combination with TRAIL 174
6.4.2.2 PP2 in combination with TRAIL 175
6.4.2.3. Integrin β1 blocking in combination with TRAIL 176
6.4.3 Investigation of an alternative experimental design to reduce variation 178
6.5 Summary of Findings **180**
6.6 Discussion **181**

Chapter 7: General Discussion **188**
7.1 Adhesion-mediated TRAIL sensitivity **188**
7.2 TRAIL sensitivity mechanisms **190**

7.3 TRAIL sensitisation *in vivo* 194

7.4 Findings in context 195

References 198

Supplementary data 223

Supplementary Chapter S1 : Apoptosis array optimization. 223

S1. Introduction 224

S1.1 Chemiluminescence/film data acquisition 225
S1.2 Fluorescence data acquisition 227
S1.3 Semi-quantitation of arrays 228

S2. Aims 229

S3. Materials & Methods 229

S3.1 Chemiluminescence detection 230
S3.2 Infrared detection 230
S3.3 Image Analysis 231
S3.3.1 Template creation 231
S3.3.2 Spot centre location 232
S3.3.3 Quantification of spot intensity 234
S3.3.4 Semi-quantitation of protein levels 236

S4.Testing the templates: comparison of chemiluminescence vs infrared data acquisition techniques 237

S4.1 Catalase spot detection 237
S4.2 Repeatability 238

S5. Discussion 240

Figures List

Chapter 1: Introduction

Figure 1.1 BCL-2 family members....22
Figure 1.2 Apoptosis pathway overview....23
Figure 1.3 Human TRAIL receptors....28
Figure 1.4 Metastatic inefficiency: potential factors contributing to tumour cell apoptosis in the circulation....42

Chapter 2: Materials and Methods

Table 2.1 Details of cell lines used....48
Table 2.2 Details of inhibitors used....50
Table 2.3 Details of primary antibodies used for western blot....56
Table 2.4 Details of siRNA used for transfections in MDA-MB-231 and 1205Lu cells....59
Table 2.5 qRT-PCR reaction mixture components and volumes....64

Figure 2.1 Optimisation of alamarBlue® assay cell seeding number for MDA-MB-231 cells....52
Figure 2.2 TUNEL staining optimisation in SW480 melanoma cells....62

Chapter 3: Hypothesis generation

Figure 3.1 TRAIL sensitivity in human cancer cell lines....71
Figure 3.2 TRAIL signals contribute to metastatic tumour cell clearance in the mouse lung....72
Figure 3.3 Low attachment leads to TRAIL sensitisation *in vitro*....74
Figure 3.4 Apoptosis protein array data for MDA-MB-231 cells cultured on normal or low attachment plates....76

Chapter 4: Disruption of transcriptional control of the cytoskeleton; TRAIL sensitisation through MRTF-A/B depletion

Table 4.1 Microarray data of MRTF-dependent genes involved in cell death....101
Figure 4.1 Signalling pathways activating Serum response factor (SRF)....84
Figure 4.2 Actin-mediated regulation of MRTF/SRF activity....86
Figure 4.3 Verification of MRTF-A and B levels and spreading defects in MDA-MB-231 clones....90

Figure 4.4 MRTF-A/B depleted MDA-MB-231 cells show increased sensitivity to TNF-α induced apoptosis but MDA-MB-231 cells are resistant to an anti-Fas antibody.....91

Figure 4.5 MRTF-A/B depletion in MDA-MB-231 results in sensitivity to TRAIL-induced apoptosis....93

Figure 4.6 Apoptosis protein array data for MDA-MB-231 cells expressing normal (C4-GFP), intermediate (C20-CFP), and low (C20-CFP TET) levels of MRTF-A/B.....95

Figure 4.7 MRTF-A/B depletion alone results in low levels of apoptosis.....96

Figure 4.8 HTRA2/Omi and $cFLIP_L$ protein levels in MRTF-A/B depleted cells.....97

Figure 4.9 Total protein levels of DR4 and DR5 increase in MRTF-A/B depleted cells, however this is not due to increased transcription.....98

Figure 4.10 Increased DR5 expression on the surface of MRTF-A/B depleted cells.....99

Figure 4.11 MRTF-A/B depleted cells depend more on DR5 for their apoptotic response to TRAIL...100

Figure 4.12 Changes in BCL-2 in MRTF-A/B depleted cells.....102

Figure 4.13 OPG mRNA and protein levels are reduced in MRTF-A/B deficient cells, but cannot protect from TRAIL *in vitro*.....104

Figure 4.14 Cell surface TRAIL expression is the same in MRTF-A/B depleted cells as controls.....105

Figure 4.15 Western blots showing robust caspase-9 activation in MRTF-A/B depleted cells.....107

Figure 4.16 Increased cleavage of BID in MRTF-A/B depleted cells.....108

Figure 4.17 NFκB, AKT and ERK1/2 activity in MRTF-A/B depleted cells.....109

Chapter 5: Targeting the integrin signalling pathway as a method of TRAIL sensitisation

Figure 5.1 Schematic representation of the pathway targeted in this chapter.....120

Figure 5.2 Pre-blocking cells with integrin β1-blocking antibody leads to cell rounding *in vitro*.....128

Figure 5.3 β1 integrin blocking sensitises MDA-MB-231 and 1205Lu cell lines to TRAIL induced apoptosis.....130

Figure 5.4 Talin expression and spreading defects in talin 1 deficient cells.....132

Figure 5.5 Talin knockdown using siRNA results in TRAIL sensitisation.....133

Figure 5.6 ILK knockdown using siRNA does not sensitise cells to TRAIL.....135

Figure 5.7 PF-228 causes a reduction in activity of p130CAS and transient adhesion defects.....136

Figure 5.8 FAK inhibition using PF-228 leads to significant TRAIL sensitivity in all three cell lines...137

Figure 5.9 PP2 inhibited SRC signalling and prevented cell attachment and spreading.....138

Figure 5.10 MDA-MB-231, 1205Lu and WM1789 cells show defective spreading after PP2 treatment.....139

Figure 5.11 PP2 treatment increased TRAIL sensitivity in the three cell lines.....140

Figure 5.12 PP2 led to decreases in survival signals in MDA-MB-231 and 1205Lu cell lines.....142
Figure 5.13 The SRC inhibitor AZD0530 increases TRAIL sensitivity.....143
Figure 5.14 SRC reductions using siRNA and shRNA in MDA-MB-231 cells.....144
Figure 5.15 Dose response curves showing TRAIL-induced reductions in viability with increasing concentrations of PP2 and AZD0530.....146
Figure 5.16 PP2 and AZD0530-induced TRAIL sensitivity correlated with active ERK1/2 and AKT reductions in MDA-MB-231 cells.....147
Figure 5.17 PP2 and AZD0530-induced TRAIL sensitivity correlated with active ERK1/2 and AKT reductions in 1205Lu cells.....148
Figure 5.18 UO126 and PI-103 efficiently reduced their targets at the concentrations used.....149
Figure 5.19 TRAIL sensitisation by PP2, UO126 and PI-103.....151
Figure 5.20 AKT inhibition also results in TRAIL sensitisation.....152
Figure 5.21 PP2 induces caspase-9 activation in MDA-MB-231 cells, while death receptor levels remain unchanged.....154

Chapter 6: PF-573228, PP2 and β1 integrin blocking in combination with a TRAIL therapy *in vivo*

Figure 6.1 Lung scanning using epifluorescent microscopy.....165
Figure 6.2 Lung foci count method.....166
Figure 6.3 Image of MatLab cell shape measurement software designed by Dr P D Allen.....168
Figure 6.4 MRTF-A/B depleted cells (C20-CFP TET) show a defect in elongation when seeded onto glass chamber slides.....169
Figure 6.5 MRTF-A/B depleted cells show spreading defects *in vivo* and are cleared more efficiently from the lung during the first 24 hr after tail vein injection.....170
Figure 6.6 rhTRAIL is effective in clearing MDA-MB-231 cells from the lung.....171
Figure 6.7 rhTRAIL clears MDA-MB-231 cells from the lung by apoptosis, without affecting the normal lung tissue.....172
Figure 6.8 Schematic outlining the *in vivo* experimental schedule.....173
Figure 6.9 FAK inhibition using PF-228 leads to mild, but not significant TRAIL sensitisation *in vivo*.....174
Figure 6.10 PP2 treatment of MDA-MB-231 cells decreases *in vivo* spreading and enhances TRAIL sensitisation.....176
Figure 6.11 Integrin β1 blocking in MDA-MB-231 cells influences spreading and reduces lung retention *in vivo*.....177
Figure 6.12 Proposal for new experimental scheme.....179
Figure 6.13 Pilot experiment using alternative experimental design shows lower variation.....180

Chapter 7: General discussion

Figure 7.1 Schematic representation of the proteins targeted in this thesis.....189

Supplementary Chapter S1: Apoptosis array optimization

Table S1. Inter and intra variability of the protein levels obtained by film and LICOR® Odyssey 239

Table S2. $\overline{Diff}$ values confirm the improved reliability of Licor® data semi-quantified using the annulus template.....240

Figure S1. Noise and dynamic range limitations of array images on film.....225

Figure S2. Evidence of signal saturation on film images of arrays.....226

Figure S3. Array image acquired using infrared detection using Licor® Odyssey 228

Figure S4 R&D System Proteome Profiler™ human apoptosis array.....230

Figure S5. A LI-COR image of a membrane showing autofluorescent contamination from the ink in the serial number..... 231

Figure S6. Example of a processed protein array aligned with a transparency overlay image.....232

Figure S7. Difference in appearance of corresponding spot pair from arrays processed using film (A) and the Licor® (B)..... 233

Figure S8. Comparison of a 1 min and 10 sec exposure to film, using an analysis tool which takes into account the increasing spot diameter..... 235

Figure S9. Spot profiles for the catalase protein pairs from two Licor® repeats.....236

Figure S10. Film images consistently lack catalase protein signal 238

Abbreviations

ALPS	Autoimmune Lymphoproliferative Syndrome
APAF1	Apoptotic protease activating factor 1
BIR	Baculovirus IAP repeat
BSA	Bovine serum albumin
CARD	Caspase activation and recruitment domain
CFP	Cyan fluorescent protein
CHK	CSK Homologous Kinase
CI	Cell index
CRD	Cysteine rich domain
CSK	C-terminal SRC Kinase
CSV	Comma-separated values
DED	Death effector domain
DD	Death domain
DIG	Digoxygenin
DISC	Death induced signalling complex
DMBA	7,12-Dimethylbenz[α]anthracene
DMEM	Dulbecco's Modified Eagle Medium
DNA-PK	DNA-dependent protein kinase
DR4	Death receptor 4
DR5	Death receptor 5
ECM	Extracellular matrix
EGF	Epidermal growth factor
ELISA	Enzyme-linked immunosorbent assay

ER	Endoplasmic reticulum
ERK	Extracellular signal-related kinase
ES	Embryonic stem cell
FACS	Fluorescent activated cell sorting
FADD	Fas-associated protein with death domain
FAK	Focal adhesion kinase
FasL	Fas Ligand
FBS	Fetal bovine serum
FGF	Fibroblast growth factor
GAPDH	Glyceraldehyde-3-phosphate dehydrogenase
GFP	Green fluorescent protein
GPI	Glycosylphosphatidylinositol
GSK-3β	Glycogen synthase kinase-3β
HDAC	Histone deacetylase
IAP	Inhibitor of apoptosis
ICAD	Inhibitor of caspase activated deoxyribonuclease
IFN	Interferon
IκB	Inhibitor of NFκB
IKK	IκB kinase complex
ILK	Integrin-linked kinase
IMD	Integrin-mediated death
IPP	ILK/PINCH/Parvin complex
I.V.	Intravenous
IVIS	*In vivo* imaging system
JAK	Janus kinase

JNK	Jun N-terminal kinase
KRB	Krebs Ringer Buffer solution
LOH	Loss of heterozygosity
LZ	Leucine zipper
MAPK	Mitogen activated protein kinase
MCA	3-methylcholanthrene
MOI	Multiplicity of infection
MOMP	Mitochondrial outer membrane potential
MRTF	Myocardin-related transcription factor
mTOR	Mammalian target of rapamycin
NFκB	Nuclear factor κ B
NK	Natural killer cell
OPG	Osteoprotegerin
P130CAS	Crk-associated substrate
PARP	Poly (ADP-ribose) polymerase
PBS	Phosphate buffered saline
PCD	Programmed cell death
PCR	Polymerase chain reaction
PDGF	Platelet-derived growth factor
PFA	Paraformaldehdye
PI3K	Phosphatidylinositide 3’-kinase
PLAD	Pre-ligand association domain
PMA	Phorbol-12-myristate-13-acetate
P/S	Penicillin/streptomycin
PVDF	Polyvinylidene fluoride

RANK	Receptor activator of NFκB
rhTRAIL	Recombinant human TRAIL
RIP	Receptor interacting protein
SCAI	Suppressor of cancer cell invasion
SCC	Squamous cell carcinoma
SCID	Severe combined immunodeficiency
SDS-PAGE	Sodium dodecyl sulphate-polyacrylamide gel electrophoresis
SFK	SRC family kinase
siRNA	Small interfering RNA
shRNA	Short hairpin RNA
SRC	v-src sarcoma (Schmidt-Ruppin A-2) viral oncogene homolog (avian)
SRE	Serum response element
SRF	Serum response factor
TBS-T	Tris-buffered Saline supplemented with 0.1% Tween20
TCF	Ternary complex factor
TNF	Tumour necrosis factor
TPA	12-*O*-tetradecanoylphorbol-13-acetate (also known as PMA)
TUNEL	Terminal deoxynucleotidyl transferase dUTP nick end labelling
TRADD	Tumour necrosis factor receptor type 1-associated DEATH domain protein
TRAIL	Tumour necrosis factor-related apoptosis-inducing ligand
TWEAK	TNF-related weak inducer of apoptosis

Chapter 1: Introduction

1.1 Cell death

Cell death is essential for the maintenance of homeostasis within the human body. Not only do cells undergo cell death in response to damage or toxic stimuli, they are also lost naturally during development and adult life (Ellis et al., 1991).

There are a number of mammalian cell death mechanisms, which exhibit very different characteristics and are triggered in response to specific stimuli (Kroemer et al., 2009). Apoptosis or 'programmed cell death' (PCD) is a method of controlled cell death which is tightly regulated (Kerr et al., 1972). Apoptosis can be triggered by multiple stimuli and executed by a number of diverse pathways, as will be discussed below.

1.1.1 Characteristics of apoptosis

When undergoing apoptosis, cells go through distinct and recognisable changes in morphology (Kerr et al., 1972, Taylor et al., 2008). These involve shrinkage of the cell, detachment of the cell from its surface, blebbing of the cell membrane, condensation of chromatin, cytoplasmic and nuclear fragmentation, and the expression of phosphatidylserine on the outer cell membrane (Kerr et al., 1972, Kroemer et al., 2009). The apoptosis process uses energy, requiring increases in gene transcription and protein synthesis, as shown by the ability of protein and RNA synthesis inhibitors to reduce the rate of apoptosis (Rawson et al., 1990). The fragmentation of the cell and its components leads to the formation of 'apoptotic bodies',

whose appearance can aid a morphological diagnosis of apoptosis. These apoptotic bodies are eventually phagocytosed by macrophages or neighbouring cells, without stimulating an immune response on the scale of necrosis.

The specific pathway controlling apoptosis was first identified in the invertebrate roundworm *Caenorhabditis elegans*. Due to the simplicity of this animal model, important components of the apoptosis signalling pathway could be identified and led to the subsequent discovery of mammalian homologues with similar roles (Ellis and Horvitz, 1986, Hengartner et al., 1992, Chinnaiyan et al., 1997).

There are two distinct pathways by which apoptosis in mammals can be initiated; the intrinsic (or mitochondrial) and extrinsic (or death receptor) pathways. Although there is cross talk between these two pathways, they involve distinct groups of proteins. Both pathways involve the activation of a family of cysteine proteases called caspases which are responsible for executing the final stages of apoptosis (Thornberry and Lazebnik, 1998). Each pathway activates a distinct set of 'initiator' caspases including caspases 8, 9 and 10 (Bratton et al., 2000), and the pathways converge with the subsequent cleavage of 'executioner' caspases 3, 6 and 7 (Salvesen and Dixit, 1999). Before outlining the distinction between the two pathways, caspases will be discussed in more detail.

1.1.2 Caspases

The first human caspase was identified as a homolog of the *CED-3* gene in *C. elegans* (Yuan et al., 1993), and human caspases now encompass a family of 12 proteases which have roles in controlling both the apoptosis pathway and inflammation. Caspases have the ability to cleave proteins adjacent to an aspartic acid residue, and exist as zymogens which require activation in order to function. Active caspases have a heterodimeric structure composed of two regions, a 20kDa large subunit and a 10KDa small subunit (Barnhart et al., 2003).

An important domain within caspases is the N-terminal pro-domain which facilitates the interaction with

the apoptotic apparatus, but is cleaved on transformation to the active form. Caspases differ in the length of their pro-domain; initiator caspases 2, 8, 9, 10 have long pro-domains while executioner caspases 3, 6, and 7 have short pro-domains (Earnshaw et al., 1999). Initiator caspases contain long domains in order to allow processing and integration into the appropriate death signalling complex. These complexes include the apoptosome and the death induced signalling complex (DISC) and will be discussed further in subsequent sections. These initiator caspases play a role in the early transmission of the apoptotic signal. After recruitment to the apoptosome or the DISC, they become activated. Activation of initiator caspases starts a cascade of cleavage, resulting in executioner caspase activation (Muzio et al., 1997).

The 'induced proximity' model was initially put forward to explain caspase activation (Salvesen and Dixit, 1999). This model hypothesised that binding of pro-caspases to complexes such as the apoptosome or the DISC leads to clustering of caspase zymogens. Due to their inherent protease activity, initiator caspases could then cleave and activate each other leading to the subsequent cleavage of executioner caspases (Yang et al., 1998, Muzio et al., 1998). Despite much initial support for this hypothesis, subsequent work found that initiator caspases could be activated without the need for cleavage (Stennicke et al., 1999) and that the formation of dimers upon recruitment to the DISC or apoptosome seemed more important for the activation of initiator caspases 8 and 9 (Boatright et al., 2003). Reconstitution of the Fas-DISC has subsequently shown that although dimerisation of procaspase-8 at the DISC is an essential initial step in caspase activation, subsequent cleavage of the inter-domain linker is required for full activation and Fas-induced apoptosis (Hughes et al., 2009).

In contrast, as executioner caspases 3, 6 and 7 exist as pre-formed dimers, their activation is solely dependent on cleavage in the inter-domain linker region (Boatright et al., 2003). Initiator caspases cleave and activate executioner caspases 3, 6 and 7, which are responsible for cleaving intracellular substrates leading to the neat and controlled disassembly of cells. For example, the cleavage of lamins leads to

pyknosis, cleavage of Inhibitor of Caspase-3-activated DNase (ICAD) results in DNA fragmentation, and cleavage of the cytoskeleton leads to characteristic membrane blebbing (Taylor et al., 2008).

1.1.3 Intrinsic pathway of apoptosis

The intrinsic pathway of apoptosis is triggered by stimuli including DNA damage, hypoxia, growth factor depletion and p53 activation (Tait and Green, 2010) and ultimately leads to the activation of the initiator caspase-9 (Hakem et al., 1998). Loss of mitochondrial outer membrane potential (MOMP) and release of cytochrome c occurs on stimulation of the intrinsic apoptotic response, control of which is carefully regulated by a balance of proteins from the BCL-2 family (Youle and Strasser, 2008).

1.1.3.1 B-cell lymphoma 2 (BCL-2) family

This family consists of both pro- and anti-apoptotic members which are split into 3 classes depending on their structure and function. Their pro- or anti-apoptotic activity is determined by the number and structure of BCL-2 homology (BH) domains that they express (see Figure 1.1). The main classes are; multidomain anti-apoptotic proteins (including BCL-2, BCL-X_L and MCL-1), multidomain pro-apoptotic proteins (including BAX and BAK) and pro-apoptotic BH3 domain-only proteins (including BID, BAD, BIM, PUMA and NOXA) (Youle and Strasser, 2008). The pro-apoptotic BH3-only proteins are activated in response to cellular stresses and initiate the apoptotic response.

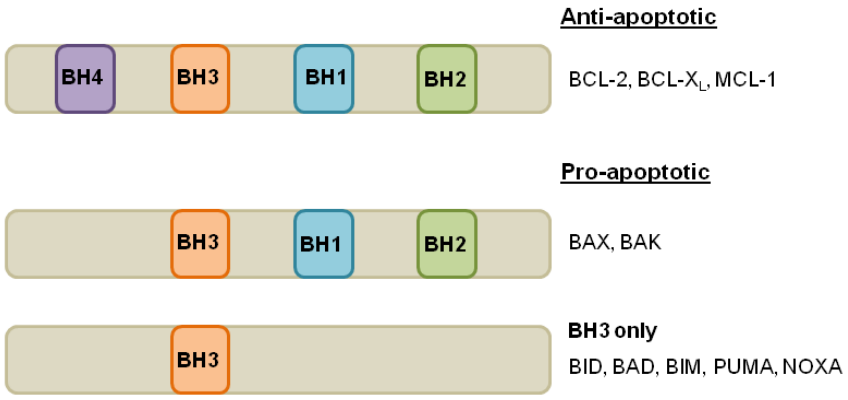

Figure 1.1 BCL-2 family members. BCL-2 family members fall into 3 classes depending on the BH domains they express. This schematic represents the structures of some of the most well characterised members of the BCL-2 family. Multidomain anti-apoptotic members carry all 4 BH domains. Pro-apoptotic BAX and BAK carry BH domains 1-3, with BH3-only proteins only containing a BH3 domain. Several members also carry transmembrane domains, not illustrated.

Cell stress stimuli often signal through pathways which can regulate BH3-only family members both at a transcriptional and post-translational level. For example, the pro-apoptotic tumour suppressor p53 can induce the transcription of BH3-only proteins NOXA and PUMA in response to DNA damage (Oda et al., 2000, Nakano and Vousden, 2001). Similarly, endoplasmic reticulum (ER) stress can activate BIM by a dephosphorylation event which prevents its proteasomal degradation (Puthalakath et al., 2007). It is well characterised that the pro-apoptotic multidomain members BAK and BAX mediate the mitochondrial permeation step that is essential for cytochrome c release and apoptosis (Wei et al., 2001). For an overview of apoptosis, see Figure 1.2.

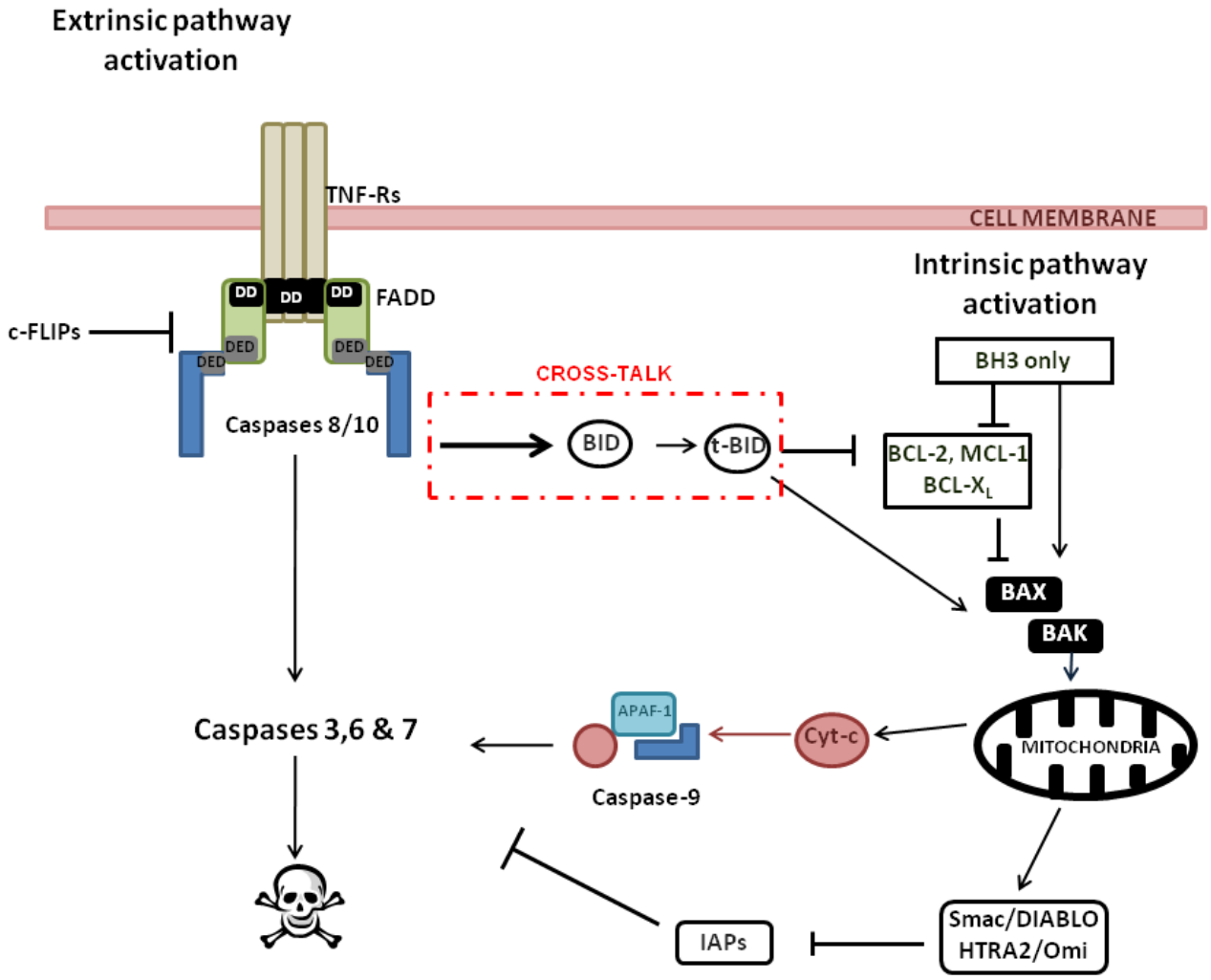

Figure 1.2 Apoptosis pathway overview. The intrinsic apoptosis pathway (right) is activated by BH3-only proteins, which activate BAX and BAK either through direct activation or displacement of anti-apoptotic factors. BAX and BAK activation causes mitochondrial membrane permeation and release of cytochrome c, SMAC/Diablo, and HTRA2/Omi into the cytosol. Cytochrome c forms the apoptosome with Apaf-1 and caspase-9 leading ultimately to executioner caspase activity. SMAC/Diablo and HtrA2/Omi act to neutralise the anti-apoptotic effects of IAPs. The extrinsic pathway (left) is activated following ligation and trimerisation of death receptors by ligands such as TNF-α, TRAIL and FasL. Trimerised receptors recruit FADD and procaspase-8 and 10 into the DISC, leading to activation of executioner caspase 3, 6 and 7. c-FLIPs antagonise death receptor signalling by mimicking caspases. Some TNF ligands such as TNF-α also require a second adaptor TRADD and are well known to signal to pro-survival pathways as well as apoptosis, but these interactions have not been included for simplicity purposes.

The anti-apoptotic family members, including BCL-2 and BCL-X_L, are either found at the mitochondrial outer membrane or translocate there following apoptotic stimuli. They act to stabilise mitochondrial membrane potential by preventing BAX and BAK-mediated mitochondrial membrane permeabilisation (Kluck et al., 1997, Yang et al., 1997).

As BH3-only proteins were shown to bind to specific anti-apoptotic family members, it was hypothesised that BAK and BAX activation was a consequence of the 'neutralisation' of anti-apoptotic control (Yang et al., 1995, Willis et al., 2005, Willis et al., 2007). However, there is some evidence that BH3-only proteins may bind and activate BAX and BAK directly (Kuwana et al., 2005). Very recent evidence has highlighted the importance of BID, BIM and PUMA on the direct activation of BAX and BAK (Ren et al., 2010). Therefore a combination of direct activity and indirect inhibition of anti-apoptotic proteins may result in activation of BAK and BAX during apoptosis (Chipuk and Green, 2008).

1.1.3.2 The apoptosome

Following the release of cytochrome c from mitochondria, a signalling complex called the apoptosome forms in the presence of ATP/dADP which contains cytochrome c, APAF-1, and caspase-9 (Li et al., 1997, Cain et al., 1999). APAFs (apoptotic protease activating factors) are adaptor proteins which contain a Caspase Activation and Recruitment Domain (CARD) in their N-terminus (Zou et al., 1997, Hofmann et al., 1997). Caspases 2 and 9 also carry CARD domains in their long pro-domain, targeting them to the apoptosome by homophilic binding to the CARD domain in APAF-1.

Also released from mitochondria on outer membrane permeation are the molecules Smac/DIABLO (Du et al., 2000) and HTRA2/Omi (Hegde et al., 2002). These proteins also play an important role in allowing pro-apoptotic signalling by inhibiting a class of molecules called Inhibitors of Apoptosis (IAPs) (Deveraux et al., 1997, Deveraux et al., 1998). IAPs, including cIAP1, cIAP2, XIAP and survivin, constitute a family which contain Baculovirus IAP Repeat (BIR) motifs allowing protein interactions (Srinivasula and Ashwell, 2008)

and can bind to caspases preventing their activation. XIAP is a potent inhibitor of executioner caspases 3 and 7 (Deveraux et al., 1997), but can also interact with the apoptosome and inhibit caspase-9 activation (Bratton et al., 2001). Smac/DIABLO and HTRA2/Omi have motifs which bind to IAPs, neutralising their anti-apoptotic regulation of caspases and enhancing cell death (Du et al., 2000, Hegde et al., 2002).

1.1.4 Extrinsic pathway of apoptosis

1.1.4.1 TNF family

The extrinsic pathway of apoptosis is triggered by the ligation of cell surface death receptors by ligands of the tumour necrosis factor (TNF) family. Although this is a large family of cytokines with diverse roles in inflammation, a subset of these proteins have been identified as having important roles in apoptosis (Hehlgans and Pfeffer, 2005). These include FasL/CD95L, TNF-α, TWEAK, and TRAIL/Apo-2L, which bind to their respective TNF receptors. Due to its selective toxicity against human tumour cells, TRAIL (tumour necrosis factor-related apoptosis-inducing ligand) is the most therapeutically promising member of the TNF family and therefore will be discussed in more detail in Section 1.2. See Figure 1.2 for an overview of apoptosis signalling.

1.1.4.2 Death induced signalling complex (DISC)

The binding of TNF ligands to trimeric receptor complexes induces the formation of the death induced signalling complex (DISC) (Kischkel et al., 1995) containing the adaptor protein FADD and caspases 8 and 10 (Muzio et al., 1996, Boldin et al., 1996). The receptors carry a Death Domain (DD) on their cytoplasmic tails, which can homophilically bind to DDs on adaptor proteins such as FADD. These homophilic bindings are essential for the formation of the DISC. Apoptotic signalling through FasL and TRAIL requires one adaptor, named FADD (Boldin et al., 1995, Chinnaiyan et al., 1995), where as TNF-α also requires a second adaptor, TRADD (Hsu et al., 1996). As well as having DDs, these adaptors also carry a Death Effector Domain (DED). Similar to the role of the DD, the DED allows homophilic binding of the adaptors with DED

domains on caspase-8 and -10 (Barnhart et al., 2003). On activation, caspases 8 and 10 can cleave and activate executioner caspases 3, 6 and 7 (Stennicke et al., 1998).

One of the most widely studied proteins which regulates DISC activity is c-FLIP (Irmler et al., 1997). c-FLIP isoforms c-$FLIP_L$, c-$FLIP_s$ and c$FLIP_R$ carry two DEDs, allowing them to bind to FADD and caspase-8 and -10, preventing caspase dimerisation and inhibiting activation. c-$FLIP_L$ also has a longer domain which contains an inactive protease domain, similar to that of caspase-8 and -10, but lacking the essential catalytic residues (Irmler et al., 1997). Over-expression of c-FLIP in BJAB cells could render them resistant to the apoptotic effects of FasL by preventing caspase-8 cleavage (Scaffidi et al., 1999). Although c-$FLIP_S$ and c-$FLIP_R$ are potent caspase-8 inhibitors, the role of c-$FLIP_L$ appears more complex (Boatright et al., 2004). Although at high levels, c-$FLIP_L$ can be anti-apoptotic through its inhibitory competition with caspase-8/10 at the DISC, at lower levels c-$FLIP_L$ may play a role in caspase-8 activation (Chang et al., 2002). However, still thought of as predominantly anti-apoptotic, and associated with apoptosis resistance in cancer, therapeutic agents targeting c-FLIPs are currently under investigation (Safa et al., 2008).

Unlike TRAIL and FasL, TNF-α binding does not preferentially induce apoptosis, instead leading to a complex involving TRADD, RIP1 and TRAF2 (Hsu et al., 1996). This complex can initiate pro-survival and pro-inflammatory signalling through NFκB. In these cells, apoptosis will only occur downstream of TNFR1 under certain conditions, such as when levels of anti-apoptotic proteins such as c-FLIPs fall too low (Micheau and Tschopp, 2003).

1.1.4.3 Caspases 8 and 10

Although caspase-8 has been better characterised, both caspase-8 and -10 have been found at the DISC. Due to their high sequence homology and the lack of a caspase-10 gene in mice, it was assumed that caspase-8 and -10 could act in a functionally redundant manner. However, the loss of caspase-10 has been shown in some cases of autoimmune lymphoproliferative syndrome (ALPS) type II, suggesting that

caspase-10 may have specific roles in controlling apoptosis in immune cells (Wang et al., 1999). It remains controversial as to whether caspase-10 can functionally replace caspase-8 at the DISC, but different caspase-10 isoforms have been shown to have specific roles in apoptotic signalling. Caspase-8 and -10 are also known to have different substrate specificities downstream of the DISC (Fischer et al., 2006, Mühlethaler-Mottet et al., 2011).

1.1.4.4 Type I and Type II cells

Despite being executed by distinct signalling pathways, there is crosstalk between the extrinsic and the intrinsic apoptosis pathways. Type I cells have been named as those which generate enough caspase-8 cleavage for full apoptosis following extrinsic pathway activation. However, a subset of cells can amplify their apoptotic response by activating the intrinsic pathway of apoptosis. These are called type II cells (Scaffidi et al., 1998, Yin et al., 1999). The cross talk between these pathways has so far been attributed to a single BCL-2 family member, BID, which is cleaved by caspase-8 resulting in a 15 kDa truncated form (Luo et al., 1998, Li et al., 1998). This truncated BID (tBID) translocates to the outer mitochondrial membrane and can directly activate BAX and BAK, leading to cytochrome c release and apoptosome formation (Eskes et al., 2000).

1.2 TNF-related apoptosis-inducing ligand (TRAIL)

TRAIL (also known as Apo-2L) was first identified in 1995 as a member of the TNF protein family with 28% identity with FasL and 23% identity with TNF (Wiley et al., 1995). Like the other family members, TRAIL is a type II transmembrane protein, but can be cleaved from the cell surface to form soluble TRAIL. Interestingly, TRAIL transcripts were found to be widely expressed in human tissue and TRAIL had the ability to induce apoptosis in a variety of cancer cell lines (Wiley et al., 1995, Pitti et al., 1996).

1.2.1 TRAIL receptors

TRAIL R1/DR4 was the first TRAIL receptor to be identified, followed closely by another four TRAIL receptors (Pan et al., 1997a, Pan et al., 1997b). Only two of these receptors, TRAIL R1/DR4 and TRAIL R2/DR5 effectively transduce apoptotic signals from TRAIL ligand binding. The other three receptors, DcR1, DcR2 and osteoprotegerin (OPG) act as decoy receptors, sequestering free TRAIL and preventing effective downstream signalling (Ashkenazi and Dixit, 1998). Whereas DR4 and DR5 contain a cytoplasmic DD sequence, allowing them to interact with the apoptotic machinery, DcR1 completely lacks a cytoplasmic region and is membrane tethered only by a GPI-anchor (Sheridan et al., 1997).

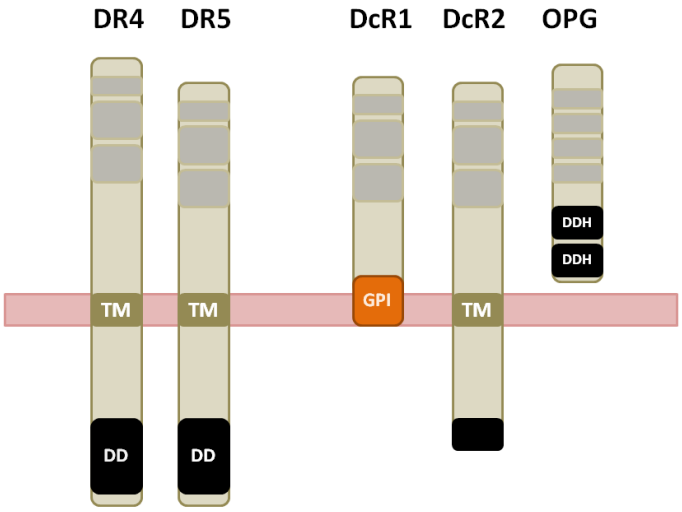

Figure 1.3 Human TRAIL receptors. All TRAIL receptors carry cysteine rich domains (CRD) in their extracellular portion which mediate ligand binding (grey boxes). DR4 and DR5 have a transmembrane (TM) portion and an intracellular death domain (DD) for apoptotic signalling. The decoy receptor DcR1 lacks a transmembrane or intracellular domain, and is instead anchored in the membrane with a GPI-anchor (GPI). DcR2 has a transmembrane domain but carries a truncated non-functional death domain. OPG is a soluble decoy receptor which contains four cysteine rich domains and two death domain homologous regions whose function is unknown. Adapted from (Wang and El-Deiry, 2003).

Despite showing more resemblance to DR4 and DR5, the C-terminal death domain of DcR2 is truncated, lacking the critical sequence which allows signal transduction (Pan et al., 1998). Osteoprotegerin is a

soluble decoy receptor for the TNF family member RANK-L, preventing it from binding to RANK to stimulate osteoclasts formation. However, OPG has also been shown to act as a soluble, low affinity decoy receptor for TRAIL (Emery et al., 1998). All receptors have cysteine rich domains (CRD) in the extracellular portion, in which the ligand binding motif is found (see Figure 1.3).

Interestingly, although mouse decoy receptors have been identified (Schneider et al., 2003), only one functional TRAIL receptor has been identified in mice, which is 43% similar to human DR4 and 49% similar to human DR5 (Wu et al., 1999).

1.2.2 TRAIL signalling

TRAIL has been shown to form tetramers, which bind to homotrimeric receptor complexes (Hymowitz et al., 1999). Although initially hypothesized that ligand binding led to trimerisation of receptors on the cell surface, it has now been shown that receptors can pre-form into complexes prior to ligand binding using a pre-ligand-binding association domain (PLAD) overlapping the extracellular CRD1 domain (Chan et al., 2000). This has also led to the finding that decoy receptors can act, not only through the sequestration of free TRAIL, but by forming inhibitory pre-ligand associations with DR4 or DR5 (Clancy et al., 2005).

Following the activation of receptors on the cell surface, downstream apoptotic signals are mediated through the clustered death domains on the cytoplasmic tails of the receptors. Similar to the activation of other death receptor ligands, as discussed in Section 1.1.4.2, DR4 and DR5 recruit FADD and caspase-8 into the DISC (Bodmer et al., 2000, Kischkel et al., 2000, Sprick et al., 2000). TRAIL, along with TNF-α, has also been shown to activate a second signalling pathway from the DISC (Schneider et al., 1997). This pathway involves the interaction of caspase-8 and FADD with the DD-containing kinase RIP1 and the adaptor protein TRAF2. RIP1 can associate with NEMO, a member of the IκB kinase (IKK) complex. This complex is responsible for signal-induced activation of NFκB signalling (Varfolomeev et al., 2005). On activation, the IKK complex can phosphorylate the NFκB inhibitor, IκBα, targeting it for degradation. On

release from IκBα, NFκB can move to the nucleus and activate gene transcription. Many of the target genes of NFκB encode anti-apoptotic proteins including cIAP1, cIAP2, XIAP, cFLIPs, BCL-2 and BCL-X_L (Wang et al., 1998, Chen et al., 2000, Micheau et al., 2001). Therefore, although pro-death signals predominate at the TRAIL-induced DISC, there is also capacity for anti-apoptotic signalling.

The DISC is known to be regulated at many levels, through post-translational modifications, survival signalling, and interaction with other components (Pennarun et al., 2010). As mentioned in Section 1.1.4.2, c-FLIPs can inhibit DISC signalling by preventing the FADD-Caspase-8/10 interaction. Expression of c-FLIP has been found to correlate with TNF resistance in human tumour cell lines and is thought to be regulated by signalling from ERK1/2, PI3K/AKT and NFκB (Yeh et al., 1998, Panka et al., 2001, Micheau et al., 2001).

TNF receptors have been shown to cluster at lipid rafts, membrane sub-domains created by the association of cholesterol and saturated phospholipids (Muppidi et al., 2004). Work in non-small cell lung cancer cells has shown that activation of death receptors in lipid rafts preferentially produces pro-apoptotic signals through activation of FADD and caspase-8, whereas non-lipid raft regions produce pro-survival signals relayed through activation of NFκB (Song et al., 2007). Therefore localization of receptors in the plasma membrane, as well as expression level can regulate TRAIL signalling to the DISC.

Other methods of receptor regulation have been reported including miRNA regulation (Ovcharenko et al., 2007) and post-translational receptor modifications, reviewed in (Pennarun et al., 2010). One example is O-glycosylation of DR4 and DR5, which is important for death receptor clustering, allowing an enhanced TRAIL response (Wagner et al., 2007).

1.2.3 Physiological roles of TRAIL

TRAIL has a well characterized role in tumour immunosurveillance, as it is expressed on a number of immune cell types including natural killer (NK) cells, macrophages and monocytes. Although this has

previously been the main focus of TRAIL research, its role in regulating immune responses under physiological conditions is becoming increasingly clear (Falschlehner et al., 2009). As well as being shown to negatively regulate erythropoiesis (Zamai et al., 2000), TRAIL can promote monocyte maturation both in a leukaemia cell line and in primary CD34+ haemopoietic progenitors (Secchiero et al., 2002). TRAIL expression on T helper2 cells has been implicated in the regulation of T helper1 cell responses (Zhang et al., 2003b) and in the regulation of CD8+ T-cell priming (Janssen et al., 2005). Further supporting its role in the control of immune responses, the loss of TRAIL signalling can accelerate the development of autoimmune diseases such as arthritis and type I diabetes in mice (Lamhamedi-Cherradi et al., 2003). TRAIL was also shown to increase proliferation and protection from apoptosis induced by trophic withdrawal in vascular endothelial cells, in a manner which was dependent on AKT and ERK1/2 signalling (Secchiero et al., 2003).

1.2.4 TRAIL as a tumour suppressor

A widely reported characteristic of TRAIL is its ability to induce apoptosis in a broad range of transformed cell types, whilst showing little or no toxicity against normal cell types (Wiley et al., 1995, Ashkenazi et al., 1999). This selectivity towards cancer cells makes it an attractive therapeutic tool. Work with TRAIL-deficient mice has been important in revealing the potential tumour suppressor role of TRAIL. These mice exhibit more rapid growth of mammary fat pad tumours and a faster rate of fibrosarcoma initiation after treatment with the chemical carcinogen 3-methylcholanthrene (MCA) (Cretney et al., 2002). Treatment of mice with a TRAIL-blocking monoclonal antibody (N2B2) leads to an increase in number and growth rate of MCA-induced fibrosarcoma, and an enhanced frequency of spontaneous lymphomas and sarcomas in p53+/- mice (Takeda et al., 2002).

However, TRAIL was shown not to be important in the development of spontaneous mammary epithelial carcinomas in a Her2/Neu model (Zerafa et al., 2005). Similarly, TRAIL deficient mice crossed with $APC^{min/+}$

mice did not show any difference in spontaneous polyp development (Yue et al., 2005). Grosse-Wilde found that although TRAIL-R deficiency did not alter the growth of primary tumours in a mouse DMBA/TPA-induced squamous cell carcinoma (SCC) model, it did profoundly enhance metastasis formation (Grosse-Wilde et al., 2008).

1.2.5 TRAIL as a metastasis suppressor

Although the tumour suppressor role of TRAIL in solid cancers remains somewhat controversial, its role in suppressing metastasis is widely reported. TRAILR-deficient mice with DMBA/TPA-induced SCC showed increased numbers of lymph node metastases which could be detected earlier (Grosse-Wilde et al., 2008). The immune system is known to regulate tumour development and metastasis through a process called 'tumour immune surveillance' (Swann and Smyth, 2007). Immune cell-mediated killing of tumour cells is thought to be a major reason why most cancer cells which enter the circulation will die. Death receptor signalling by NK cells is essential for the clearance of metastatic tumour cells (Screpanti et al., 2001). TRAIL has been implicated in the cytotoxic action of monocytes, CD4+ T-cells and NK cells on tumour cells (Griffith et al., 1999, Kayagaki et al., 1999). TRAIL-deficient mice were shown to have significantly more liver metastasis after intrasplenic tumour cell injections than control mice (Cretney et al., 2002), and there is much evidence suggesting an important role for TRAIL in NK cell-mediated tumour cell clearance in the liver. This will be discussed further in Section 1.4.1.

1.2.6 TRAIL resistance in cancer

Initially, the presence of decoy TRAIL receptors went some way to providing an explanation for why normal tissues were resistant to TRAIL killing, despite expressing high levels of mRNA for both TRAIL and its receptors DR4 and DR5 (Pan et al., 1997b). However, recent work suggests that TRAIL-resistance in non-transformed cells may not be simply due to differences in the balance of activating and decoy TRAIL receptors. Numerous papers have reported little or no correlation between decoy receptor level and

TRAIL sensitivity, with expression levels of DR4 shown to better correlate with TRAIL sensitivity in a panel of normal and tumour cell lines (Kim et al., 2000). In a panel of melanoma cell lines, DR4 and DR5 expression levels correlated with TRAIL sensitivity (Zhang et al., 1999), with loss of death receptor expression during metastatic progression (Zhuang et al., 2006). Alterations in clathrin-mediated endocytosis of death receptors has been implicated as one mechanism of receptor downregulation in breast and colon cancer cells (Jin et al., 2004, Zhang and Zhang, 2008).

There have also been reports of TRAIL resistance in human tumour cells resulting from mutations in death receptors. The genes encoding the four death receptors, DR4, DR5, DcR1 and DcR2, are found clustered on chromosome 8p21-22 and this region is frequently mutated in cancers. Loss of heterozygosity (LOH) in this region was reported by Emi in a number of cases of liver, colorectal and lung carcinoma (Emi et al., 1992) and subsequently reported in other cancer types including breast cancer (Yaremko et al., 1995). Polymorphisms have since been identified in DR4, conferring a dominant negative effect on normal DR4 function and resulting in TRAIL resistance despite high DR4 protein expression (Kim et al., 2000, Chen et al., 2009). DR4 and DR5 polymorphisms and LOH in 8p21-22 were found to be more common in breast cancer patients with metastasis compared to those with intraductal carcinoma (Shin et al., 2001). Hypermethylation in the promoter regions of decoy receptors has been reported in a range of cancer types (Shivapurkar et al., 2004). Promoter hypermethylation has also been reported for DR4 in a range of cancers, including melanoma and ovarian cancer cell lines, and correlated with increased TRAIL resistance (Horak et al., 2005, Bae et al., 2008).

FADD mutations have been reported in rare cases of non-small cell lung and colon cancer (Soung et al., 2004), and caspase-8 expression is reported to be lower in neuroblastoma and correlates with metastatic progression (Stupack et al., 2006). Alterations in intrinsic pathway components have also been implicated in TRAIL resistance. Increased c-FLIP levels were shown in a panel of TRAIL resistant cell lines (Kim et al.,

2000) and TRAIL sensitivity in some melanoma cell lines was attributed to greater release of Smac/DIABLO from the mitochondria (Zhang et al., 2001) .

Despite having the lowest affinity for TRAIL out of all the TRAIL receptors, there is increasing evidence that OPG has a role in controlling the TRAIL response. Alongside its normal role in controlling RANKL signalling in osteoclastogenesis (Emery et al., 1998), OPG can also bind to TRAIL and prevent it from initiating apoptosis. Bone marrow stromal cells and osteoblasts in the bone microenvironment produce high levels of OPG which were shown to protect MDA-MB-436 breast cancer cells from TRAIL-induced apoptosis *in vitro* (Neville-Webbe et al., 2004). High levels of OPG were also found to be secreted from breast, colon and prostate cancer cells in concentrations which were high enough to confer a TRAIL-protective effect *in vitro* (Holen et al., 2002, Holen et al., 2005). Serum OPG levels were shown to be higher in pancreatic and colorectal cancer patients and to correlate with metastatic progression in colon cancer patients (Lipton et al., 2002, De Toni et al., 2008).

In light of this evidence, there appears to be multiple players which act together to control TRAIL resistance. Tumour cells develop a shift in the balance of these players, allowing resistance to pro-apoptotic TRAIL signals. There are many ways in which this balance can altered, including receptor expression or epigenetic control, mutations in DISC components, alterations in the levels of apoptosis inhibitors, and signalling from the environment. It appears that there is not one universal mechanism for TRAIL resistance, and this mechanism is likely to differ between cancer cell types and individuals.

1.2.7 TRAIL therapies

Due to the selectivity of TRAIL in killing cancer cells without normal cell toxicity, and its ability to kill a range of cancer cells independent of their p53 status (Ashkenazi et al., 1999), TRAIL therapies have emerged which show promising potential. Although apoptosis induced by FasL and TNF-α is important and has been reported to be physiologically relevant in metastasis, therapies designed to mimic the apoptotic

effect of these molecules have been problematic. Anti-tumour TNF-α therapies have led to high levels of systemic toxicity (Moritz et al., 1989), most likely due to its ability to regulate inflammation via NFκB activation. Similarly, systemic Fas therapies in mice were found to be problematic due to acute hepatocyte toxicity and FasL resistance in tumour cells (Ogasawara et al., 1993, Rensing-Ehl et al., 1995).

1.2.7.1 Recombinant human TRAIL

Pre-clinical data has shown that a recombinant form of human TRAIL has a half life of 32 min in non-human primates and exhibits no toxicity at the doses tested (up to 10 mg/kg/day). Serum concentrations in chimpanzees following a 5mg/kg intravenous dose were around 10 μg/ml after 1 hr, much higher than those typically used for *in vitro* cytotoxicity assays (Kelley et al., 2001). rhTRAIL was also able to induce apoptosis *in vivo* in a mouse xenograft model after a single intraperitoneal dose, with daily doses inhibiting the growth of established tumours and preventing the development of new ones (Ashkenazi et al., 1999). Leucine zipper TRAIL, a stable dimerised form of recombinant TRAIL, also showed potent anti-tumour activity with no toxic side effects (Walczak et al., 1999). In 2000, it was reported that recombinant human (rh)TRAIL administration could induce apoptosis in human brain slices (Nitsch et al., 2000) and in human hepatocytes (Jo et al., 2000), bringing into doubt its potential as an anti-cancer agent. However subsequent studies confirmed that hepatotoxicity is only found after administration of highly aggregated forms of recombinant TRAIL (Lawrence et al., 2001).

With subsequent pre-clinical studies showing the effective anti-tumour activity of rhTRAIL in a number of cancer models in the absence of toxicity, it was taken into clinical trials (Johnstone et al., 2008). Phase I dose escalation studies showed that rhTRAIL (also known as dulanermin) was safe and well tolerated at doses up to 30mg/kg (Herbst et al., 2010). Further results from phase II trials are expected in the near future.

1.2.7.2 DR4 and DR5 monoclonal antibodies

Although rhTRAIL can bind to both DR4 and DR5, giving it the potential for greater clinical effectiveness, there is also the possibility that it could be bound and sequestered by TRAIL decoy receptors. To prevent this, several monoclonal antibodies against DR5, including MD5-1 and TRA-8, were generated and showed promising anti-tumour and anti-metastatic effects in mouse models with low toxicity (Ichikawa et al., 2001, Takeda et al., 2004). Fully humanized agonistic antibodies for DR4 and DR5 have since been developed, which show some clinical advantages over rhTRAIL. As they have higher specificity for their target, they are expected to have increased potency over rhTRAIL. They also have a half life of 15 to 20 days, much longer than the 30 min reported for rhTRAIL (Camidge et al., 2007). In addition to this, these antibodies have been shown to attract immune cells *in vivo*, which can act to enhance tumour clearance (Haynes et al., 2010).

Several antibodies have been created which target DR5 with high selectivity, including apomab, PRO95780, and lexatumumab. All of these antibodies exhibit potent anti-tumour activity *in vivo*. Similar to rhTRAIL, both intraperitoneal and intravenous administration of these antibodies led to significant tumour delay or regression in mouse models (Adams et al., 2008, Malin et al., 2011). Despite some reported toxicity against hepatocytes and testicular germ cells *in vitro* (Mori et al., 2004, McKee et al., 2006), all the antibodies are reported to be well tolerated in phase I trials (Camidge et al., 2007, Plummer et al., 2007, Camidge et al., 2010).

The antibody mapatumumab, which selectively targets DR4, also showed potent anti-tumour effects in pre-clinical studies. Treatment of xenografts in nude mice with 10 mg/kg of mapatumumab led to a 97% decrease in tumour volume 25 days after the onset of the treatment regime (Pukac et al., 2005). Similarly, phase I trials with mapatumumab show low toxicity and maximum tolerated dose was not reached, although no objective responses were reported (Hotte et al., 2008). Phase II trials of mapatumumab

monotherapy have also shown few objective responses in both advanced non-small cell lung cancer and refractory colon cancer (Greco et al., 2008, Trarbach et al., 2010).

Data from these early trials suggest that disease stabilization may be the best end point for determining the activity of the agents, which is in line with the evidence implicating an important role for TRAIL in the control of metastasis. Despite promising pre-clinical results, early phase trials using TRAIL monotherapy has shown a limited number of positive responses. Although around two thirds of tested cell lines are TRAIL sensitive *in vitro*, as discussed in Section 1.2.6, they can rapidly develop mechanisms to overcome this sensitivity. Therefore the application of TRAIL as a monotherapy may be limited and recent work has been looking at combinations of TRAIL therapies with other targets.

1.2.7.3 Combination studies

Recombinant human TRAIL in combination with 5-fluorouracil or the topoisomerase inhibitor CPT-11 led to substantial tumour regression in mouse xenograft models, suggesting synergistic activity of rhTRAIL with chemotherapeutic agents (Ashkenazi et al., 1999). This interaction was also synergistic in the control of metastasis, and was shown to be synergistic even in the presence of inactivating p53 mutations (Ravi et al., 2004). This was due to chemotherapy-induced downregulation of JAK/STAT signalling which caused a reduction in BCL-X_L and XIAP expression. This led to higher levels of apoptosis and was p53-independent due to TRAIL activation of BID, and subsequent activation of the intrinsic pathway of apoptosis. Cancer chemotherapeutics have also been reported to increase death receptor levels, providing another mechanism for potentiating the TRAIL response (Gibson et al., 2000). Similar synergistic interactions have been shown with combinations of chemotherapeutic agents and both apomab and mapatumumab *in vitro* (Pukac et al., 2005). Phase I studies with combinations of TRAIL therapies and chemotherapeutics have been well tolerated and display potential anti-cancer effects, and these are being taken into phase II trials (Leong et al., 2009, Soria et al., 2010). Pre-clinical studies have also suggested that TRAIL therapies can act

synergistically with radiotherapy, widening the possible therapeutic scope of these drugs (Marini et al., 2006).

In light of our knowledge on TRAIL resistance mechanisms, TRAIL therapies are being tested in combination with drugs which can act on the apoptosis pathway to enhance sensitivity. Proteasome inhibitors such as bortezomib can prevent proteasomal degradation of the NFκB inhibitor IκB, preventing NFκB-mediated survival signals. In combination with TRAIL therapies, such proteasome inhibitors have shown promising effects *in vitro* (Voortman et al., 2007). Pre-clinical evidence shows a synergistic interaction of inhibitors of NFκB signalling with TRAIL therapies in mouse xenograft models (Khanbolooki et al., 2006). Similarly histone deacetylase inhibitors (HDAC inhibitors) can upregulate death receptor levels and also show promising results *in vitro* and in pre-clinical tumour models in combination with TRAIL therapies (Srivastava et al., 2010).

However, the proteasome was also shown to be necessary for rapid death receptor induced apoptosis in a number of cell lines, including HeLa and MCF7, suggesting that proteasome inhibitors may actually delay death receptor induced apoptosis in certain cell lines (Sohn et al., 2006). Evidence has also been presented of hepatotoxicity with combinations of TRAIL and certain chemotherapeutic drugs, and with TRAIL and high concentrations of bortezomib (Ganten et al., 2006, Koschny et al., 2007). In combination experiments with TRAIL and HDAC inhibitors, high doses of HDAC inhibitors led to significant on-target toxicity in mice (Martin et al., 2011). Therefore particular care must be taken when designing combination TRAIL therapies, to assess the likely hepatotoxicity or other toxicity effects.

Small molecule inhibitors targeting other members of the apoptosis pathway have also been tested in combination with TRAIL therapies, including XIAP inhibitors, BCL-2 inhibitors and SMAC mimicking peptides, discussed further in (Kruyt, 2008). Inhibitors of the PI3K pathway such as LY294002 and gefitinib

(Iressa) have also been shown to enhance TRAIL sensitivity *in vitro* through the reduction in AKT signalling and a downregulation of XIAP (Shrader et al., 2007).

Therefore TRAIL has great clinical potential and is likely to be most effective when combined with other agents. As discussed earlier, tumour cells can develop many and varied resistance mechanisms, allowing them to overcome the TRAIL-induced death signal. Many of these combination agents are likely to be effective only in certain cell lines as the response of a cell line will depend on the specific resistance mechanism developed. Finding a mechanism to sensitise a wide range of cancer cell lines to TRAIL *in vitro*, could provide a useful target for a TRAIL combination agent.

1.3 Metastasis

With 12.7 million new cancer cases having occurred worldwide in 2008 and cancer causing 1 in 4 deaths in the UK, it is a disease which puts significant burden on the health service and affects almost all individuals in some way (Jemal et al., 2011). One distinct hallmark of cancer is the ability of cancer cells within the primary tumour to invade local tissue and metastasise in the blood or lymph system to other parts of the body (Hanahan and Weinberg, 2011). Not only must cells survive the transition to a new environment, they must survive and colonise at the new site. Metastasis is the main reason for treatment failure in cancer patients and it is estimated that around 90% of cancer patients die from metastasis.

Metastasis is a multi-step process in which cancer cells extravasate from the primary tumour, invade into the surrounding tissue and eventually reach the blood or lymphatic system. On arrival at an appropriate secondary site, these cells then extravasate into the new tissue. In 1986, Price et al. found that after injection into mice, K1735 melanoma cells split into two distinct groups. These were low metastatic clones, with low viability in the lung after 24 hrs, and highly metastatic clones which showed a higher proportion of viable clones in the lung (Price et al., 1986). This paper highlights that metastasis depends

on the inherent properties of the disseminated cancer cells, with a subset of cells within a heterogeneous tumour acquiring the necessary characteristics to disseminate and survive.

1.3.1 Metastatic inefficiency and apoptosis

In early studies following intravenous (i.v.) injection of radiolabelled tumour cells into mice, high numbers of cells were predominantly located in the lung at early time points, with lower numbers in the liver. However, by 24 hr there was a dramatic loss of tumour cells from the lung and liver with high urine radiation counts, indicating that the cells had died (Fidler, 1970). When comparing the fate of cells with high and low metastatic potential, equal numbers of cells were found in the lung at early time points after i.v. injection. Again, by 24 hr the differences between these variants were very apparent, with non-metastatic cell variants being cleared much more effectively (Price et al., 1986). For non-metastatic cell lines, there was often fewer than 1% of cells remaining in the lung at 24 hr after i.v injection (Fidler, 1970). This shows that circulating cancer cells, despite their inherent metastatic ability, can arrest in the lung at early time points but only those cells with the ability to overcome the hostile barrier of the new environment will survive. This observation has been termed metastatic inefficiency, describing the propensity of the majority of circulating cells to die before secondary colonisation. This phenomenon is the focus of the work in this thesis, and will therefore be discussed in preference to other steps of the metastatic cascade.

Wong et al. also showed that non-metastatic cells were cleared more effectively from the lung following tail vein injection into mice. Using TUNEL staining, they showed that these cells underwent significantly more apoptosis than metastatic cell lines. They also showed that by increasing apoptosis resistance in these cells through overexpression of the anti-apoptotic protein BCL-2, the number of cells in the lung at 24 hrs could be increased 5 fold (Wong et al., 2001). This apoptosis was later confirmed with a non-metastatic and metastatic melanoma cell line using a BAD-GFP construct which is relocated to the

mitochondria during apoptosis (Kim et al., 2004). Over expression of BCL-2 could also increase metastasis in a spontaneous breast cancer model (Del Bufalo et al., 1997). By comparing *in vitro* apoptosis resistance with metastatic potential, researchers found that the apoptotic sensitivity of human breast and prostate cancer cell lines *in vitro* correlated with their *in vivo* metastatic potential (McConkey et al., 1996, Glinsky et al., 1997). Similarly, loss of the pro-apoptotic tumour suppressor p53 led to enhanced metastasis in a mouse model of hepatocellular carcinoma (Lewis et al., 2005). Together, this evidence reveals that apoptosis plays a vital role in metastatic inefficiency.

Importantly, despite being widely characterised in experimental models of metastasis in animals, there is also clinical evidence of metastatic inefficiency. Despite high levels of tumour cells being present in the circulation of cancer patients, this will not always lead to detectable metastasis (Glaves et al., 1988). In the case of breast cancer, many of the circulating tumour cells detected in the blood of patients were been shown to be apoptotic by TUNEL staining for DNA fragmentation (Méhes et al., 2001).

There are a number of reasons why circulating tumour cells may undergo apoptosis on entry into the circulation (Mehlen and Puisieux, 2006), as outlined in Figure 1.4. One potential reason is due to the shear stress experienced on exposure to the high pressure and flow rates within the vasculature. Mechanical deformation experienced during circulation can lead to higher levels of apoptosis in non-metastatic mouse melanoma cells compared to their metastatic counterparts (Weiss et al., 1993). Similarly, culture of human colorectal cells in a rotational culture system, which recreates shear stress similar to that experienced in the vasculature, induces higher rates of apoptosis than those cultured in a monolayer or static 3D culture (Laguinge et al., 2004).

Cells can also fall prey to immune surveillance, or undergo spontaneous cells death (anoikis) following detachment from the primary tumour. Although other immune cell types have been shown to interact with circulating tumour cells, much research has focused on the role of natural killer (NK) cells in

metastatic cell clearance. NK cells are lymphocytes which make up 10-20% of the mononucleocyte cells in peripheral blood, and mediate killing of cells which lack major histocompatibility complex I (Zamai et al., 2007). On activation, NK cells become highly cytotoxic, increasing their surface expression of FasL, TRAIL and the cytolytic protein perforin (Arase et al., 1995, Johnsen et al., 1999, Smyth et al., 1999).

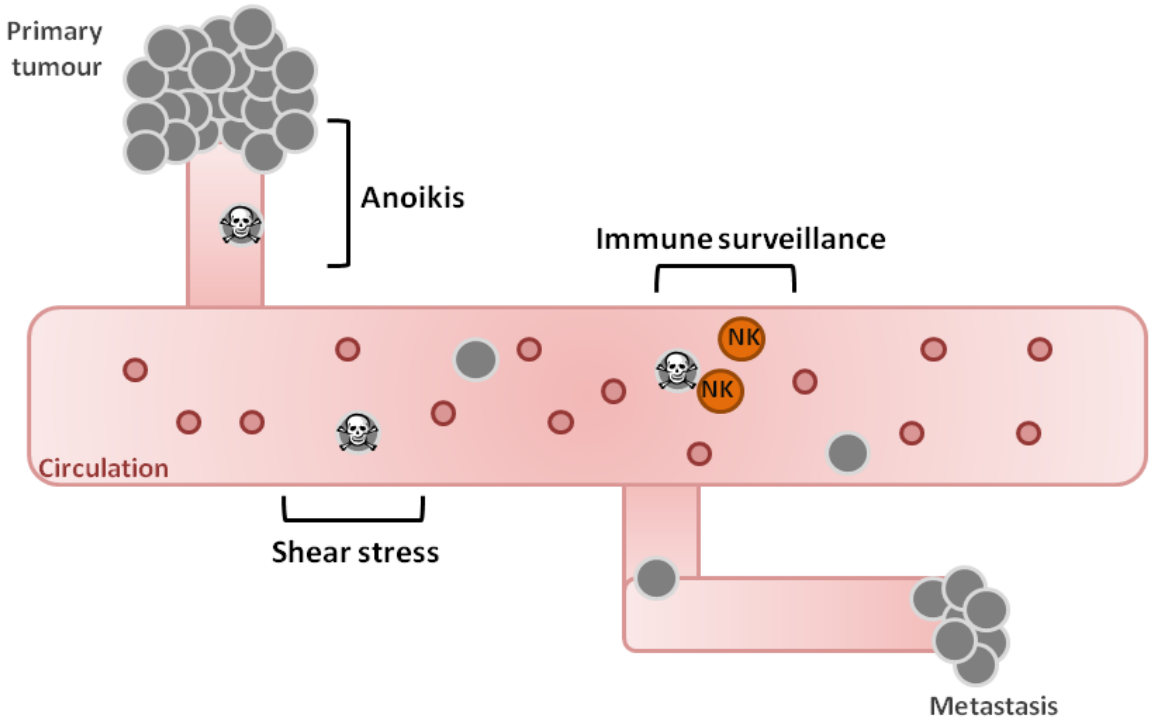

Figure 1.4 Metastatic inefficiency; potential factors contributing to tumour cell apoptosis in the circulation. Cancer cells (grey) extravasating from the primary tumour into the blood during haematogenous spread may undergo anoikis following detachment. Once in the blood, shear stress and high blood flow may induce apoptosis. Immune cells such as natural killer (NK) cells also play an important role in the immune surveillance of circulating tumour cells. Adapted from (Mehlen and Puisieux, 2006).

On extravasation and entry into the circulation, cancer cells can be seen bound to platelets (Nieswandt et al., 1999). This interaction is protective to cancer cells, as anti-coagulation drugs can reduce metastasis. These bound platelets are thought to act as a physical shield, protecting circulating cancer cells from NK-mediated lysis (Nieswandt et al., 1999, Palumbo et al., 2005).

Depletion of NK cells in mice dramatically increases the number of lung and liver nodules in experimental metastasis models (Takeda et al., 2001). When a mouse fibrosarcoma cell line was injected i.v. into untreated mice, only 5% of the injected cells were retained in the lung. When mice were depleted of NK cells, this figure rose dramatically to 93% of cells retained (Nieswandt et al., 1999). TRAIL, FasL and perforin have all been implicated in the cytotoxic effect of NK cells on tumour cells *in vitro* (Kayagaki et al., 1999, Takeda et al., 2001, Seki et al., 2003), however the contribution of each agent *in vivo* appears to be dependent on metastatic site.

The literature acknowledges an important role for TRAIL in NK-mediated killing of tumour cells in the liver during metastasis, which may reflect the fact that a subset of liver NK cells constitutively expresses TRAIL (Takeda et al., 2001). TRAIL on other NK cell populations is induced only on activation of NK cells by cytokines. These liver NK cells could kill tumour cell targets *in vitro* using a combination of FasL, TRAIL and perforin-mediated killing. *In vivo* experiments also demonstrated the importance of TRAIL, FasL and perforin in controlling liver metastasis (Takeda et al., 2001, Seki et al., 2003).

Perforin was shown to be required in the NK-mediated control of lung metastasis in an experimental and spontaneous model of metastasis *in vivo* (Smyth et al., 1999, Seki et al., 2003). FasL also plays an important role in controlling metastatic outgrowth in the lung (Owen-Schaub et al., 1998, Hall et al., 2004). However the importance of TRAIL remains controversial, with some studies suggesting no role for TRAIL in NK cell mediated clearance of lung metastasis (Cretney et al., 2002). As TRAIL expression can be induced on NK cells following exposure to cytokines such as IL-2, IL-12 and IFN-γ (Kayagaki et al., 1999, Mark J Smyth, 2001), TRAIL's contribution to NK cytotoxicity is likely to depend on the location, activation state, and signals surrounding NK cells. This may depend not only on the organ being investigated, but on the inherent immune background of the mouse strain used in each experiment.

1.3.2 Anoikis

Anoikis is used to describe apoptotic cell death which is stimulated following detachment of cells from a matrix (Frisch and Francis, 1994). It has been shown to be another factor regulating metastasis, as tumour cells must detach in order to circulate in the blood. For cells to survive in the circulation, they must develop mechanisms to resist anoikis (Simpson et al., 2008).

The expression of heterodimeric integrin receptors on the cell surface is essential for the attachment of cells to a matrix (discussed further in Section 5.1). Integrins form focal adhesions through which signals are relayed by adaptors and kinases such as integrin-linked kinase, talin, focal adhesion kinase (FAK) and SRC (Nagaprashantha et al., 2011). Overexpression or over-activation of almost all members of this complex has been reported to confer anoikis resistance in cancer cells, as discussed further in Chapter 5. Activation of FAK and SRC can lead to anoikis resistance in cells *in vitro* (Frisch et al., 1996, Beierle et al., 2009). These kinases can activate survival pathways such as phosphotidylinositide 3'-kinase (PI3K), mitogen activated protein kinase (MAPK) and NFκB (Schlaepfer et al., 1994, Chen et al., 1994, Schlaepfer and Hunter, 1997), which themselves regulate the expression of apoptosis pathway components such as caspase-9, BAD, BIM, cFLIPs and IAPs (Datta et al., 1997, Wang et al., 1998, Cardone et al., 1998, Micheau et al., 2001, Reginato et al., 2003).

There is also evidence that the death receptor pathway of apoptosis can mediate anoikis. Expression of dominant negative FADD or high levels of cFLIP could protect detached cells from anoikis by preventing caspase-8 cleavage (Rytömaa et al., 1999, Shain et al., 2002, Mawji et al., 2007). FAK was also shown to regulate FADD and caspase-8 signalling through its control of the DD-containing kinase RIP1 (Kurenova et al., 2004). Fas signalling has been implicated in anoikis, as a number of cell lines were shown to be more sensitive to the apoptotic effects of FasL following detachment (Aoudjit and Vuori, 2001, Shain et al., 2002), and blocking Fas signalling in detached intestinal epithelial cells could protect them from anoikis

(Rosen et al., 2002). Adhesion of PC3 prostate cancer cells could also render them more resistant to the pro-apoptotic effects of TNF-α, suggesting that adhesion may be a general mechanism behind resistance to apoptosis by death receptor ligands (Fornaro et al., 2003). In support of this, Goldberg showed that anchored MCF7 breast cancer cells had lower TRAIL expression, and was one of the first studies showing detached cells had higher TRAIL sensitivity (Goldberg et al., 2001). Subsequently, the carcinoembryonic antigen (CEA), able to drive metastasis in colon cancer cells lines, was shown to confer anoikis resistance through its ability to bind to DR5 and prevent activation of caspase-8 (Samara et al., 2007). FAK was also shown to mediate TRAIL sensitivity in HL60 leukaemia cells through its ability to regulate AKT, and a number of apoptotic proteins including XIAP, BCL-X_L and RIP (Tamagiku et al., 2004).

These studies provided the first evidence that controlling cell adhesion, either by detachment or disruption of integrin signalling, could provide a potential mechanism by which to sensitise metastatic tumour cells to TRAIL therapy. On arrival of metastatic cells at the secondary organ, tumour cells are seen to spread along the vasculature and to begin to proliferate intravascularly (Wong et al., 2002, Im et al., 2004). Therefore inhibiting the adhesion of tumour cells to the vasculature may allow a longer window of opportunity for TRAIL sensitisation. Due to the importance of NK-expressed TRAIL in the immune clearance of circulating tumour cells, such a sensitisation mechanism could not only make cells more susceptible to exogenous TRAIL therapies but also to endogenous TRAIL on immune cells.

1.4 Aims

In light of this evidence, and the need to develop novel methods of sensitising resistant cancer cells to TRAIL therapy, the aim of this thesis is to investigate whether disrupting cell adhesion can sensitise metastatic tumour cells to TRAIL-induced apoptosis *in vitro* and *in vivo*. A number of models will be used to investigate this, as outlined below:

i) Initial work will aim to verify previous suggestions that detachment can sensitise cancer cells to TRAIL-induced apoptosis. Cancer cells will be identified with varying TRAIL sensitivity and their response to TRAIL tested on normal and low attachment plates. Apoptosis protein arrays will be used to investigate potential mechanistic reasons for the TRAIL sensitivity seen.

ii) To further develop this work, a model will be used in which MDA-MB-231 breast cancer cells are rendered deficient in the ability to transcribe genes essential for cell adhesion and spreading. The effect of this defect on TRAIL sensitivity will be investigated, and analysis made to identify potential differences in the TRAIL pathway which may account for the TRAIL sensitivity seen.

iii) Cell adhesion will then be disrupted at the level of the integrin signalling pathway, using siRNA or inhibitors and their effect on TRAIL sensitisation determined.

iv) Following the identification of potential TRAIL sensitising agents in the cell adhesion pathway, the final aim is to test whether these agents could enhance metastatic lung clearance *in vivo* in combination with rhTRAIL therapy. This will require the development of a metastasis assay, and the development of software allowing the measurement of cell morphology *in vivo*.

Chapter 2: Materials and Methods

2.1 Cell culture

2.1.1 Cell lines and maintenance

Table 2.1 outlines the cell lines used in this study, the person or organisation from which they were obtained, and the conditions used for their maintenance. All fetal bovine serum (FBS) was heat inactivated for 30 min at 56^{o}C. Dulbecco's Modified Eagle Medium (DMEM) and penicillin/streptomycin (P/S) were purchased from GIBCO® (Invitrogen, Paisley, UK). Cells were subcultured in a bioMAT class II sterile laminar flow hood and maintained in an incubator at 37^{o}C with 20% oxygen and 5% carbon dioxide.

Cells were thawed rapidly in a water bath at 37^{o}C after removal from liquid nitrogen. Once thawed, they were diluted in 10 x volume of complete media, centrifuged at 240 x *g* for 4.5 min, resuspended in complete media, and seeded into a T75^{2} flask. On confluency, cells were split by rinsing with sterile phosphate buffered saline (PBS), adding 0.05% Trypsin-EDTA (GIBCO®) at a volume of 5 ml per T175^{2} flask and allowing cells to lift for 5 min at 37^{o}C. Trypsin was then diluted with 10 x volume of medium, which was then spun at 240 x *g* for 4.5 min in a centrifuge, and a small fraction added to a new flask of fresh medium. The density of reseeding was dependent of the experiments to be performed. Cells were routinely checked for mycoplasma using a Cambrex MycoAlert® Mycoplasma Detection Assay kit (Cambrex).

Name	Type	Source	Conditions
MDA-MB-231	Breast carcinoma	Prof R Treisman (LRI, London)	DMEM (10% FBS)
-Clone C4-GFP			DMEM (10% FBS, 5 µg/ml blasticidin, 100 µg/ml G418)
-Clone C20-CFP			DMEM (10% FBS, 5 µg/ml blasticidin, 100 µg/ml G418, 200 mg/ml zeocin)
WM1789-GFP	Melanoma (radial phase)	Dr M Herlyn (Wister Institute,PA)	MCDM153 medium: L-15 medium (4:1), 4% FBS, 1% P/S, 5mg insulin (pL), 2mmol/L $CaCl_2$
1205Lu-GFP	Melanoma (vertical phase)	Dr M Herlyn (Wister Institute,PA)	DMEM (10% FBS, 1% P/S)
SW480	Colon carcinoma	ATCC ® (# CCL-228)	DMEM (10% FBS, 1% P/S)
Jurkat	T-cell leukaemia	ATCC® (#TIB-152)	RPMI (10% FBS, L-glutamine)

Table 2.1 Details of cell lines used.

2.1.2 Freezing cells

Cells were suspended in a freeze medium containing 70% DMEM, 20% FBS, and 10% DMSO (Sigma Chemical Company) and aliqouted into 1.5 ml cryovials. Vials were placed in a Nalgene® Mr Frosty filled with 200 ml isopropanol at room temperature, and placed at -80^{o}C for 24 hr prior to long term storage in liquid nitrogen.

2.1.3 Counting cells

Cells were counted using a nucleocounter (Chemometec), which uses cassettes containing propidium iodide to stain the cell nuclei. Lysis of the cell samples prior to cassette loading allows the free nuclei to be labelled, therefore providing a total cell count. This method has been shown to be as equally accurate as traditional haemocytometer methods, with higher reproducibility (Shah et al., 2006).

2.2 Cell-based assay protocols

2.2.1 Low attachment plates

For experiments requiring inhibition of cell attachment, cells were cultured on low attachment plates (Corning Life Sciences).

2.2.2 TNF ligands

For *in vitro* apoptosis induction, cells were treated with recombinant human TRAIL (Peprotech), anti-Fas monoclonal antibody (clone CH-11) (MBL), or recombinant human TNF-α (Peprotech). All ligands were used at the concentrations indicated in the figure legends.

2.2.3 Integrin blocking

Prior to integrin blocking, 96 well plates were coated with 10 µg/ml of fibronectin from human plasma (Sigma) or human collagen I (VWR), at a volume of 30 µl per well. The protocol for coating is briefly outlined below.

Fibronectin was diluted to 10 µg/ml in Phosphate Buffered Saline (PBS), added to the wells of the microtiter plate, and left at 37^{o}C for 1 hr prior to use. Collagen I was made up in 2 mM Hydrochloric acid, and diluted to 10 µg/ml. This solution was then added to the wells of the microtiter plate for 2 hr, before being aspirated and the plates left to dry overnight.

For *in vitro* integrin blocking, cells were counted and suspended in complete medium at 1x10^{5} cells/ml. Cells suspensions were then either left untreated, or incubated with 5 µg/ml of monoclonal anti-human Integrin β1 blocking antibody (R&D Systems #MAB17781), anti-human integrin β3-blocking antibody (Millipore #MAB2023Z), or anti-human integrin β1-stimulating antibody (Millipore #MAB2250Z) for 1 hr on ice on a low speed rocking platform.

After incubation, cells were plated onto the coated 96 well plates and left to attach for 4 hr before TRAIL addition. When performing phalloidin staining, the above was performed in coated chamber slides (Lab-Tex®, Thermo scientific) and cells fixed for staining 4 hr after seeding.

2.2.4 Inhibitor treatments

The inhibitors used in this thesis are outlined below.

Name	Function	Company	Concentration	Treatment
Z-VAD-FMK	Pan-caspase inhibitor	R&D Systems	10 µM	1 hr prior to TRAIL addition
PP2	SRC family kinase inhibitor	Sigma	Range (mostly 10 µM)	1 hr prior to TRAIL addition
PP3	Non-functional PP2 analog	Sigma	Range (mostly 10 µM)	1 hr prior to TRAIL addition
AZD0530 (Saracatinib)	SRC inhibitor	Selleck	Range (mostly 25 µM)	1 hr prior to TRAIL addition
UO126	MEK1/MEK2 inhibitor	Sigma	5 µM	1 hr prior to TRAIL addition
PI-103	PI3K inhibitor	Piramid Pharma	0.8 µM	1 hr prior to TRAIL addition
AKT inhibitor	Pan AKT inhibitor	Merck (Kind gift from lab of Dr E O'Neill)	5µM	1hr prior to TRAIL addition
PF-573,228	FAK inhibitor	Tocris	Range (mostly 10 µM)	1hr prior to TRAIL addition

Table 2.2 Details of inhibitors used.

2.2.5 Death receptor blocking

The function of TRAIL receptors DR4 and DR5 was blocked using monoclonal antibodies HS101 and HS201, respectively (Enzo Life Sciences). These antibodies were added to pre-seeded cells at a concentration of 10 μg/ml for 30 min before the addition of TRAIL.

2.2.6 Other reagents

Recombinant OPG was purchased from R&D Systems.

2.2.7 Caspase 3/7 activity

Caspase 3/7 activity was measured using a luminescence assay, during which caspase 3 and 7 from lysed cells cleaves a luminogenic substrate containing the DEVD caspase-cleavage target sequence (Caspase 3/7 Glo® Assay, Promega). Cleavage of the DEVD-containing substrate releases aminoluciferin, a substrate for luciferase. $1x10^4$ cells were seeded per well into a white walled 96 well microtiter plate and left to adhere overnight. They subsequently underwent the appropriate treatment, and TRAIL was added at the appropriate time after treatment. Caspase activity was shown to be maximal at 3 hr after TRAIL treatment for all cell lines (see Figure 3.1B); therefore Caspase3/7 Glo® substrate was added 3 hr after TRAIL treatment in a 1:1 ratio with the cell medium. The plate was covered in foil, incubated for 1 hr at room temperature, and then luminescence read on a plate reader (Tecan Infinite® M200).

2.2.8 Cell viability

Cell viability was measured using alamarBlue® assay (Invitrogen). AlamarBlue® reagent contains resazurin, a cell-permeable, non-fluorescent blue dye which is converted to a red-fluorescent dye, resorufin, following reduction. The metabolic activity of living cells reduces the alamarBlue® reagent, giving an indication of the number of viable cells present. For this assay, cells were seeded overnight at a density of $1x10^4$ cells per well in a 96 well plate. The following morning, cells were treated with the appropriate drug/chemical and left for 24 hr. AlamarBlue® solution was then added at 10% of the total volume per

well. After around 4 hr, the plates were read at 560 nm (excitation), 590 nm (emission). The gain was set to 90 for all experiments to allow comparison between plates. To ensure that the plates were being read within the linear range of the alamarBlue® fluorescence, this assay was optimized for each cell line, at a range of cell seeding densities. Figure 2.1 shows that $1x10^4$ cells per well was an optimum seeding density, as its linear range had a wide time scale and a wide range of absorbance readings. Data in this thesis is expressed as a % reduction in viability after TRAIL treatment, compared to paired non-TRAIL treated controls for each condition.

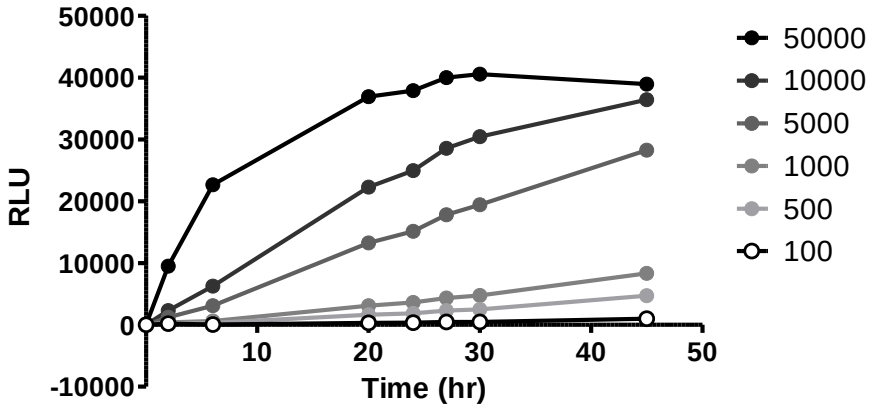

Figure 2.1 Optimisation of alamarBlue® assay cell seeding number for MDA-MB-231 cells. The indicated number of cells were seeded into each well of a 96 well plate, and 10 min later alamarBlue® added at 10% culture volume and read on a plate reader at various time intervals.

2.2.9 Cell spreading measurements

Cell spreading *in vitro* was measured using the xCELLigence system from Roche Applied Science. This system uses E-plates, containing microelectrodes in an array across the bottom of the plate. The presence of cells on top of the electrodes results in electrical impedance, measured with the unit Cell Index (CI), which is greater when more cells are present. If the same cell number is incubated in the wells, the CI becomes a measure of the quality of cell attachment. The E-plate was initially coated in 10 µg/ml fibronectin, 25 µl of medium was added to each well and a blank step ran on the xCELLigence machine.

Cells were then loaded into the wells with $4x10^4$ cells per well. Plates were left to equilibrate at room temperature for 20 min before being loaded into the xCELLigence machine inside a 37°C incubator, and measurements taken every 3 min for 150 runs.

2.3 Western blot

2.3.1 Preparation of cell lysates

Cells were either spun down and resuspended in lysis buffer, or lysed directly from the tissue culture plate by the addition of ice cold lysis buffer. For western blots investigating levels of apoptosis related proteins, spent media was also collected from the plates, spun down at 240 x *g* for 1 min and combined with the rest of the lysate. Lysis buffer was purchased from Thermoscientific (Loughborough, UK) and was composed of 25 mM Tris-HCl (pH7.6), 150 mM NaCl, 1% NP-40, 1% sodium deoxycholate, 0.1% SDS. This buffer was then supplemented with protease inhibitor cocktail (Roche), and phosphatase inhibitor cocktail (Sigma). Resuspended lysates were rotated for 30 min at 4°C, and then spun at 10,000 x *g* for 10 min at 4°C. The supernatant was then transferred to a new Eppendorf tube on ice and either used immediately, or stored at -20°C for later use.

2.3.2 Quantification of protein concentration

Protein concentrations were determined using a BCA assay (Thermoscientific) using reagents provided in the kit. Briefly, a standard curve of concentrations was created using BSA, ranging from 0 µg/ml to 2000 µg/ml. The unknown samples were diluted 1/12.5 with water and also added to the plate in duplicate. The reagents supplied in the BCA kit were then combined, reagent A (containing sodium carbonate, sodium bicarbonate, bicinchoninic acid and sodium tartrate in 0.1 M sodium hydroxide) and reagent B (4% cupric sulfate) in a 50:1 ratio and 200 µl added to each sample and standard curve in the plate. The plate was then incubated at 37°C for 30 min and the absorbance read at wavelength 562 nm

using a plate reader (Tecan). The standard curve was used to calculate the actual concentration of sample in µg/µl.

2.3.3 Sample preparation

Western blots always used between 10-30 µg whole cell lysate. The volume of lysate which contained the chosen amount of protein (eg. 25 µg) was added to an Eppendorf tube, along with 1 mM DTT, and NuPAGE® LDS sample buffer at 25% the volume of the total sample volume. The remaining volume was made up with water. Samples were then boiled for 10 min at 70°C.

2.3.4 Gel electrophoresis

Protein samples were loaded onto a gel and separated by sodium dodecyl sulphate-polyacrylamide gel electrophoresis (SDS-PAGE). RunBlue® pre-cast gels were purchased from Expedeon and were used at either 4-12% gradient, or 16% gradient. Prior to use, the gels were washed and loaded into a Novex mini-cell tank (Invitrogen), which was filled with running buffer. SDS running buffer was supplied by RunBlue® (2-5% tricine, 2-4% tris-hydroxymethylaminomethane, 0.1-2.5% sodium dodecyl sulphate, 0.002-0.5% sodium bisulfate) and diluted 1 in 20 with water. Samples were loaded using loading tips (Greiner), along with precision plus protein™ standards (Bio-Rad), and ran for 55 min at 185 V.

2.3.5 Blotting protocol

After being separated using gel electrophoresis, the protein samples were transferred from the gel onto a 48 cm^2 polyvinylidene fluoride (PVDF) transfer membrane (Immobilon™ from Millipore). The membrane was activated by washing for 5 min in 100% methanol. The transfer was performed using a XCell II™ blot module in which the gel and membrane were sandwiched between two sheets of Whatman paper, and compacted into the module with sponges. The transfer was performed in transfer buffer (0.2 M Tris base with 0.09 M glycine in dH_20) at a voltage of 30 V for 1 hr 15 min.

Following transfer, membranes were blocked for 1 hr on an orbital shaker at room temperature in 5% milk TBS-T (using 5% (w/v) skimmed milk powder (Marvel), made up with Tris-buffered saline supplemented with 0.1% Tween-20 (TBS-T)). Following blocking, the membrane was briefly washed in TBS-T and the primary antibody added.

The primary antibodies used are outlined in Table 2.3, along with the antibody buffer components and concentration. All primary antibodies were applied to the membrane overnight at 4^{o}C on a tube roller (Stuart).

Following primary antibody incubation, membranes were washed 3 times for 5 min in TBS-T on an orbital shaker, and then incubated with HRP-conjugated secondary antibody at room temperature for 1 hr. Membranes were then re-washed prior to development.

2.3.6 Membrane development

Once washed, the membrane was exposed to either Amersham^{TM} enhanced chemiluminescence ECL or ECL+ solution (GE healthcare), depending on the primary antibody used. Membranes were then protected from light using an autoradiography cassette (Fisher), exposed to film (Fuji) and developed using an XoGraph processor (XoGraph Imaging Systems).

2.3.7 Stripping of membranes

In order to allow membranes to be probed with multiple primary antibodies, membranes were stripped for 15 min at 37^{o}C using Restore^{TM} Western Blot Stripping Buffer (Pierce). Stripping buffer was composed of 7-10% glycine, 3-5% aliphatic carboxylic acid.

2.3.8 Primary antibodies

Protein Name	Company (order#)	Species	Primary Dilution	Secondary Dilution	Buffer
Actin	Sigma Aldrich (#A1978)	Mouse	1/10000	1/10000	5% milk TBS-T
p-AKT (Ser 473)	Cell Signaling (#9271)	Rabbit	1/2000	1/5000	5% BSA TBS-T
Total AKT	Cell Signaling (#9272)	Rabbit	1/1000	1/5000	5% milk TBS-T
BCL-2	Millipore (#04-436)	Rabbit	1/1500	1/4000	5% milk TBS-T
BID	Cell Signaling (#2002)	Rabbit	1/1000	1/4000	5% milk TBS-T
P130Cas (Tyr165)	Cell Signaling (#4015)	Rabbit	1/1000	1/5000	5% BSA TBS-T
Caspase-8	R&D Systems (#AF1650)	Rabbit	1/2000	1/4000	5% milk TBS-T
Caspase-9	Cell Signaling (#9502)	Rabbit	1/1000	1/4000	5% milk TBS-T
Caspase-10	MBL (#M059-3)	Mouse	1/1000	1/4000	5% milk TBS-T
cFLIP	Alexis (#ALX-804-428)	Mouse	1/500	1/3000	5% milk TBS-T
DR5	R&D Systems (AF721)	Goat	1/500	1/5000	5% milk TBS-T
DR4	Imgenex (#IMG-141A)	Mouse	1/166	1/2000	5% milk TBS-T
ERK1/2 (phospho-p44/42)	Cell Signaling (#9101)	Rabbit	1/1000	1/5000	5% BSA TBS-T
Total ERK1/2	Cell Signaling (#9102)	Rabbit	1/1000	1/5000	5% milk TBS-T
FAK	BD (#610087)	Mouse	1/500	1/4000	5% milk TBS-T
FAK (Tyr^{861})	Abcam (#ab4804)	Rabbit	1/1000	1/5000	5% BSA TBS-T
HTRA2/Omi	Abcam (#ab21307)	Rabbit	1/1000	1/3000	5% milk TBS-T
IκBα	Abcam (#ab32518)	Rabbit	1/10,000	1/5,000	5% milk TBS-T
ILK	Cell Signaling (#3862)	Rabbit	1/1000	1/5000	5% BSA TBS-T
Integrin β1	Abcam (#ab52971)	Rabbit	1/500	1/3000	5% milk TBS-T
Integrin β3	Cell Signalling (#4702)	Rabbit	1/1000	1/5000	5% milk TBS-T
MRTF-A	Santa Cruz (#sc-21558)	Goat	1/1000	1/4000	5% milk TBS-T

MRTF-B	Santa Cruz (#sc-47282)	Goat	1/1000	1/4000	5% milk TBS-T
PARP-1 (F-2)	Santa Cruz (#sc-8007)	Mouse	1/1000	1/5000	5% milk TBS-T
Paxillin	Cell Signaling (#2542)	Rabbit	1/1000	1/5,000	5% BSA TBS-T
Paxillin (Tyr^{118})	Cell Signaling (#2541)	Rabbit	1/1000	1/5,000	5% BSA TBS-T
SRC	Cell Signaling (#2109)	Rabbit	1/1000	1/5000	5% BSA TBS-T
Talin 1	Gift Dr. D Critchley (Leicester)	Mouse	1/50	1/3000	5% milk TBS-T
Talin 2	Gift Dr. D Critchley	Mouse	1/50	1/3000	5% milk TBS-T

Table 2.3 Details of primary antibodies used for western blot

2.4 Osteoprotegerin ELISA

In order to detect secreted osteoprotegerin (OPG) from MDA-MB-231 cells, $1x10^4$ cells were seeded into a 24 well plate, as previously described (Neville-Webbe et al., 2004). These were left to grow for 72 hr, and then the medium was collected and stored at -20^oC. The number of cells at the 72 hr point were counted using a Nucleocounter. This allowed the normalisation of secreted OPG levels to the proliferation rate of the cells. A human OPG Instant ELISA kit was purchased from Bender Medsystems, and performed according to the manufacturer's protocol. Briefly, 50 µl of sample was added to each sample well in duplicate into the ELISA plate, which was incubated for 3 hr at room temperature on a microplate shaker (100 rpm). The plate was then washed, before TMB substrate (3,3',5,5' – tetramethylbenzidine) solution was added and allowed to develop. The reaction was stopped when the highest standard reached an optimal density value of 0.6-0.65. The absorbance was then read at 450 nm on a plate reader. A standard curve was created using Microsoft Excel, and sample values calculated from the standard curve. These average sample values were then multiplied by the dilution factor, and normalised to the proliferation rate of the cells from which each medium sample was taken.

2.5 Human Apoptosis Array

Proteome Profiler™ Human Apoptosis Array Kits (R&D Systems) were used to measure the relative expression of 35 apoptosis related proteins. MDA-MB-231 cells were lysed using Lysis Buffer provided in the array kit. Protein concentration was measured using a BCA assay (Thermoscientific). As outlined in the manufacturer's protocol, the supplied membranes were blocked on a platform rocker for 1 hr at room temperature with Array Buffer provided. Following this, a solution of 1.5 ml volume was created using Array Buffer and a volume of whole cell protein lysate equal to 350 µg. These lysate solutions were incubated on the membranes overnight at 4°C. The following day, membranes were washed with Wash Buffer 3 times for 10 min. The membranes were then incubated for 1 hr with a solution containing 15 µl of reconstituted Antibody Detection Cocktail diluted in Array Buffer. The membranes were then washed, and incubated for 30 min at room temperature with a solution containing a 1/2000 dilution of Streptavidin-HRP. After re-washing, the membrane was exposed to either Amersham™ enhanced chemiluminescence ECL or ECL+ solution (GE Healthcare). Membranes were then developed by film exposure and development as described in section 2.3.6. For further information about the image analysis software designed specifically for semi-quantitation of these arrays, and for data on the investigation of other imaging methodologies for these arrays, see Supplementary Chapter 1.

2.6 Transfection protocols

2.6.1 siRNA transfection

All siRNA was purchased from Dharmacon (Thermoscientific) and reconstituted in siRNA buffer (300 mM KCl, 30 mM HEPES-pH7.5, 1.0 mM MgCl2) for storage at -80°C. For use, the appropriate volume of siRNA was diluted in 200 µl serum-free DMEM and incubated for 5 min in an Eppendorf tube prior to mixing with Dharmafect transfection reagent (also diluted in 200 µl DMEM for 5 min). Once combined, the

siRNA/Dharmafect mixture was left for 20 min with frequent gentle mixing. The siRNAs used are outlined in Table 2.4.

siRNA target	Description	Concentration of siRNA needed	Volume transfection reagent needed
Control	ON-TARGETplus non-targeting pool (Thermoscientific)	Variable (dependent on experiment)	Variable (dependent of experiment)
Human ILK	ILK human siRNA ON-TARGET plus SMARTpool (Thermoscientific)	25 nM (MDA-MB-231) 50 nM (1205Lu)	2 µl (MDA-MB-231) 3 µl (1205Lu)
Human SRC	SRC human siRNA ON-TARGET plus SMARTpool (Thermoscientific)	Range tested	Range tested
Human Talin 1	Talin 1 human siRNA ON-TARGET plus SMARTpool (Thermoscientific)	25 nM	2 µl

Table 2.4 Details of siRNA used for transfections in MDA-MB-231 and 1205Lu cells.

Cells for transfection were seeded the afternoon prior to transfection at $1x10^5$ cells per well of a 6 well plate in antibiotic free medium. After preparation of the siRNA mixture, medium was aspirated from cells and replaced with 400 µl of pre-mixed siRNA/Dharmafect and the volume made up to 2 ml with antibiotic free medium. The medium was changed on the cells after 7 hr. For verification of knockdown via western blot, cells were harvested and lysed at 72 hr post-transfection. For TRAIL assays, 55 hr after transfection, cells were trypsinised, recounted and reseeded in 96 well plates and left to attach overnight before subsequent treatment.

2.6.2 shRNA expression

Cells were seeded at $1.6x10^4$ cells per well in a 96 well plate the evening before transfection. The day of transfection, medium containing 8 µg/ml Polybrene® was added to promote interaction of the pseudoviral capsid and the cell membrane. Control or SRC shRNA lentiviral particles (Santa Cruz Biotechnology) were

added to each well at volumes equal to a Multiplicity of Infection (MOI) of 2 and left to incubate overnight. The medium was changed the following day, to complete medium (without Polybrene®). In the following days, cells were passaged into 24 well plates and selected using 5 µg/ml puromycin. For limiting dilution, cells were diluted to a concentration giving approximately 1 cell per 100 µl medium and seeded into a 96 well plate for selection and clonal expansion.

2.7 Immunofluorescence staining

2.7.1 TUNEL staining

For *in vitro* terminal deoxynucleotidyl transferase dUTP nick end labelling (TUNEL) assays, cells were seeded overnight in a 6 well plate at a density of 1 million cells. Cells were then incubated with TRAIL (100 ng/ml) for 6 hr. Optimisation was performed on a TRAIL sensitive positive control cell line SW480 to determine the optimal TRAIL treatment time. As shown in Figure 2.2, 24 hr treatment led to significant nuclear fragmentation making the cells to difficult to count, whereas 6 hr TRAIL treatment led to easily distinguishable cells whose apoptotic state could be clearly determined. After the 6 hr treatment, spent media containing floating dead cells was kept, and the remaining cells trypsinised and then pooled with the spent media. The pooled cells from each condition were centrifuged at 10,000 x *g* for 5 min and resuspended in 1% paraformaldehyde (PFA) for fixation. After fixation the cells were re-centrifuged, resuspended in an equal volume of phosphate buffered saline (PBS) and spun onto a microscope slide using a cytospin cytocentrifuge (Shandon). Cells were spun onto slides at 120 x *g* for 2 min.

For TUNEL staining of lung sections, slides were rehydrated in PBS for 5 min and then incubated in 1% PFA for 10 min, followed by 2 washes in PBS for 5 min.

Following the above mentioned preparation techniques and fixation, slides could then be immersed in a Coplin jar containing pre-cooled (−20^{o}C) ethanol:acetic acid mix in a ratio of 2:1 for 5 min at −20^{o}C.

Following this permeabilisation step, slides were washed in PBS. The TUNEL staining Apoptag® kit was purchased from Millipore and performed in accordance with manufacturer's protocol. Briefly, slides were coated with equilibration buffer for 20 sec. TdT enzyme was added in a dilution containing 70% reaction buffer and 30% TdT enzyme and incubated for 1 hr in a humidifying chamber at 37^{o}C. For negative controls, the TdT enzyme was replaced with PBS. Following this incubation, slides were added to stop/wash buffer for 10 min at room temperature. Slides were then washed in PBS, before incubation in the dark with a mixture of 53% blocking buffer solution and 47% digoxygenin (DIG) at room temperature for 30 min. Slides were then washed again in PBS before the addition of Hoechst (1/1000 in PBS) for nuclear staining. Vectashield® mounting medium was used to add coverslips to slides, before images were taken using an epifluorescent microscope (Leica). For *in vitro* TUNEL staining, cells were scored as positive (expressing red colour) or negative (only blue nuclear stain visible), with scoring aided by the use of UTHSCSA Image Tool 2.00 software for Windows. Cells were counted from 10 random fields for each condition, from 3 separate experiments. For *ex vivo* TUNEL staining, TUNEL positive staining was counted using Image J software (Image J), with any signals with a pixel value of below 0.2 being discarded as noise. For each condition, cells were counted from 10 fields across the centre of the lung, from 4 sections of the same lung and each experiment was repeated 3 separate times.

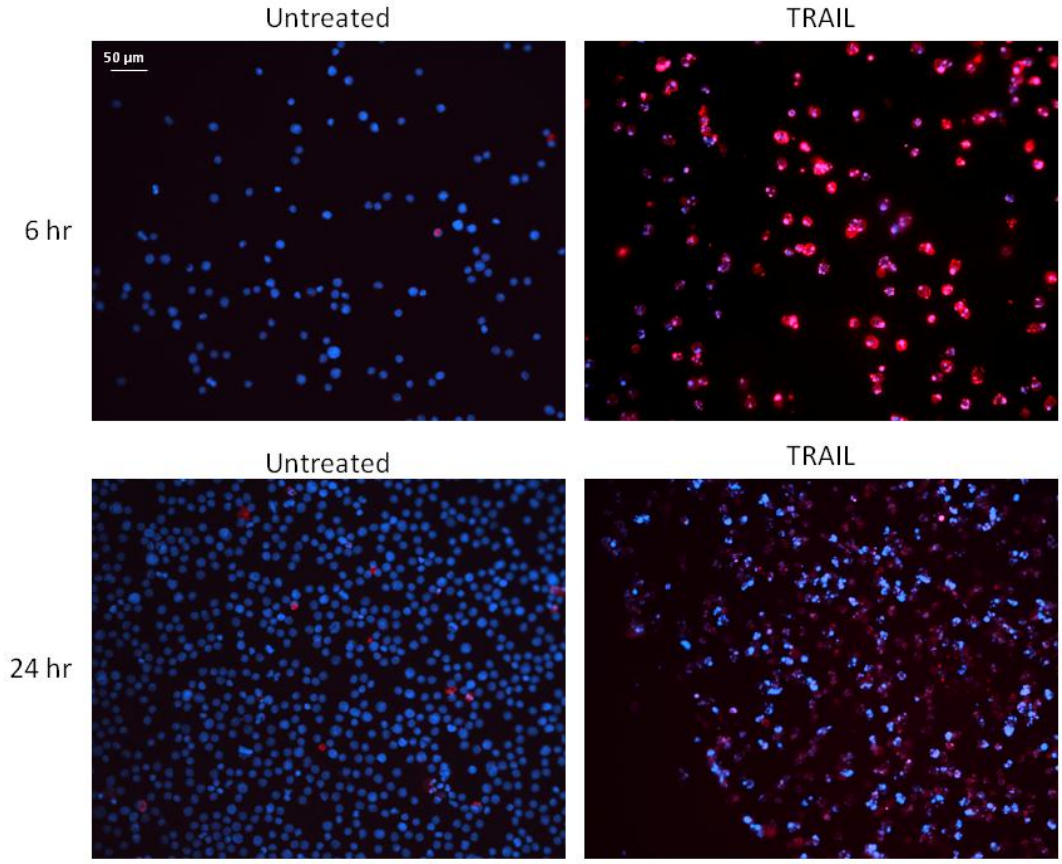

Figure 2.2 TUNEL staining optimisation in SW480 melanoma cells. TRAIL sensitive SW480 cells were treated for 6 hr or 24 hr with 100 ng/ml TRAIL. Resultant TUNEL staining shows that by 24 hr, TRAIL treated cells have severely fragmented nuclei, making the determination and scoring of single cells very difficult. Red staining highlights fragmented DNA resulting from cell death, blue staining highlights the cell nucleus.

2.7.2 Phalloidin staining

Cells were grown in 4 well glass chamber slides overnight. The next day the medium was removed, slides rinsed in PBS, and then fixed for 10 min in 4% PFA. The slides were then washed in PBS before being permeabilised for 10 min in 0.1% Triton-X in PBS. Slides were blocked using TNB Blocking Buffer (0.1 M Tris-HCL pH7.5, 0.15 M NaCl, 0.5% Blocking Reagent) (Perkin Elmer) for 45 min at room temperature. Phalloidin-TRITC (Sigma) solution was then added to cells in a dilution of 1/100 in TNB blocking buffer for 30 min at room temperature in the dark. Slides were washed in PBS before the addition of Hoechst

(1/1000 in PBS) for nuclear staining. Slides were mounted as previously described, and images obtained using either an epifluorescent microscope (Leica) or a confocal microscope (Zeiss).

2.8 Flow cytometry

For analysis, $5x10^5$ cells were suspended in 100 µl FACS buffer (PBS supplemented with 10% FBS) and stained appropriately. For DR4 and DR5 staining, cells were stained with 1 µl per sample of monoclonal antibodies HS201 and HS202 (Enzo Life Sciences), respectively, and TRAIL staining was performed using 2 µl per sample of monoclonal TRAIL antibody (C92B9) (Cell Signalling). All samples were incubated with antibodies at 4^{o}C for 30 min on a plate shaker. Following this, samples were washed twice by centrifugation at 240 x *g* followed by resuspension in 200 µl FACS buffer. Samples were then incubated on ice for 30 min in the dark with 1 µl of secondary antibody. For HS201 and HS101, this was anti-mouse IgG conjugated to Alexa Fluor 633 (Invitrogen), with anti-rabbit IgG conjugated to Alexa Fluor 633 (Invitrogen) for TRAIL staining. Samples were washed twice in FACS buffer before being measured using a FACScalibur (BD Biosciences), and analyzed with FloJo software. Using FloJo software, viable cells were gated according to forward/side scatter and their fluorescence was represented in histograms. The geometric mean of the fluorescent intensity for each sample was calculated using FloJo.

2.9 PCR

2.9.1 RNA Extraction

Cells were lysed directly from culture using 1 ml of TRIzol® reagent (Invitrogen) per well of a 6 well plate. Cells were left for 5 min to lyse, before being transferred to Eppendorf tubes. Chloroform was added to each sample at a volume of 0.2 ml per 1 ml TRIzol® reagent and shaken vigorously for 15 sec. The samples were then centrifuged at 2-8^{o}C at 10,000 x *g* for 15 min. The aqueous phase containing the RNA was transferred to a new tube and mixed with 0.5 ml of isopropanol per 1 ml of original TRIzol® mixture.

Samples were then centrifuged for 10 min at the above conditions to create an RNA pellet. The supernatant was removed from this pellet, and the pellet was washed in 1 ml of 75% ethanol. This mixture was then centrifuged at 10,000 x *g* for 5 min. The supernatant was then carefully removed, and the pellet allowed to air dry until completely dry. The RNA was then dissolved in 20-30 µl of RNase-free water and concentration measured the next day using a Nanodrop ND-1000 Spectrophotometer (Invitrogen).

2.9.2 qRT-PCR reaction

RNA was amplified and detected using SuperScript® III Platinum® SYBR® Green One-Step qRT-PCR Kit (Invitrogen) using the volumes of reagents outlined below. The total volume of the PCR reaction mixture was made up to 25 µl for each reaction using RNase free water (Sigma).

Component	Volume (µl)
SuperScript® III/RT/Platinum *Taq* mix	0.5
2 x SYBR® reaction mix	13
10 µM Forward Primer	1
10 µM Reverse Primer	1
RNA template	Volume containing 500ng (≈1)

Table 2.5 qRT-PCR reaction mixture components and volumes

The primers sequences used were:

OPG Forward : 5’GAAGGGCGCTACCTTGAGAT 3’

Reverse : 5’ ACAGGGTGCTTTAGATGACG 3’

DR4 Forward : 5’CATCGTGCCCTTTGACTCCTG 3’

Reverse : 5’GCGTTCCGTCCAGTTTTGTTG 3’

DR5 Forward : 5’TGCACCACGACCAGAAACAC 3’

Reverse : 5’ATCACCGACCTTGACCATCC 3’

GAPDH Forward : 5'GAAGGTGAAGGTCGGAGTC 3',

Reverse : 5'GAAGATGGTGATGGGATTTC 3'.

The qRT-PCR was run for 1 cycle of 30 min at 42^{o}C for reverse transcription, followed by a 10 min cycle at 95^{o}C for dsDNA denaturation. This was then followed by 40 cycles of 30 sec/95^{o}C, 30 sec/57^{o}C and 60 sec/72^{o}C. To ensure that a specific product was obtained, a melt curve analysis was performed after each PCR reaction, with a 1 min/95^{o}C denaturation step, a 30 sec/55^{o}C annealing step followed by a 30 sec melting step at 95^{o}C. Gene-specific products were measured using Mx3005P Real-Time PCR System and MxPro software version3 (Stratagene). Ct values were normalized to GAPDH and converted into fold change values relative to the control condition using the $2^{\Delta\Delta Ct}$ method.

2.10 *In vivo* work

2.10.1 Animals

Mice used were 6-8 wk old female Severe Combined Immunodeficient (SCID) mice (Harlan) kept in individually ventilated cages. Unless stated differently in the figure legend, animals were injected with $3x10^5$ cells (100 µl of a $3x10^6$ cells/ml solution in DMEM with no FBS) into the lateral tail vein. Lungs were isolated at either 4 hr or 24 hr following injection, as described in Section 2.10.4 and reported previously (Al-Mehdi et al., 2000, Im et al., 2004).

2.10.2 Preparation of cells for *in vivo* injection

Prior to injection, cells were trypsinised and counted, as described in Section 2.1.3. Once counted, a volume containing $3x10^6$ cells was removed and re-spun in a centrifuge at 240 x *g* for 4.5 min. The cell pellet was then resuspended in 1 ml of serum-free DMEM and the number of cells recounted. The cells were then respun, and resuspended in serum-free DMEM to a concentration of exactly $3x10^6$ cells per ml and stored on ice until injection.

For *in vivo* blocking experiments, cells were pre-blocked with either β1-blocking antibody (10 μg/ml), mouse IgG control antibody (10 μg/ml) (R&D Systems), PP2 (10 μM) or PF-573228 (10 μM) for 30 min on ice on a plate rocker.

2.10.3 Recombinant human TRAIL

For *in vivo* experiments, recombinant human TRAIL was kindly supplied by the lab of Professor Wafik El-Deiry (University of Pennsylvania). Purity and activity were verified in the El-Deiry lab prior to shipment. Due to relatively rapid precipitation of recombinant human TRAIL following purification, it required long term storage in 50% glycerol:50% PBS buffer. Before injection into animals, the required amount of rhTRAIL was diluted in a 10 fold higher volume of PBS. This was then concentrated using Amicon® Ultra-4 Centrifugal Filter Devices with molecular weight cut off of 10K, and re-diluted to the required concentration in sterile PBS. This could then be stored for up to 7 days at 4^{o}C before precipitation. For *in vivo* lung clearance assays, mice were injected 4 hr after tumour cell injection with an intravenous injection of 5mg/kg.

2.10.4 Lung isolation protocol

Mice were anaesthetized using an intraperitoneal injection (250 μl) of a solution composed of 2:1:1 ratio of water, Hypnorm® (Vetapharma) and Hypnovel® (Roche), respectively. Following this, mice were spread onto a cork board, the skin and fascia over the neck removed, and the trachea exposed. A small nick was made in the trachea into which a cannula could be inserted. A piece of cotton was threaded underneath the trachea and tied in order to hold the tube in place. The cannula was connected to a ventilator, and the lungs artificially ventilated at a respiration rate of 60 breaths per minute and pressure of 6.0 cm H_20. The skin and fascia over the abdomen was then opened to expose the vena cava, which was subsequently cut to exsanguinate the animal. Following exsanguination, the rib cage was opened and pinned back to expose the lungs and heart. The left atrium was removed from the heart, and a small cut made in the right

ventricle into which a cannula could be inserted to push Krebs Ringer Buffer solution through the lungs by gravity-driven perfusion. Krebs Ringer Buffer Solution contained KCl (0.3532 g/L), NaCl (6.9240 g/L), $MgSO_4.7H_20$ (0.2922 g/L), $NaHCO_3$ (2.09 g/L), KH_2P0_4 (0.1616 g/L), $CaCl_2.2H_20$ (0.1868 g/L), 5 % (w/v) dextran, 10 mM glucose at pH7.4.

Once cleared of blood, the ventilation was stopped and the trachea, lungs and heart were carefully removed from the animal and connected to a homemade chamber. This chamber was made by cutting a square out of a petri dish and inserting a thin 57 mm x 64 mm glass coverslip (Agar scientific). The lungs could then be placed onto the coverslip for imaging with an inverted microscope. A three-way valve was inserted into the top of the petri dish, into which the tracheal cannula could be attached. This allowed the inflation of the lungs using a syringe, and the maintenance of lungs in an inflated condition. An image of the chamber is shown in Chapter 6, Figure 6.1A.

2.10.5 Lung imaging protocol

The left lobe of the lung was imaged using a 10x objective lens on an inverted microscope (Leica), and images taken of each field as the lobe was scanned. This method is further discussed in Chapter 6.

2.10.6 Lung isolation protocol for immunofluorescence

When lung tissue was required for immunofluorescence, lungs were perfused as described above in section 2.10.4 with KRB, however lungs were then perfused with 50 ml paraformaldehyde (4%). They were then stored overnight in a solution 25% (w/v) sucrose in PBS.

2.10.7 Lung sectioning and counting

Following overnight storage in sucrose, lungs were embedded in O.C.T™ Compound (Tissue-Tek®) and frozen using Cryo Freeze Aerosol containing 1,1,1,2 tetrafluoroethane (Agar Scientific). Lungs were then sectioned using a cryostat (Bright Instruments) to sections of thickness 15 µm (for TUNEL staining) and

18 µm (for tumour cell counting). Sections were mounted onto SuperFrost®Plus microscope slides (VWR International). GFP positive tumour cells were counted by scanning and counting the number of tumour cells across a whole lung section. This was repeated for 6 different lung sections and an average taken.

Chapter 3: Hypothesis generation

3.0 Hypothesis

Culturing cancer cells on low attachment plates can sensitise them to TRAIL-induced apoptosis *in vitro*.

3.1 Aims

A previous report has suggested that detaching cancer cells from their matrix *in vitro* can enhance their sensitivity to apoptosis induced by exogenous TRAIL (Goldberg et al., 2001). The aim of this chapter is to verify that these effects could be reproduced in a range of cancer cell lines by performing 'proof of principle' experiments using cells cultured on normal or low attachment plates.

To meet the hypothesis, the main aims of this chapter are:

• To investigate TRAIL sensitivity in a selection of human cancer cell lines

• To investigate TRAIL sensitivity in these cell lines when cultured on normal or low attachment plates.

3.2 Results

3.2.1 TRAIL sensitivity in human cancer cell lines

To identify appropriate cell lines for use in future experiments, the TRAIL sensitivity of four human cancer cell lines was tested *in vitro*. A dose-response experiment was performed with concentrations of recombinant human TRAIL used in previous reports (Goldberg et al., 2001). For this experiment, viability reduction was used as an indicator of apoptosis and measured 24 hr after TRAIL treatment (Figure 3.1A). All cell lines showed a dose-dependent reduction in viability with increasing TRAIL, up to a concentration of 200 ng/ml. At this concentration, the colon carcinoma cell line SW480 exhibited a substantial 80% reduction in viability in response to TRAIL. The triple negative human breast cancer cell line MDA-MB-231 showed greater TRAIL resistance, with a 33% reduction in viability after 200 ng/ml TRAIL. Two human melanoma cell lines were also tested; 1205Lu derived from a highly metastatic vertical phase melanoma, and WM1789 derived from a poorly metastatic radial phase melanoma (Juhasz et al., 1993, Satyamoorthy et al., 1997). WM1789 cells showed a 42% reduction in viability after 200 ng/ml TRAIL, compared to only 11% reduction in the more TRAIL resistant 1205Lu cells. The TRAIL sensitivity of these melanoma cells matches with their reported ability to metastasise (Juhasz et al., 1993).

As viability reductions are only an indicator of apoptosis, the TRAIL sensitivity was confirmed by increases in caspase 3/7 activity after TRAIL treatment (Figure 3.1B). This activity was measured by the ability of cells to cleave a luminogenic caspase 3/7 substrate. The caspase 3/7 activity peaked 3 hr after TRAIL treatment for 3 out of the 4 cell lines tested. Caspase 3/7 activity in MDA-MB-231 cells only increased slightly beyond 3 hr, therefore a 3 hr time point was used in future experiments. The most TRAIL sensitive SW480 cell line showed a 19 fold increase in caspase 3/7 activity relative to untreated controls, compared with only a 5 fold increase in the more TRAIL-resistant 1205Lu cells 3 hr after TRAIL treatment (Figure 3.1B). Therefore the extent of caspase 3/7 activity matched with the viability reductions shown in Figure 3.1A.

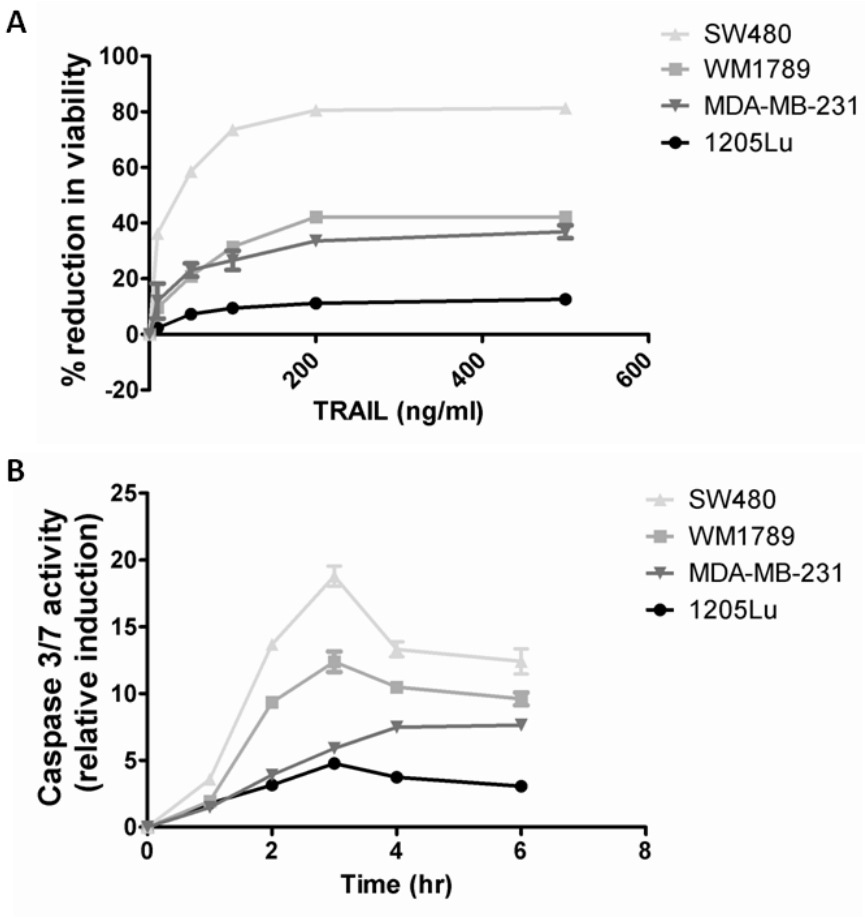

Figure 3.1 TRAIL sensitivity in human cancer cell lines. **A** SW480, MDA-MB-231, WM1789, and 1205Lu cell lines were treated for 24 hr with the indicated concentrations of TRAIL and viability measured using an AlamarBlue® viability assay. The four cell lines show varying TRAIL sensitivity, with 1205Lu showing the highest resistance and SW480 the highest sensitivity. **B** The four cell lines were treated with TRAIL (100 ng/ml) for the indicated durations, and caspase 3/7 activity measured using a Caspase 3/7 Glo® assay. Data expressed is caspase 3/7 activity after TRAIL treatment relative to an untreated control for each cell line. The extent of caspase activity matched the viability reductions, confirming that TRAIL was inducing apoptosis. Data for SW480 and melanoma cell lines were collected by Dr Satoshi Hino (whilst at ROB, Oxford). Graphs show mean +/- SEM for **(A)** n=5,**(B)** n=3.

3.2.2 The importance of TRAIL in the mouse lung *in vivo*

Previous unpublished work carried out by Dr Satoshi Hino in our laboratory examined the role of endogenous TRAIL in the clearance of circulating tumour cells from mouse lung. SCID mice were injected into the tail vein with either WM1789 or 1205Lu melanoma cells. Lungs were extracted, and quantitative

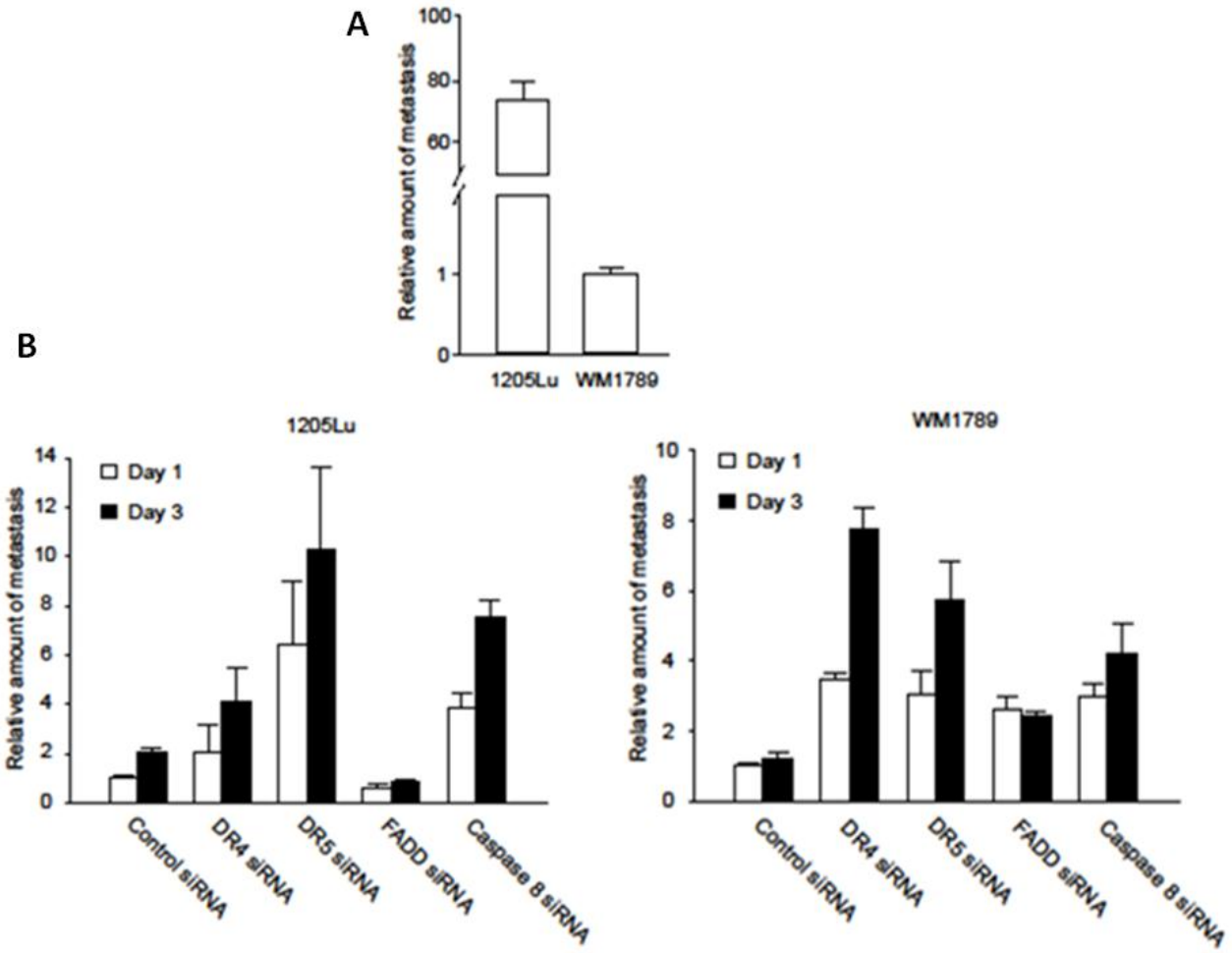

Figure 3.2 TRAIL signals contribute to metastatic tumour cell clearance in the mouse lung. Unpublished work performed by Dr S. Hino. Tumour cells were injected into the tail vein of SCID mice and lungs were removed at indicated time points after injection. Relative amounts of metastasis was calculated using an Alu RT-PCR method. **A** Relative amount of cells in the lung at day 1 after i.v. injection of 1205Lu relative to WM1789 cells confirms that 1205Lu are more metastatic **B** siRNA knockdown of components of the extrinsic apoptosis pathway increased the number of cells in the lung at day 1 and 3 relative to cells treated with control siRNA at day 1. All data is mean +/- SEM.

RT-PCR was used to detect the relative amounts of the human Alu sequence in the mouse lung, a method previously described by (Schneider et al., 2002). The results confirmed previous reports that 1205Lu are more metastatic than WM1789 cells, as 1205Lu cells showed almost 80 times higher Alu expression in the lung than their non-metastatic counterparts (Figure 3.2A). Components of the TRAIL-mediated extrinsic apoptosis pathway, including DR4, DR5, FADD and caspase-8 were transiently knocked down using siRNA. The knockdown was confirmed at the protein level and resulted in *in vitro* TRAIL resistance (data not

shown). Following siRNA-mediated depletion of these proteins, cells were injected into the tail vein of SCID mice, and the number of cells in the lung was quantified at days 1 and 3 after injection. As shown in Figure 3.2B, by making both cell lines more resistant to endogenous TRAIL signals, the number of cells retained in the lung was increased. For 1205Lu cells, inhibiting TRAIL signalling through DR5 led to a 10 fold increase in the number of cells in the lung at day 3. In WM1789 cells, DR4 silencing led to 8 fold higher lung retention than controls 3 days after injection. Therefore endogenous TRAIL signals also appear to play an important role in cancer cell clearance *in vivo*.

3.2.3 TRAIL sensitivity on low attachment plates

Following a previous study reporting that detached MCF7 breast cancer cells show both greater TRAIL expression and higher TRAIL sensitivity (Goldberg et al., 2001), it was hypothesised that cell adhesion may play an important role in TRAIL sensitivity. To investigate this hypothesis *in vitro*, both melanoma cell lines and MDA-MB-231 cells were cultured on normal or low attachment plates. Low attachment plates have a hydrophilic surface which prevents full attachment. After seeding onto low attachment plates, cells adhere weakly and fail to spread compared to those on normal plates.

Before TRAIL sensitivity was investigated, levels of anoikis were measured in cells on low attachment plates compared to normal plates. As anoikis-sensitive cell lines undergo apoptosis following detachment (Frisch and Francis, 1994), this could potentially influence their TRAIL response by pushing them further towards a threshold necessary to undergo apoptosis. To determine the levels of anoikis in these cells under normal and low attached conditions, cells were seeded in the appropriate conditions for 12 hr before caspase 3/7 activity was measured and samples blotted for PARP cleavage. PARP is an enzyme whose cleavage to shorter fragments is indicative of apoptosis (Kaufmann et al., 1993). As shown in Figure 3.3A, there was no difference in cleaved caspase 3/7 levels for any of the three cell lines, and no apparent PARP cleavage after culture in low attachment conditions (Figure 3.3B).

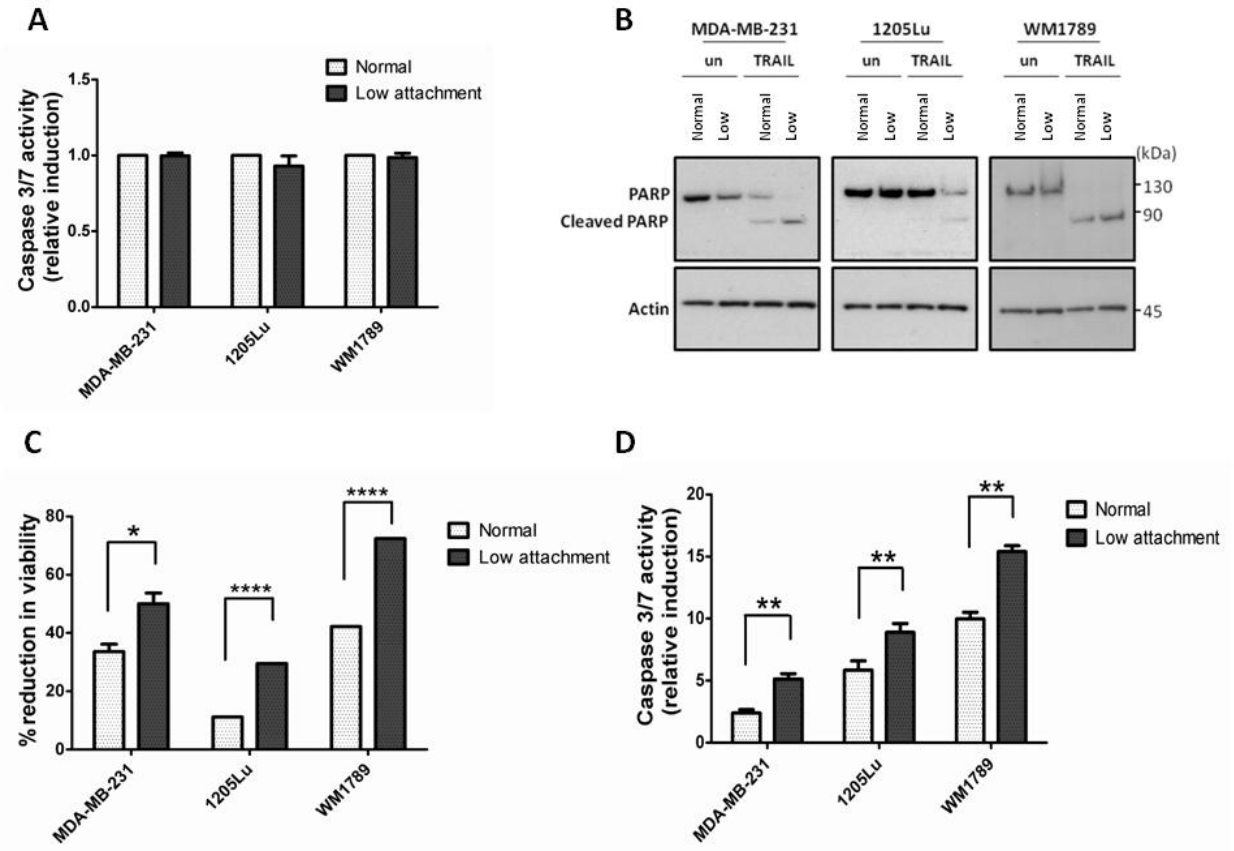

Figure 3.3 Low attachment leads to TRAIL sensitisation *in vitro*. **A** Anoikis, as assessed by caspase 3/7 activity, was not detected in MDA-MB-231, 1205Lu or WM1789 cells 12 hr after seeding. **B** PARP cleavage was not detected in cells 12 hr after seeding into either condition, but increased after a 4 hr treatment with 200 ng/ml TRAIL, particularly in cells in low attachment conditions (low)**. C** Cells in low attachment conditions showed reduced viability 24 hr after TRAIL treatment compared to attached cells. Values are relative to untreated cells for each condition. **D** Cells in low attachment conditions also showed increased caspase 3/7 activity 3 hr after TRAIL treatment. **(D)**. Data for 1205Lu and WM1789 cells in **C** was collected by Dr S Hino. All data mean +/- SEM; n=3; **(C)** unpaired t-test; **(D)** paired t-test; * p<0.05, **p<0.01, **** p<0.0001.

However, following TRAIL treatment, cells cultured on low attachment plates showed much more robust PARP cleavage than those that attached and spread normally (Figure 3.3B). This increased TRAIL sensitivity was further confirmed by a greater reduction in viability of low attachment cells following TRAIL treatment (Figure 3.3C). MDA-MB-231, 1205Lu and WM1789 were 17%, 18%, and 30% less viable, respectively, after TRAIL treatment when cultured on low attachment plates compared to control cells cultured on normal plates. These cells also showed 5.4, 2.7, and 3.6 fold higher caspase 3/7 activity after TRAIL treatment, compared to TRAIL-treated cells which spread normally (Figure 3.3D).

3.2.4 Increased death receptor expression in detached cells.

The Proteome Profiler™ Human Apoptosis Array from R&D Systems allows the detection of 35 apoptosis related proteins, and can be semi-quantified using methods outlined in Supplementary Chapter S1. Lysates were made from MDA-MB-231 cells cultured for 12 hr either on normal or low attachment plates and incubated with the apoptosis array.

Compared to MDA-MB-231 cells cultured on normal plates, those cultured on low attachment plates showed the largest increases in protein expression for the TRAIL receptor DR5 (40% increase), and the TNF-α receptor TNFR1 (Figure 3.4). TNFR1 was the only significant change detected; increasing by 75% in cells in low attachment conditions compared to those under normal culture conditions. A non-significant 30% increase was detected in cleaved caspase-3 protein levels in MDA-MB-231 cells cultured in low attachment conditions compared to control cells. There were also non-significant reductions in the protein levels of c-IAP2 (29% reduction), survivin (29% reduction) and claspin (42% reduction). The mitochondrial serine protease HTRA2/Omi and the cell cycle regulator p27 showed non-significant 20% increases in protein expression.

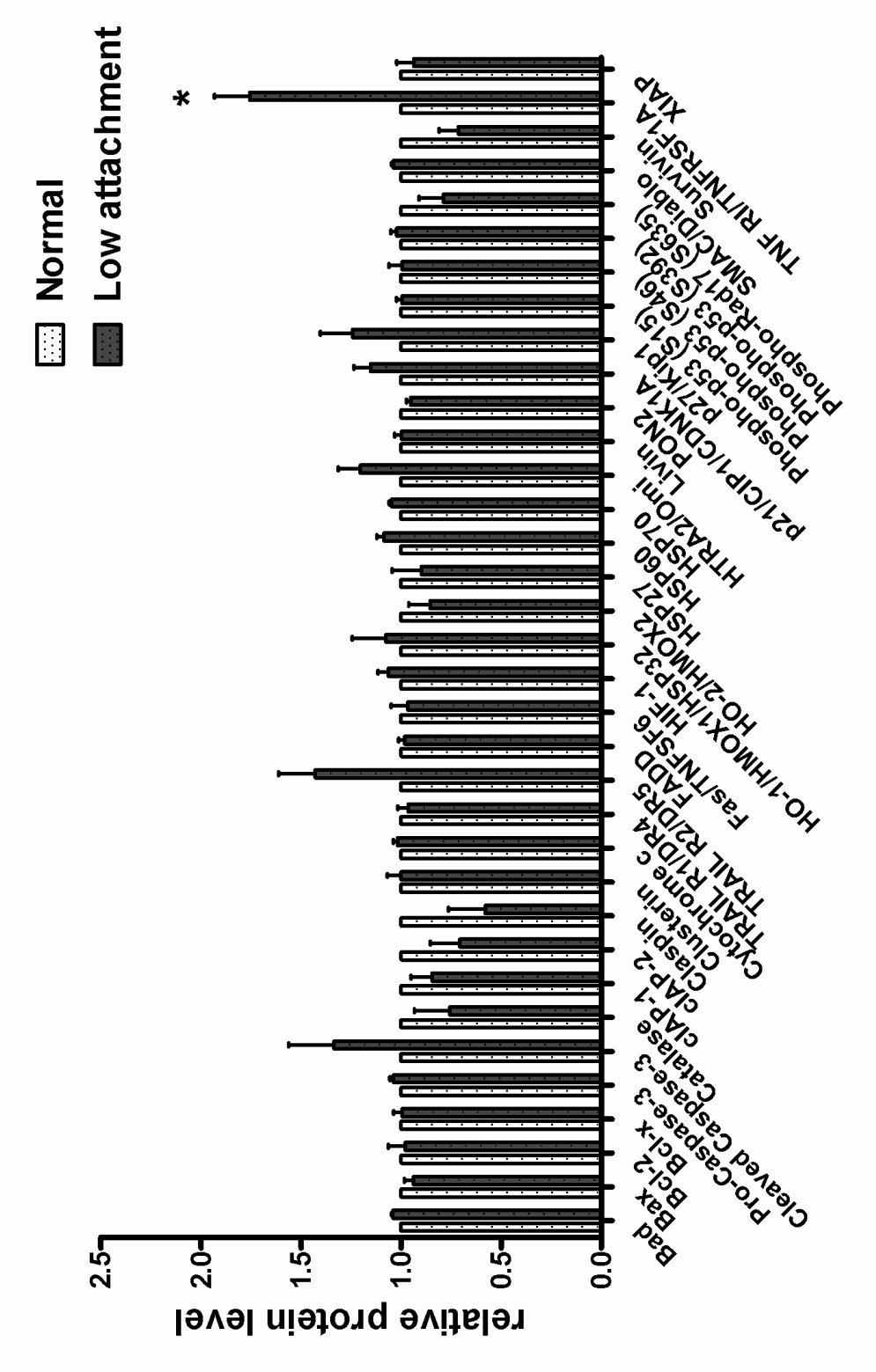

Figure 3.4 Apoptosis protein array data for MDA-MB-231 cells cultured on normal or low attachment plates. MDA-MB-231 cells were cultured on normal or low attachment plates for 12 hr before lysis, and 350 µg of whole cell lysate was incubated with the array membranes. Data expressed is relative change in protein levels from cells in low attachment conditions compared to normally attached cells. Array signals were semi-quantified and normalised as outlined in Supplementary Chapter S1. Mean +/- SEM, n=3 paired t-test

*p<0.05.

3.3 Summary of findings

• MDA-MB-231 human breast cancer, 1205Lu and WM1789 human melanoma, and SW480 human colorectal cancer cell lines show different levels of TRAIL sensitivity; with SW480 the most sensitive and 1205Lu the most resistant.

•Blockade of apoptotic TRAIL signalling in human melanoma cell lines 1205Lu and WM1789 increases the incidence of metastatic lung colonies in mice, highlighting the importance of endogenous TRAIL signals in the lung.

•Culturing anoikis-resistant breast and melanoma cell lines on low attachment plates renders them more sensitive to TRAIL-induced apoptosis *in vitro* than those cultured on normal plastic.

•MDA-MB-231 cells under low attachment conditions show increases in the protein expression of death receptors DR5 and TNFR1.

3.4 Discussion

Due to its proven cancer selectivity and its importance in controlling tumour development and progression, the TRAIL pathway has arisen as a promising target for cancer therapy (Ashkenazi et al., 1999). A broad spectrum of cancer cells exhibit TRAIL sensitivity, however the extent of this sensitivity varies greatly between cell lines. This resistance poses a problem for the use of TRAIL therapies in treating cancer. Combining TRAIL therapies with drugs which can sensitise cells to its toxic effect are likely to yield the greatest effects in patients (Wu, 2009). The work presented in this chapter proves the hypothesis that culturing MDA-MB-231, 1205Lu and WM1789 cells on low attachment plates can sensitise them to TRAIL-induced apoptosis *in vitro*. This work is important in exposing the cell adhesion/spreading pathway as a potential target for the development of TRAIL sensitising agents.

To meet the first aim of this chapter, TRAIL sensitivity was determined for four human cancer cell lines. Due to their high sensitivity, SW480 colon cancer cells were not used in the remainder of this work. Human cell lines were used preferentially over mouse cell lines, as mouse cells have a slightly different TRAIL signalling pathway with only one TRAIL receptor and no caspase-10 (Wu et al., 1999). It was important to include the relatively TRAIL resistant 1205Lu melanoma cells in future investigations, as any method developed to sensitise tumour cells to TRAIL must show efficacy in TRAIL resistant cells. Using cell lines derived from both breast cancer and melanoma meant that future work performed with these cell lines could separate cell-type specific effects from general responses affecting multiple cancer cell types.

The work performed by Dr Satoshi Hino (Figure 3.2), is important for setting the context for the work in this thesis. His work identified an important role for death receptor mediated apoptosis in the clearance of the two melanoma cell lines from the mouse lung, as disruption of DISC signalling increased lung colonisation. Although Fas and TNF-α also induce apoptosis through the extrinsic pathway via FADD and caspase-8, knockdown of TRAIL receptors DR4 and DR5 led to similar increases in metastasis. Melanoma cells rendered resistant to TRAIL showed up to a 10 fold increase in lung retention three days after tail vein injection. This data show that endogenous TRAIL does play an important role in the clearance of tumour cells from the lung. This finding is contrary to a number of previous studies which have suggested that FasL and perforin are more important than TRAIL signals in clearing cancer cells from the lung (Owen-Schaub et al., 1998, Smyth et al., 1999, Hall et al., 2004), however many of these studies have only focused on the role of NK cell-derived death signals. The nature of this experiment does not allow the identification of the TRAIL source, but TRAIL expression has also been detected in human lung tissue including lung vascular endothelial cells (Spierings et al., 2004), and can be induced on a number of other immune cells including CD4+ lymphocytes and monocytes (Griffith et al., 1999, Dorothée et al., 2002) . This work also does not identify TRAIL as the sole mechanism for tumour cell clearance; therefore it is likely that important roles still exist for Fas Ligand and perforin. Nevertheless, this work suggests that the

development of an *in vivo* TRAIL sensitising agent will not only sensitise cells to TRAIL administered therapeutically, but also to endogenous TRAIL signals in the lung.

The second aim of this chapter was to investigate whether MDA-MB-231, 1205Lu and WM1789 human cancer cell lines could be sensitised to TRAIL-induced apoptosis *in vitro* using low attachment plates to prevent full adhesion and spreading. These experiments were performed to further validate results seen in MCF7 human breast cancer cells (Goldberg et al., 2001) when cultured in low attachment conditions. In support of the hypothesis, all three cell lines cultured on low attachment plates exhibited enhanced TRAIL sensitivity compared to those cultured on normal plastic. The three cell lines showed no evidence of anoikis under low attachment conditions, confirming previous reports of anoikis resistance in MDA-MB-231 cells (Attwell et al., 2000). This suggests that TRAIL sensitisation was due to specific sensitivity to TRAIL, and not a consequence of cells being in a spontaneously apoptotic state. These findings were further supported by Grosse-Wilde et al., who showed that sarcoma cells derived from a mouse squamous cell carcinoma model could be sensitised to exogenous TRAIL treatment when cultured on polyHEMA to prevent attachment, despite also showing little susceptibility to anoikis (Grosse-Wilde et al., 2008). This suggests that matrix attachment may be a general mechanism mediating TRAIL resistance in tumour cells.

To further investigate potential mediators of the TRAIL sensitisation response in MDA-MB-231 cells, global protein changes in the apoptosis pathway were investigated using a Proteome Profiler^{TM} Human Apoptosis Array (Figure 3.4). This showed increases in death receptors DR5 and TNFR1, along with subtle decreases in several intrinsic apoptosis pathway components. These initial findings suggest that death receptor levels could be altered in response to cell detachment, and implicate a possible role for the intrinsic pathway in mediating the death receptor signalling pathway in these cells. These findings have also been supported by subsequent work showing increases in DR4 and DR5 expression following matrix detachment of colon and oesophageal cancer cell lines (Laguinge et al., 2008, Liu et al., 2009). This

provides evidence that detachment-induced alterations at the receptor level could account for the increased TRAIL sensitivity seen in these experiments. Although increases in Fas were not seen in this array, MDA-MB-231 cells are shown in Chapter 2 to be FasL resistant and therefore may have a more unresponsive Fas signalling pathway. Due to the significant increase in TNFR1 expression in low attachment cells, it is likely that these cells would also show increased sensitivity to TNF-α induced apoptosis. Although this is therapeutically less interesting, it presents an avenue for future research.

Reduced levels of the IAPs, cIAP-2 and survivin, detected in the protein array may enable an enhanced caspase cleavage response to apoptotic stimuli, due to their ability to inhibit caspase cleavage (Deveraux et al., 1998). Previous research has reported increases in cIAP and XIAP in non-malignant epithelial cells following detachment, as a mechanism of anoikis avoidance (Liu et al., 2006b). Although the apoptosis array also showed variable increases in the level of cleaved caspase-3 in low attachment cells, indicative of anoikis, this could not be confirmed by either caspase 3/7 activity or PARP cleavage assays. HTRA2/Omi levels were also increased by 20% in cells in low attachment conditions. As HTRA2/Omi can bind to and neutralise inhibitors of apoptosis (IAPs), it was initially hypothesised that the function of this protein was pro-apoptotic (Hegde et al., 2002). However, it has been suggested that the true role of HTRA2/Omi may be mitochondrial preservation and that its IAP binding motif may act to allow IAPs to ubiquitinate it for degradation. This may act as a protective mechanism against mitochondrial proteins that have leaked out into the cytoplasm (Vaux and Silke, 2003). In addition, Vaux and Silke argue that substantial mitochondrial damage may result in the release of multiple mitochondrial proteins with IAP binding motifs, and this could act to drive apoptosis as a further protective mechanism against large-scale mitochondrial damage. Therefore it is unclear how small alterations in HTRA2/Omi protein levels may affect apoptotic responses.

One limitation of these arrays is that they focus only on whole cell protein expression. A common feature of regulation within the apoptosis signalling pathway is relocation or post-translational modification of

proteins rather than expression levels. For example, TRAIL receptor signalling can be modulated not only by protein expression level but by membrane localisation to lipid rafts, mutation, membrane recycling, and post-translational modification (Muppidi et al., 2004, Wagner et al., 2007, Chen et al., 2009). Equally mitochondrial pro-apoptotic proteins such as HTRA2/Omi are located in the inner mitochondrial space, only influencing apoptosis after mitochondrial membrane permeation. Therefore, although increased HTRA2/Omi protein levels could lead to a more robust and rapid apoptotic response following mitochondrial permeation, it is the translocation to the cytoplasm which is the most important indicator of the functional state of the protein. Many of the changes seen in this array may only indicate a potential effect, and one cannot assume that a functional effect will result. However, these arrays do give an indication of pathway-wide alterations, allowing more rapid identification of potential targets than performing individual Western blots. Future work will need to follow up these targets in order provide a direct link between their expression levels and the TRAIL sensitivity observed. Following on from this initial use of the apoptosis arrays, work was performed in collaboration with Dr D. Allen to investigate other methods of acquiring data from these array membranes, outlined in Supplementary Chapter 1.

The data presented in this chapter supports the initial hypothesis that culturing cancer cells on low attachment plates can sensitise them to TRAIL-induced apoptosis *in vitro*, confirming the earlier report in detached human mammary carcinoma MCF-7 cells (Goldberg et al., 2001). The work performed by Satoshi Hino highlighted an important role for endogenous TRAIL in the clearance of human melanoma cells from the mouse lung. Therefore development of a TRAIL-sensitising agent could work in combination not only with therapeutic TRAIL strategies, but with endogenous TRAIL signals to enhance the clearance of metastatic tumour cells. This initial work forms the basis of the hypothesis in this thesis; that cell adhesion pathways could be targeted in order to enhance responses to TRAIL *in vitro* and *in vivo*. The following chapters present the process by which this hypothesis was strengthened and tested in a number of models. In Chapter 4, the transcriptional control of the cytoskeleton is targeted, using MDA-MB-231

lacking MRTF-A and B, transcriptional controllers of many cytoskeletal genes. More specific members of the integrin signalling pathway are targeted in Chapter 5, and these targets are used in Chapter 6 to develop *in vivo* assays to allow sensitisation effects to be measured in an experimental mouse model of metastasis.

Chapter 4:
Disruption of transcriptional control of the cytoskeleton: TRAIL sensitisation through MRTF-A/B depletion

4.0 Hypothesis

Depletion of MRTF-A and B in MDA-MB-231 breast cancer cells causes adhesion and spreading defects *in vitro* and leads to an enhanced apoptotic response to TRAIL and other TNF family ligands.

4.1 Introduction

4.1.1 Myocardin-related transcription factors and Serum response factor

Myocardin-related transcription factors (MRTFs) are transcriptional co-activators for the transcription factor Serum response factor (SRF) (Miralles et al., 2003, Guettler et al., 2008). SRF is a widely conserved and expressed transcription factor that binds to targets containing a CArG box sequence $CC(A/T)_6GG$. SRF regulates the transcription of many immediate early genes, cytoskeletal genes and certain muscle-specific gene sets and plays an essential role in cellular homeostasis (Johansen and Prywes, 1995, Miano, 2010). Due to its role in controlling cytoskeletal gene expression (Sun et al., 2006), MRTF/SRF signalling has been implicated in cell spreading, adhesion, invasion and metastasis (Morita et al., 2007, Medjkane et al., 2009, Brandt et al., 2009).

SRF is a pleiotropic transcription factor and there are currently around 50 identified SRF cofactors which can interact with SRF to control the transcription of restricted gene sets. Two pathways have been identified which lead to SRF activation, as outlined in Figure 4.1 (Gineitis and Treisman, 2001).

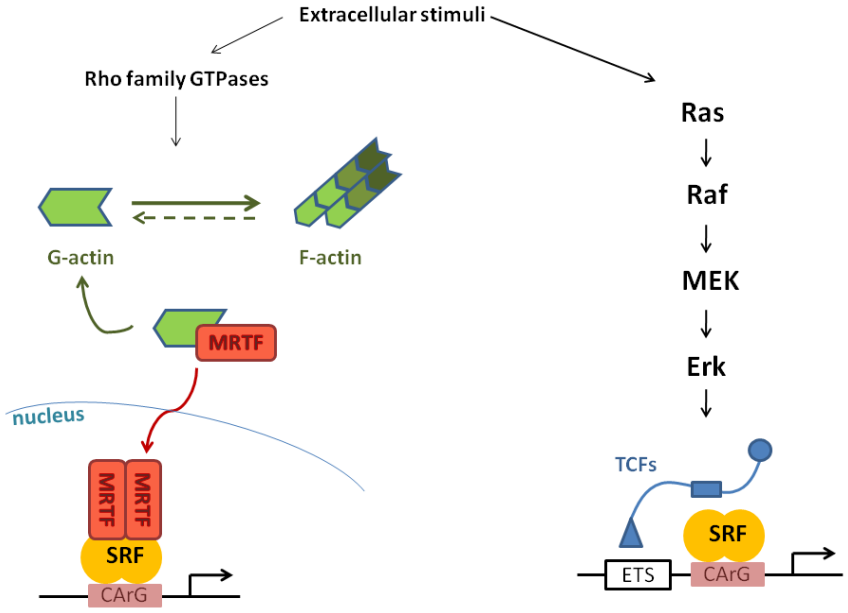

Figure 4.1 Signalling pathways activating Serum response factor (SRF). SRF activity is mediated by two signalling pathways: Rho activation through MRTFs such as MRTF-A and B, and MAPK activation through Ternary complex factors (TCFs). Adapted from (Posern and Treisman, 2006).

The first identified pathway involves members of the Ternary complex factor (TCF) subfamily (ELK1, SAP1 and SAP2), transcription factors that can complex with SRF at the Serum response element (SRE) (Shaw et al., 1989). They contain an ETS domain which binds to an ETS site upstream of the SRE. Phosphorylation of TCFs by mitogen signalling through MAPK can lead to the formation of a complex with SRF, allowing serum responsive transcription of immediate early genes including *C-FOS* (Marais et al., 1993).

The second pathway is activated by extracellular signalling through Rho GTPases, and mediated by MRTFs (Miralles et al., 2003, Guettler et al., 2008), including MRTF-A, MRTF-B and myocardin. Myocardin can strongly activate SRF to control cardiac and smooth muscle-specific gene transcription (Wang et al., 2001),

but its expression is mainly restricted to these tissues. In contrast, MRTF-A and B have broader expression profiles (Wang et al., 2002). MRTF-A is also known as MAL, MKL-1 and BSAC.

4.1.2 MRTFs and the cytoskeleton

SRF activation through MRTFs can lead to the transcriptional activation of a large number of cytoskeletal genes including talin, vinculin, profilin and integrin β1 (Miano et al., 2007). There have been over 150 SRF-dependent target genes identified, of which around 45% have roles in contractility and/or the cell cytoskeleton (Sun et al., 2006). MRTF-A and -B contain three RPEL domains in the N-terminal end which are responsible for actin binding, two N-terminal basic sites for binding to SRF and nuclear localisation, and a transcriptional activation domain at the C-terminus (Miralles et al., 2003). Although most of the work characterising the regulation of MRTF-A and -B has focused on MRTF-A, they are thought to be regulated in the same manner and act cooperatively to control the transcription of cytoskeletal and focal adhesion genes (Medjkane et al., 2009).

Drugs such as latrunculin B, which sequester monomeric G actin, can reduce transcription of SRF target genes, whereas the actin-disrupting mycotoxin cytochalasin D can activate transcription of SRF target genes. The discovery that SRF activity could be controlled by actin dynamics led to the discovery that SRF signalling works in a positive feedback loop, controlling cytoskeletal transcription whilst being regulated itself by actin dynamics (Sotiropoulos et al., 1999).

4.1.3 MRTF/SRF activation

MRTF-A/B activation requires Rho pathway signalling, and the interaction between MRTF and Rho-actin signals normally controls whether it is located in the cytoplasm or the nucleus (Figure 4.2). MRTF-A/B are present in complexes with G-actin in the cytoplasm and undergo constant nuclear shuttling (Figure 4.2).

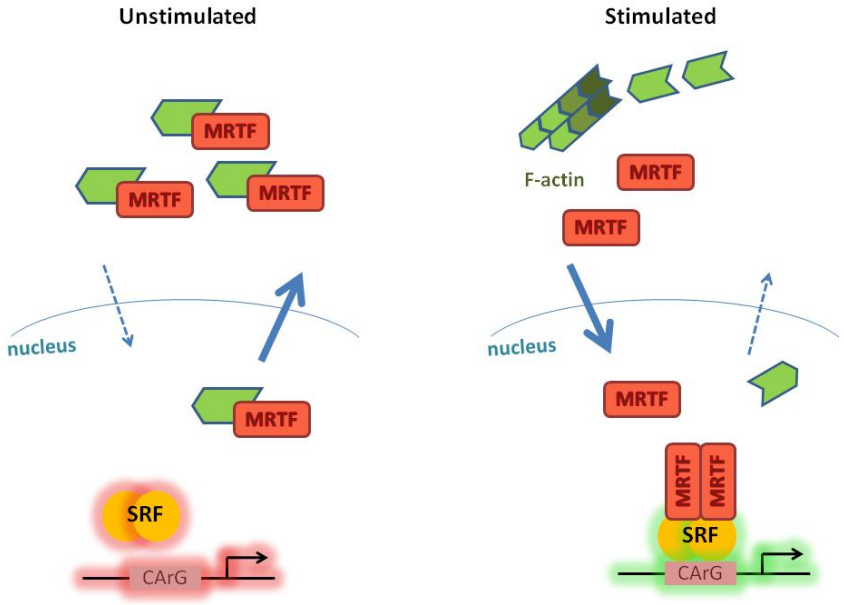

Figure 4.2 Actin-mediated regulation of MRTF/SRF activity. In unstimulated cells **(left)** monomeric G-actin (green arrow) is bound to MRTF-A/B in the cytoplasm and the nucleus, with rapid export of nuclear MRTF-A/B leading to high cytoplasmic levels. This prevents MRTF-dependent SRF target gene transcription. When stimulated **(right),** for example by serum, G-actin monomers polymerise to form F-actin, releasing MRTF. A change in the balance of import/export signalling drives MRTF nuclear import, with reductions in nuclear export. Together, these factors drive the nuclear accumulation of free MRTF-A/B which can bind SRF and drive SRF target gene transcription. Adapted from (Vartiainen et al., 2007).

In the resting state, SRF activation is prevented by a combination of MRTF-A/B interaction with G-actin in both the cytoplasm and the nucleus, and an enhanced propensity for MRTF-A/B nuclear export (Vartiainen et al., 2007). Activation of Rho signalling leads to the polymerisation of G-actin monomers to form F-actin filaments. As shown in Figure 4.2, this reduction in the G-actin pool releases MRTF-A/B, which can enter the nucleus to activate their targets. The nuclear export rate is reduced in stimulated cells, helping to drive the nuclear accumulation of MRTF. In the nucleus, MRTF-A/B bind as dimers to SRF and drive the transcription of SRF-dependent target genes. Although some cells, including MDA-MB-231 cells, show constitutive nuclear localisation of MRTF-A/B, their ability to drive SRF target gene transcription is still regulated by Rho stimulation, suggesting that binding to nuclear actin plays an important role in MRTF/SRF pathway regulation (Vartiainen et al., 2007).

4.1.4 MRTFs and cancer

As MRTF target genes are implicated in diverse biological pathways including cell-type specific development, motility and actin dynamics, dysregulation can facilitate cancer development and progression (Scharenberg et al., 2010). The human MRTF-A gene was initially discovered through its involvement in a translocation event commonly reported in infant acute megakaryocytic leukaemia (Ma et al., 2001, Mercher et al., 2001).

MRTF/SRF signalling has also been implicated in invasion and metastasis. Through their ability to drive the transcription of cytoskeletal genes, MRTF-A/B have been shown to regulate focal adhesion and stress fibre formation. As a result, MRTF-A/B depleted MDA-MB-231 cells demonstrate reduced adhesion and motility, and are less metastatic than control cells (Morita et al., 2007, Medjkane et al., 2009). Recent work has found that SCAI (suppressor of cancer cell invasion) can bind to SRF in the nucleus to form an inhibitory ternary complex. Loss of SCAI, as observed in a panel of tumour samples, allows robust MRTF/SRF dependent transcription of β1 integrin, greatly increasing the invasive potential of cells (Brandt et al., 2009).

Interestingly, mouse mrtf-A was discovered in an early mouse screen looking to identify genes which can confer resistance to TNF-α induced apoptosis (Sasazuki et al., 2002). This is one of the only a few reports directly linking MRTF signalling to apoptosis.

4.2 Aims

Following on from Chapter 3, which showed that impairing cell adhesion using low attachment plates could induce TRAIL sensitivity in three cancer cell lines, the aim of this chapter is to investigate TRAIL sensitivity in cancer cells which constitutively exhibit cytoskeletal defects. MRTF-A/B depletion in MDA-MB-231 cells is a good model in which to investigate this, as loss of SRF-dependent cytoskeletal gene transcription results in reduced stress fibres, focal adhesions, and morphological defects (Medjkane et al., 2009). As mrtf-A was first discovered due to its ability to protect cells from TNF-α induced apoptosis in mice (Sasazuki et al., 2002), I was interested to see whether MRTF-A and -B could confer the same protection in human cell lines, and whether this protection was also relevant to the TNF superfamily ligand TRAIL.

In summary, the main aims of this chapter are:

• To confirm MRTF-A and B depletion in MDA-MB-231 cells and resultant cell spreading defects.

• To investigate the effects of MRTF-A and B reduction on sensitivity to apoptosis induced by TNF-α, FasL and TRAIL.

•To investigate potential mechanisms behind any sensitisation seen by using an apoptosis protein array and following up previously published microarray data in MRTF-A and B depleted MDA-MB-231 cells (Medjkane et al., 2009).

4.3 Methods

4.3.1 Cell lines

MDA-MB-231 human breast cancer cells were supplied as a kind gift from Prof. R Treisman (LRI, London). Two clones were used, named C4-GFP and C20-CFP, and have been previously described (Medjkane et al., 2009). Briefly, C4-GFP cells were MDA-MB-231 control cells which contain a GFP expression plasmid along with a Tet repressor construct. C20-CFP cells were MDA-MB-231 cells containing a CFP expression plasmid, along with a Tet repressor construct and tetracycline inducible shRNA for MRTF-A and MRTF-B.

4.4 Results

4.4.1 MRTF-A and B depletion in MDA-MB-231 cells

To test the shRNA system, C20-CFP cells were either untreated or treated with 1 µg/ml of tetracycline for 72 hr for full depletion (referred to as C20-CFP TET). Figure 4.3A shows that even without tetracycline treatment, C20-CFP cells show partial reduction of MRTF-A levels, which is fully abrogated, along with a 75% reduction in MRTF-B, 72 hr after tetracycline treatment. MRTF-A/B depletion in MDA-MB-231 cells has been previously shown to cause cell rounding, reduced stress fibres and reduced focal adhesions (Medjkane et al., 2009). To confirm this, cells were seeded onto chamber slides for 12 hr prior to staining with phalloidin for actin, along with Hoechst nuclear stain (Figure 4.3B). In support of the previous findings, MRTF-A/B depleted cells showed a more arborised phenotype, lacking stress fibres and exhibiting spreading defects. Although not measured directly in this work, as outlined by Medjkane et al., MRTF-A/B depleted cells could also be observed to be less adherent than their control counterparts.

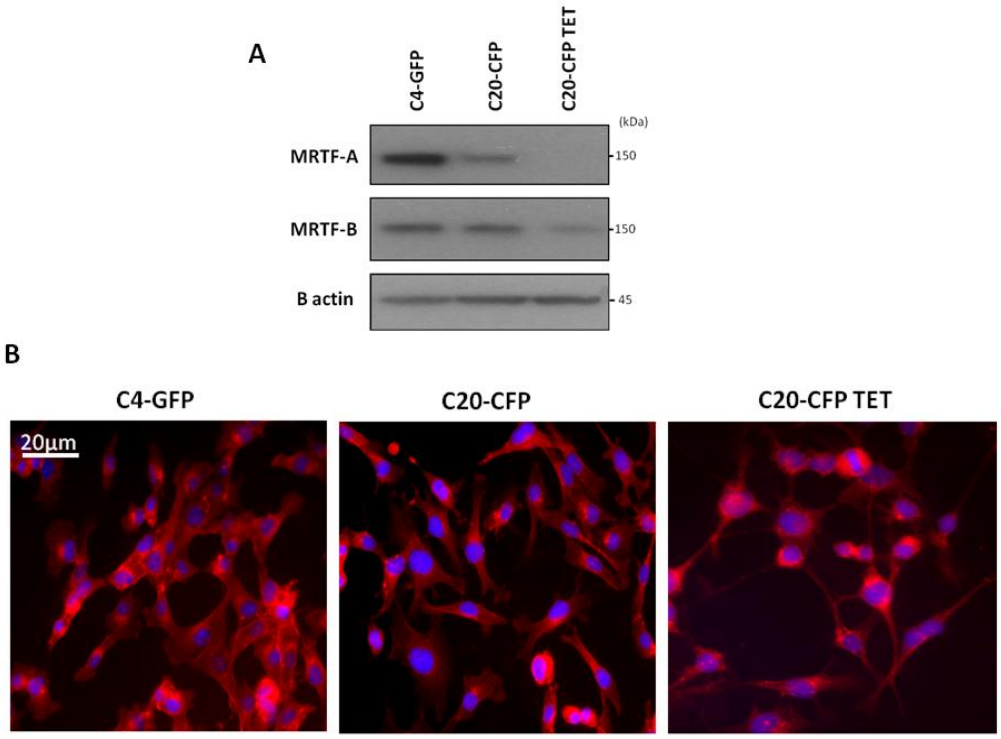

Figure 4.3 Verification of MRTF-A and B levels and spreading defects in MDA-MB-231 clones. A Western blot with MRTF-A and B specific antibodies shows efficient depletion of MRTF-A and B after 72 hr tetracycline treatment (1 µg/ml) in C20-CFP TET cells. **B** Staining showing control cells (C4-GFP), MRTF-A and B depleted cells (C20-CFP TET), along with those expressing an intermediate level of MRTF-A and B (C20-CFP). F-actin was stained with phalloidin (red) and the nucleus with Hoechst (blue). C20-CFP TET cells show marked morphological defects.

4.4.2 Sensitivity of MRTF-A and B depleted clones to Tumour necrosis factor family ligands.

Cells were seeded and allowed to attach for 12 hr prior to treatment with recombinant TNF-α, agonistic anti-Fas antibody, or recombinant TRAIL. In control C4-GFP cells, TNF-α treatment led to a 2% increase in viability compared to untreated controls (Figure 4.4A). In contrast, C20-CFP expressing partial reduction in MRTF-A/B showed a 5.5% reduction in viability after 24 hr of TNF-α treatment. This increased to 10.6% reduction on full depletion of MRTF-A/B in C20-CFP TET cells. Similarly, caspase 3/7 activity was 3.5 fold higher in C20-CFP cells than C4-GFP control cells, rising to 7 fold higher in fully depleted C20-CFP TET cells (Figure 4.4B).

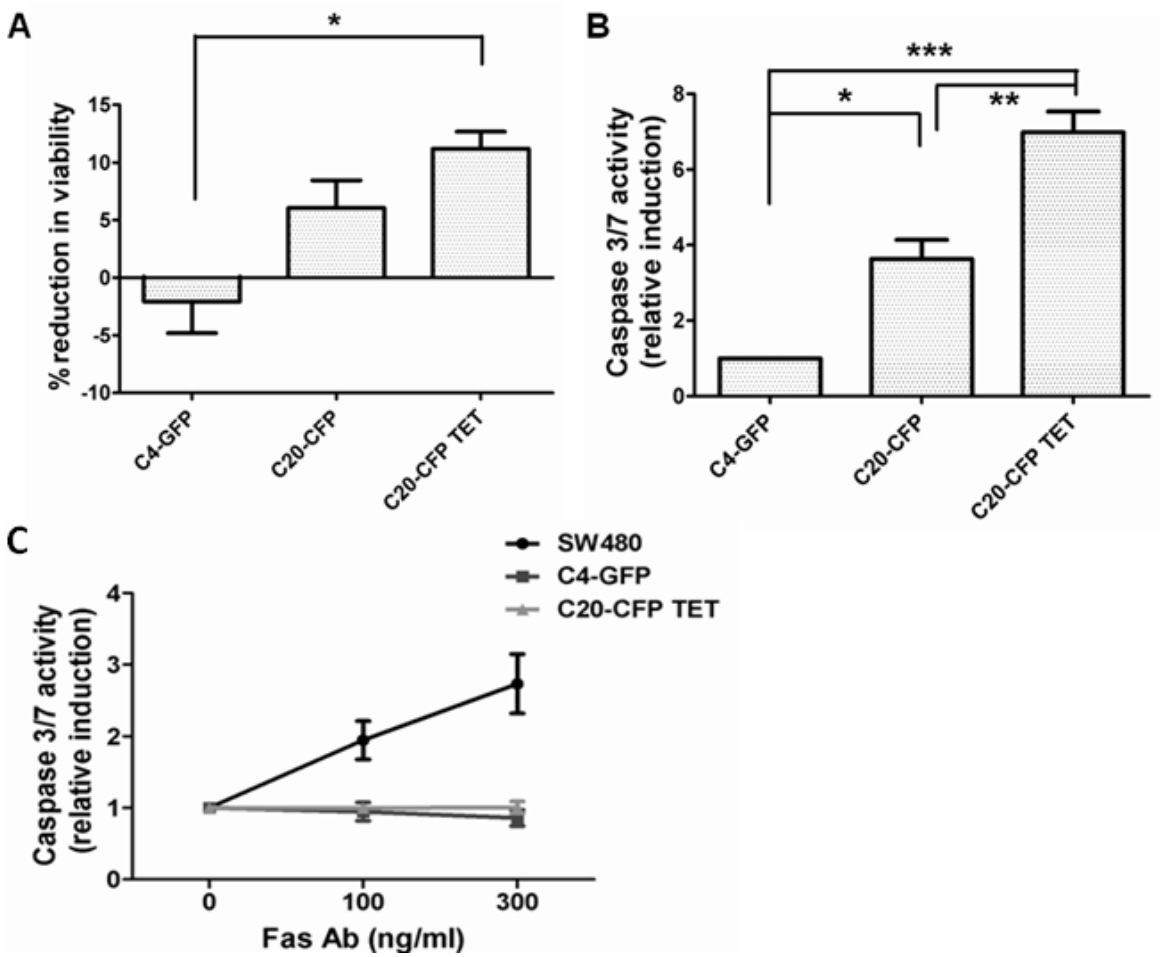

Figure 4.4 MRTF-A/B depleted MDA-MB-231 cells (C20-CFP TET) show increased sensitivity to TNF-α induced apoptosis but MDA-MB-231 cells are resistant to an anti-Fas antibody. A Viability was measured in cells either untreated or treated for 24 hr with 300 ng/ml TNF-α. MRTF-A/B depleted cells show a greater reduction in viability after TNF-α treatment. **B** Cells were treated with 300 ng/ml TNF-α for 3 hr and caspase 3/7 activity measured using a Caspase 3/7 Glo® assay. Caspase 3/7 activity is higher in MRTF-A/B depleted cells after TNF-α treatment, confirming apoptosis. **C** Dose-response experiment for cells incubated for 3 hr with indicated concentrations of anti-Fas antibody (Ab) (CH-11), showing caspase 3/7 activity relative to untreated controls. The colon carcinoma cell line SW480 was used as a positive control, confirming FasL resistance in MDA-MB-231 cells. Graphs show mean +/- (SEM) n=3. ANOVA (Tukey post-test) * $p<0.05$, ** $p<0.01$, *** $p<0.001$

MDA-MB-231 cells have previously been shown to be resistant to the apoptotic effects of agonistic Fas antibodies (Yu et al., 1999, Toillon et al., 2002). To confirm this, the MDA-MB-231 cells were treated for 3 hr with anti-Fas antibody, and caspase 3/7 activity determined (Figure 4.4C). Due to their high sensitivity to FasL-induced apoptosis, SW480 were used as a positive control and showed a 3 fold increase in caspase

3/7 cleavage following treatment with 300 ng/ml of anti-Fas antibody. As expected, treatment of both C4-GFP and C20-CFP TET cells with an anti-Fas antibody did not stimulate caspase 3/7 activity.

C4-GFP, C20-CFP and C20-CFP TET cells were then treated with 100 ng/ml recombinant human TRAIL. The viability of MRTF-A/B depleted cells was 25% lower than control cells 24 hr after TRAIL treatment (Figure 4.5A). Pre-treatment of cells with 10 μM pan-caspase inhibitor Z-VAD-FMK completely abrogated the TRAIL response in all cell lines, confirming that TRAIL was acting through caspase activation (Figure 4.5B). To further confirm that the TRAIL sensitivity was a result of increased apoptosis, caspase 3/7 activity was measured in the three cell lines after TRAIL treatment. Figure 4.5C shows that C20-CFP cells showed a 1.8 fold higher caspase 3/7 response after TRAIL treatment than control C4-GFP cells, with over 2 fold higher activity in fully depleted C20-CFP TET cells. As a control, C4-GFP control cells were treated with tetracycline, however this did not induce any greater caspase 3/7 activity than C4-GFP alone. MRTF-A/B depleted cells also showed a significant increase in TUNEL positive cells 6 hr after treatment with TRAIL compared with C4-GFP control cells and C20-CFP cells. Representative images of TUNEL staining are shown in Figure 4.5E.

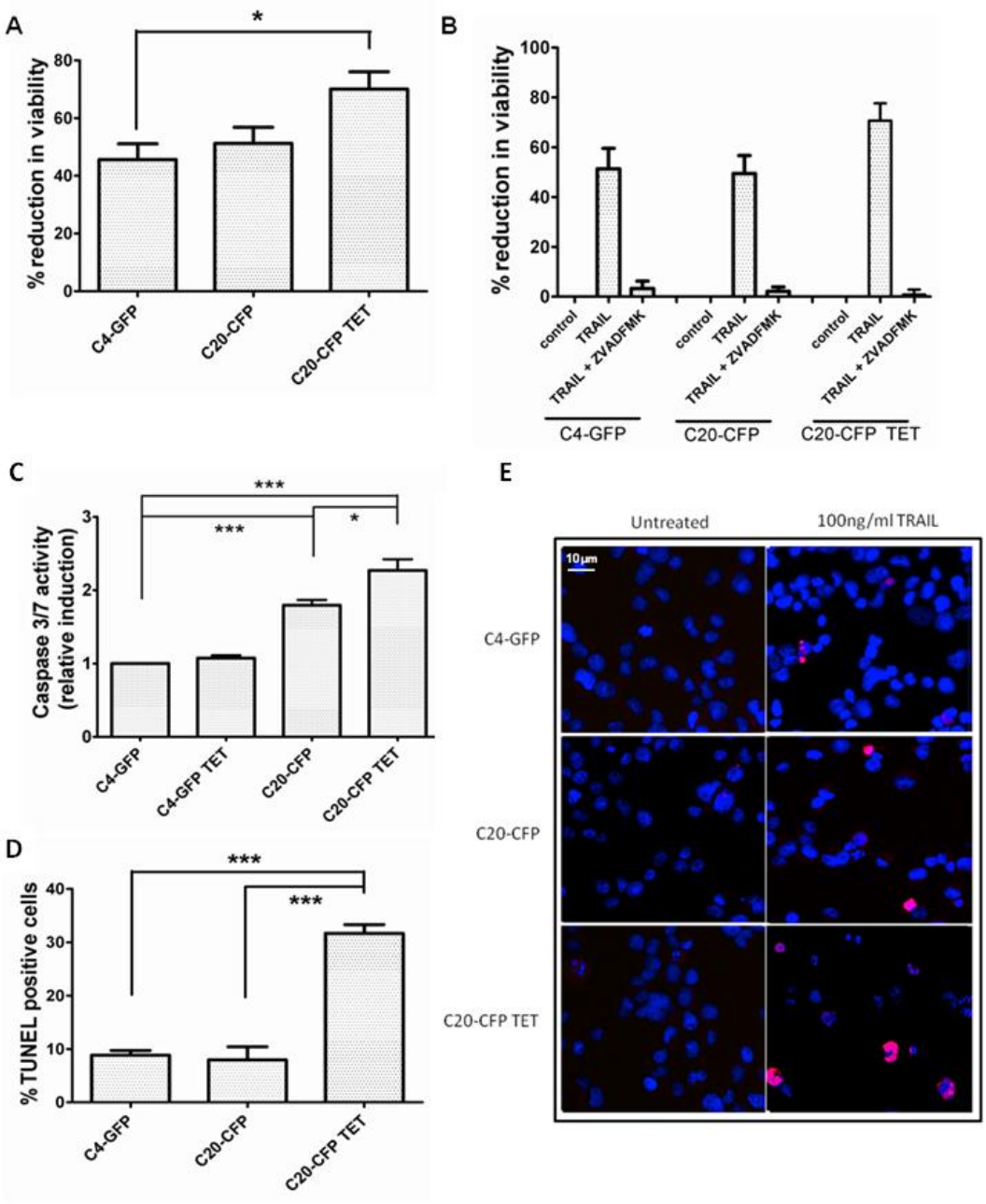

Figure 4.5 MRTF-A/B depletion in MDA-MB-231 results in sensitivity to TRAIL-induced apoptosis. A Cells treated with 100ng/ml TRAIL for 24 hr showed a significant reduction in viability as measured using the alamarBlue® assay. **B** This effect could be completely blocked after a 1 hr pre-incubation of cells with a pan-caspase inhibitor Z-VAD-FMK (10μM) prior to TRAIL addition. **C** MRTF-A/B depleted cells treated for 3 hr with 100 ng/ml TRAIL showed higher caspase 3/7 activity relative to C4-GFP controls and C20-CFP cells. **D** Cells were treated with 100 ng/ml of TRAIL 6 hr prior to TUNEL staining, with representative images shown in **E**. Graphs show mean +/- SEM **(A)** n=8; **(B)** n=3; **(C)** n=4 ; **(D)** n=3; ANOVA (Tukey Post-test) * $p<0.05$ *** $p<0.001$

4.4.3 Analysis of apoptosis-related protein changes

To investigate potential reasons behind the TRAIL sensitivity seen in MRTF-A/B depleted cells, whole cell lysates from each cell line were incubated with the Human Apoptosis Proteome Profiler™ Array described in Chapter 3 and Supplementary Chapter S1. As shown in Figure 4.6, there was a significant 23% increase in protein expression of phosphorylated Rad17 in MRTF-A/B depleted cells compared to controls, along with variable and non-significant increases in HIF-1 and p27/KIP. In direct relation to the extrinsic pathway of apoptosis, both C20-CFP and fully depleted C20-CFP TET cells showed significant increases in protein expression of DR4 (up to 37% higher), DR5 (up to 45% higher), and TNFR1 (75% higher) compared to control cells. There were also subtle increases in the protein levels of Fas. Interestingly, C20-CFP TET cells also showed 30% higher levels of the mitochondrial serine protease HTRA2/Omi, previously detected as increased in cells cultured on low attachment plates (Chapter 3). Similarly, cleaved caspase 3 levels were also increased in MRTF-A/B depleted cells up to 2.7 fold higher than controls, however this value showed high variability between repeats. The spontaneous increases in active caspase 3 levels indicated that MRTF-A/B depleted cells may be undergoing anoikis following MRTF-A/B depletion.

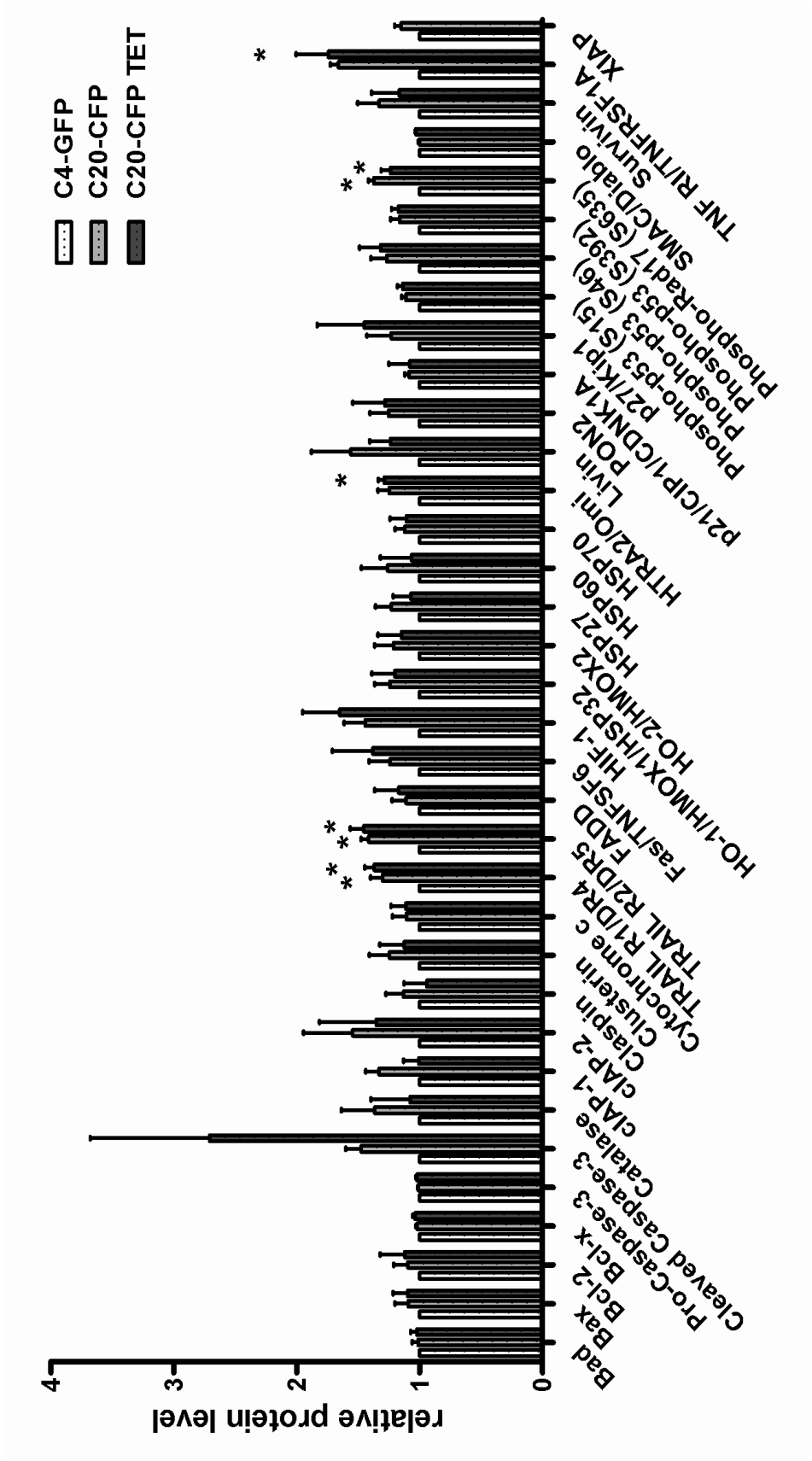

Figure 4.6 Apoptosis protein array data for MDA-MB-231 cells expressing normal (C4-GFP), intermediate (C20-CFP), and low (C20-CFP TET) levels of MRTF-A/B. Cells were cultured for 12 hr before lysis and 350 µg of whole cell lysate was incubated with the array membrane. Data expressed is relative change in protein levels compared to control C4-GFP cells. Array signals were semi-quantified and normalised as outlined in Supplementary Chapter S1. Mean +/- SEM, n=3 ANOVA (Tukey post-test) * $p<0.05$

To investigate this further, cells were taken from culture and TUNEL stained (Figure 4.7A). TUNEL staining showed only a 3% increase in the levels of DNA fragmentation in MRTF-A/B depleted cells, with a 1.9% increase in C20-CFP cells expressing intermediate levels of MRTF-A/B. Neither of these increases were significant. To verify this result, cells were blotted for PARP cleavage. Figure 4.7B shows that, although there were slight reductions in the expression of full-length PARP in MRTF-A/B depleted cells, the 90 kDa cleaved PARP form could not be detected. Anoikis is therefore unlikely to be playing a major role in influencing the TRAIL response.

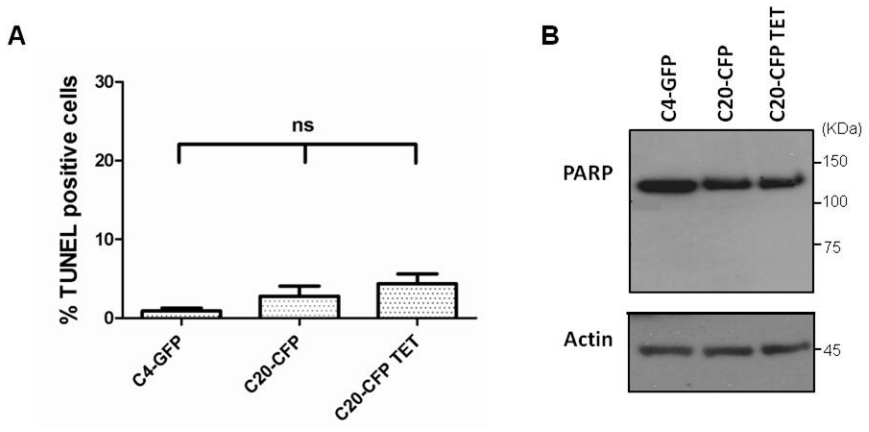

Figure 4.7 MRTF-A/B depletion alone results in low levels of apoptosis. A TUNEL staining in untreated cells shows slight increases in TUNEL positive cells with MRTF-A/B depletion, however this was not significant. **B** Western blotting for full length and cleaved PARP in MRTF-A/B depleted cells using whole cell lysates showed slight reductions in full length PARP; however accompanying increases in PARP fragments at 90kDa were undetectable.

To further investigate the HTRA2/Omi protein levels, Western blots were performed with a different antibody and new samples. As the apoptosis array lacked antibodies detecting the c-FLIP isoforms, important inhibitors of the extrinsic apoptosis pathway (Section 1.1.4.2), samples were also tested for this protein. As shown in Figure 4.8A, up to 2 fold increases could be detected in HTRA2/Omi protein level in MRTF-A/B depleted cells compared to controls, however these differences were only seen in three out of

seven repeats. The expression level of the c-FLIP long isoform c-$FLIP_{L,}$ was not associated with the level of TRAIL sensitivity, and c-$FLIP_s$ was undetectable in this cell line. Therefore it is unlikely that alterations in the whole cell levels of these proteins can account for the consistent TRAIL sensitivity effect.

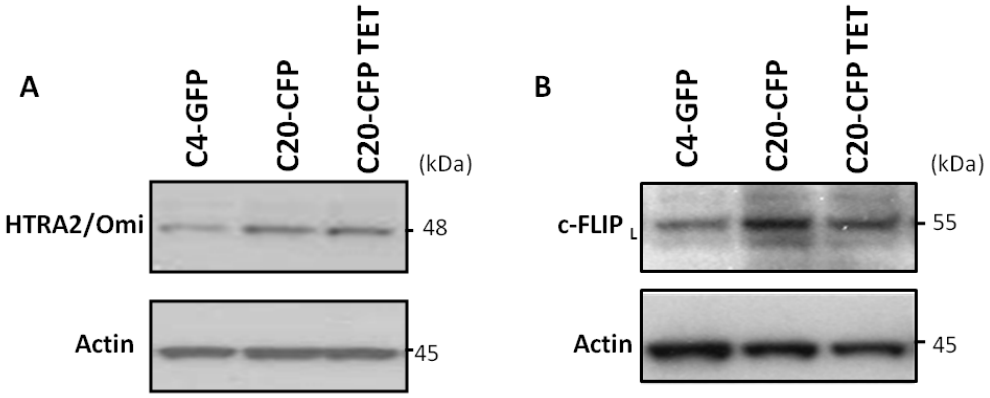

Figure 4.8 HTRA2/Omi and c-$FLIP_L$ protein levels in MRTF-A/B depleted cells. A Whole cell lysates of untreated cells showing increases in HTRA2/Omi protein levels in MRTF-A/B depleted C20-CFP TET cells. **B** c-$FLIP_L$ levels were unchanged in MRTF-A/B depleted cells.

4.4.3.1 Alterations in death receptor signalling in MRTF-A/B depleted cells.

To verify the increases in the expression level of TRAIL receptors DR4 and DR5 observed in the apoptosis protein array, whole cell lysates were blotted with independent antibodies for DR4 and DR5 (Figure 4.9A). This confirmed that C20-CFP cells showed a 2.5 fold increase in DR5 expression level compared to control C4-GFP cells, rising to a 7.5 fold increase on full MRTF-A/B depletion. Similarly, whole cell protein expression of DR4 was 1.74 fold higher in C20-CFP cells, and 2.7 fold higher in C20-CFP TET cells, compared to controls. Quantitative real time PCR was used to measure mRNA levels of DR4 and DR5 from control and MRTF-A/B depleted cells from culture (Figure 4.9B).

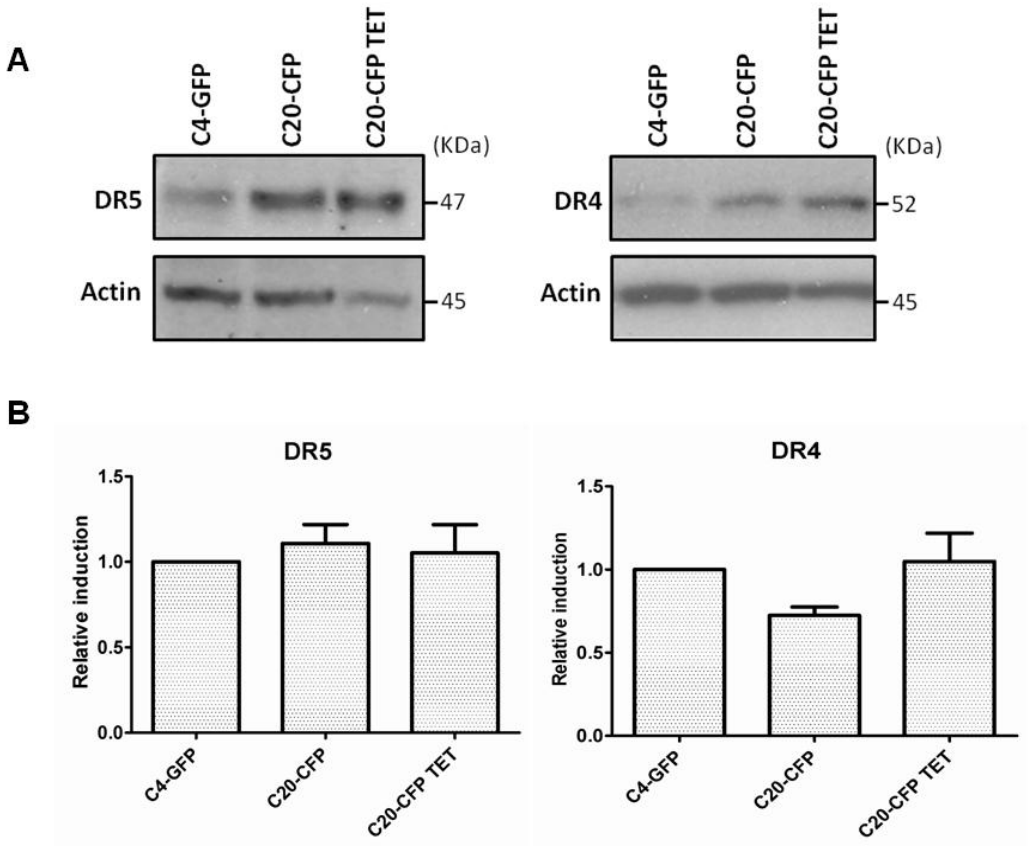

Figure 4.9 Total protein levels of DR4 and DR5 increase in MRTF-A/B depleted cells, however this is not due to increased transcription. Whole cell lysates were blotted for DR5 and DR4 or RNA extracted and subjected to quantitative real time PCR. **A** Representative images of Western blots of whole cell lysates for DR5 (left) and DR4 (right), showing increased levels of both death receptors in MRTF-A/B depleted cells (C20-CFP TET), as highlighted previously in the apoptosis array. **B** There is no difference in DR5 mRNA levels between the three cell lines. The Ct values were normalized to GAPDH and relative expression calculated using the $2^{\Delta\Delta Ct}$ method. Mean +/- SEM n=4

There was no significant difference in DR5 or DR4 mRNA levels in MRTF-A/B depleted cells compared to C4-GFP controls. This suggests that the whole cell protein level increases seen in figure 4.9A were not a result of increased transcription, and may therefore be due to reduced degradation. To investigate the expression of these receptors on the cell surface, cells were stained with DR4 and DR5 antibodies and analysed by flow cytometry (Figure 4.10).

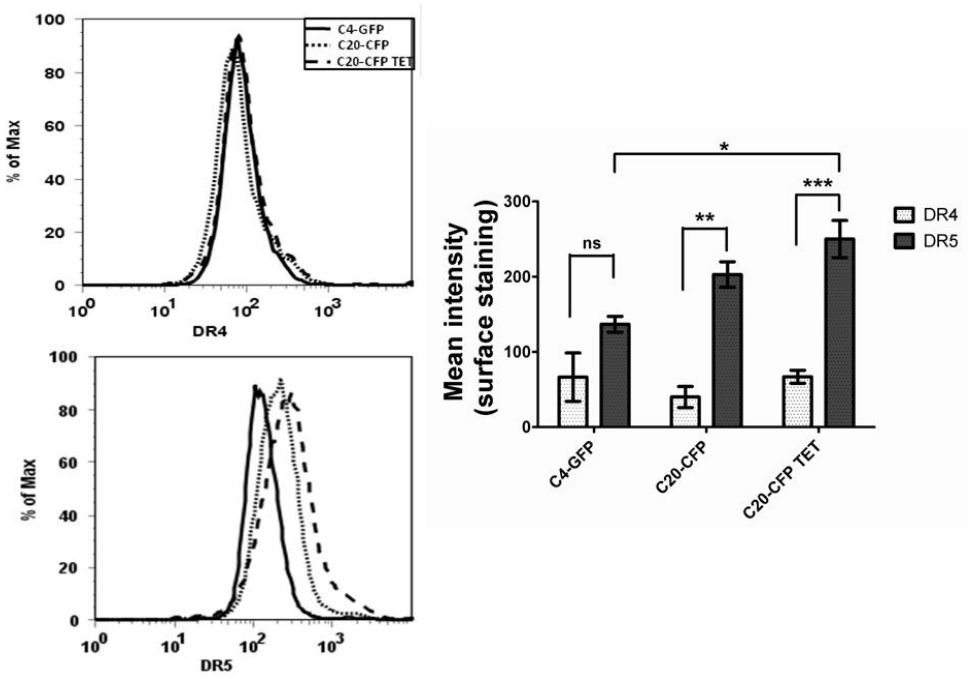

Figure 4.10 Increased DR5 expression on the surface of MRTF-A/B depleted cells. Cells were incubated for 30 min on ice with monoclonal antibodies for DR4 and DR5 before flow cytometry. (*Left*) shows histograms, representative of flow cytometry data showing increased cell surface staining of DR5 (*bottom left*) with DR4 levels unaltered (*top left*). The bar chart (*right*) shows quantitated fluorescent intensity of staining from 3 independent experiments. Mean +/- SEM; n=3; ANOVA (Tukey post-test) *p<0.05 ** p<0.01 *** p<0.001 ns=not significant.

Flow cytometric analysis revealed that C20-CFP cells have 50% more DR5 expression on their surface than control C4-GFP, with an 84% increase in fully MRTF-A/B depleted C20-CFP TET cells. In contrast, DR4 expression levels remained unchanged. This meant that the ratio of DR4:DR5 expression on the cell surface increased from 1:2 in control C4-GFP cells to almost 1:4 in MRTF-A/B depleted cells.

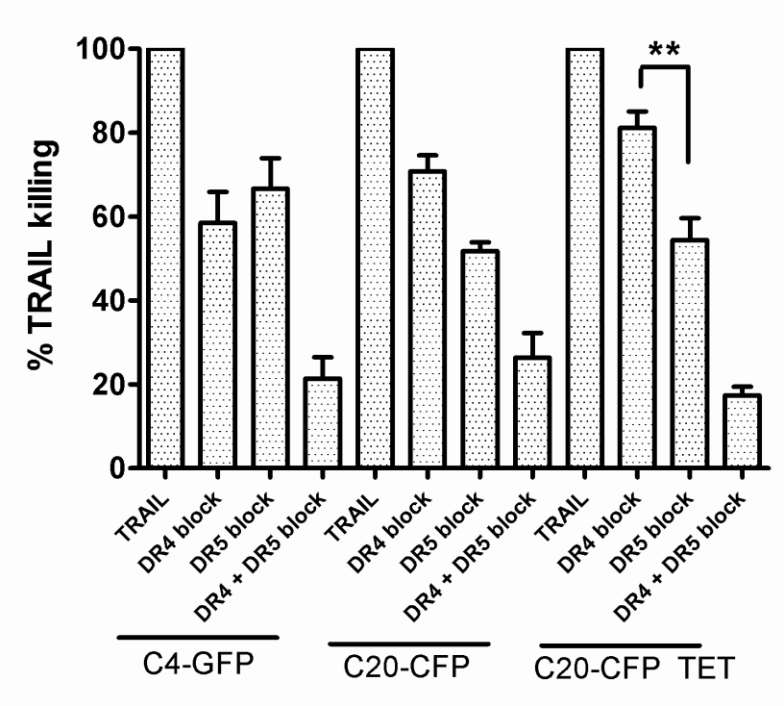

Figure 4.11 MRTF-A/B depleted cells depend more on DR5 for their apoptotic response to TRAIL. Death receptors were blocked by a 30 min incubation with 10 µg/ml of DR4 or DR5 blocking antibodies prior to TRAIL treatment (100 ng/ml) for 24 hr, and viability determined using alamarBlue®. DR4 and DR5 blocking in control (C4-GFP) cells prevents TRAIL-induced viability reductions to the same extent. However, in intermediate and fully MRTF-A/B depleted cells, DR4 was less essential for the TRAIL response. Mean +/- SEM n=5 ANOVA (Tukey post-test) ** $p<0.01$

To investigate whether signalling through DR5 was more important than DR4 in mediating the apoptotic TRAIL signal in MRTF-A/B depleted cells, cells were pre-treated with DR4 and DR5 blocking antibodies 30 min prior to TRAIL treatment (Figure 4.11). Blocking the function of both DR4 and DR5 individually could reduce TRAIL sensitivity by around 40% in control C4-GFP cells, which was increased to a 79% reduction when both receptors were blocked. However, in MRTF-A/B depleted cells, DR5 block could reduce 46% of the TRAIL response, where as DR4 blocking could only reduce it by 19%. The data show a shift in death receptor signalling in MRTF-A/B depleted cells to a predominantly DR5-mediated response, suggesting that alterations in the cell surface expression level of TRAIL receptors could account for some of the increased TRAIL sensitivity seen in MRTF-A/B depleted cells.

4.4.4 MRTF-dependent genes previously identified using microarray

TRAIL sensitivity mechanisms in MRTF-A/B depleted cells were then further investigated using previously published microarray data which identified MRTF-dependent genes (Medjkane et al., 2009).

Gene	Gene name	Control	Control + CD	MRTF-A/B depleted	MRTF-A/B depleted + CD	Fold change dep/control
TNFRSF11B	tumour necrosis factor receptor superfamily, member 11b (osteoprotegerin)	50	60	14	14	**0.28**
DAPK1	death-associated protein kinase 1	228	178	76	79	**0.33**
TNFSF18	tumour necrosis factor (ligand) superfamily, member 18	88	71	35	31	**0.40**
TNFRSF21	tumour necrosis factor receptor superfamily, member 21 (DR6)	683	648	363	378	**0.53**
PDCD6	programmed cell death 6	393	373	212	206	**0.54**
BCL-2	B Cell lymphoma 2	146	140	83	80	**0.57**
TNFRSF12a	tumour necrosis factor receptor superfamily, member 12a (TWEAKR)	587	699	2035	2370	**3.47**
TNFSF10	tumour necrosis factor (ligand) superfamily, member 10 (TRAIL)	51	51	84	96	**1.65**
PDCD4	programmed cell death 4 (neoplastic transformation inhibitor)	105	103	168	163	**1.60**

Table 4.1 Microarray data of MRTF-dependent genes involved in cell death, adapted from (Medjkane et al., 2009). This table includes information from previously published microarray data of MRTF-dependent genes using MDA-MB-231 cells. The top 6 genes (highlighted in blue) are those whose expression decreases with MRTF-A/B depletion, where as the bottom 3 genes (highlighted in red) are those whose levels increase with MRTF-A/B depletion.

This array, outlined by Medjkane et al. compared genes which were affected not only by MRTF-A/B depletion, but MRTF activation following treatment with 5 µM cytochalasin D. Cytochalasin D is a cell

permeable mycotoxin which can interfere with the interaction of G-actin and MRTF (Sotiropoulos et al., 1999). This allows the release of MRTF into the nucleus to activate SRF, and is equivalent to full activation.

Analysis of these microarray data for genes involved in apoptosis signalling highlighted nine genes whose expression was altered following MRTF-A/B depletion. Interestingly, two of the genes with the largest expression difference were osteoprotegerin (*OPG*), the soluble TRAIL decoy receptor, and *TRAIL* itself. *OPG*, also known as *TNFRSF11B*, showed a 72% reduction in gene expression in MRTF-A/B depleted cells compared to control cells. In contrast, *TRAIL* (*TNFSF10*) expression levels were 65% higher in MRTF-A/B depleted cells compared to controls. Other highly altered apoptotic genes included *DAPK1* and *TWEAKR* (*TNFRSF12a*). *BCL-2* levels were also shown to be reduced in MRTF-A/B depleted cells but no protein changes had been detected in the apoptosis array. Western blot for BCL-2 with a different antibody to the array showed up to 60% reduction in BCL-2 protein expression in MRTF-A/B depleted cells compared to control cells, however again such a large difference was only seen in two out of seven repeats (Figure 4.12) and an average of the changes across the repeats showed no significant difference overall.

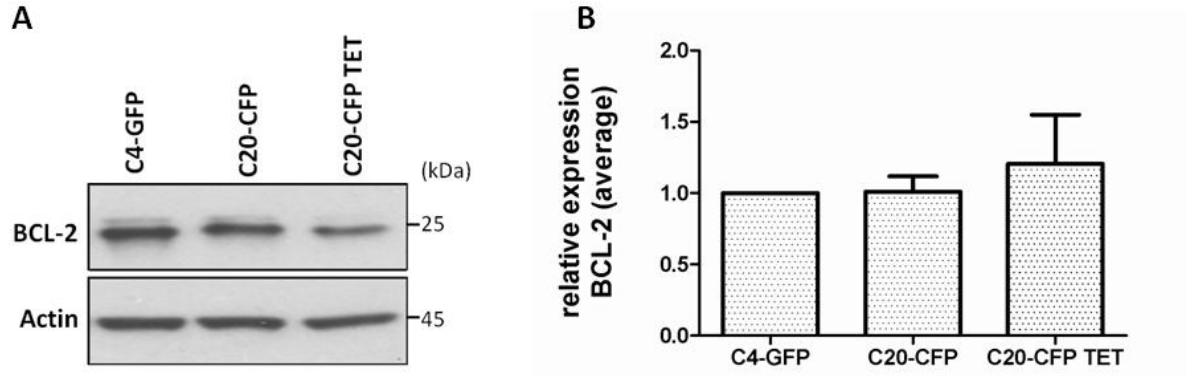

Figure 4.12 Changes in BCL-2 in MRTF-A/B depleted cells. A Example of Western blot of whole cell protein levels of BCL-2 which showed reduction in MRTF-A/B depleted cells. **B** Average BCL-2 expression (normalised to actin expression) from seven individual repeats, showing no overall change in expression level in MRTF-A/B depleted cells.

4.4.4.1 OPG and TRAIL expression

The remaining work focused on the reported changes in *OPG* and *TRAIL* gene expression, as these were deemed the most likely to influence the TRAIL sensitivity response. Osteoprotegerin, as discussed in Section 1.2.6, is a low affinity, soluble decoy receptor for TRAIL (Emery et al., 1998). MDA-MB-231 cells have been shown to secrete OPG (Neville-Webbe et al., 2004), thus it is conceivable that expression differences could influence TRAIL sensitivity in this model. The microarray data reported a 72% decrease in *OPG* expression in MRTF-A/B depleted cells compared with controls. This suggested that reduced OPG secretion in MRTF-A/B depleted cells could allow more TRAIL ligand to reach the cell surface, inducing a greater apoptotic response.

To investigate this further, the microarray results were confirmed using quantitative real time PCR analysis on the three MDA-MB-231 cell lines (Figure 4.13A). In support of the microarray findings (Medjkane et al., 2009), MRTF-A/B depleted cells did have significantly reduced levels of OPG mRNA compared to control cells. These levels correlated with the MRTF expression in the three cell clones, with C20-CFP cells showing a 48% reduction in *OPG* expression compared with C4-GFP control cells, with a 63% reduction in fully depleted C20-CFP TET cells. Conditioned medium was then collected from cells grown for 72 hr, and subjected to ELISA to measure secreted OPG protein concentrations. Control C4-GFP cells secreted 484 pg/ml of OPG into the medium over 72 hr. In contrast, C20-CFP cells only secreted 250 pg/ml and this fell to 163 pg/ml in fully depleted C20-CFP TET cells. Therefore the reduction in OPG transcription means that less protein is being secreted into the medium by MRTF-A/B depleted cells. To investigate whether these differences were physiologically relevant, medium on MRTF-A/B depleted cells was reconstituted with 500 pg/ml of recombinant OPG, representing the concentration secreted by MRTF proficient C4-GFP cells. A positive control of 100 ng/ml recombinant OPG could reduce the TRAIL response by 37% in C20-CFP TET

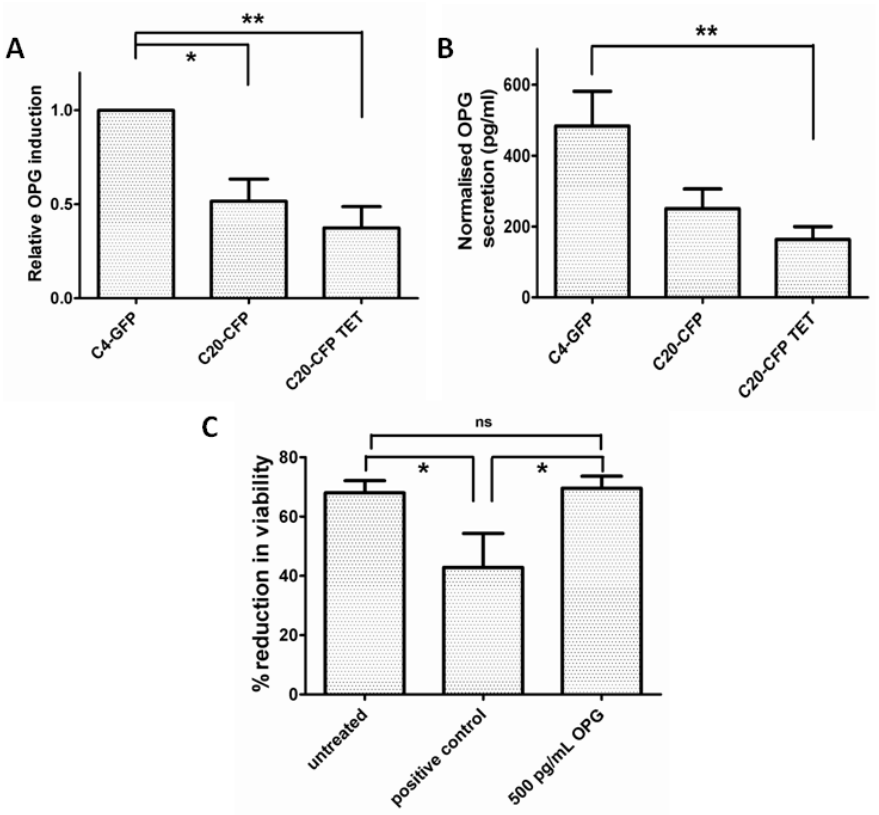

Figure 4.13 OPG mRNA and protein levels are reduced in MRTF-A/B deficient cells, but cannot protect from TRAIL *in vitro*. A Quantitative real time PCR was performed on the three MDA-MB-231 cell lines. The Ct values were normalized to GAPDH and relative expression calculated using the $2^{\Delta\Delta Ct}$ method. This confirmed reductions in OPG mRNA levels in MRTF-A/B depleted cells. **B** Cells were seeded in 6 well plates, conditioned medium collected after 72 hr of growth, and subject to ELISA for OPG. This confirmed reduced OPG protein secretion in MRTF-A/B depleted cells. **C** MRTF-A/B depleted C20-CFP TET cells were treated with 100 ng/ml TRAIL in combination with either 500 pg/ml recombinant OPG or 100 ng/ml as a positive control. Viability was determined after 24 hr using the alamarBlue® assay. OPG did not have a protective effect at the concentration secreted by control cells. Mean +/- SEM **(A)** n=3; **(B)** n=11; **(C)** n=6 ANOVA (Tukey post-test) * $p<0.05$ ** $p<0.01$ ns= not significant

cells, however 500 pg/ml was not a high enough concentration of OPG to confer any TRAIL protection. Therefore OPG secretion differences are unlikely to account for the TRAIL sensitivity seen in this model.

Levels of TRAIL mRNA were reported to be increased by 65% in MRTF-A/B depleted cells (Medjkane et al., 2009). To measure whether TRAIL expression was increased on the cell surface, giving the potential for paracrine TRAIL signalling between cells, cells were labelled with a TRAIL antibody and analysed by flow cytometry. Jurkat cells were used as a positive control (Figure 4.14A and C), because as reported

previously, a 16 hr treatment with phorbol-12-myristate-13-acetate (PMA) can induce a 6 fold increase in surface TRAIL expression (Baetu et al., 2001). However, no difference was detected in surface TRAIL expression between control and MRTF-A/B depleted cell lines (Figure 4.14B and C).

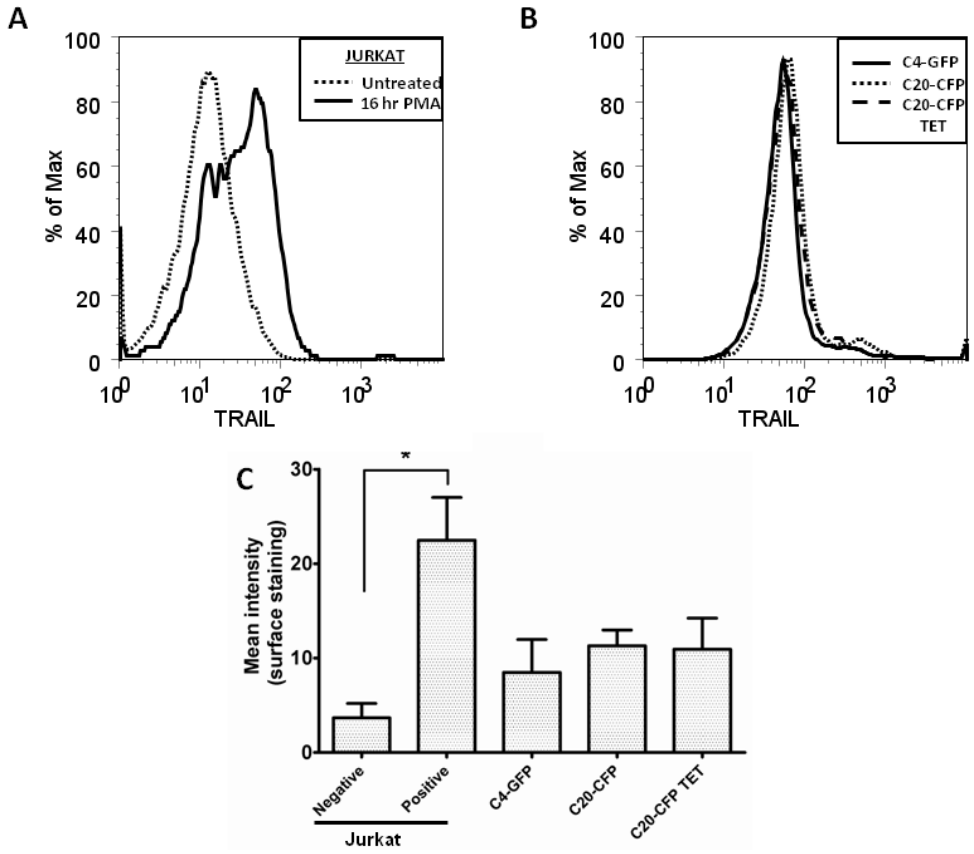

Figure 4.14 Cell surface TRAIL expression is the same in MRTF-A/B depleted cells as controls. Cells were incubated with a primary TRAIL antibody followed by an Alexa fluor 633- conjugated secondary antibody. For a positive control, Jurkat immortalized T-lymphocyte cells (TRAIL negative) were treated for 16 hr with 100 ng/ml phorbol-12-myristate-13-acetate (PMA). **A** Treatment of TRAIL-negative Jurkat cells with PMA resulted in large TRAIL expression increases, illustrated in a representative histogram. **B** None of the three experimental cell lines showed any differences in surface TRAIL expression as shown by a representative histogram. **C** The average geometric mean intensity of surface staining confirms these observations. Mean +/- SEM n=3 ANOVA (Tukey post-test) *p<0.05

4.4.5 Caspase activation

TRAIL acts through the extrinsic pathway of apoptosis, as discussed in section 1.1.4, therefore one would expect increased activation of caspase-8 in the more TRAIL sensitive MRTF-A/B deficient cells. Due to the reported non-specificity of selective caspase inhibitors (Berger et al., 2006), Western blotting was performed to investigate the levels of caspase-8, 9 and 10 activity following TRAIL treatment. As shown in Figure 4.15, all 3 cell lines showed cleavage of procaspase-8, procaspase-10, and procaspase-9 to their intermediate or fully cleaved forms at increasing time points up to 2 hr following treatment with 100 ng/ml of TRAIL. At 2 hr after TRAIL treatment, MRTF-A/B depleted cells showed 1.6 fold higher levels of the 18 kDa cleaved form of caspase-8 compared to control cells. After normalisation, the fold increases in intermediate and cleaved forms of caspase-10 did not associate with the observed increase in apoptosis. In contrast, cleavage of procaspase-9 to its 37 and 35 kDa cleavage products was much more rapid and robust in MRTF-A/B depleted cells compared to control cells. At 1 hr post-TRAIL treatment, MRTF-A/B depleted cells showed 2.65 higher levels of cleaved caspase-9 than C4-GFP cells and 1.22 fold higher than C20-CFP cells.

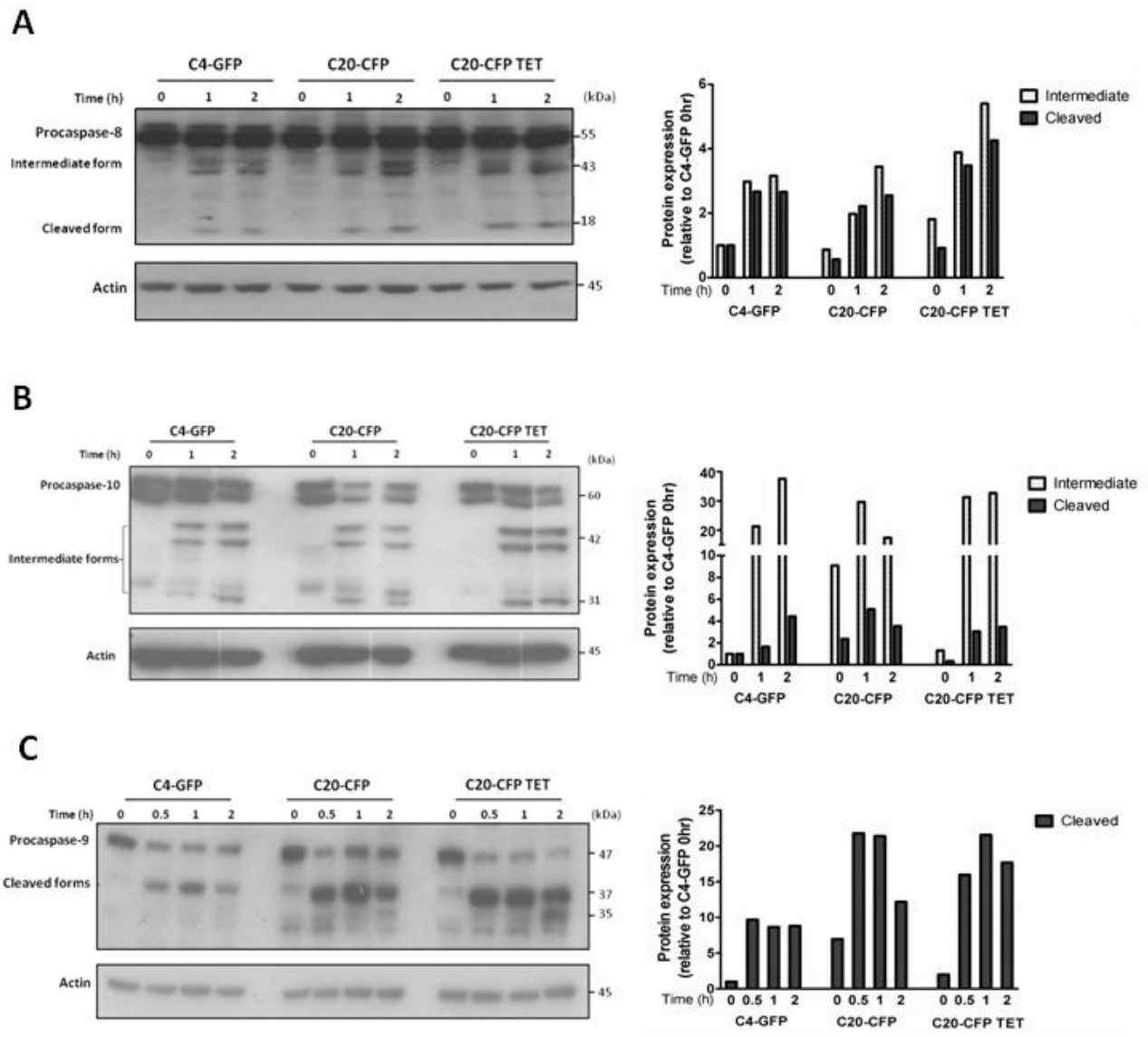

Figure 4.15 Western blots showing robust caspase-9 activation in MRTF-A/B depleted cells. Cells were cultured in 6 well plates for 12 hr prior to TRAIL treatment (100 ng/ml) for the indicated durations. Cells were lysed along with spent media. Blots shown alongside quantitation of protein expression of intermediate and cleaved forms, normalised to actin and relative to C4-GFP 0hr time point. **A** Cleavage of procaspase-8 into cleavage products was slightly higher in C20-CFP TET cells. **B** Cleavage of procaspase-10 to its intermediate cleavage showed little difference following normalisation to actin. **C** Much greater procaspase-9 cleavage occurred in C20-CFP TET cells compared to control C4-GFP cells. Blot in B all ran on same gel but one time point was removed between 1 and 2 hr due to misloading.

As caspase-8 activates caspase-9 through cleavage of the BCL-2 family member BID, levels of BID and its truncated form were investigated by Western blotting (Figure 4.16). MRTF-A/B depleted C20-CFP TET cells showed 2.5 fold higher expression of BID compared to control cells. After a 2 hr treatment with TRAIL,

tBID levels increased in MRTF-A/B depleted cells, remaining undetectable in control cells. Therefore through increased tBID cleavage and caspase-9 activation, MRTF-A/B depleted cells show enhanced amplification of the intrinsic pathway of apoptosis.

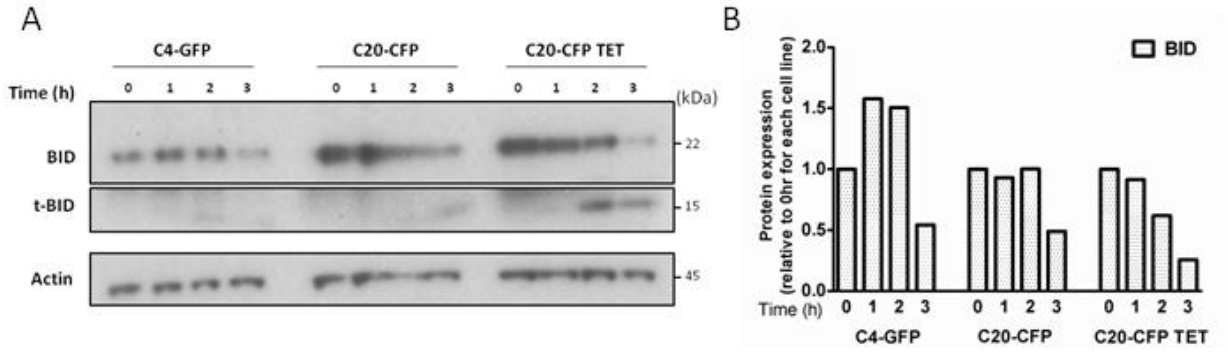

Figure 4.16 Increased cleavage of BID in MRTF-A/B depleted cells. Cells were seeded in 6 well plates for 12 hr before treatment for the indicated durations with 100ng/ml TRAIL. **A** MRTF-deficient C20-CFP TET cells show elevated levels of BID and tBID, which is almost undetectable in control cells. All bands from same gel, but split as a longer exposure was required for tBID detection. **B** Western blot quantified by total BID level, normalised to actin, relative to 0 hr time point for each cell line.

4.4.6 NFκB, AKT and ERK1/2 activity

As discussed in section 1.3.2, signalling through AKT, MAPK and NFκB can provide essential survival signals to cells, preventing them from undergoing apoptosis. There is much evidence that AKT, ERK1/2 and NFκB signalling can control expression of intrinsic apoptosis family members and could therefore influence the balance between extrinsic and intrinsic apoptosis signalling. NFκB signalling can be activated downstream of death receptors and lead to the transcription of anti-apoptotic proteins such as IAPs, with high levels of NFκB associated with TRAIL resistance (Wang et al., 1998). To investigate NFκB activity in the three cell lines, Western blotting was performed for levels of IκBα, a protein which negatively regulates NFκB by sequestering it in the cytoplasm of the cell (Scheidereit, 2006). Therefore low levels of IκBα are commonly used as a marker for NFκB activity. As shown in Figure 4.17A, NFκB activity was higher in MRTF-A/B depleted cells after TRAIL treatment, as shown by a much faster reduction in IκBα. This suggests that the NFκB activity is unrelated to TRAIL sensitivity in these cells. Survival signalling through the MAPK pathway

and PI3K/AKT is also activated downstream of the cell surface and can control the levels of intrinsic apoptosis family members (Shrader et al., 2007, Zhang et al., 2003a).

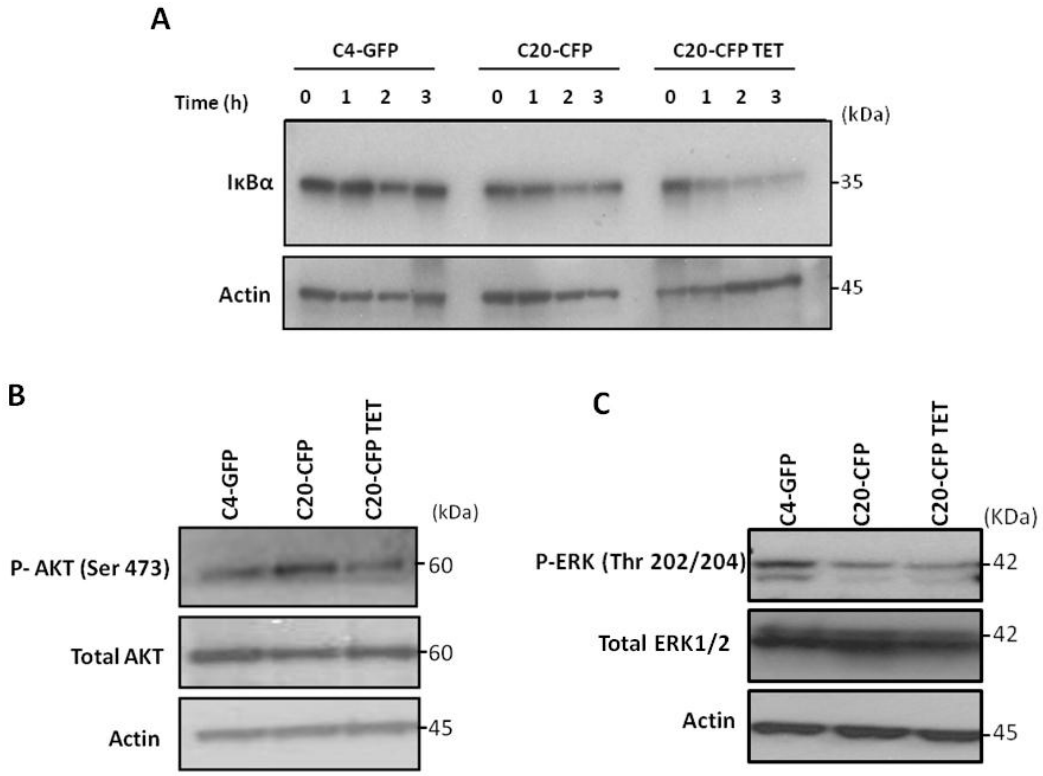

Figure 4.17 NFκB, AKT and ERK1/2 activity in MRTF-A/B depleted cells. A Cells were seeded 12 hr prior to treatment with 100 ng/ml TRAIL for the indicated durations. MRTF-A/B depleted cells show greater reductions in IκBα levels after TRAIL treatment than control cells, indicative of higher NFκB activation. **B** Phosphorylated AKT (Ser 473) levels did not correlate with TRAIL sensitivity in the three cell lines **B** MRTF-A/B depleted C20-CFP TET cells show reductions in active ERK1/2 (ERK Thr202/204) with total ERK1/2 levels staying the same.

Cells were blotted for their expression of activated phosphorylated AKT at Ser473, a commonly used phosphorylation site, along with activated ERK1/2 (Thr202/204), and total AKT and total ERK1/2. Phosphorylated AKT in these MDA-MB-231 cells was barely detectable and did not correlate with TRAIL sensitivity (Figure 4.17B). In contrast, there was ~30% reduction in level of phosphorylated ERK1/2 (Thr 202/204) in MRTF-A/B depleted cells compared to C4-GFP control cells (Figure 4.17C), with no alteration in total ERK1/2 level. Therefore reductions in ERK1/2 survival signalling could contribute to the increased sensitivity to apoptosis after TRAIL treatment in MRTF-A/B depleted cells.

4.5 Summary of findings

• MDA-MB-231 cells carrying tetracycline inducible shRNA for MRTF-A and B show strong reductions in MRTF-A/B expression after treatment with tetracycline, and exhibit marked cytoskeletal defects in accordance with previous studies.

• There is a low level of anoikis in MRTF-A/B cells compared to control cells.

•MRTF-A/B depleted cells show increased sensitivity to apoptosis induced by TNF-α and TRAIL, but MDA-MB-231 cells are resistant to the apoptotic effects of an anti-Fas agonistic antibody.

•Protein levels of both DR4 and DR5 are increased in MRTF-A/B depleted cells, however only DR5 is increased at the cell surface and DR5 shows increased importance over DR4 in TRAIL signal transduction.

•MRTF-A/B depleted cells show reductions in osteoprotegerin mRNA and protein secretion; however, these did not confer TRAIL protection *in vitro*.

•There is more rapid and robust tBID cleavage and caspase-9 activation in MRTF-A/B depleted cells, along with mild reductions in anti-apoptotic protein BCL-2 and increases in pro-apoptotic mitochondrial protein HTRA2/Omi.

•MRTF-A/B cells show reduced signalling through ERK1/2, however AKT and NFκB activity does not correlate with TRAIL sensitivity.

4.6 Discussion

Cells depleted of MRTF-A and B show marked defects in spreading and adhesion, associated with a reduced capacity for invasion and metastasis (Medjkane et al., 2009). The work presented in this chapter confirms the hypothesis that MRTF-A and B depleted MDA-MB-231 cells are also more sensitive to apoptosis induced by members of the TNF family. This provides further evidence that cell

spreading/adhesion is a good target for TRAIL sensitisation, as well as adding a further relatively uncharacterised role for MRTF/SRF signalling in apoptosis resistance.

To meet the first aim of this chapter, efficient knockdown of MRTF-A and B was confirmed. MRTF-B expression was not completely eliminated in this system, suggesting either inefficient shRNA expression or the need for some basal MRTF-B expression to maintain survival. Little work has been done investigating the different roles of MRTF-A and B and whether or not they show complete functional redundancy. There is some evidence of MRTF-B having distinct and independent functions from MRTF-A, with knock-out mice of both variants exhibiting different phenotypes (Li et al., 2006, Wei et al., 2007). However the knockdown achieved was great enough to confer the adhesion and spreading defects characteristic of this model (Medjkane et al., 2009). C20-CFP cells without tetracycline treatment showed partial reduction in MRTF levels. This resulted from 'leak' in the inducible system, whereby C20-CFP cells show some basal transcription of the MRTF-A/B shRNA in the absence of tetracycline. This characteristic was previously highlighted (Medjkane et al., 2009), and may result from low concentrations of tetracycline present in serum (unpublished observations, Dr Y Cao). However, these characteristics meant that 3 clones could be used, with full, medium, and reduced levels of MRTF-A and B (C4-GFP, C20-CFP and C20-CFP TET, respectively). Reduction in MRTF-A and B led to marked cytoskeletal and morphological defects as previously reported (Medjkane et al., 2009). As these cells showed constitutive reductions in MRTF-A and B, investigating potential alterations in the apoptosis pathway was easier than for cells on low attachment plates, as the cell phenotype was less dependent on the adherence conditions and so could be easily manipulated. These cells therefore provided a good model by which to investigate the effect of global cytoskeletal defects on sensitivity to TNF family ligands.

MRTF-A/B depleted cells showed increased sensitivity to apoptosis induced by TNF-α *in vitro,* with the extent of sensitivity correlating with MRTF A/B expression level. Interestingly, mouse mrtf-A was first

identified by its ability protect mouse embryonic fibroblast cells from TNF-α induced apoptosis (Sasazuki et al., 2002). This is the first time since the publication of that important work that a similar effect has been shown in human cells with MRTF-A. In fact, MRTF-A/B depletion was enough to switch the cell's response from pro-survival to pro-apoptotic signalling following TNF-α stimulation. Results of an apoptosis protein array showed that MRTF-A/B depleted cells express significantly increased levels of TNFR1 protein. Although increased receptor protein levels could provide an explanation for this sensitivity, the array only showed whole cell lysate protein increases, giving no indication of protein localisation. Further work is required to confirm increased levels of TNFR1 at the cell surface.

FasL has been reported to be involved in the clearance of tumour cells from the circulation (Owen-Schaub et al., 1998, Screpanti et al., 2001). However MDA-MB-231 cells were found to be resistant to the apoptotic effects of an anti-Fas agonistic antibody, in line with previous reports (Yu et al., 1999, Toillon et al., 2002). However, small increases in Fas protein level were detected in MRTF-A/B depleted cells compared to control cells, suggesting that receptor protein levels could be influenced by cell adhesion. In support of this, Fas levels were shown to be increased in a range of non-malignant and malignant cells following detachment (Aoudjit and Vuori, 2001, Mawji et al., 2007). Therefore it is possible that MRTF-A/B depletion in a FasL-sensitive cell line may also increase sensitivity to apoptosis induced by FasL. As discussed in Section 1.2.7, systemic FasL and TNF-α treatments have limited therapeutic application in cancer. As sensitizing tumour cells to TRAIL has more clinically relevant applications, the remainder of the work focused on the TRAIL response. Similar to TNF-α, depletion of MRTF-A/B led to increased sensitivity to TRAIL-induced apoptosis shown by a range of apoptotic detection techniques.

The third aim of this chapter was to investigate potential mechanisms for this TRAIL sensitivity using protein arrays and previously collected microarray data. When comparing the apoptosis protein array in MRTF-A/B depleted cells to that shown in Figure 3.4 looking at MDA-MB-231 cells on normal and low

attachment plates, the proteins consistently changed in both cases were cleaved caspase-3, DR5, TNF-R, and HTRA2/Omi. Increases in cleaved caspase-3 are indicative of spontaneous apoptosis or anoikis in MRTF-A/B depleted cells, however these apoptosis levels were less than 5% when determined by TUNEL staining and PARP cleavage. Previous work had also shown undetectable levels of anoikis in these cells using propidium iodide staining and flow cytometric analysis (Medjkane et al., 2009). This again confirms the specificity of the TRAIL-induced apoptosis in response to disrupted adhesion. HTRA2/Omi showed up to 2 fold increase in MRTF-A/B depleted cells when verified by a second Western blot. This value was highly variable and therefore confident conclusions cannot be made as to its role in the TRAIL sensitivity response.

The apoptosis protein array also highlighted changes in some cell cycle and DNA damage control proteins. Increases were seen in the cyclin dependent kinase inhibitor p27, which could explain why these MRTF-A/B depleted cells proliferate at a slightly slower rate than the parental cells. Increased levels of phospho-RAD17 in MRTF-A/B depleted cells also indicate these cells may exhibit a certain level of genotoxic stress. Interestingly there is also an increase in the hypoxia-induced transcription factor HIF-1 in MRTF-A/B depleted cells. These changes may reflect increased levels of oxidative stress in MRTF-A/B depleted cells, as oxidative stress can stabilise HIF1 and lead to DNA damage (Kietzmann and Görlach, 2005). In support of this prediction, several genes involved in metabolism and control of reactive oxygen species are known to have putative CArG boxes and are therefore likely to be regulated by MRTF-A/B (Sun et al., 2006). Interestingly HTRA2/Omi has also been implicated in the stabilisation of the mitochondrial membrane potential following oxidative stress, which may explain the variable increases detected in HTRA2/Omi protein (Krick et al., 2008). As these markers of genotoxic stress were not seen in the apoptosis array of detached cells in Chapter 3, it is likely that they result from disrupted expression of MRTF-dependent metabolic genes rather than the disruption of cell adhesion. Although not in the scope of this thesis, there is potential for future work to investigate the effect of MRTF-depletion on these pathways.

A limitation of the arrays presented in this chapter is that they showed high variation in the level of a number of proteins, meaning that only the more robust changes reach significance. One way to reduce the variation between repeats would be to use infrared detection techniques rather than chemiluminescence to acquire array images, as discussed in Supplementary Chapter S1. It is also possible that negative results from the array may reflect poor antibody performance, and therefore proteins which show no expression difference should not be confidently ruled out without further investigation.

However the array did highlight significant increases in the levels of the extrinsic apoptosis pathway death receptors, DR4 and DR5. Quantitative RT-PCR showed that MRTF-A/B depletion was not affecting mRNA levels of these TRAIL receptors, suggesting that the protein increase may result from reduced receptor degradation. FACS analysis of surface expression of these receptors showed that only DR5 expression was increased on the cell surface of MRTF-A/B depleted cells, suggesting that DR4 is maintained in the cytoplasm. Previous unpublished work by Dr S Hino has shown that low surface DR4 expression levels in 1205Lu melanoma cells was due to increased retention of DR4 in the cytoplasm. Similarly, DR4 localisation was also found to be predominantly cytoplasmic in TRAIL resistant BT474 human breast cancer cells (Zhang and Zhang, 2008). TRAIL receptors are internalised and recycled through clathrin-mediated endocytosis after TRAIL stimulation, with inhibitors of this process being shown to enhance TRAIL sensitivity in MDA-MB-231 cells by maintaining surface receptor expression (Zhang et al., 2009b). As clathrin-mediated endocytosis and recycling depends upon the actin cytoskeleton (Kaksonen et al., 2006), it is possible that gross cytoskeletal alterations in MRTF-A/B depleted cells could disrupt this vesicular transport network, leading to altered recycling and membrane transport of receptors such as the death receptors. Experiments with DR4 and DR5 blocking antibodies showed that DR5 function was also more important than DR4 in mediating TRAIL sensitivity in MRTF-A/B depleted cells. This is likely to be due its increased expression at the cell surface. In the presence of both DR4 and DR5 blocking antibodies, all three cell lines still showed some TRAIL signalling which suggests that the concentration of blocking

antibodies used was not high enough to block all receptor sites. Several recent studies have also outlined the importance of DR5 in mediating anoikis in anoikis-sensitive cell lines (Samara et al., 2007, Laguinge et al., 2008). In support of this, recent evidence has shown increased cell surface localisation of DR5 in detached oesophageal cancer cells. In detached cells, DR5 was relocalised to the cell membrane from the golgi apparatus and a DR5 agonist was more toxic in these detached cells (Liu et al., 2009). Although this suggests an important role for DR5 in mediating anoikis and detachment-induced apoptosis, a recent study by Kočí et al. found that levels of DR4 and DR5 in detached human colon adenocarcinoma cells were unchanged, with TRAIL sensitivity being mediated through reductions in AKT signalling (Kočí et al., 2011). Therefore, despite DR5 increases being seen in a range of cancer cell lines following detachment, this effect may still be cell line-dependent.

Microarray data previously published using these cell lines highlighted differences in nine apoptosis-related proteins which were MRTF-dependent (Table 4.1). Data presented in this chapter supports the MRTF-dependent expression of the soluble TRAIL decoy receptor osteoprotegerin, as reductions in both mRNA and secreted protein level were detected in MRTF-A/B depleted cells. A 63% reduction in OPG mRNA was found in MRTF-A/B depleted cells by RT-PCR, similar to the 72% decrease previously published from the microarray (Medjkane et al., 2009). As discussed in Section 1.2.6, OPG has been shown to have a protective role for breast cancers *in vitro* and the level of OPG secretion seen in these MDA-MB-231 cells corresponded with previous reports of this cell line (Holen et al., 2005). However, reconstitution experiments showed that the differences in protein secretion seen between these cell lines *in vitro* were not large enough to cause any TRAIL protection at the TRAIL concentration used throughout these experiments. Therefore, it is unlikely that OPG secretion is responsible for the differential TRAIL sensitivity observed between these cell lines. In support of this, recent work has suggested that OPG activity is not able to neutralise the effects of rhTRAIL treatment *in vivo* (Zinonos et al., 2011). The difference in TRAIL transcription reported in the microarray could not be confirmed by FACS analysis of cell surface TRAIL

expression. This does not rule out a role for secreted soluble TRAIL, as secretion into the culture medium could also induce apoptosis in an autocrine or paracrine manner. This could be investigated further, however differences would only be likely to affect levels of spontaneous apoptosis and not the response of cells to endogenous TRAIL treatment.

Investigation into the other targets from the microarray was not in the scope of this thesis, and it was deemed that they were less likely to be directly involved in TRAIL signalling. However, we cannot rule out the possibility that these other genes may affect the TRAIL sensitivity response and further work should be done to investigate the role of MRTF in controlling these genes. TNFRSF12a (TWEAKR) shows particularly high expression levels in MRTF-A/B depleted cells compared to control cells, and TWEAK has been shown to weakly induce apoptosis (Chicheportiche et al., 1997). As TWEAK is one of the least well characterised members of the TNF superfamily, work linking it to MRTF signalling would be novel and interesting.

TRAIL is known to activate apoptosis through the extrinsic apoptosis pathway mediated by caspase-8, as discussed in Section 1.1.4. However, in some cells cross talk between the extrinsic and intrinsic pathway can occur through the cleavage of BID to truncated BID and subsequent activation of caspase-9. As shown in figures 4.15 and 4.16, MRTF-A/B deficient cells exhibited slight increases in caspase-8 and caspase-10 cleavage which may result from the increased surface DR5 expression. However, they also showed robust cleavage of caspase-9, increased levels of BID, and increased cleavage of BID to its truncated form. Therefore it appears that MRTF-deficient cells amplify their death response by utilizing the intrinsic pathway of apoptosis, characteristic of type II cells. This amplification is likely to result from alterations in the levels of BCL-2 family proteins, the balance of which controls apoptosome formation and caspase-9 cleavage. Although no BCL-2 family proteins showed expression changes in the apoptosis array, *BCL-2* expression levels were shown to be reduced on the microarray in MRTF-A/B depleted MDA-MB-231 cells. In fact, SRF has been shown to bind to, and regulate the transcription of BCL-2 during early embryonic

mouse development by binding to a CArG box its promoter region (Schratt et al., 2004). Similarly, very recent work has just identified a role for MRTF-A in driving the transcription of the anti-apoptotic protein MCL-1, contributing to brain derived neurotrophic factor (BDNF)-induced neuroprotection in rat cortical neurons (Cao et al., 2011). This was also shown to be through the binding of SRF to a CArG box region in the promoter of MCL-1. Western blotting for BCL-2 with a separate antibody did detect reductions in BCL-2 level, although variable. Reductions in BCL-2 expression may allow more robust activation of caspase-9 by allowing greater activation of BAX and BAK, and more robust apoptosome signalling. Although *MCL-1* was not identified as an MRTF-dependent gene in MDA-MB-231 cells (Medjkane et al., 2009), due to its recent link to MRTF-A, further work could investigate MCL-1 protein levels in this model.

Survival signalling pathways such as NFκB, MAPK/ERK and PI3K/AKT can be regulated by cell adhesion, and have been shown to influence apoptotic signalling, especially through the control of intrinsic apoptosis pathway members (Wang et al., 1998, Chen et al., 2000, Sonoda et al., 2000, Reginato et al., 2003). Therefore alterations in these pathways in MRTF-A/B depleted cells could account for the increased caspase-9 cleavage. However, NFκB activity was higher in MRTF-A/B depleted cells, suggesting that NFκB is not acting to protect MRTF-proficient cells from apoptosis. Levels of active AKT in MDA-MB-231 showed no correlation with TRAIL sensitivity, levels of phosphorylated ERK1/2 were significantly reduced in MRTF-A/B depleted cells compared to control cells. As ERK1/2 has been shown to affect levels of intrinsic pathway components, including the expression of BCL-2 and cleavage of BID (Holmström et al., 2000, Galante et al., 2009), reduced ERK1/2 signalling could provide an explanation for the increase in intrinsic apoptosis activation in MRTF-A/B depleted cells.

In conclusion, this chapter presents novel and important findings that MRTF-A/B depletion in MDA-MB-231 cells can lead to TRAIL sensitivity and sensitivity to TNF-α induced apoptosis *in vitro*. These data contribute to the MRTF field by adding a new role to MRTF's pleiotropic control network. As developing

resistance to apoptosis is a key step in tumour progression and metastasis (Hanahan and Weinberg, 2000), MRTF-A/B could influence these processes both through cytoskeletal control of motility and invasion, and through their ability to influence apoptosis. These findings also contribute to our understanding of the regulation of TRAIL resistance. The TRAIL sensitivity reported here is likely to result from a combination of increased DR5 expression on the cell surface, and increased activation of the intrinsic apoptosis pathway due to reduced survival signalling through ERK1/2.

One limitation of this system is that SRF has many targets including adhesion and cytoskeletal proteins, as well as proteins involved in transcription, signalling, transport and metabolism (Sun et al., 2006). For this reason, it is a relatively unattractive target for therapy. Interestingly a specific small molecule Rho inhibitor, CCG-1423, has been identified which can interfere with MRTF/SRF driven transcription (Evelyn et al., 2007). This inhibitor could be used to verify the effects seen in this thesis, with the important advantage of being applicable to clinical use. However, the next aim of this thesis was to identify more viable therapeutic targets. As discussed in the following chapter, such a target would ideally be a specific protein involved in adhesion, whose interactions are well defined and understood and for which specific inhibitors are available. As integrins play an important part in mediating the interaction between cells and their matrix, the integrin signalling pathway was targeted.

Chapter 5: Targeting the integrin signalling pathway as a method of TRAIL sensitisation

5.0 Hypothesis

Targeting of specific focal adhesion complex proteins can sensitise tumour cells to TRAIL-induced apoptosis.

5.1 Introduction

To discover more specific targets for detachment-induced TRAIL sensitisation, components of the focal adhesion complex were targeted. This complex of adhesion molecules and adaptor proteins mediates integrin signalling from the cell surface. The following section will outline some of the key members of this complex (Figure 5.1).

5.1.1 Integrins

Integrins are cell surface receptors that exist as heterodimers of α and β subunits, and mediate the binding of cells to extracellular matrix (ECM) molecules such as fibronectin, laminin and collagen (Tamkun et al., 1986). There are 18 α and 8 β integrin subunits in mammals, with heterodimeric combinations of

each resulting in 24 possible integrin molecules. Each of these integrin combinations has affinity for particular ECM ligands, playing vital roles in transducing extracellular cues into intracellular responses (Miranti and Brugge, 2002, Humphries et al., 2006).

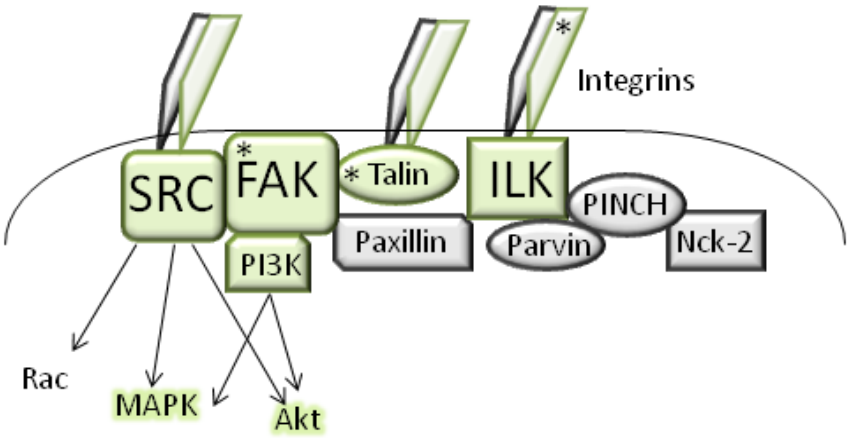

Figure 5.1 Schematic representation of the pathway targeted in this chapter. A simplified pathway representing the main molecules targeted in this chapter (highlighted green). Attachment of cells to an extracellular matrix involves the ligation of integrin receptors. Many proteins form complexes with β integrin tails, including talin, paxillin, and ILK. ILK forms a signalling hub, which signals through α- and β-parvin, and PINCH1. A different signalling hub passes to the kinases FAK and SRC by a series of adaptor proteins, including talin.

On ligation to the correct substrate, clustered and activated integrins initiate the formation of a set of signalling molecules and adaptors called the focal adhesion complex. Integrins recruit adaptor proteins, such as α-actinin and talin to their cytoplasmic β integrin tails (Otey et al., 1990, Rees et al., 1990), leading to activation of Rho GTPases and intracellular kinases. Through these connections, they can regulate many processes, including cytoskeleton remodelling and cell survival (Miranti and Brugge, 2002). They can also interact co-operatively with growth factor receptors and oncogenes, creating a complex signalling network downstream of the cell surface (Miyamoto et al., 1996, Moro et al., 1998).

Integrins play multiple and varied roles in tumour progression and metastasis, involving growth, invasion and apoptosis (Desgrosellier and Cheresh, 2010). As well as being implicated in angiogenesis (Brooks et al., 1994), they can also facilitate interactions between tumour cells and the surrounding microenvironment,

including mediating the protective interactions between platelets and tumour cells, and between tumour cells and the vasculature during metastasis (Felding-Habermann et al., 2001, Wang et al., 2004, Carbonell et al., 2009). β1 integrins were shown to play a role in the induction of a mouse model of human mammary carcinoma (White et al., 2004), and increased expression in human breast cancer patients has been associated with disease progression and poor prognosis (Yao et al., 2007). In line with this, β integrin blocking antibodies can reduce progression, invasion, and increase apoptosis *in vitro* whilst reducing metastasis *in vivo* (Fujita et al., 1992, Park et al., 2006). Therapies targeting α5β1, αvβ3 and α2β1 are currently in clinical trials (Ricart et al., 2008, Mita et al., 2011), with an RGD-mimetic, cilengitide, being the first integrin-targeting agent to reach phase III clinical trials (Reardon et al., 2008).

Cell attachment has been extensively shown to modulate cell survival, including resistance to chemotherapy, irradiation and FasL treatment (Sethi et al., 1999, Cordes et al., 2006, Estrugo et al., 2007). Integrin signalling has been implicated in the regulation of a number of apoptosis proteins including BCL-2 (Fukai et al., 1998, Matter and Ruoslahti, 2001), BAX (Gilmore et al., 2000), survivin (Fornaro et al., 2003), and cFLIP (Shain et al., 2002). Integrins have also been shown to regulate survival through a process termed integrin-mediated death (IMD). Independent from anoikis, IMD describes cell death which is triggered by unligated integrins. This pathway, outlined by Stupack et al., was shown to involve caspase-8, independent of death receptors or DISC formation (Stupack et al., 2001). In cell lines with little caspase-8, this pathway could be mediated by cytochrome c and caspase-9 (Bonfoco et al., 2000). IMD suggests a protective mechanism, evolved to prevent cells from growing in inappropriate surroundings. Therefore due to their important role in tumour cell-matrix interactions, and their ability to control apoptosis signalling pathways, integrins were chosen as a potential TRAIL-sensitising target for this thesis.

5.1.2 Talin

First discovered as a cytoskeletal protein localised to cell-ECM contacts, talin is now known to play an important role in the transduction of signals at focal adhesions (Burridge and Connell, 1983, Horwitz et al., 1986). Talin consists of a globular head containing a FERM region and a flexible rod domain, and can bind both to β integrin tails and to actin (Rees et al., 1990). Through binding to β integrin tails, talin mediates the final stage of integrin activation, allowing integrin heterodimers to adopt an active conformation and increase their ligand-binding affinity (Calderwood et al., 1999, Tadokoro et al., 2003). This ability of talin to promote integrin activation is termed 'inside-out' signalling (Moser et al., 2009). Through its rod domain, talin can also bind to other focal adhesion proteins such as vinculin and FAK, helping to form the focal adhesion complex (Burridge and Mangeat, 1984, Chen et al., 1995).

Mammals carry two talin genes, which give rise to the forms talin 1 and talin 2 (Monkley et al., 2001). Talin 1 has been best characterised as having essential roles in integrin-mediated signalling at focal adhesions, whereas the contribution of talin 2 has remained largely uninvestigated. Talin 1 is also ubiquitously expressed in mammalian tissues, whereas talin 2 is expressed in more specific locations including brain and striated muscle (Senetar and McCann, 2005).

Downregulation of talin leads to cell adhesion and spreading defects in a range of cells (Albigès-Rizo et al., 1995, Priddle et al., 1998). By utilising human umbilical vein endothelial cells (HUVECs), which lack talin 2, Kopp et al showed that RNA silencing of talin 1 causes reductions in cell spreading, focal adhesion formation, stress fibre formation and migration (Kopp et al., 2010). In fibroblasts expressing both talin 1 and talin 2, RNA silencing of both forms was required to cause cell spreading defects (Zhang et al., 2008). Interestingly, these results showed that talin is not required for initial attachment and spreading of cells onto fibronectin, but plays an important role in the maintenance of cell spreading, focal adhesion formation and force generation.

Very recent data has started to directly implicate talin in cancer invasion and metastasis. Talin 1 mRNA expression level was found to be almost 7 fold higher in oral squamous cell carcinoma (SCC) patient samples than normal epithelium, and was associated with poor patient outcome (Lai et al., 2011). Talin 1 expression levels were also shown to increase with tumour grade in prostate cancer patient samples. Over expression of talin 1 in prostate cancer cells could promote anoikis resistance, and increase the activation of the PI3K/AKT and ERK1/2 survival pathways (Sakamoto et al., 2010). This was the first report to directly link talin 1 signalling to apoptosis sensitivity; however no research has been done coupling talin 1 to death receptor signalling. Therefore talin was also chosen as a molecule to target in this chapter.

5.1.3 SRC and FAK

Integrins do not exhibit kinase activity and therefore recruit kinases into focal adhesions. Two of the most well studied kinases at focal adhesions are the non-receptor tyrosine kinases, SRC and FAK.

C-SRC was first identified as the cellular homolog to the viral gene *v-src*, which could lead to transformation in chicken sarcoma (Rous, 1911, Collett et al., 1978, Czernilofsky et al., 1980). There are now known to be nine SRC family kinase (SFK) members in humans; SRC, YES, FYN, LYN, HCK, LCK, BLK, FGR and YRK. SRC, YES and FYN are expressed in most tissues, with the other members expressed primarily in haematopoietic cells (Thomas and Brugge, 1997). SRC is kept in a deactivated state by phosphorylation of a regulatory Tyr^{530} by the kinases C-terminal SRC Kinase (CSK) and CSK Homologous Kinase (CHK) (Okada and Nakagawa, 1989, Chow et al., 1994). Dephosphorylation of Tyr^{530} and autophosphorylation of Tyr^{419} is required for full SRC activation (Thomas and Brugge, 1997).

FAK was identified as a tyrosine kinase that was phosphorylated both by integrin attachment and during v-SRC transformation (Kanner et al., 1990, Schaller et al., 1992, Lipfert et al., 1992). Along with binding to focal adhesion components such as paxillin, talin and p130CAS, FAK binds to SRC (Zhao and Guan, 2009).

Autophosphorylation at a Tyr^{397} residue in FAK during activation creates a high affinity binding site for SRC, which can further phosphorylate and activate FAK (Schaller et al., 1994).

SRC and FAK are localised to focal adhesions on activation (Kaplan et al., 1994), and promote cell adhesion, spreading and motility through their ability to bind and regulate focal adhesion proteins such as paxillin and p130CAS (Kanner et al., 1990, Richardson et al., 1997, Tachibana et al., 1997). Both kinases have been implicated in focal adhesion turnover, as SRC and FAK-deficient cells show enlarged focal adhesions and reductions in motility (Ilić et al., 1995, Fincham and Frame, 1998, Webb et al., 2004). This results from impaired focal adhesion disassembly, preventing cell migration and invasion (Ilić et al., 1995, Webb et al., 2004). SRC and FAK can also promote and mediate signalling from growth factor receptors such as EGF-R, PDGF-R, and FGF-R, through a number of mechanisms including receptor phosphorylation and heterocomplex formation (Tice et al., 1999, Ishizawar et al., 2007, Sieg et al., 2000). FAK and SRC also mediate survival signalling through their ability to activate the MAPK/ERK and PI3K/AKT pathways (Schlaepfer et al., 1994, Chen et al., 1996, Fincham et al., 2000b, Lu et al., 2003). Both kinases have been implicated in apoptosis resistance, particularly in anoikis-resistance following detachment (Frisch et al., 1996, Duxbury et al., 2004a, Beierle et al., 2009), with many invasive cancer cells showing particularly high expression levels (Sakuma et al., 2009). They can influence a number of intrinsic apoptosis proteins including IAPs, BCL-2, BIM, MCL-1 and p53 (Sonoda et al., 2000, Matter and Ruoslahti, 2001, Woods et al., 2007, Sakuma et al., 2009), along with the extrinsic apoptosis proteins caspase-8 and RIP (Xu et al., 2000, Kurenova et al., 2004). Over-expression of FAK in HL60 leukaemia cells could confer TRAIL resistance through a reduction in caspase-8 and increases in XIAP, BCL-X_L and RIP (Tamagiku et al., 2004). Therefore FAK and SRC were also chosen as potential targets for TRAIL sensitisation in this chapter.

Many studies have implicated SRC signalling in tumour progression and metastasis (Boyer et al., 2002, Trevino et al., 2006), with activation reported in many human cancer types (Irby et al., 1999, Irby and

Yeatman, 2000). Similarly, increased FAK expression can be detected in a broad range of cancer types, with high expression in invasive cancers (Weiner et al., 1993, Cance et al., 2000). For this reason, FAK and SRC have great potential for therapeutic targeting. Specific SRC inhibitors including AZD0530 (saracatinib), bosutinib, and dasatinib show promising anti-tumour and anti-metastatic effects in preclinical studies, and are currently in clinical trials (Nam et al., 2005, Jallal et al., 2007, Green et al., 2009). FAK inhibitors such as PF-573,228, PF-562,271 and TAE226 also show high specificity for FAK and show promising anti-tumour activity in preclinical studies (Slack-Davis et al., 2007, Roberts et al., 2008).

5.1.4 Integrin-linked kinase (ILK)

Initially identified as a binding partner of β integrin tails, ILK also plays a role in transducing signals from the cell surface and controlling cell adhesion (Hannigan et al., 1996, Attwell et al., 2003). ILK has ankyrin repeat motifs at its N-terminus which allow binding to other proteins, a pleckstrin homology domain which binds to phosphatidylinositol 3,4,5-trisphosphate (PIP_3) (Delcommenne et al., 1998), and a C-terminal sequence which contains a putative ser/thr kinase domain (Hannigan et al., 1996). As this kinase domain lacks well-conserved motifs believed to be required for protein kinase activity, ILK has been labelled by some as a pseudokinase. However, there is mounting evidence that ILK can exhibit kinase activity and so the debate about the function of this domain continues (Hannigan et al., 2011). ILK forms a complex called the IPP complex, named after its interacting partners ILK, PINCH and parvins (Tu et al., 1999, Nikolopoulos and Turner, 2000, Tu et al., 2001). PINCH1 and PINCH2 bind to the ankyrin repeat motif in ILK (Braun et al., 2003), whereas parvins-α, β, and γ bind to the kinase domain of ILK (Yamaji et al., 2001). ILK can control signalling pathways such as AKT and glycogen synthase kinase-3β (GSK-3β) (Delcommenne et al., 1998), as well as regulating actin, paxillin, and other proteins involved directly in cytoskeletal regulation (Nikolopoulos and Turner, 2000, Wu, 2005).

ILK has been implicated in the development and progression of cancer in animal models (White et al., 2001, Gao et al., 2011). In humans, over-expression of ILK has been reported in some cancer types, including prostate, ovarian and colon (Graff et al., 2001, Marotta et al., 2001, Ahmed et al., 2003), but not all, and may reflect the differentiation state of the cancer rather than the malignant potential (Haase et al., 2008).

ILK activation has been shown to confer anoikis resistance in a number of cell lines and regulate apoptosis, mainly through its ability to activate AKT signalling (Attwell et al., 2000). Reduction of ILK expression in bladder cancer cells could increase apoptosis through the reduction of anti-apoptotic BCL-2 protein levels and the induction of pro-apoptotic BAX (Gao et al., 2011). Similarly, inhibition of PINCH1 was shown to have radiosensitising and chemosensitising effects in a range of cancer cell lines through its regulation of AKT (Eke et al., 2010). As a result, small molecule inhibitors have been developed that target ILK, and these were shown to reduce proliferation and induce apoptosis in a number of cancer cell lines including breast and glioblastoma (Koul et al., 2005, Troussard et al., 2006) and in a mouse model of lung cancer (Liu et al., 2006a). However, one inhibitor QLT0267, was shown to lack specificity, resulting in radiosensitivity effects which were ILK-independent (Eke et al., 2009b). Furthermore, constitutively active ILK has been shown to contribute to radiation-induced death, acting pro-apoptotically through interaction with caspase-8 and 9 (Cordes, 2004, Hess et al., 2007). These reported pro- and anti-apoptotic roles of ILK bring into question the therapeutic application of ILK inhibitors, but present another interesting target to investigate TRAIL sensitivity effects.

5.2 Aims

As shown in Chapters 3 and 4, detachment of cells or interruption of cell adhesion and spreading by global cytoskeletal disruption can lead to increased sensitisation of cancer cells to TRAIL-induced apoptosis *in vitro*. In order to find potential targets for enhancing a TRAIL therapy *in vivo*, different members of the integrin signalling pathway were disrupted in turn. To verify the hypothesis that targeting the integrin signalling pathways at the focal adhesion complex could sensitise cancer cells to TRAIL, the aims of this chapter are as follows;

• To target β1 and β3 integrins, talin, integrin-linked kinase, SRC and FAK in MDA-MB-231 and 1205Lu cells *in vitro* using inhibitors and/or RNA silencing.

•To test these depleted cells for sensitivity to TRAIL- induced apoptosis

5.3 Results

5.3.1 Beta integrin blocking

As integrin subunits β1 and β3 have been implicated in the initial establishment of tumour cell metastasis (Felding-Habermann et al., 2001, Wang et al., 2004, Carbonell et al., 2009), the role of these subunits in TRAIL sensitivity was investigated. First, the expression of integrin β1 and β3 subunits was investigated in MDA-MB-231 and 1205Lu cells by Western blot (Figure 5.2A). Both MDA-MB-231 and 1205Lu cells expressed the integrin β1 receptor, with 4 fold higher expression levels in MDA-MB-231 cells. In contrast, only 1205Lu cells showed detectable β3 integrin subunit expression.

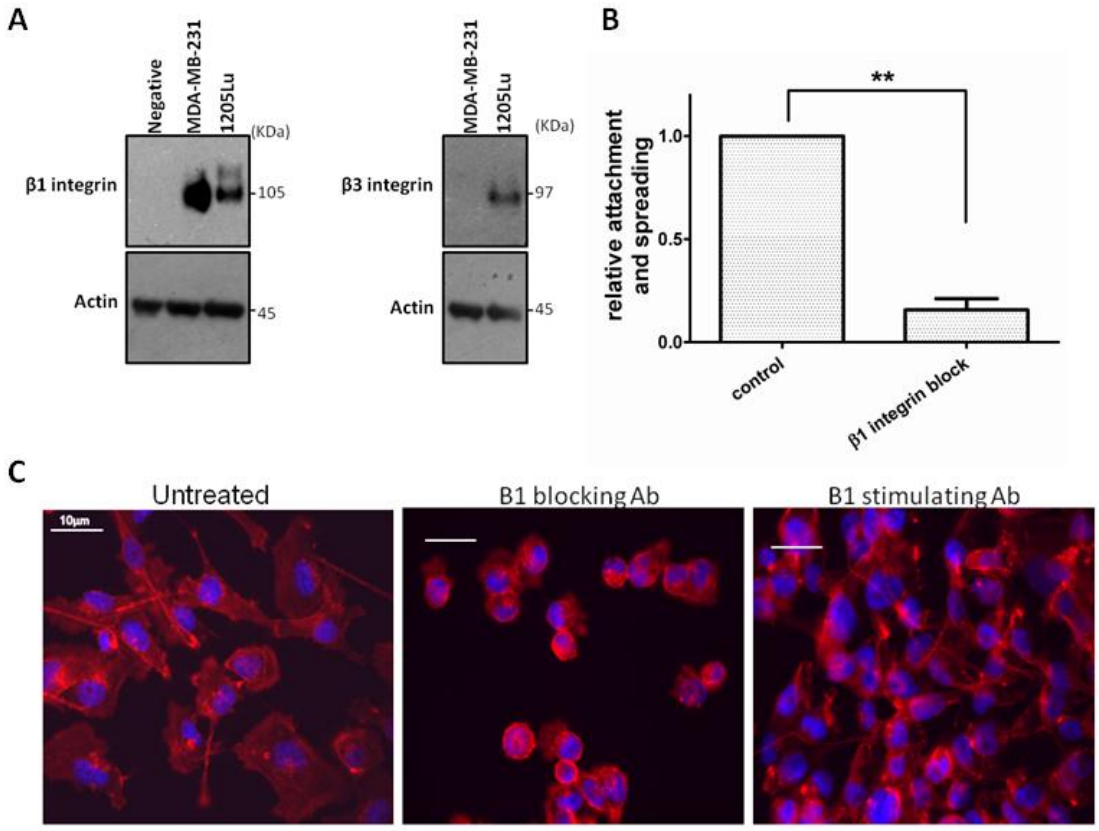

Figure 5.2 Pre-blocking cells with integrin β1-blocking antibody leads to cell rounding *in vitro*. A Western blot was performed with MDA-MB-231 and 1205Lu whole cell lysates and probed for β1 and β3 subunit expression. The negative control for β1 expression was Esb murine lymphoma cells with genetic ablation of β1 integrin (Carbonell et al., 2009). Only 1205Lu cells expressed the β3 integrin subunit. **B** MDA-MB-231 cells were pre-blocked for 1 hr with β1-blocking antibody (5 μg/ml) and seeded onto fibronectin (10 μg/ml) coated xCELLigence plates (see Section 2.2.9 for detailed methods). Significant attachment and spreading defects were observed 2 hr after seeding in cells pre-blocked with β1-blocking antibody. **C** MDA-MB-231 cells were either untreated, or pre-blocked with β1-blocking or β1-stimulating antibodies, before seeding onto human collagen I coated chamber slides for 4 hr. F-actin was stained using phalloidin (red) and nuclear Hoechst (blue) staining. These cells show marked cell rounding compared to untreated or β1 stimulating antibody control. Mean +/- SEM n=3 paired t-test **p<0.01

Next, a β1-blocking antibody was tested for its ability to prevent attachment and spreading of MDA-MB-231 cells on both fibronectin and collagen, common ECM substrates for the β1 integrin subunit. Pre-incubation of MDA-MB-231 for 1 hr with β1-blocking antibody led to an 85% inhibition of attachment and spreading on fibronectin 2 hr after seeding compared to untreated controls (Figure 5.2B). Pre-blocked cells were also seeded onto collagen I coated chamber slides for 4 hr and F-actin stained using a TRITC-

labelled phalloidin toxin. Figure 5.2C confirms that β1-blocking antibody pre-treatment resulted in marked cell rounding compared to both untreated cells and those pre-treated with a β1-stimulating antibody.

Following this, it was investigated whether reduced attachment mediated by integrin blocking was accompanied by an increased sensitivity to TRAIL-induced apoptosis. MDA-MB-231 and 1205Lu cells were blocked for 1 hr with either β1-blocking, β1-stimulating, or β3-blocking antibodies before being plated onto fibronectin or collagen I coated plates. At 4 hr after seeding, cells were treated with TRAIL for 24 hr and their viability measured (Figure 5.3A). Blocking of the β1 integrin subunit in MDA-MB-231 reduced viability by a further 19% after TRAIL treatment compared to untreated controls when seeded on fibronectin, and a further 13% when seeded on collagen I (Figure 5.3A). Similarly, β1 integrin blocking in 1205Lu cells enhanced TRAIL sensitivity by 8% after TRAIL treatment on fibronectin and 7% on collagen I, compared to untreated controls (Figure 5.3B). Treatment with a β3-blocking antibody had very little effect on MDA-MB-231 cells, as expected due to the lack of expression shown in Figure 5.2A. In 1205Lu cells, β3 blocking led to a 7% increase in TRAIL sensitisation on fibronectin but not on collagen.

To rule out any influence of anoikis or integrin-mediated death on these results, β1-blocked cells were tested for spontaneous increases in caspase 3/7 activity after seeding. As shown in Figure 5.3C, in the absence of TRAIL, no significant increases in caspase 3/7 activity could be seen in either cell line after integrin β1-blocking relative to unblocked cells.

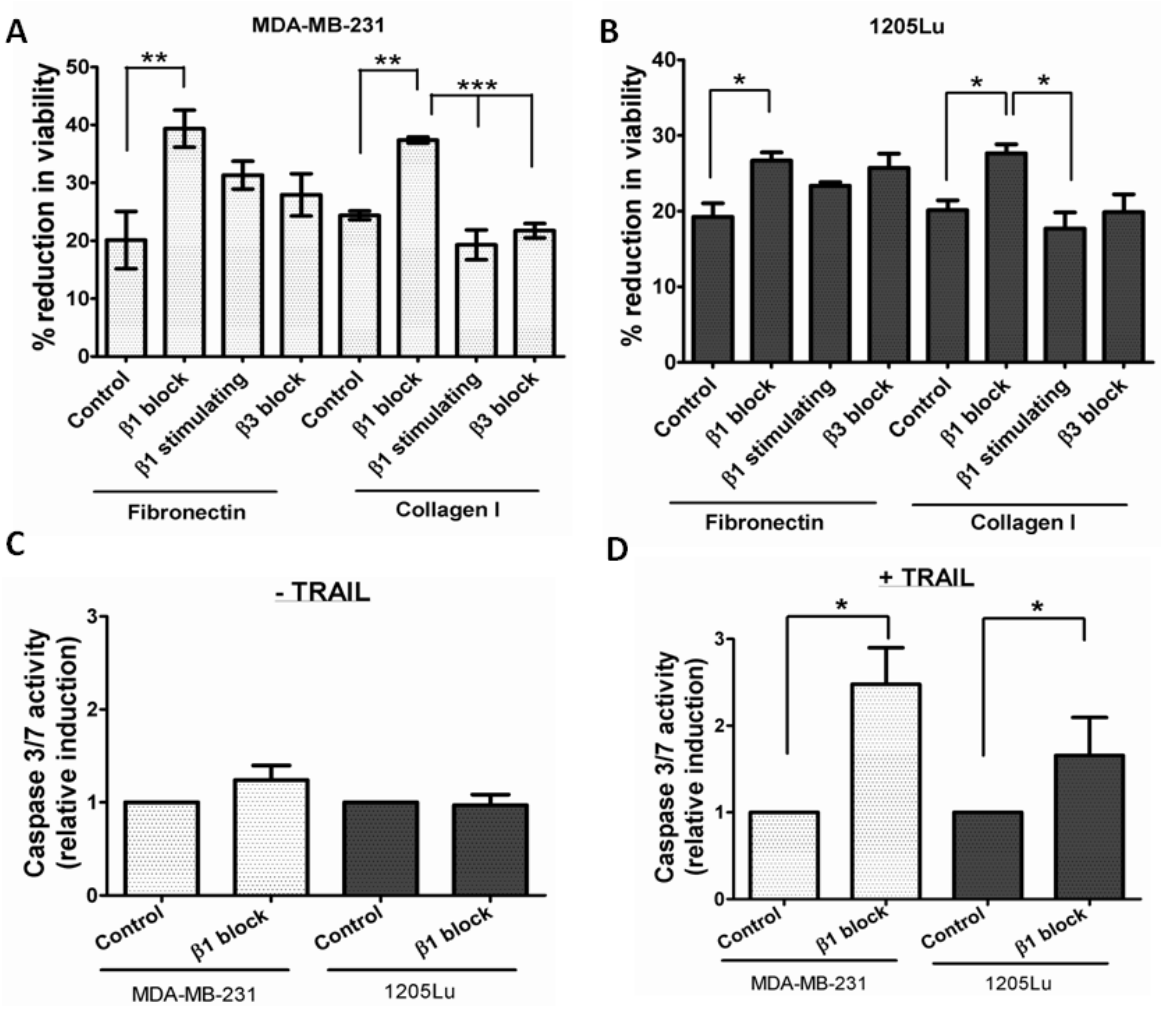

Figure 5.3 β1 integrin blocking sensitises MDA-MB-231 and 1205Lu cell lines to TRAIL induced apoptosis. MDA-MB-231 and 1205Lu cells were either untreated or pre-incubated for 1 hr with 5 µg/ml β1-blocking or β1-stimulating antibodies prior to seeding onto fibronectin or collagen I coated plates (10 µg/ml). Four hours after seeding, cells were treated with TRAIL (100 ng/ml for MDA-MB-231 and 200 ng/ml for 1205Lu). Viability reductions were determined using alamarBlue® assay (at 24 hr) or Caspase 3/7 Glo® assay (at 3 hr). **A** MDA-MB-231 cells show TRAIL sensitisation after β1 blocking on both fibronectin and collagen I. β3 blocking caused sensitisation only in 1205Lu cells on fibronectin. **B** 1205Lu cells show TRAIL sensitisation after both β1 and β3-blocking on fibronectin, but only after β1-blocking on collagen I. **C** Caspase 3/7 activity of cells cultured on fibronectin coated plates was not significantly altered by β1 blocking alone (-TRAIL), but was increased in both cell lines after β1 integrin pre-block and TRAIL treatment (+ TRAIL) **(D)**. Mean +/- SEM (**A** n=7 (fibro) n=5 (collagen)) (**B** n= 6(fibro) n=8 (collagen)) (**C &D** n=6) ANOVA (Tukey post-test) * p<0.05 ** p<0.01 *** p<0.001

To confirm that the enhanced viability reductions after TRAIL treatment in β1-blocked cells were a result of increased apoptosis, both cell lines were pre-blocked with β1-blocking antibody and caspase 3/7

activity was measured 3 hr after TRAIL addition (Figure 5.3D). Compared to unblocked control cells, β1-blocked MDA-MB-231 cells showed 2 fold higher caspase 3/7 activity after TRAIL treatment, with 1.4 fold higher levels in 1205Lu cells.

5.3.2 Knockdown of talin 1 using siRNA

As discussed in Section 5.1.2, talin is an important molecule which links the tail of β integrins to actin, and plays a key role in integrin activation. New evidence suggests that talin 1 also has roles in metastasis (Sakamoto et al., 2010, Lai et al., 2011). Western blotting was performed to investigate the expression profiles of talin 1 and talin 2 in MDA-MB-231 and 1205Lu cells. Figure 5.4A shows that talin 1 is the prevailing isoform in both cell lines. MDA-MB-231 cells have undetectable levels of talin 2, with levels of talin 2 in 1205Lu cells being much weaker than talin 1.

Previous studies have reported compensatory increases in talin 2 following depletion of talin 1 (Kopp et al., 2010). To investigate this, cells were transfected with siRNA for talin 1 and harvested for Western blot 72 hr post-transfection. Transfection of MDA-MB-231 cells with talin 1 siRNA gave a strong reduction in talin 1 protein expression, but did not lead to a compensatory increase in the levels of talin 2 protein within 72 hr (Figure 5.4B). This suggests that knockdown of talin 1 is sufficient to eliminate overall talin signalling.

Cells expressing siRNA for talin 1 were then tested for their ability to attach and spread *in vitro*. MDA-MB-231 cells were either untreated, or transfected with control non-targeting siRNA or talin 1 siRNA and seeded onto fibronectin coated plates 72 hr post-transfection (Figure 5.4C). Cell attachment and spreading was monitored over 2 hr, with talin 1 depleted cells showing a 20% reduction in the ability to attach and spread on fibronectin compared to untransfected (parental) and control transfected cells.

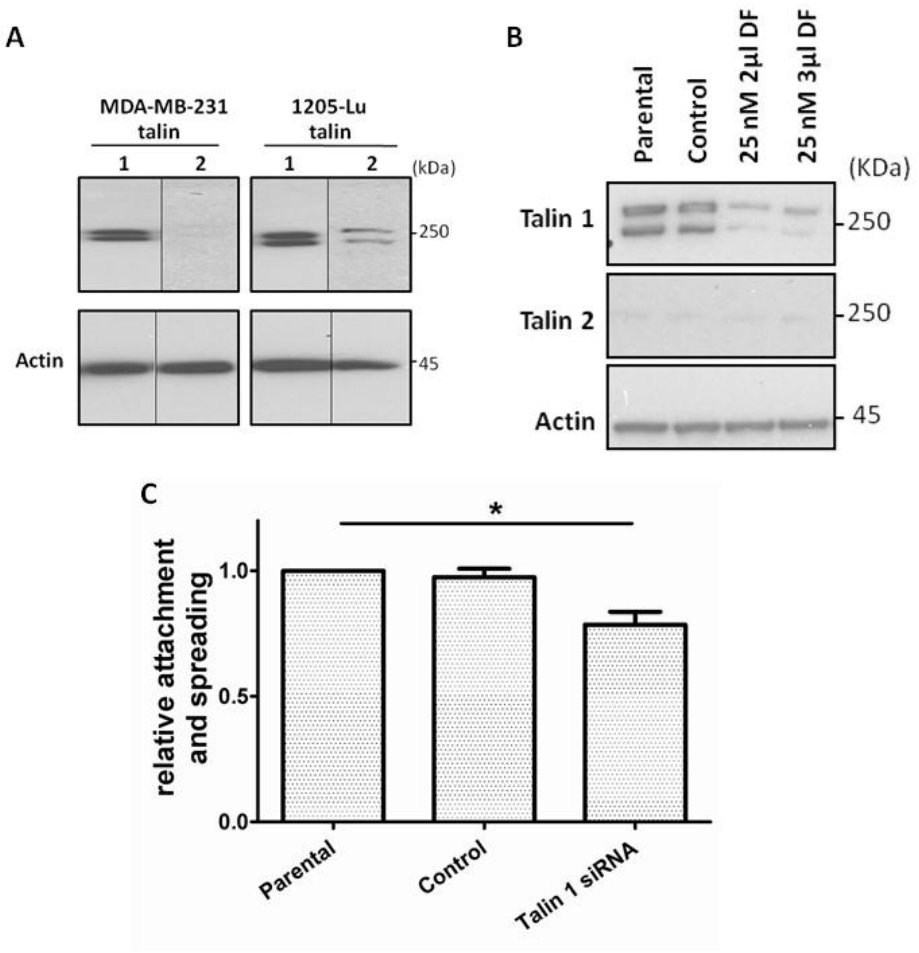

Figure 5.4 Talin expression and spreading defects in talin 1 deficient MDA-MB-231 and 1205Lu cells. Whole cell lysates were prepared from MDA-MB-231 or 1205Lu cells either untreated (parental), or transfected with non-targeting (control) or talin 1 siRNA. The siRNA was used at 25 nM, with either 2 or 3 µl of Dharmafect reagent (DF). At 72 hr post-transfection, samples were taken for Western blot or seeded onto fibronectin (10 µg/ml) coated E-plates for xCELLigence measurements. **A** Talin 1 is the prevalent isoform in both cell lines. **B** Knockdown of talin 1 in MDA-MB-231 cells did not cause any compensatory increase in talin 2 at 72 hr post-transfection. The doublet indicates possible degradation of talin 1 into its rod and head domain. The antibody only recognises the rod domain, but cleavage of the head domain (50kDa) from the rod domain in part of the sample could result in the presence of a lower band. **C** MDA-MB-231 cells transfected with talin 1 siRNA (25 nM and 2 µl DF) showed attachment and spreading defects 2 hr after seeding. Values were calculated relative to untransfected (parental) cells. Mean +/- SEM n=3 ANOVA * $p<0.05$

The effect of talin 1 knockdown on TRAIL sensitivity was then tested. Efficient knockdown of talin 1 was confirmed by Western blot in figure 5.5A for both MDA-MB-231 and 1205Lu cell lines. These cell lines both showed a decrease in talin 1 protein expression greater than 85% compared to control cells transfected with non-targeting siRNA.

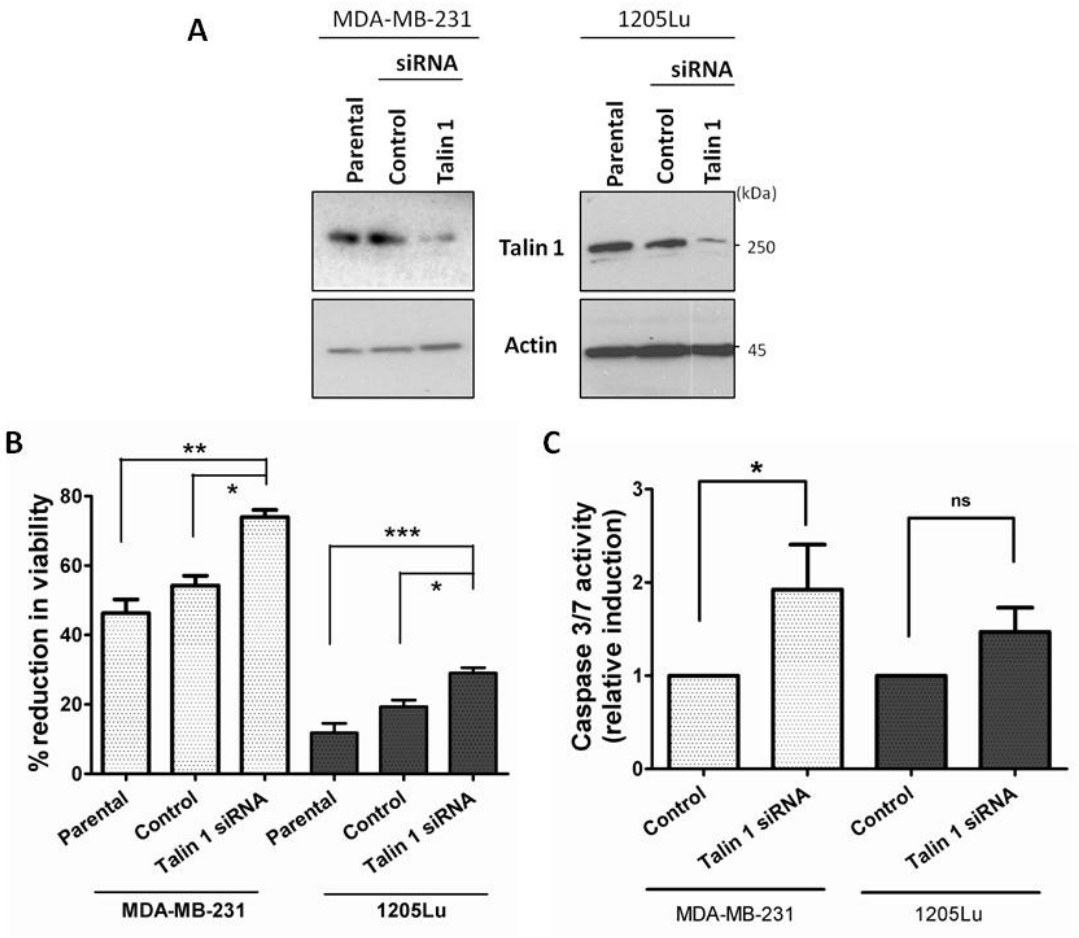

Figure 5.5 Talin knockdown using siRNA results in TRAIL sensitisation. MDA-MB-231 and 1205Lu cells were either untreated (parental), or transfected with non-targeting (control) or talin 1 siRNA at 25 nM concentration with 2 µl Dharmafect reagent. Cells were lysed for Western blot or seeded for apoptosis assays 72 hr post-transfection. **A** Western blot confirms knockdown of talin 1. **B** Greater viability reductions are observed in talin 1 knockdown cells 24 hr following TRAIL treatment using the alamarBlue® assay. **C** Increased caspase 3/7 activity 3 hr after TRAIL treatment using Caspase Glo assay. TRAIL was used at a concentration of 100 ng/ml in MDA-MB-231 cells and 200 ng/ml in more TRAIL resistant 1205Lu cells. Mean +/- SEM (**B** MDA-MB-231 n=4, 1205Lu n=5) (**C** MDA-MB-231 n=4, 1205Lu n=3). ANOVA (Tukey post-test) * $p<0.05$, ** $p<0.01$, *** $p<0.001$, ns= not significant.

A viability assay showed that talin 1 depletion in MDA-MB-231 cells led to a 20% increase in TRAIL sensitivity compared to control transfected cells. In 1205Lu cells this TRAIL sensitivity was slightly lower, with viability reduced by a further 10% after TRAIL treatment in talin 1-depleted cells (Figure 5.5B). Talin 1-depleted MDA-MB-231 cells showed 2 fold higher caspase 3/7 activity after treatment with TRAIL than control transfected cells, with 1.5 fold higher activity after talin depletion in 1205Lu cells (Figure 5.5C).

This again confirms that the viability reductions seen after TRAIL treatment correspond to increases in apoptosis.

5.3.3 Knockdown of ILK using siRNA

As discussed in Section 5.1.4, there is much evidence for ILK playing an important role in mediating the integrin signalling response through the formation of a heterotrimeric complex with PINCH1 and parvins, and survival signalling through AKT. To investigate a role for ILK in the TRAIL sensitivity response, siRNA was used to knockdown ILK in both MDA-MB-231 and 1205Lu cell lines. As shown in figure 5.6A, ILK siRNA gave an efficient knockdown of 97% in MDA-MB-231 cells and 88% in 1205Lu cells compared to cells transfected with non-targeting siRNA (control) 72 hr after transfection (quantified from Western blot). After plating onto fibronectin for 2 hr, ILK depleted MDA-MB-231 cells showed no observable attachment and spreading defects (Figure 5.6B).

Treatment of parental or transfected cells with TRAIL for 24 hr showed no difference in TRAIL sensitivity between control and ILK siRNA transfected cells (Figure 5.6C). The control transfected 1205Lu cells showed a 10% increase in TRAIL sensitivity compared to untransfected cells; however, ILK siRNA did not enhance this further. This non-specific sensitivity is likely to be a result of the high levels of siRNA needed to efficiently deplete ILK in this cell line. These results suggest that ILK does not play a major role in attachment and TRAIL sensitivity in these cell lines.

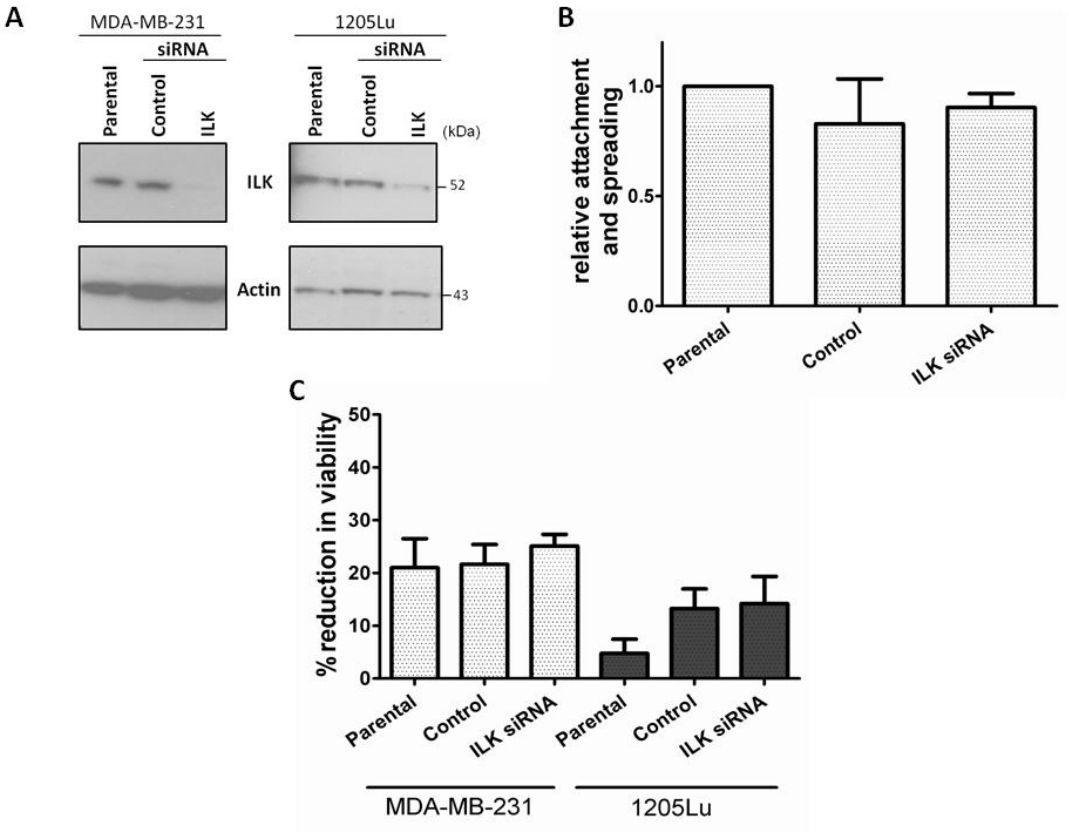

Figure 5.6 ILK knockdown using siRNA does not sensitise cells to TRAIL. A Western blot of whole cell lysates showing efficient knockdown of ILK in both cells 72 hr post-transfection compared to untreated or control (non-targeting siRNA). MDA-MB-231 cells were transfected with 25 nM siRNA (2 µl Dharmafect reagent), 1205Lu cells were transfected with 50 nM siRNA (2 µl Dharmafect reagent). Cells were lysed 72 hr post-transfection. **B** There was no attachment and spreading defect in ILK knockdown cells 72 hr post-transfection when re-seeded for 2 hr onto fibronectin using the xCELLigence machine. AlamarBlue® viability assay showed no ILK-specific sensitisation to TRAIL (100 ng/ml MDA-MB-231, 200 ng/ml 1205Lu). Mean +/- SEM (**B** n=3) (**C** n=5)

.

5.3.4 FAK inhibition using PF-573,228

As outlined in section 5.1.3, the non-receptor tyrosine kinases SRC and FAK play a major role in the translation of focal adhesion signals into multiple cellular changes (Kaplan et al., 1994, Schaller et al., 1992). To investigate whether they could control TRAIL sensitivity, MDA-MB-231 and 1205Lu cells were treated with the FAK inhibitor PF-573,228 (Slack-Davis et al., 2007).

MDA-MB-231 cells were treated with increasing concentrations of PF-228 and lysed for Western blot of activated p130CAS, a downstream focal adhesion component (Tachibana et al., 1997). Concentrations of PF-228 above 5 µM led to a reduction in p130CAS activity, indicating FAK inhibition (Figure 5.7A). Cells were pre-treated with PF-228 and seeded onto fibronectin coated plates (Figure 5.7B). After 1 hr, PF-228 treated cells showed a 21% reduction in the ability to attach and spread, although this was transient as values returned to those of untreated cells by 2 hr (data not shown).

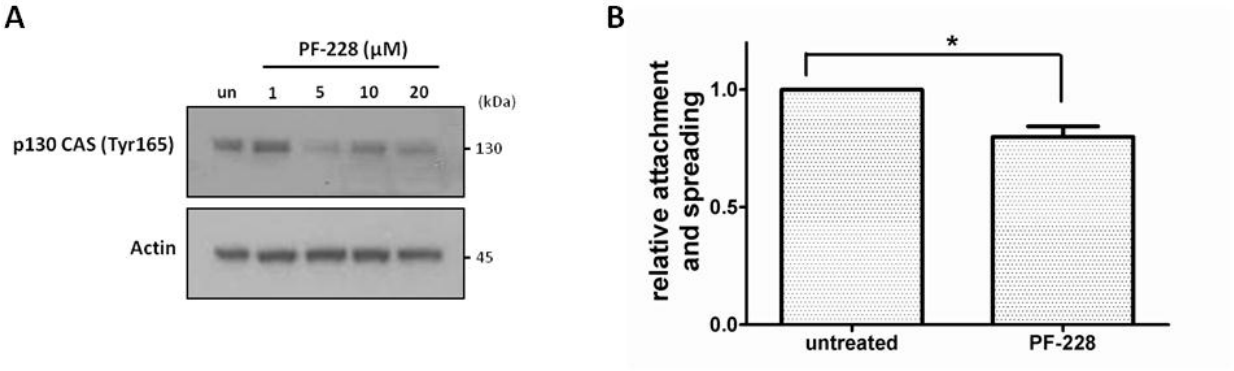

Figure 5.7 PF-228 causes a reduction in activity of p130CAS and transient adhesion defects. A MDA-MB-231 cells were treated with the indicated concentrations of PF-228 for 1 hr prior to lysis. Reductions in the activity of p130CAS are seen with concentrations of 5 µM PF-228 or above. **B** MDA-MB-231 cells were pre-blocked with PF-228 (10 µM) and seeded onto fibronectin (10 µg/ml) coated E-plates in the xCELLigence machine. Defects in attachment and spreading were seen 1 hr after seeding compared to untreated controls. Mean +/- SEM n=5 paired t-test *p<0.05

Following verification of the activity of PF-228, a dose-response experiment was performed with increasing concentrations of PF-228 incubated with cells for 1 hr prior to TRAIL addition. As a control, equal volumes of DMSO were added to cells 1 hr before TRAIL. Cell viability was measured 24 hr after TRAIL addition. In MDA-MB-231 cells (Figure 5.8A), treatment with 5 µM PF-228 slightly reduced the viability after TRAIL treatment compared to cells treated with DMSO and TRAIL. After a 10 µM treatment, viability was significantly reduced by 23% compared to DMSO treated cells. Similarly, 1205Lu cells (Figure 5.8B) showed mild TRAIL sensitivity at concentrations of PF-228 as low as 1 µM, with a significant increase in sensitivity at 10 µM when the TRAIL-induced viability was reduced by a further 22% compared to

controls. This effect was also investigated in another cell line, the WM1789 melanoma cell line tested in Chapter 3 (Figure 5.8C). These cells also showed TRAIL sensitivity increases at PF-228 concentrations as low as 1 µM, reaching significance with 5 µM PF-228, where viability was reduced by a further 22% after TRAIL treatment compared to DMSO treated controls.

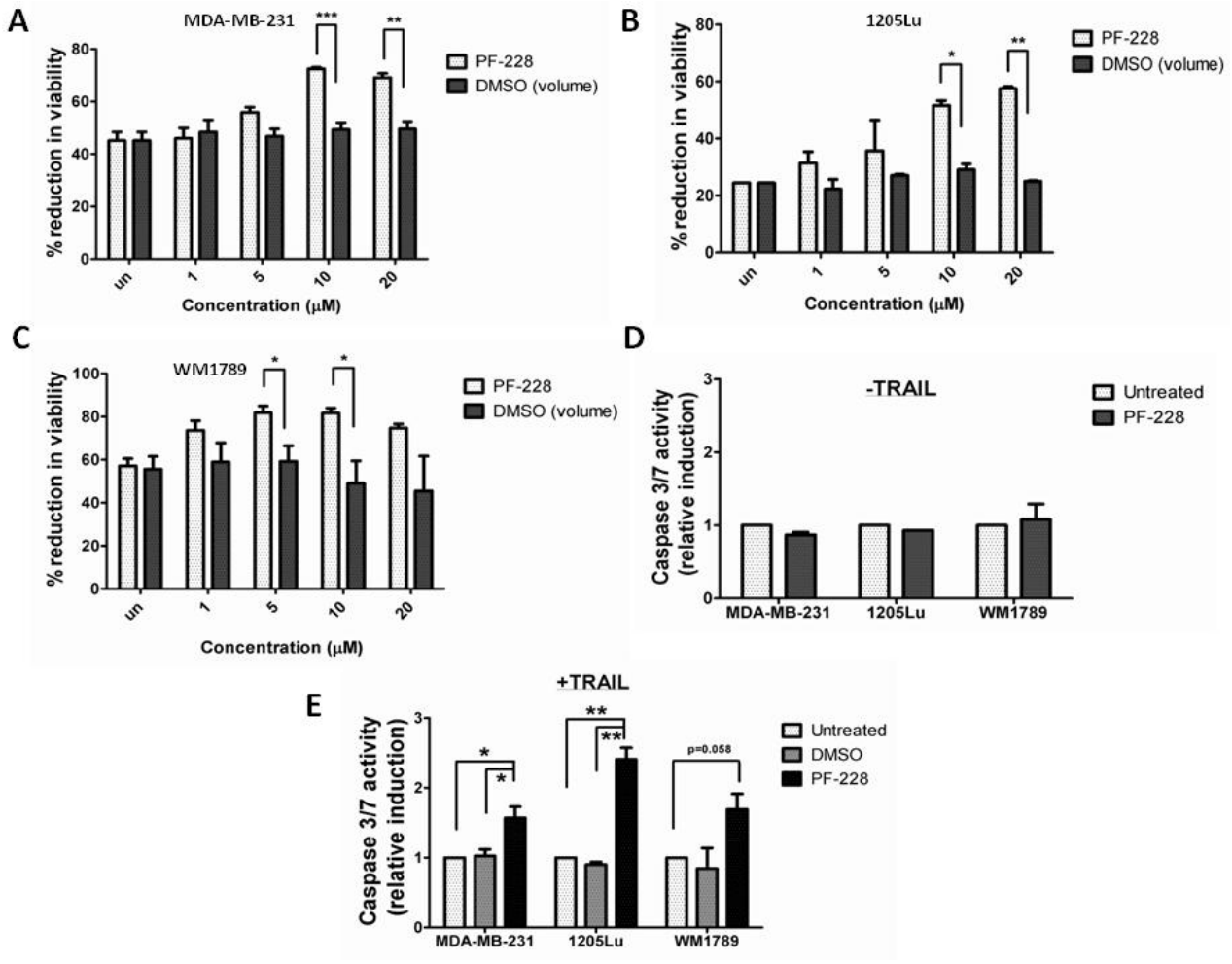

Figure 5.8 FAK inhibition using PF-228 leads to significant TRAIL sensitivity in all three cell lines. MDA-MB-231 **(A),** 1205Lu **(B)** and WM1789 **(C)** cells were pre-treated for 1 hr with the indicated concentrations of PF-228 or equal volumes of DMSO. TRAIL was added after 1 hr, viability measured after 24 hr and expressed as % reduction compared to paired non-TRAIL treated controls for each treatment. TRAIL was used at 100 ng/ml for MDA-MB-231, 200 ng/ml for 1205Lu, and 50 ng/ml for WM1789. **D** Caspase 3/7 activity was measured 4 hr after PF-228 (10 µM) addition (-TRAIL) using the CaspaseGlo® assay and showed no difference in activity in any cell line compared to untreated controls. **E** TRAIL was added to cells 1 hr after PF-228 (10 µM) treatment, and caspase 3/7 activity measured after 3 hr (+ TRAIL). TRAIL treatment led to higher caspase 3/7 activity in PF-228 treated cells compared to untreated or DMSO treated controls. Mean +/- SEM **(A)** n=6; **(B)** n=3; **(C)** n=5; **(D)** n=3; **(E)** n=3 ANOVA (Tukey post-test) * p<0.05 ** p<0.01 *** p<0.001

Pre-treatment of all three cell lines with 10 µM PF-228 did not cause spontaneous apoptosis as measured by caspase 3/7 activity 4 hr after treatment with PF-228 (Figure 5.8D). In contrast, after TRAIL treatment, all three cell lines showed an enhancement of caspase 3/7 activity after pre-incubation with PF-228 compared to untreated cells or those pre-treated with DMSO (Figure 5.8E). For MDA-MB-231 and 1205Lu cells, this enhanced activity was significantly higher than in controls, with activity increased by 56% and 140%, respectively. In WM1789 cells, caspase 3/7 activity was increased by 70% compared to controls; however, this did not reach significance at $p<0.05$.

5.3.5 SRC inhibition using PP2 and AZD0530

SRC was initially targeted using the broad spectrum SFK inhibitor PP2, at a concentration previously reported to inhibit spreading of colon cancer cells on fibronectin (Jones et al., 2002). A non-functional analogue, PP3, was used as a control.

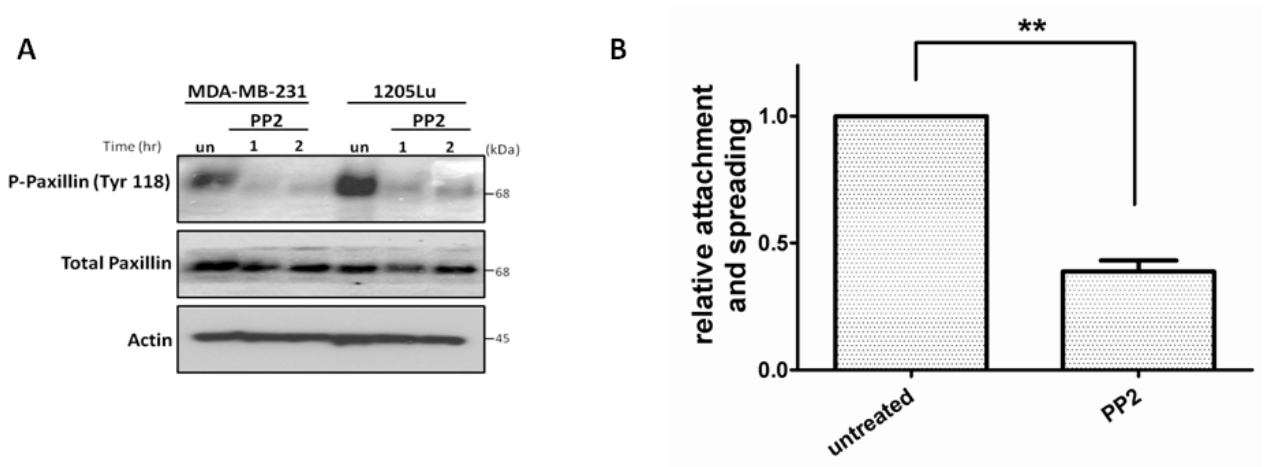

Figure 5.9 PP2 inhibited SRC signalling and prevented cell attachment and spreading. Cells were treated for the indicated durations with PP2 (10 µM) and subject to Western blotting. MDA-MB-231 cells were pre-incubated for 1 hr with PP2 prior to seeding onto fibronectin coated E-plates and cell attachment and spreading measured at 2 hr using the xCELLigence machine. **A** PP2 treatment led to efficient reduction in the phosphorylated form of paxillin over 2 hr, compared to total paxillin levels. **B** Pre-treatment with PP2 led to a significant decrease in the relative attachment and spreading of MDA-MB-231 cells compared to untreated controls. Mean +/- SEM n=3 paired t-test ** $p<0.01$

As shown in figure 5.9A, a 1 hr treatment with PP2 led to a robust reduction in the levels of phosphorylated focal adhesion protein paxillin (Tyr118), whereas total paxillin levels were unchanged. After seeding for 2 hr onto fibronectin, PP2-treated MDA-MB-231 cells showed a 61% reduction in the ability to attach and spread (Figure 5.9B). To verify this spreading defect, PP2 and PP3-treated MDA-MB-231, 1205Lu and WM1789 cells were stained with TRITC-phalloidin (Figure 5.10). Treatment with PP2 induced marked morphological changes in all three cell lines, characterised by cell rounding, with PP3-treated cells remaining unaffected.

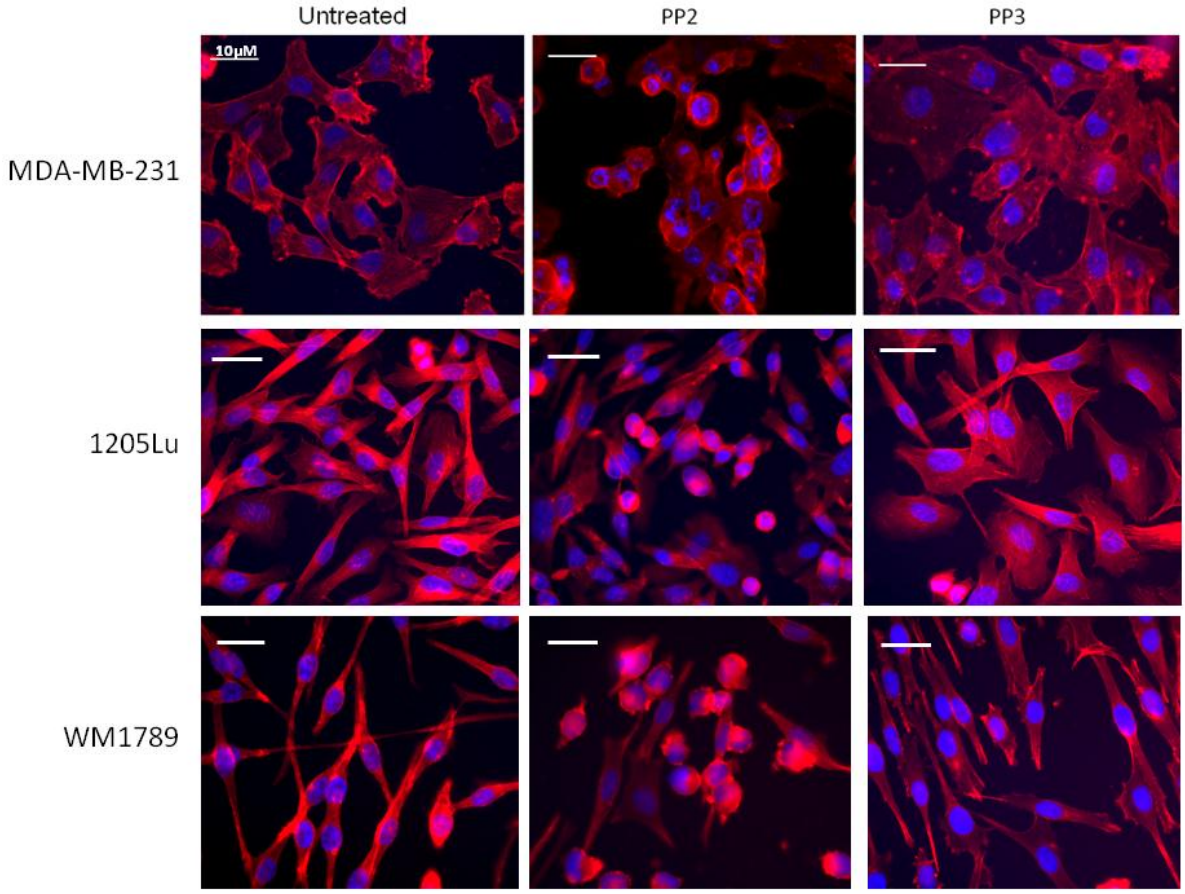

.

Figure 5.10 MDA-MB-231, 1205Lu and WM1789 cells show defective spreading after PP2 treatment. Cells were seeded for 12 hr onto glass chamber slides, before treatment for 1 hr with PP2 or PP3 (10 µM). Staining was then performed with phalloidin (red) and Hoechst (blue) and indicated PP2-specific morphological defects.

All three cell lines were treated with PP2 for 1 hr prior to TRAIL addition and the viability was measured (Figure 5.11A). After TRAIL addition, MDA-MB-231 cells pre-treated with PP2 showed viability levels which were 19% lower than PP3 treated cells. Similarly, PP2 and TRAIL reduced viability by a further 16% in 1205Lu cells, and 21% in WM1789 cells compared to PP3 and TRAIL. To investigate whether PP2 treatment alone could induce apoptosis, caspase 3/7 activity was measured 4 hr after PP2 treatment (Figure 5.11B).

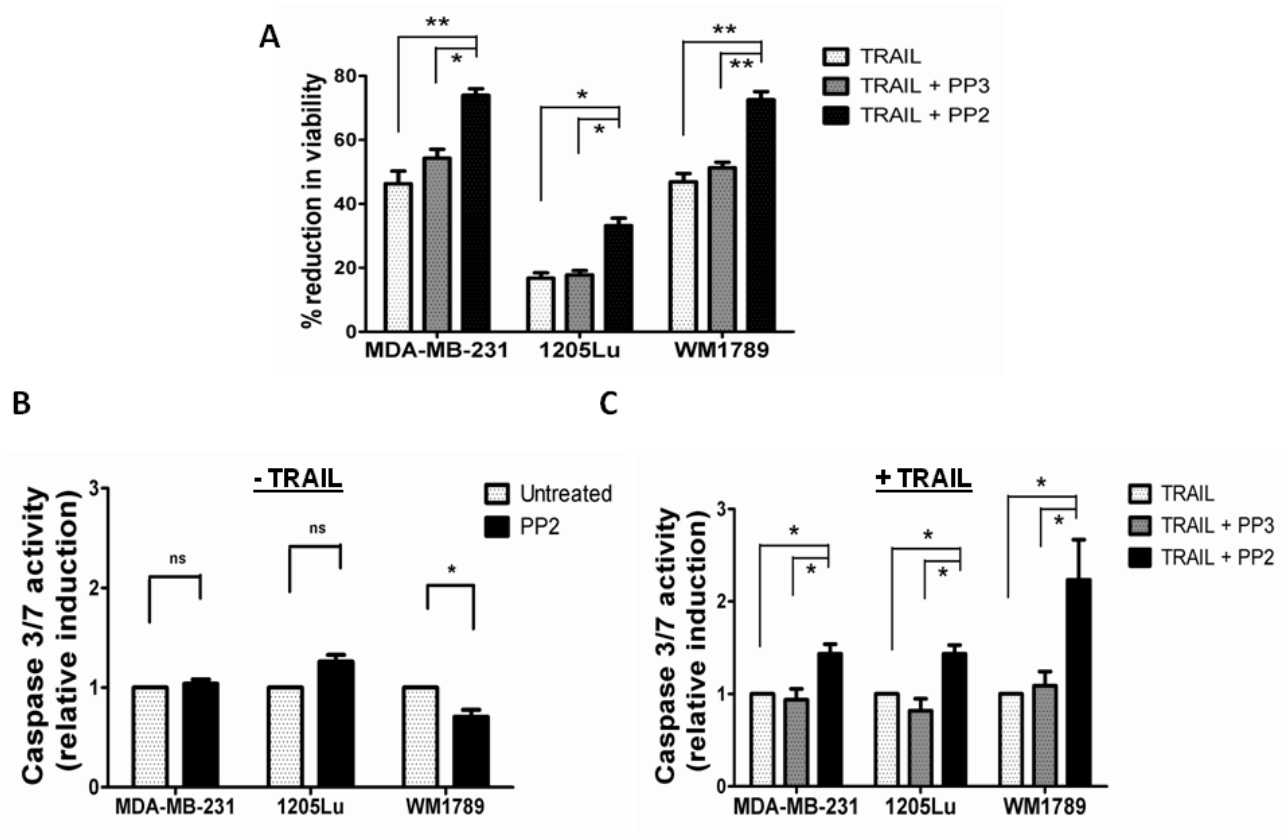

Figure 5.11 PP2 treatment increased TRAIL sensitivity in the three cell lines. A Addition of PP2 (10 μM) to cells 1 hr before TRAIL addition led to greater reductions in viability 24 hr after TRAIL treatment compared to cells which were untreated or pretreated with PP3 (10 μM). **B** None of the cell lines showed significant increases in spontaneous apoptosis 4 hr after PP2 treatment (-TRAIL). **C** PP2 treated cells showed significant increases in caspase 3/7 activity 3 hr after TRAIL addition (+ TRAIL). The control inhibitor PP3 had no effect on any cell line. TRAIL was used at 100 ng/ml (MDA-MB-231), 200 ng/ml (1205Lu), 50 ng/ml (WM1789). Graphs show mean +/- SEM (**A**) n=4 (MDA) n=9 (1205Lu & WM1789); **(B)** n=5 (MDA & WM1789) n=3 (1205Lu); **(C)** n=4 (MDA) n=3 (1205Lu) n=6 (WM1789); A and C ANOVA (Tukey post test); B paired t-test * $p<0.05$ ** $p<0.01$

Although there was a slight increase in caspase 3/7 activity in 1205Lu cells (26% increase from controls) upon PP2 treatment, this was not significant. MDA-MB-231 and WM1789 cells showed no signs of spontaneous apoptosis. In comparison, following TRAIL treatment, cells pre-treated with PP2 showed significantly higher caspase 3/7 activity compared to untreated cells or cells pre-treated with the control inhibitor PP3 (Figure 5.11C). This confirms that the TRAIL sensitivity seen in Figure 5.10A is a result of increased levels of apoptosis following treatment with TRAIL and PP2 in combination.

As mentioned, SRC can control activation of AKT and ERK1/2, either directly or through association with FAK (Schlaepfer and Hunter, 1997, Fincham et al., 2000a). To investigate a role for these proteins in controlling the TRAIL sensitivity response downstream of SRC, their activity was measured by Western blot 1 hr and 2 hr after PP2 treatment (Figure 5.12). Levels of the NFκB inhibitor IκB were also measured, as an indication of NFκB activity. After 2 hr of PP2 treatment, MDA-MB-231 cells showed robust reductions in the activity of AKT and ERK1/2, as judged by their level of phosphorylation relative to total levels. Phosphorylation of AKT at Ser473 is a widely used marker of AKT activity. Despite low expression of activated AKT, a decrease in phosphorylation level could still be seen. Interestingly, there was also an increase in the level of IκBα protein, indicating a reduction in NFκB signalling. 1205Lu cells also showed large decreases in phosphorylated AKT (Ser 473) and ERK (Thr202/204) levels, however did not show similar changes in NFκB activity. Total levels of AKT and ERK were subsequently measured and shown in a later blot (Figures 5.16 and 5.17).

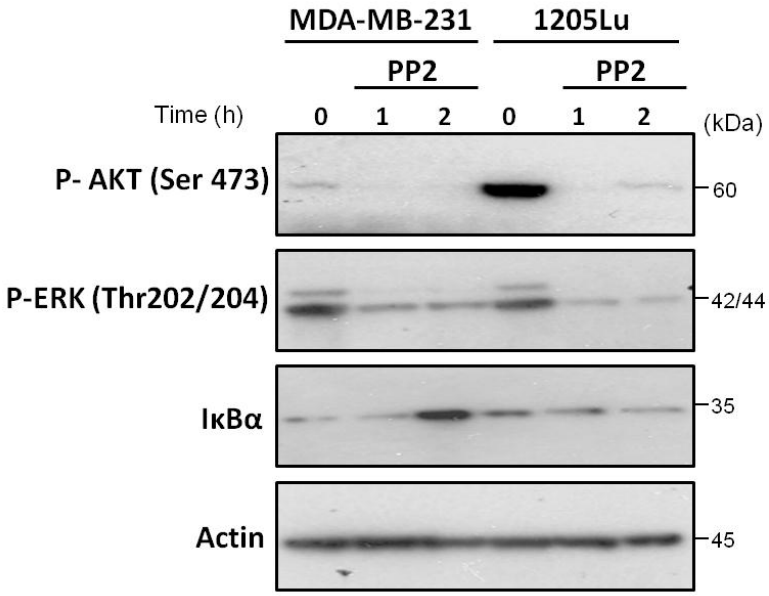

Figure 5.12 PP2 led to decreases in survival signals in MDA-MB-231 and 1205Lu cell lines. Cells were treated for the indicated times with PP2 (10 μM) before whole cell lysates were sampled. PP2 led to reductions in the activation of AKT and ERK1/2 at 1 hr after treatment. MDA-MB-231 cells also showed increases in IκBα levels after 2 hr.

To verify the TRAIL sensitivity effect seen by PP2 in these cell lines, a second inhibitor was used, the highly selective SRC/ABL inhibitor AZD0530. Cells were treated for 1 hr with AZD0530 before treatment with TRAIL and viability measured after 24 hr (Figure 5.13). An equal volume of DMSO was added to cells as a control. Compared to treatment with DMSO and TRAIL, AZD0530 in combination with TRAIL reduced viability by a further 23% in MDA-MB-231 cells and 19% in 1205Lu cells.

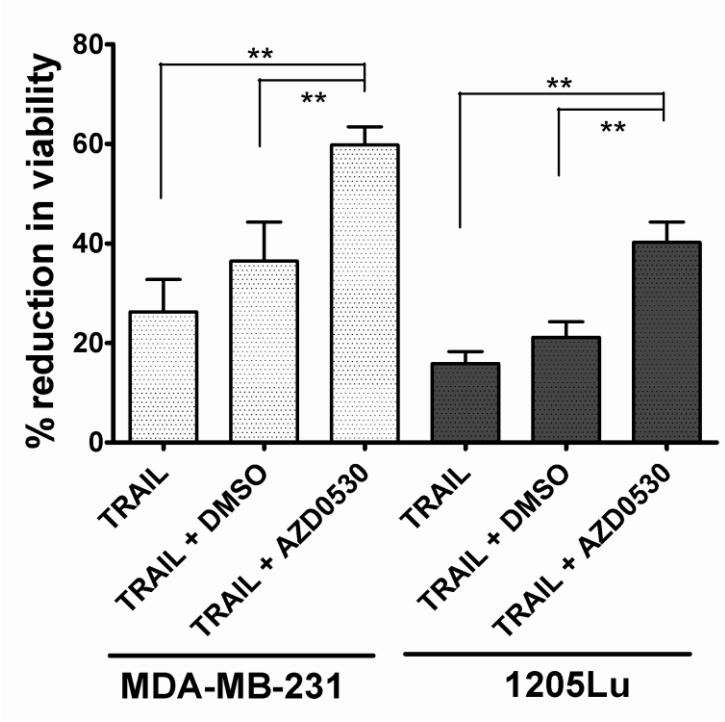

Figure 5.13 The SRC inhibitor AZD0530 increases TRAIL sensitivity. A 1 hr treatment with AZD0530 (50 µM for MDA-MB-231, 25 µM for 1205Lu) prior to TRAIL addition (100 ng/ml MDA-MB-231 cells, 200 ng/ml 1205Lu cells) led to greater reductions in viability compared to cells treated with equal volumes of DMSO or not treated with an inhibitor. Viability was measured 24h after TRAIL addition. Mean +/- SEM n=4 ANOVA (Tukey post-test) ** p<0.01

5.3.6 SRC knockdown using shRNA

MDA-MB-231 cells were transiently transfected with SRC siRNA, and cells harvested after 72 hr for Western blot. A range of concentrations and incubation times were tested (Figure 5.14A), none of which showed any change in SRC total protein level. Following this, lentiviral delivery of SRC shRNA was performed to create stable cell lines lacking SRC protein. At a Multiplicity of Infection of 2, MDA-MB-231 cells showed a 50% reduction in total SRC protein levels, resulting in caspase 3/7 cleavage which was 44% higher than in control transfected cells after TRAIL treatment (Figure 5.14B). However, after two passages, the SRC expression in these cells returned to control levels, along with the TRAIL sensitivity.

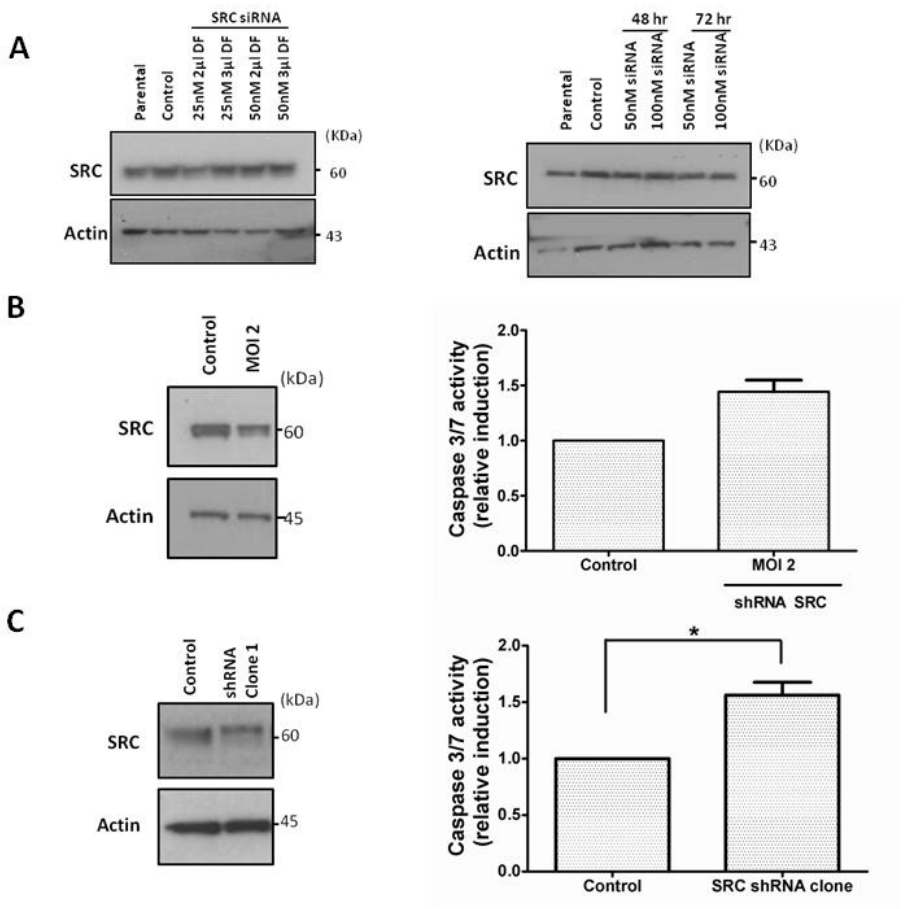

Figure 5.14 SRC reductions using siRNA and shRNA in MDA-MB-231 cells. A Treatment of MDA-MB-231 cells with the indicated concentrations of SRC siRNA and Dharmafect transfection reagent (DF) did not cause any knockdown of total SRC levels compared to untreated (parental) or non-targeting siRNA (control) transfected cells. (Left blot) cells were collected for analysis 48 hr post-transfection. (Right blot) No knockdown could be seen with higher concentrations of siRNA (5 µl DF) at either 48 hr or 72 hr post-transfection. **B** MDA-MB-231 cells were infected with SRC shRNA lentiviral particles at the indicated Multiplicity of Infection (MOI) and Western blot performed 72 hr post-transfection. At 55 hr post-transfection, cells were seeded overnight and then treated with TRAIL for 3 hr before caspase 3/7 activity was measured using CaspaseGlo® assay. **C** MDA-MB-231 cells were re-transfected at MOI2 and clones were isolated by limiting dilution. The clone with the highest SRC reduction was treated with TRAIL as above. Even partial SRC depletion led to enhanced TRAIL sensitivity. Mean +/- SEM **(B)** n=2 **(C)** n=3 paired t-test * $p<0.05$

Therefore cells were re-transfected and clonal populations were isolated by limiting dilution, however the clones with the lowest SRC expression only showed a 20% reduction in SRC protein levels compared to control transfected cells (Figure 5.14C). However they did show stable knockdown, allowing TRAIL sensitivity to be measured in a number of experimental repeats. These showed that, despite the low level

of knockdown, SRC-depleted cells still exhibited 56% higher caspase 3/7 activity after TRAIL treatment than control transfected cells (Figure 5.14D). This suggests a specific role for SRC activity in the control of TRAIL resistance.

5.3.7 ERK1/2 and AKT activity is affected by SRC inhibitors and correlates with TRAIL sensitivity

To further investigate the potential mechanism behind the TRAIL sensitivity seen with the SRC inhibitors PP2 and AZD0530, and to investigate why PP2 shows higher TRAIL sensitisation effects, experiments were performed to correlate the TRAIL sensitivity response with the activity of the two SRC inhibitors. Dose-response curves were performed for both inhibitors in both cell lines, measuring TRAIL sensitivity by the reduction in viability shown 24 hr after TRAIL treatment (Figure 5.15). PP2 induces TRAIL sensitivity at concentrations as low as 5 μM in both MDA-MB-231 cells (Figure 5.15A) and 1205Lu cells (Figure 5.15B). This sensitivity increased further with increasing doses of PP2 up to 20 μM. In contrast, AZD0530 resulted in TRAIL sensitivity at higher concentrations of 50 μM in MDA-MB-231 cells and 25 μM in 1205Lu cells.

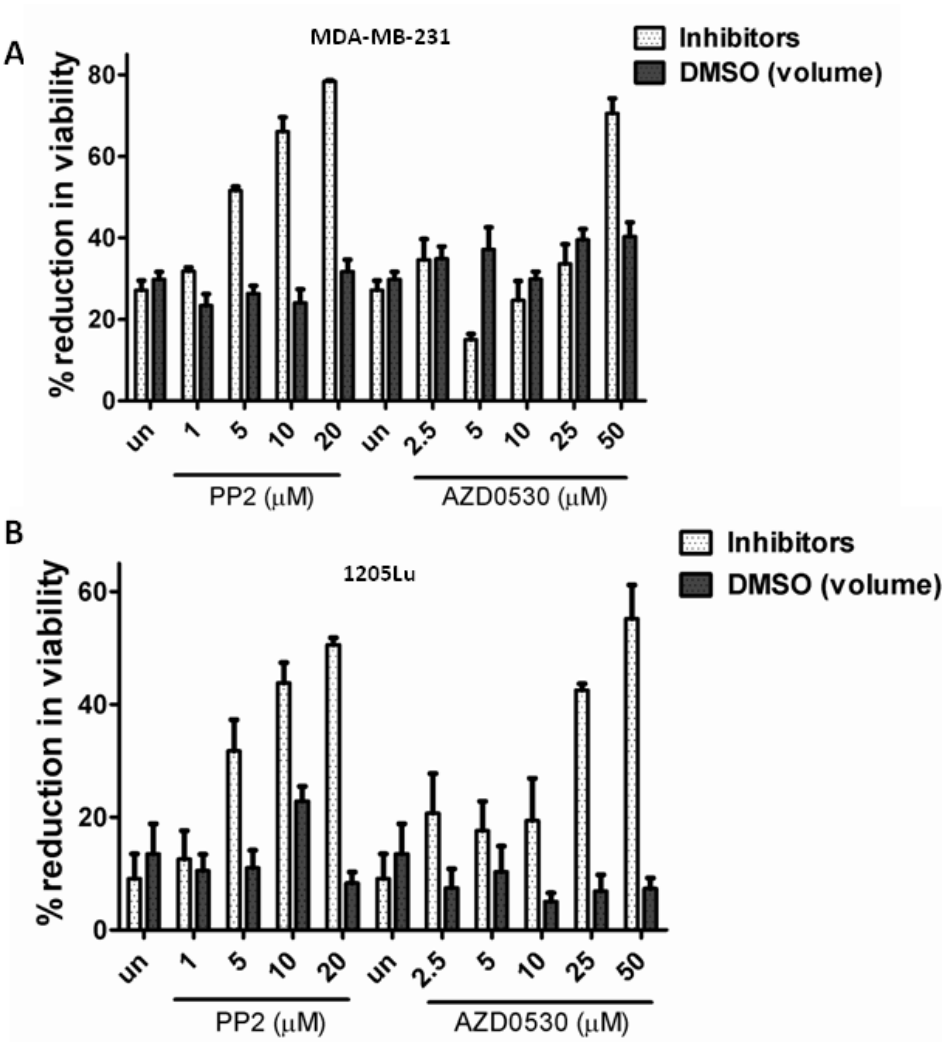

Figure 5.15 Dose response curves showing TRAIL-induced reductions in viability with increasing concentrations of PP2 and AZD0530. A MDA-MB-231 cells and **(B)** 1205Lu cells were treated for 1 hr with the indicated concentrations of DMSO, PP2 or AZD0530. TRAIL was then added (100 ng/ml for MDA-MB-231, 200 ng/ml for 1205Lu) and viability measured after 24 hr using alamarBlue®. Compared to DMSO, PP2 led to TRAIL sensitisation at 5 μM concentration in both cell lines, whereas AZD0530 induced TRAIL sensitisation only at much higher concentrations. Mean +/- SD n=1 (triplicate)

Western blots were performed in MDA-MB-231 cells (Figure 5.16) and 1205Lu cells (Figure 5.17) to investigate the relationship between the onset of TRAIL sensitivity and the ability of the inhibitors to abolish signalling through their downstream targets.

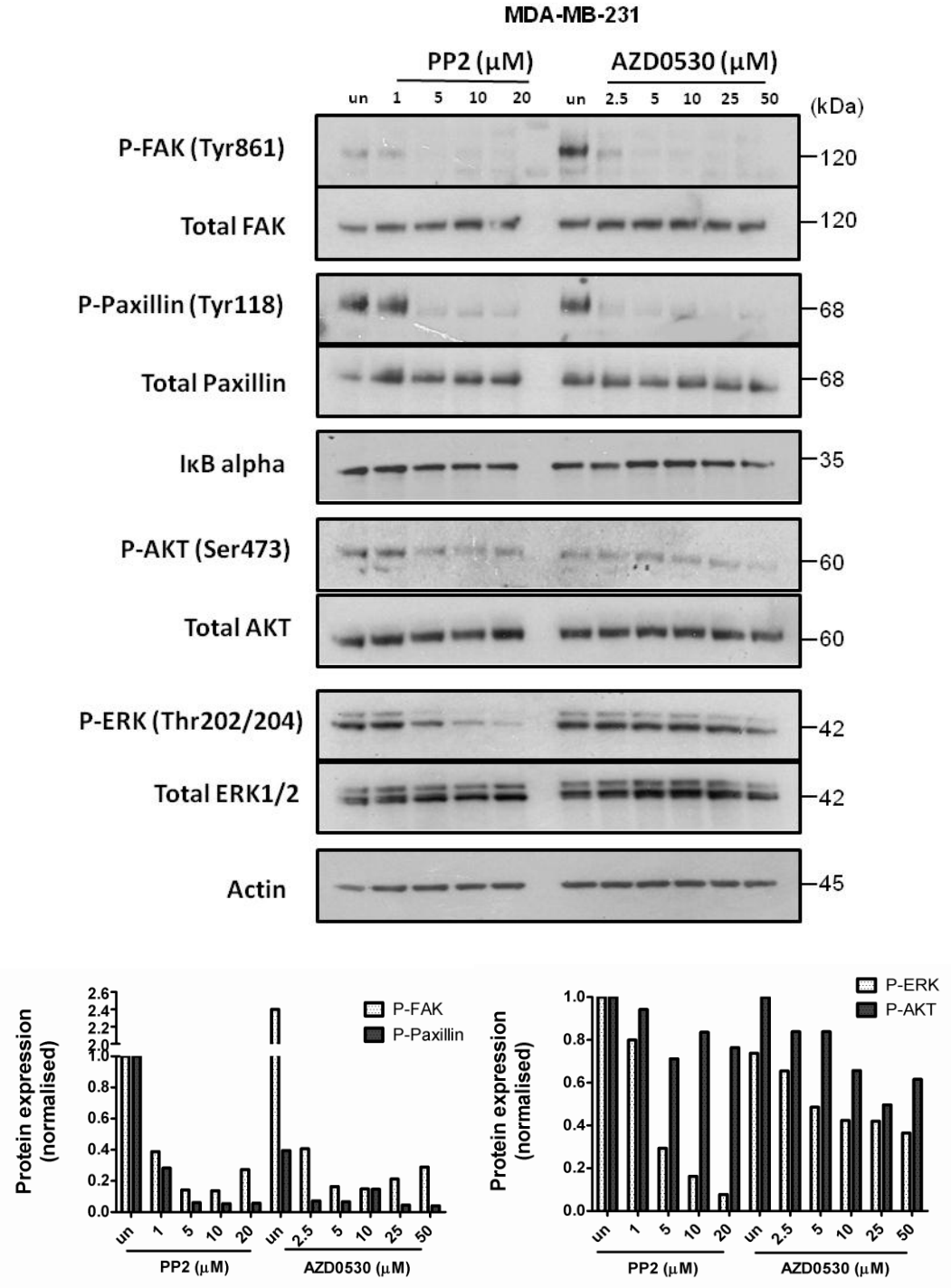

Figure 5.16 PP2 and AZD0530-induced TRAIL sensitivity correlated with active ERK1/2 and AKT reductions in MDA-MB-231 cells. Western blot of a range of downstream signalling proteins in MDA-MB-231 cells following treatment for 1 hr with the indicated concentrations of PP2 or AZD0530. Graphs show phospho FAK, paxillin, ERK and AKT levels quantified and normalised to actin and total levels of each protein and displayed relative to PP2 untreated. This was to account for apparent underloading in the first lane.

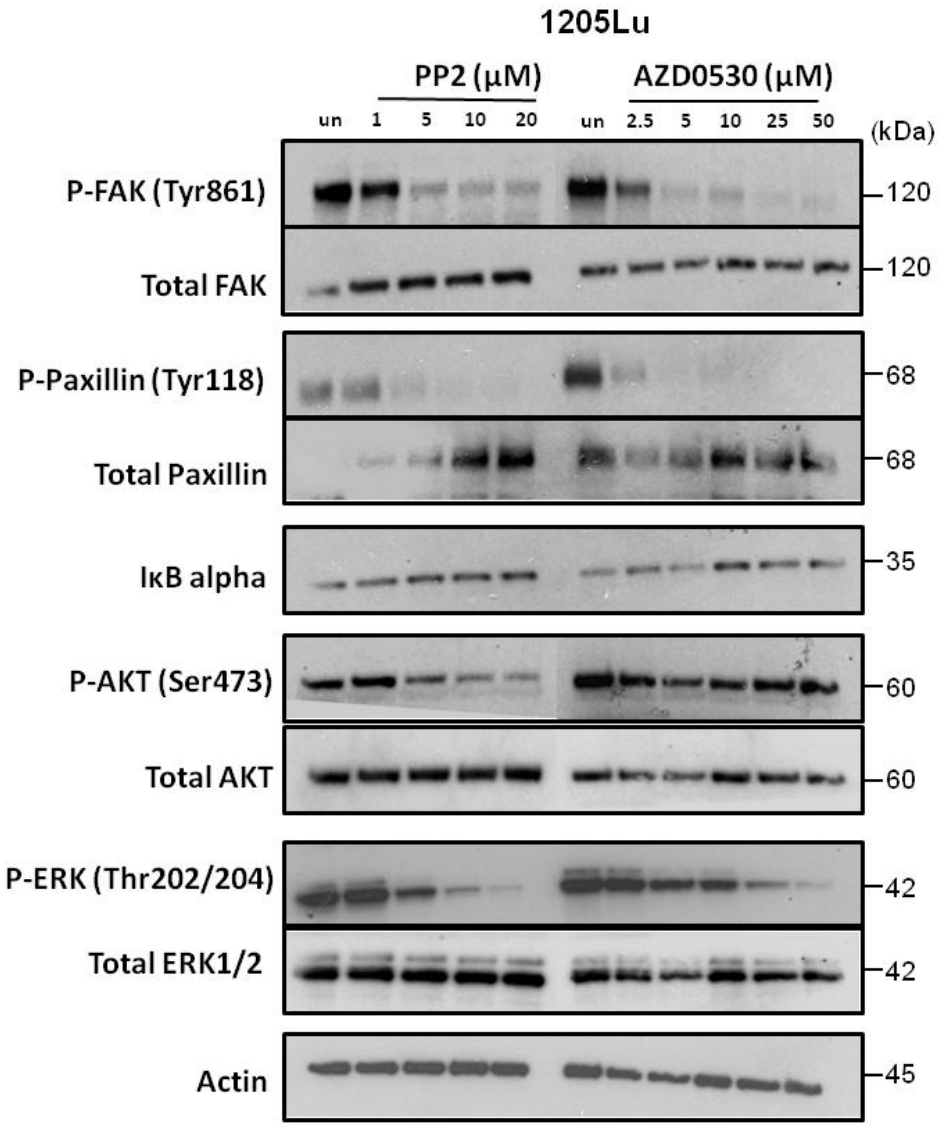

Figure 5.17 PP2 and AZD0530-induced TRAIL sensitivity correlated with active ERK1/2 and AKT reductions in 1205Lu cells.

Western blot of a range of downstream signalling proteins in 1205Lu cells following treatment for 1 hr with the indicated concentrations of PP2 or AZD0530.

In both cell lines, PP2 led to a reduction in the phosphorylation of FAK on Tyr861 and paxillin on Tyr118. These phosphorylation sites were used as they are known to be phosphorylated by active SRC. AZD0530 also led to rapid reduction in phosphorylated FAK and paxillin, even at concentrations as low as 1 μM in MDA-MB-231 cells. This did not correlate with the onset of observed TRAIL sensitivity, which could only be demonstrated at 25μM and above (Figure 5.15). However, the onset of TRAIL sensitivity did match

extremely well with the ability of PP2 and AZD0530 to reduce activity of ERK1/2 and AKT, as shown by phosphorylation of ERK1/2 on Thr202/204 and AKT on Ser473.

5.3.8 ERK1/2 and PI3K/AKT inhibitors

Reductions in AKT activity have been shown to enhance the TRAIL apoptotic response in NSCLC and leukaemia cells (Kandasamy and Srivastava, 2002, Tamagiku et al., 2004), whereas the MEK inhibitor UO126 increased TRAIL-induced apoptosis in human melanoma cells (Zhang et al., 2003a). To investigate whether the AKT and ERK1/2 reductions caused by the SRC inhibitors would be sufficient to cause TRAIL sensitivity in MDA-MB-231 and 1205Lu cells, cells were pre-treated for 1 hr with PI3K inhibitor PI-103 or MEK inhibitor UO126 prior to TRAIL treatment (Figure 5.18).

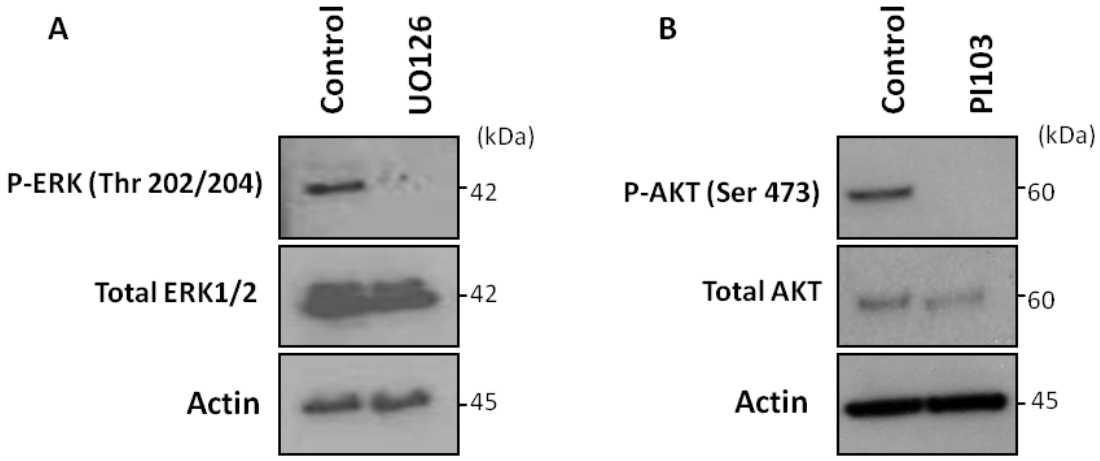

Figure 5.18 UO126 and PI-103 efficiently reduced their targets at the concentrations used. Cells were treated with UO126 (5 μM) and PI-103 (0.8 μM) for 1 hr prior to lysis. **A** Western blots showing the reduction of active ERK1/2 (Thr 202/204) 1 hr after treatment of MDA-MB-231 cells with UO126. **B** Phosphorylated AKT (Ser 473) levels were reduced 1 hr after PI-103 treatment in 1205Lu cells. 1205Lu cells were used for AKT detection because they express much higher protein levels than MDA-MB-231 cells.

UO126 reduced the levels of activated phosphorylated ERK1/2 (Thr202/204) in MDA-MB-231 cells by over 90% (Figure 5.18A), and PI-103 reduced phosphorylated AKT in 1205Lu cells by 100% (Figure 5.18B). The total levels of these proteins remained unchanged.

Thus, MDA-MB-231 and 1205Lu cells were pre-treated for 1 hr with UO126 or PI-103 and then treated with TRAIL. Cells were also pre-treated with combinations of UO126, PI-103 or PP2 prior to TRAIL treatment (Figure 5.19). Reductions in viability were measured 24 hr after TRAIL treatment and expressed as relative TRAIL sensitivity using untreated control cells as a baseline. As previously shown, PP2 alone led to a 2 fold increase in TRAIL sensitivity in both cell lines compared to control cells (Figure 5.19A and B). As expected, the control inhibitor PP3 did not affect TRAIL sensitivity. In both MDA-MB-231 and 1205Lu cells, the MEK inhibitor UO126 increased TRAIL sensitivity by around 45% compared to untreated cells. Similarly, the PI3K inhibitor PI-103 increased sensitivity by 40% in MDA-MB-231 cells and 78% in 1205Lu cells compared to untreated controls. UO126 and PI-103 together additively enhanced the TRAIL sensitivity in both cell lines, increasing it by 2 fold compared to controls. Interestingly, in MDA-MB-231 cells, a combination of PP2, UO126 and PI-103 led to a 2.8 fold increase in TRAIL-induced caspase 3/7 activity, suggesting that in MDA-MB-231 cells, SRC may not be acting solely through ERK1/2 and PI3K to regulate TRAIL resistance. 1205Lu cells also saw greater viability reductions with PP2 in combination with UO126 and PI-103, than UO126 and PI-103 alone, but to a lesser extent than that seen in MDA-MB-231 cells.

To confirm that these reductions in viability are concomitant with increases in apoptosis, cells were pre-treated for 1 hr with the inhibitors before TRAIL addition. Four hours after TRAIL treatment, cells were lysed and blotted for PARP and its cleaved form (Figure 5.19C & D). The 90kDa cleaved PARP fragment could be observed in control cells after TRAIL treatment along with a reduction in full length PARP. Cells treated with PP2, UO126, PI-103 or combinations of the three showed an appearance of the 90kDa cleaved form of PARP, along with larger decreases in full length PARP. The percentage of total and cleaved PARP in each condition was quantified and indicated in a bar chart beside each blot. The pattern of PARP cleavage seen with the different drug treatments mirrored the viability reduction shown in Figure 5.19A &B, confirming that these viability reductions were a result of apoptosis.

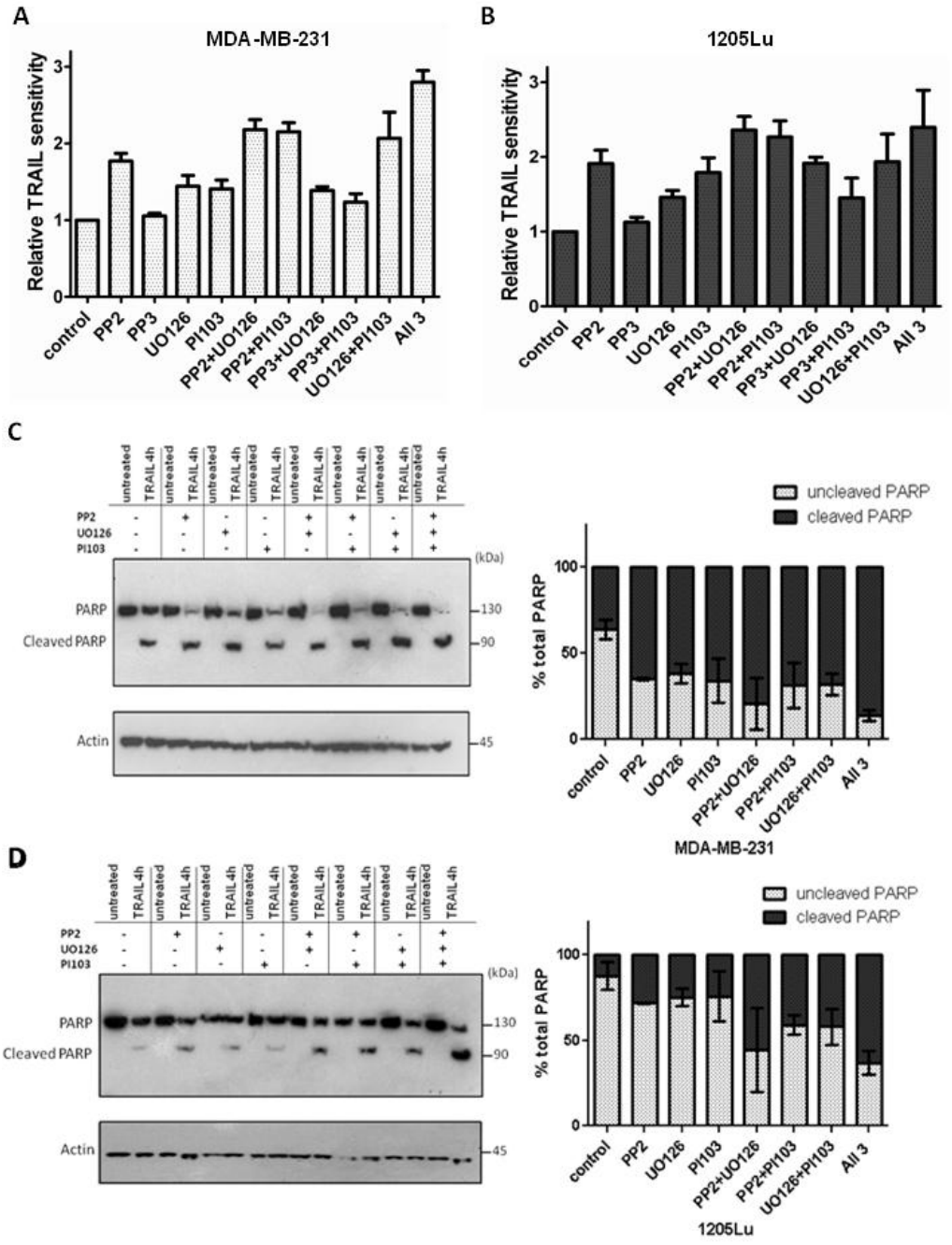

Figure 5.19 TRAIL sensitisation by PP2, UO126 and PI-103. Cells were treated for 1 hr with PP2 (10 μM), UO126 (5 μM), and PI-103 (0.8 μM) prior to TRAIL addition for 24 hr. Viability was then determined with the alamarBlue® assay and expressed as relative TRAIL sensitivity compared to untreated control cells for each condition. **A** Shows TRAIL sensitivity by PP2, UO126 and PI-103 in MDA-MB-231 cells. **B** Shows similar TRAIL sensitivity changes in 1205Lu cells. **C** Four hours after TRAIL treatment, cells were lysed and blotted for full length and cleaved PARP, confirming increased apoptosis in cells pre-treated with combinations of inhibitors in MDA-MB-231 cells. Data are expressed with a representative blot (left) and as quantification of percentage of PARP cleavage averaged from 2 independent blots **D** Similar PARP cleavage patterns were evident in 1205Lu cells. Mean +/- SEM (**A &B** n=6); (**C&D** n=2)

As PI-103 is an inhibitor of PI3K, DNA-PK and mTORC1 (Raynaud et al., 2007), a pan AKT inhibitor was used to determine whether AKT inhibition through PI-103 was responsible for the TRAIL sensitisation observed.

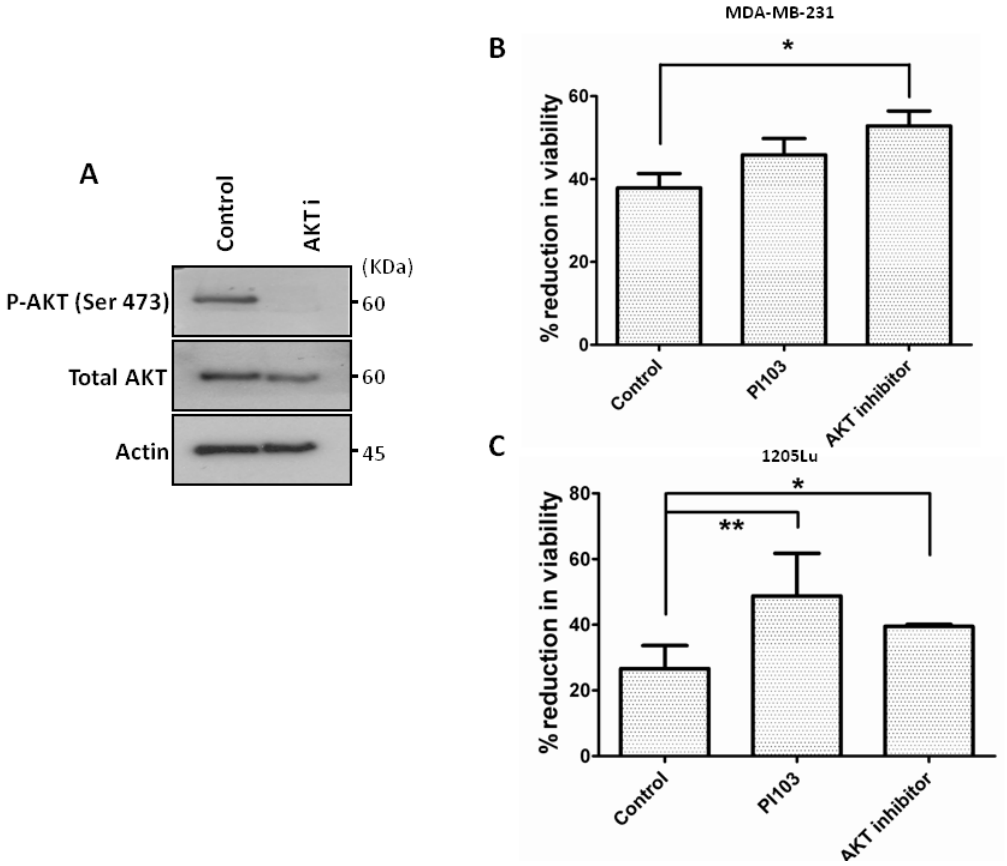

Figure 5.20 AKT inhibition also results in TRAIL sensitisation. **A** 1205Lu cells were treated for 1 hr with an AKT inhibitor (AKTi) (5 μM) and blotted for phosphorylated AKT (P-AKT) on Ser473. The inhibitor resulted in complete ablation of AKT phosphorylation. **B** After a 1 hr treatment with the inhibitor, cells were treated with TRAIL for 24 hr and viability measured using alamarBlue®. MDA-MB-231 pre-treated with the AKT inhibitor showed greater reductions in viability after TRAIL treatment (100 ng/ml) compared to untreated controls. This level was similar to that induced by PI-103. **C** Similar sensitisation results were seen with 1205Lu cells after TRAIL treatment (200 ng/ml). Mean +/- SEM **(A)** n=7; **(B)** n=4 ANOVA (Tukey post-test) *p<0.05 ** p<0.01

As shown in figure 5.20, this AKT inhibitor reduced phosphorylation of AKT on Ser 473 by 100% and increased the TRAIL-induced viability reduction by 15% in MDA-MB-231 cells and 13% in 1205Lu cells. This was comparable to the sensitisation effects seen by PI-103. Therefore the TRAIL sensitivity effect is likely to result from inhibition of AKT downstream of PI3K.

5.3.9 PP2 enhances caspase-9 activation

As presented in Chapter 4, MRTF-A/B depleted MDA-MB-231 cells also showed a reduction in survival signalling through ERK1/2, and exhibited amplification through the intrinsic pathway of apoptosis after TRAIL treatment (Figure 4.15 & 4.17). They also showed increases in protein expression of DR4 and DR5 (Figure 4.9). In contrast to MRTF-A/B depletion, MDA-MB-231 cells treated with PP2 or PP3 showed no correlation between DR4 and DR5 expression level and TRAIL sensitivity (Figure 5.21A), but did show increased caspase-9 activity. Cells were pre-treated for 1 hr with PP2 before TRAIL addition. Samples were taken at intervals after TRAIL treatment and caspase-9 activation determined by Western blot. In untreated MDA-MB-231 cells, TRAIL treatment led to an increase in cleaved caspase-9 after 2 hr (Figure 5.21B). In contrast, MDA-MB-231 cells pre-treated with PP2 showed caspase-9 cleavage as early as 1 hr after TRAIL treatment, with a complete loss of procaspase-9 by 1.5 hr. To investigate this caspase-9 activity in 1205Lu cells, a similar Western blot was performed. 1205Lu control cells treated with TRAIL did not show significant caspase-9 cleavage over the time points investigated, whereas PP2-treated cells showed robust cleavage at 2 hr after TRAIL addition (Figure 5.21C). This suggests that the reduction in survival signalling seen in PP2-treated cells may allow increased activation of the intrinsic apoptosis pathway, similar to that seen in MRTF-A/B depleted cells.

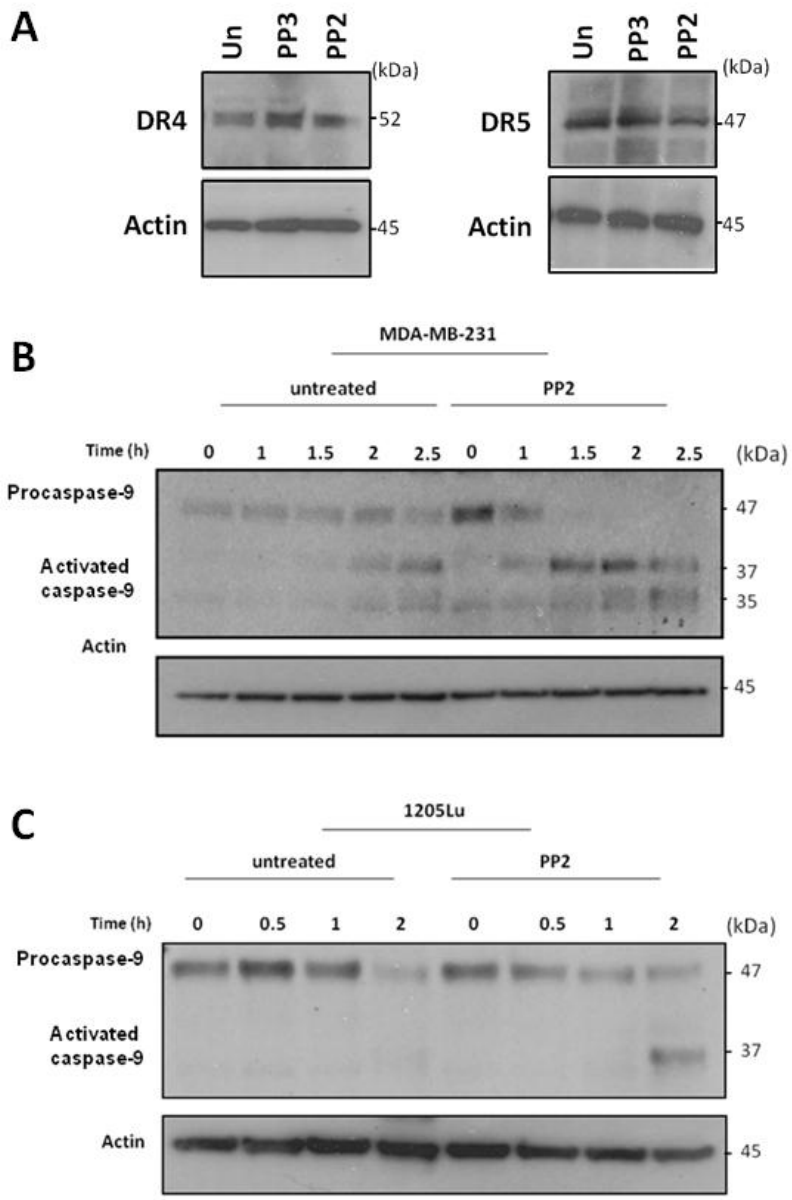

Figure 5.21 PP2 induces caspase-9 activation in MDA-MB-231 cells, while death receptor levels remain unchanged. A Western blots of MDA-MB-231 cells untreated or treated with PP2 or PP3 (10 μM) for 1 hr, showing no correlation between the expression of DR4 and DR5 and TRAIL sensitivity. **B** MDA-MB-231 and 1205Lu **(C)** cells were either left untreated, or were treated with 10 μM PP2 for 1 hr, prior to TRAIL treatment for the indicated durations (MDA-MB-231 cells 100 ng/ml TRAIL, 1205Lu cells 200 ng/ml TRAIL). Both cell lines showed robust caspase-9 cleavage after PP2 treatment.

5.4 Summary of findings

• β1 and β3 integrin blocking and talin 1 reduction can sensitise MDA-MB-231 and 1205Lu cells to TRAIL-induced apoptosis *in vitro*.

• ILK depletion using siRNA does not affect TRAIL-induced apoptosis in either cell line.

•Inhibitors to SRC and FAK can sensitise MDA-MB-231 and 1205Lu cells to TRAIL-induced apoptosis.

•Knockdown of SRC using shRNA can sensitise MDA-MB-231 cells to TRAIL-induced apoptosis.

•The SRC inhibitors PP2 and AZD0530 appear to sensitise cells to TRAIL-induced apoptosis partly through downregulation of AKT, ERK1/2 and/or NFκB, with cells showing enhanced caspase-9 cleavage.

•MEK and PI3K/AKT inhibitors can also sensitise MDA-MB-231 and 1205Lu cells to TRAIL, although the TRAIL sensitivity effect is greater when PP2 is used, or when UO126 and PI-103 are combined.

5.5 Discussion

The data presented in this chapter confirm the hypothesis that targeting specific components of the integrin signalling pathway can sensitise tumour cells to TRAIL-induced apoptosis. In accordance with the two aims stated at the beginning of this chapter, MDA-MB-231 and 1205Lu cell lines were treated with inhibitors or siRNA for β integrins, talin, ILK, SRC and FAK, and their TRAIL sensitivity was determined.

Firstly, the direct attachment of cells to their matrix was blocked at the level of the β integrin receptor. Pre-blocking MDA-MB-231 and 1205Lu cells with integrin β1-blocking antibodies led to the inhibition of cell attachment and spreading. Integrin β1 has also been shown to mediate the adherence of MDA-MB-231 cells to blood vessels *in vivo* during metastatic outgrowth in the brain (Carbonell et al., 2009). Enhanced sensitivity to TRAIL-induced apoptosis was seen in β integrin-blocked cells compared to controls, shown by greater reductions in viability and enhanced caspase 3/7 activity after TRAIL treatment.

β3-integrins bind to fibronectin but not collagen, whereas β1-integrins bind to a broader range of extracellular matrix substrates (Humphries et al., 2006). The data in Figure 5.3 are consistent with this, as β1-block led to TRAIL sensitisation on both fibronectin and collagen, whereas β3-blocking caused sensitisation only on fibronectin. The effect of β3-blocking was only evident in 1205Lu cells, due to lack of the β3-integrin subunit in MDA-MB-231 cells. The ability of 1205Lu cells to signal through both β1 and β3 integrins, compared with only β1 in MDA-MB-231 cells, may also provide some explanation as to why 1205Lu cells show less enhanced TRAIL sensitivity compared to MDA-MB-231 cells when these subunits were individually blocked. The addition of β1 integrin blocking antibodies to adherent neuroblastoma cell lines *in vitro* has been shown to induce spontaneous apoptosis through integrin-mediated death, with apoptosis peaking at 18 hr after treatment (Bonfoco et al., 2000). However, at the time points used for the TRAIL sensitivity assays described in this thesis, there was no measurable apoptosis in β1-blocked cells compared to controls. This again suggests the specificity of the TRAIL sensitivity response. However, a more thorough analysis using PARP cleavage or TUNEL staining could be performed over a range of time points to strengthen this finding.

The second component targeted was talin, which was depleted using siRNA for talin 1. Due to the low expression of talin 2, and the lack of observed compensatory increases after talin 1 depletion in MDA-MB-231 cells, talin 1 depletion alone was deemed sufficient to allow significant overall reductions in talin protein. Talin depletion led to TRAIL sensitivity in both cell lines; however, the sensitivity of talin-depleted 1205Lu cells was two-fold less than that observed in MDA-MB-231 cells. This is likely to reflect their higher expression level of talin 2, as talin 2 can function in place of talin 1 in controlling integrin signalling and attachment (Zhang et al., 2008, Kopp et al., 2010). Knockdown of both talin 1 and talin 2 isoforms in 1205Lu cells may result in TRAIL sensitivity differences comparable to those in MDA-MB-231 cells. In contrast to previous studies reporting talin depletion to reduce the spreading of HUVECs by 70% (Kopp et al., 2010), talin depletion in MDA-MB-231 cells surprisingly did not lead to a large delay in cell attachment

and spreading in this study. This discrepancy could be due to the nature of the attachment surface used in each experiment. In the previous report, HUVEC cells were seeded onto tissue culture plastic. However, the experiments in this chapter were performed on fibronectin-coated surfaces, which promote greater spreading. In support of this, other studies have shown that spreading defects in talin deficient mouse embryonic stem (ES) cells and HeLa cells were more marked on laminin or collagen than on fibronectin (Albigès-Rizo et al., 1995, Priddle et al., 1998). This may be related to the observation that talin depletion in these cells also led to defects in β1 integrin signalling. As attachment to laminin and collagen relies on β1 subunits, spreading may be more impaired on these surfaces than fibronectin which can also be bound by other integrins such as αvβ3 and αvβ6. Recent work has implicated talin in the metastatic process, with high expression levels seen in invasive oral squamous cell carcinoma and in human prostate cancer samples (Sakamoto et al., 2010, Lai et al., 2011). Similarly, talin 1 has also recently been implicated in anoikis resistance through its activation of AKT in prostate cancer cells (Sakamoto et al., 2010). The work in this chapter presents the first report directly linking talin to death receptor-mediated apoptosis, showing that talin activity is important in the regulation of TRAIL sensitivity in a human breast cancer and a melanoma cell line.

The next protein to be targeted was integrin-linked kinase (ILK). Due to certain small molecule ILK inhibitors being reported to show non-specific effects (Eke et al., 2009b), this protein was targeted using siRNA. ILK was chosen due to previous reports implicating its ability to control apoptosis downstream of integrins (Attwell et al., 2000, Troussard et al., 2006). Despite a report that ILK inhibition causes cell spreading defects in the prostate line PC3 (Attwell et al., 2003), MDA-MB-231 cells showed no spreading defect after ILK depletion. However, this finding is in accordance with a report that MDA-MB-231 cells treated with the ILK inhibitor QLT0267 spread normally (Troussard et al., 2006). Therefore the ability of ILK to regulate cell adhesion and spreading at focal adhesions may be cell line dependent. Although implicated in the control of apoptosis through its ability to activate AKT, ILK depletion using siRNA did not

sensitise either MDA-MB-231 or 1205Lu cells to TRAIL-induced apoptosis. This is surprising given that an AKT inhibitor was able to confer TRAIL sensitisation. This suggests that if ILK is reducing AKT activity in this system, it may be being compensated for by signalling through other pathways at the focal adhesion, such as through SRC or FAK. Despite conferring apoptosis protection in a number of bladder cancer cell lines (Gao et al., 2011), ILK has also been shown to relay pro-apoptotic signals through caspase-8 and 9 following irradiation (Hess et al., 2007). Therefore the role of ILK in apoptosis appears complex and has yet to be fully understood. In light of recent evidence of pro- and anti-apoptotic roles for ILK, its potential use as a therapeutic agent should be investigated with caution (Eke et al., 2009a).

The FAK inhibitor PF-228 was shown to be effective in reducing phosphorylation of its target protein p130CAS, and in conferring TRAIL sensitivity in MDA-MB-231, 1205Lu and WM1789 cell lines at concentrations shown to be previously effective *in vitro* (Slack-Davis et al., 2007). This supports a previous finding that TRAIL sensitivity in HL60 leukaemia cells could be modulated by expression of activated FAK (Tamagiku et al., 2004). Although FAK has been shown to influence apoptosis in certain cell lines through its ability to regulate p53 (Golubovskaya et al., 2005), due to the p53 mutant status of MDA-MB-231 cells (Petitjean et al., 2007), it is unlikely to be playing an important role in this cell line. Recent work has also shown that the DD-containing kinase RIP can shuttle between FAK and FAS in a number of cell lines, switching cells between anti-apoptotic and pro-apoptotic signalling (Kurenova et al., 2004). Following reductions in FAK, RIP could preferentially mediate FAS signalling, resulting in apoptosis (Kamarajan et al., 2010). It is possible that RIP may control TRAIL signalling in a similar manner. It has also recently been shown that ovarian cancer ascites can induce TRAIL resistance in ovarian cancer cell lines through integrin-mediated FAK and AKT activity (Lane et al., 2010). These studies suggest that FAK may control TRAIL resistance at multiple levels, and further work will be needed to identify the exact mechanism of sensitivity in these cell lines.

The broad spectrum SFK inhibitor PP2 led to robust TRAIL sensitisation in both cell lines, with the more selective SRC inhibitor AZD0530 showing sensitisation at higher concentrations. TRAIL sensitivity was also reported in two cell lines (hepatoma and colon cancer) *in vitro* after treatment with PP2 and AZD0530 (De Toni et al., 2007), along with the observation of increased efficacy of PP2 compared with AZD0530. As these inhibitors may be affecting other kinases at the concentrations used in this thesis, RNA silencing was also used to reduce SRC levels in MDA-MB-231 cells. SRC knockdown using shRNA also led to an increase in TRAIL sensitivity in MDA-MB-231 cells, identifying a specific role for SRC in the control of TRAIL resistance. In these studies, shRNA targeting SRC only gave up to 50% reduction in SRC expression, despite an attempt to isolate clonal populations by limited dilution. After several rounds of passaging, the SRC depleted cells were lost from the cell population and the phenotype reverted to normal. It is likely that the SRC depleted cells cannot compete with the selective advantage of cells expressing little, or none of the shRNA construct. However, as partial knockdown of SRC still gave a TRAIL sensitivity response, it is possible that full knockdown would increase this response further.

The TRAIL sensitivity seen in both MDA-MB-231 and 1205Lu cells after treatment with PP2 or AZD0530 corresponded with the ability of each inhibitor to reduce signalling through ERK1/2 and AKT. In support of this finding, SRC siRNA and signalling inhibitors have been shown to reduce ERK1/2 and AKT activity in a broad range of cancer cell lines *in vitro* and reductions have also been detected in SRC-depleted tumours *in vivo* (Duxbury et al., 2004b, Trevino et al., 2006, Jallal et al., 2007). The observation that the ERK1/2 and AKT reductions do not correspond with the ability of the inhibitors to reduce paxillin or FAK activity highlights the complexity of signalling downstream of cell attachment. In the cell lines tested in this chapter, the broad spectrum SFK inhibitor PP2 was most effective at reducing the activity of these 'nodal points' of survival signalling in comparison to the more specific AZD0530 or shRNA, explaining the sensitivity results seen in this chapter and in a previous study (De Toni et al., 2007). This may reflect an as yet uncharacterised inhibitory activity of PP2 or may result from the direct effect on cell spreading and

actin turnover (Martin and Leder, 2001). Alternatively, it may reflect PP2's increased specificity towards other SRC-family kinase members compared with shRNA or AZD0530. SFK members such as FYN and YES are also ubiquitously expressed, and FYN can bind to FAK at focal adhesions (Schaller et al., 1994, Cobb et al., 1994). Mutations in all three SFKs; SRC, YES and FYN, lead to much more severe phenotypes both *in vitro* and *in vivo* than mutations in each member alone, suggesting an element of functional redundancy and compensation between these family members (Klinghoffer et al., 1999). Interestingly, increased FYN activity was shown to promote metastasis in pancreatic cell lines *in vivo* and to confer apoptosis resistance through an increase in the BAX/BCL-2 ratio (Chen et al., 2010). Further investigations into the roles of specific SFK members in the TRAIL sensitivity response would be interesting and could be performed using siRNA depletion of each specific family member.

As UO126, PI-103 and a specific AKT inhibitor could also sensitise cells to TRAIL, it seemed likely that SRC mediates a significant proportion of its TRAIL resistance through its activation of the ERK1/2 and AKT pathways. ERK1/2 has been shown to play a role in TRAIL resistance in melanoma cell lines (Zhang et al., 2003a), and more recently to regulate detachment-induced TRAIL sensitivity of skin carcinoma cells *in vitro* (Grosse-Wilde et al., 2008). Similarly, a number of studies over the past year have implicated AKT activity in the regulation of TRAIL sensitivity in ovarian, neuroblastoma, and a number of breast cancer cell lines *in vitro* (Xu et al., 2010, Goncharenko-Khaider et al., 2010, Opel et al., 2011). However, PP2 was able to enhance TRAIL sensitivity even in the presence of UO126 and PI-103, although this was less marked in 1205Lu cells than in MDA-MB-231 cells. This may suggest that ERK1/2 and AKT are not the only signalling pathways regulating TRAIL sensitivity following PP2 treatment, and that the increased NFκB signalling seen in MDA-MB-231 cells after PP2 treatment may also play a role. It also may reflect incomplete inhibition of ERK and AKT by each agent individually, with complete kinase inhibition being achieved with a combination of the three agents. Further experiments could investigate the levels of other survival

pathway components downstream of SRC and FAK, including NFκB, p38 and JNK (Almeida et al., 2000, Rosen et al., 2002).

The TRAIL sensitivity that resulted from PI-103 treatment was shown to be mediated through AKT inhibition, and is unlikely to be mediated through the ability of PI-103 to directly inhibit mTOR or DNA-PK (Raynaud et al., 2007). In support of this, a recent study showed that inhibition of mTOR could not induce TRAIL sensitivity in neuroblastoma cell lines *in vitro*, whereas siRNA for the PI3K subunits could (Opel et al., 2011). Interestingly, in these neuroblastoma cell lines PI-103 treatment did not affect DR4 or DR5 expression, but enhanced BID cleavage and caspase-9 activity after TRAIL treatment. This also supports the findings presented in this chapter, as total levels of DR4 and DR5 in PP2-treated MDA-MB-231 cells were unchanged. Although this may not reflect expression levels on the cell surface, De Toni et al. also reported no differences in cell surface expression levels of DR4 and DR5 after PP2 treatment in Chang liver cells (De Toni et al., 2007). Although De Toni et al. showed increased caspase-8 activity after PP2 treatment, the work in this chapter shows that robust amplification of apoptosis also occurs through intrinsic apoptosis pathway activation in MDA-MB-231 and 1205Lu cells. As discussed in section 5.1, disruption of downstream ERK1/2 and AKT activation after dysregulation of the integrin signalling pathway has been shown to influence a number of apoptotic proteins, including IAPs, BIM, BAX, and FLIPs (Sonoda et al., 2000, Gilmore et al., 2000, Aoudjit and Vuori, 2001, Reginato et al., 2003, Fornaro et al., 2003). It has also been postulated that cytoskeletal rearrangements could release the pro-apoptotic molecules BMF and BIM from their microtubule-mediated regulation (Puthalakath et al., 2001). Therefore there may be many reasons why these cells exhibit increased caspase-9 cleavage, and further work remains to be done to identify the full mechanism behind the TRAIL sensitisation in these cells. Equally, although work in this thesis has focused on the canonical apoptosis initiator caspases 8,9 and 10, recent work has implicated caspase-2 in the control of apoptosis following treatment with drugs which disrupt the actin

cytoskeleton. Therefore it is possible that apoptosis may be mediated by other caspases, not investigated in the scope of this thesis (Ho et al., 2008).

In conclusion, the data in this chapter show that the integrin signalling pathway provides a number of targets for TRAIL sensitisation, and appears to regulate TRAIL resistance, at least in part, through activation of AKT and ERK1/2. Although previous studies have implicated integrin signalling pathway members in regulating anoikis, few have looked at their effects on TRAIL sensitivity. This is the first comprehensive study linking a number of integrin signalling pathway components to TRAIL resistance. It also suggests that activation of proteins such as talin 1, SRC and FAK could not only act as biomarkers for increased motility and invasion, but also for increased resistance to TRAIL therapies. Inhibitors of many of these targets already exist, and are being tested in pre-clinical studies, clinical trials, or are already being used in the clinic. Therefore combining existing inhibitors with a TRAIL therapy could sensitise cancer cells to TRAIL-induced apoptosis *in vivo*. The potential of this will be explored in the final chapter of this thesis.

Chapter 6: PF-573228, PP2 and β1 integrin blocking in combination with a TRAIL therapy *in vivo*

6.0 Hypothesis

Pre-blocking MDA-MB-231 cells with FAK inhibitor PF-573,228, SFK inhibitor PP2 or a β1 blocking antibody can sensitise them to the apoptotic effects of recombinant human TRAIL administration in an experimental mouse model of metastasis.

6.1 Introduction

The work presented so far in this thesis reveals that disruption of cell adhesion and spreading can sensitise MDA-MB-231 and 1205Lu cells to TRAIL-induced apoptosis *in vitro*. Despite showing great promise in preclinical studies (Ashkenazi et al., 1999, Malin et al., 2011), clinical trial data with TRAIL therapies suggest they will be most effective in combination with sensitizing agents (Greco et al., 2008, Trarbach et al., 2010). Although inhibition of integrins, SRC and FAK reduce metastasis in animal models, their role in controlling TRAIL sensitivity is only recently becoming apparent (Tamagiku et al., 2004, Zhang et al., 2009a, Liu et al., 2009). In light of these studies, and the evidence presented in Chapters 3-5, targeting these

proteins in combination with a TRAIL therapy *in vivo* may allow more efficient clearance of metastatic tumour cells from the circulation.

As discussed earlier, an important factor contributing to metastatic inefficiency is the susceptibility of circulating tumour cells to death induced by a number of factors (Wong et al., 2001, Takeda et al., 2001, Laguinge et al., 2004). Although different cell types display varying extents of loss over these early time points, the majority of circulating tumour cells are lost within the first 24hrs after injection into the circulation (Fidler, 1970, Price et al., 1986). As the aim of this project is to investigate the sensitivity of tumour cells to TRAIL signals within the first 24 hr, an assay was required to measure the loss of tumour cells from the lung over these early time points. For blocking agents such as integrin β1-blocking antibodies and PP2, which prevent effective attachment and spreading *in vitro*, it would be interesting to monitor the shape of these cells inside the mouse after injection to investigate whether this effect could be seen *in vivo*. The use of fluorescent labels has greatly enhanced our ability to visualise the metastatic process in more detail (Sahai, 2007).

6.2 Aims

To investigate the hypothesis stated above, the aims for this Chapter are as follows:

•To develop a method of quantifying the number of tumour cells present in the lung at early time points following tail vein injection into mice.

•To develop an automated assay to assess tumour cell morphology within the pulmonary vasculature of the mouse and to test this assay using the MRTF-A/B depleted cells described in Chapter 3.

•To test the ability of recombinant human trail to clear MDA-MB-231 tumour cells from the mouse lung at early time points following injection.

•To investigate whether inhibition of the cell adhesion pathway by targeting β1 integrin, SRC and FAK can sensitise MDA-MB-231 cells to the apoptotic effect of recombinant TRAIL *in vivo*.

6.3 Method development

6.3.1 An assay to quantify tumour cells present in the lung

6.3.1.1 Lung removal

Following tail vein injection, mice were anaesthetised and a tracheotomy performed, allowing the lung to be artificially ventilated (described in Section 2.10.4). The heart was then used to perfuse KRB solution around the lungs, clearing them of blood and unattached tumour cells. The KRB solution was of a physiological composition, allowing the lung to be kept fresh and in a good condition for up to 3 hr after removal. The lung was then removed and carefully placed onto a specially designed chamber into which the lung was rested onto a coverslip. The trachea was connected to a 3-way valve in the chamber, allowing the lung to be inflated onto the surface of the coverslip (Figure 6.1A).

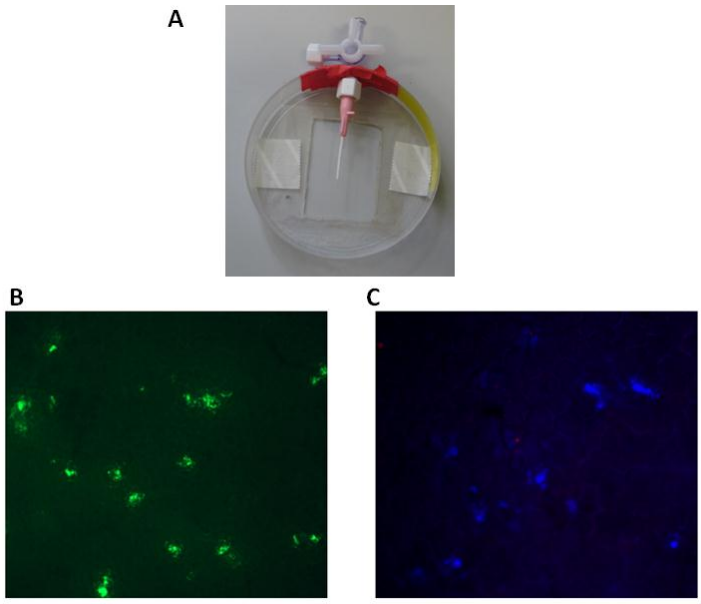

Figure 6.1 Lung scanning using epifluorescent microscopy. A Image of chamber used for lung imaging. **B** Representative images of lungs scanned at 10 x magnification of lungs containing either C4-GFP control MDA-MB-231 cells or C20-CFP MDA-MB-231 cells **(C)**, 4 hr after injection into the tail vein of SCID mice.

To get a representative value for the amount of tumour cells present in the lung, an epifluorescent microscope was used to scan the whole of the left lobe of the lung and images taken (Figure 6.1B and C).

6.3.1.2 Lung cell counts

The number of cells on the lung images could be counted using Image Tool version 2.00 (UTHSCSA) software. This software has a 'count and tag' tool, allowing the researcher to 'tag' parts of the images to aid counting (Figure 6.2).

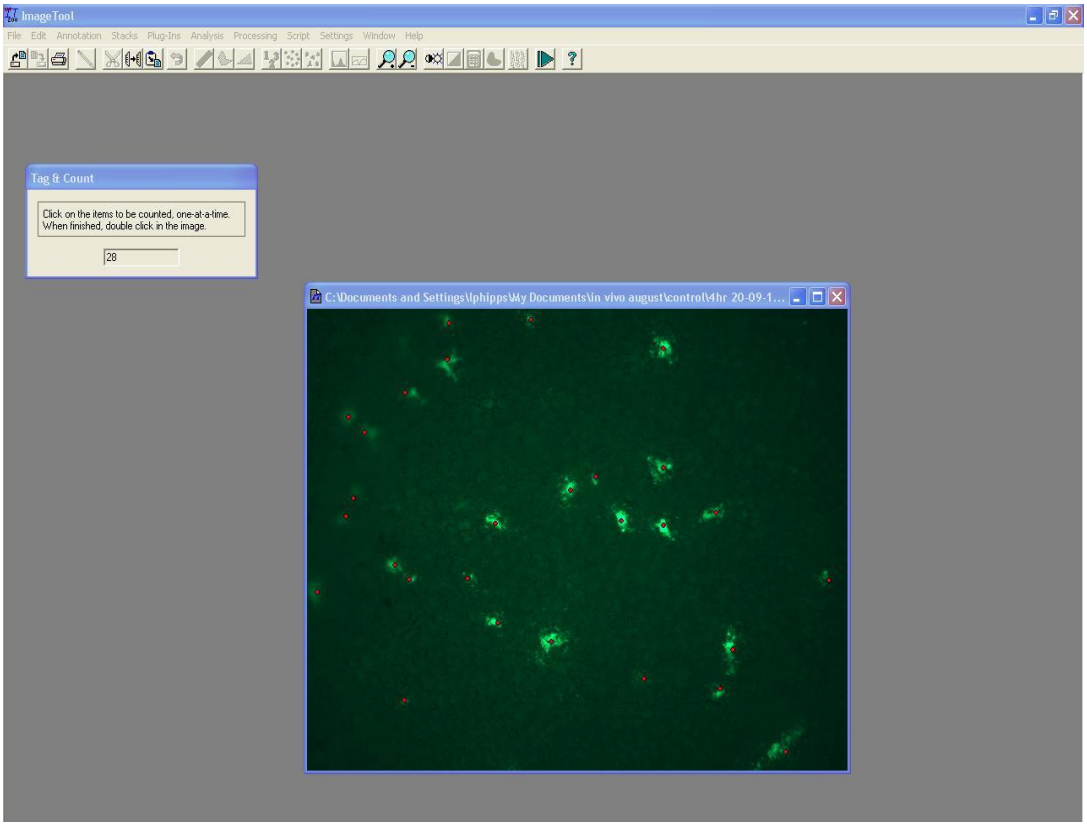

Figure 6.2 Lung foci count method. Screen shot of Image Tool 2.00 software used to tag and count foci according to the criteria outlined below.

In order to maintain consistent counting, the following rules were followed:

1. Bright foci were counted as one cell.
2. Blurred or faint glowing was counted as one cell.

3. Any foci which could be distinguished as multiple cells could be counted as such, however if a large foci could not be distinguished then it was counted as one cell.
4. Small fragments are counted as 'fragments' and were not included in the final analysis.
5. Cells which were half in frame were only counted on the right and bottom edges of the image to prevent multiple counting of the same foci.

6.3.2 An assay to measure cell shape within the pulmonary vasculature of a mouse

MRTF-A/B depletion, β1 integrin blocking, and PP2 treatment all resulted in marked defects in adhesion and spreading *in vitro*. To measure the phenotype of these cells *in vivo*, an assay was developed which used confocal microscopy to create 3D cell images. Software was developed to quantitate the longest length measurement for each cell.

6.3.2.1 Obtaining z-stacks

In order to measure the longest length of single cells within the vasculature of the mouse lung at 4 hr and 24 hr after tumour cell injection, lungs were visualised using an inverted confocal microscope (Zeiss). After counting on the epifluorescent microscope, as detailed above, lungs were taken to the confocal microscope, and imaged using a 40 x oil lens. Once a cell was located within the lung, z-stacks were made over the whole cell volume using Zen 2009 software (Zeiss).

6.3.2.2 Analysing z-stacks

Software was designed and created by Dr. P D Allen (ROB, Oxford) using MatLab 2008 (MathWorks), which allowed the user to define the borders of the cell to be measured by altering the gray level measurement. The software then gives the user a longest length (μm) and volume (μm^3) measurement of each cell. An image of the software is shown below (Figure 6.3), including the screen in which the user can outline the cell of interest (right), the 3D generated image of the cell created (left) and the measurements given out (outlined in the red box).

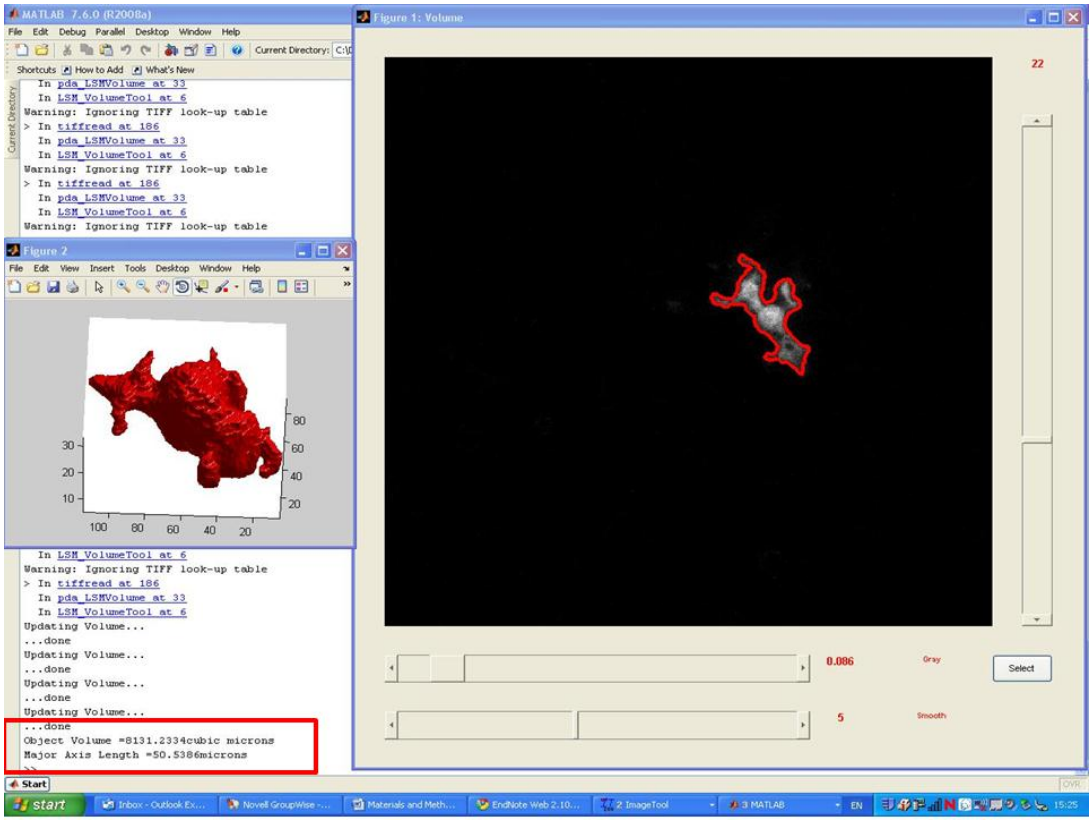

Figure 6.3 Image of MatLab cell shape measurement software designed by Dr P D Allen. The software uses the z-stack image in LSM file format (stack of .tif images), to allow the user to scroll through the stack using the rolling bar on the far right. By altering the gray level value using the rolling bar at the bottom the user can outline the cell of interest. This cell can then be selected, and the software gives the object volume and longest length measurements (red box) and a 3D reconstruction of the cell.

6.3.3 Validation of *in vivo* methodology using MRTF-A/B depleted cells

As discussed in Chapter 4, MRTF-A/B depleted MDA-MB-231 cells show marked cell spreading defects and enhanced TRAIL sensitivity *in vitro*, presenting a good target to test the above techniques. To investigate the range of cell lengths observed with these cell lines *in vitro*, longest length measurements were taken for the MRTF-control and depleted cells used in Chapter 4 after culture on glass chamber slides (Figure 6.4). The length values varied in a Gaussian distribution, with most cells longer than 20 µm. Therefore for analysis, any object with a longest length measurement of less than 15 µm was classed as a 'fragment' of cell and discounted from subsequent analysis. These measurements confirmed that C4-GFP control cells

have a more spread phenotype, with most common longest length measurement of 50 µm, compared to only 30 µm in MRTF-A/B depleted C20-CFP TET cells.

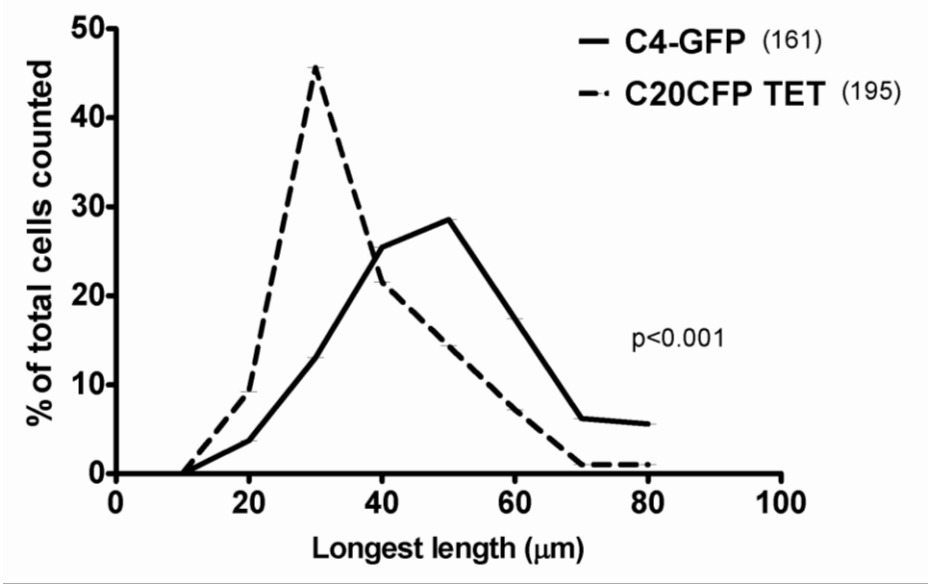

Figure 6.4 MRTF-A/B depleted cells (C20-CFP TET) show a defect in elongation when seeded onto glass chamber slides. C4-GFP control or C20-CFP TET (MRTF-A/B depleted) cells were cultured on glass chamber slides for 12 hr. Longest length was measured on 2D images using Zen2008 Software (Zeiss). MRTF-A/B depleted cells showed marked cell spreading defects, similar to results outlined in Chapter 4. Number of cells counted shown in brackets. Significance calculated using Chi squared test.

The *in vivo* length measurement tool was then used to investigate whether these spreading defect seen *in vitro* in MRTF-A/B depleted cells could also be seen *in vivo*. Z-stacks were taken of cells from the lungs of mice at 4 hr and 24 hr after tail vein injection of C4-GFP or C20-CFP TET cells and longest length measured using the MatLab measurement tool (Figure 6.6A). At 4 hr, C20-CFP TET cells showed shorter length measurements compared to control cells, with few cells spreading longer than 40 µm in length. In comparison, control cells spread up to 80 µm in length, although this difference did not reach significance. By 24 hr post-injection there was no difference in cell length distribution between the two cell lines. This finding validates the MATLAB length tool, showing it to be an effective method of analysing cell shape *in vivo* at 4 hr post-injection.

As previously published, MRTF-A/B depleted C20-CFP TET show enhanced clearance from the lung over 24 hr following tail vein injection (Medjkane et al., 2009). To validate the lung quantitation measurement technique outlined in Section 6.3, these experiments were repeated. Western blots were performed to confirm MRTF-A/B depletion in C20-CFP TET cells prior to injection (Figure 6.6B).

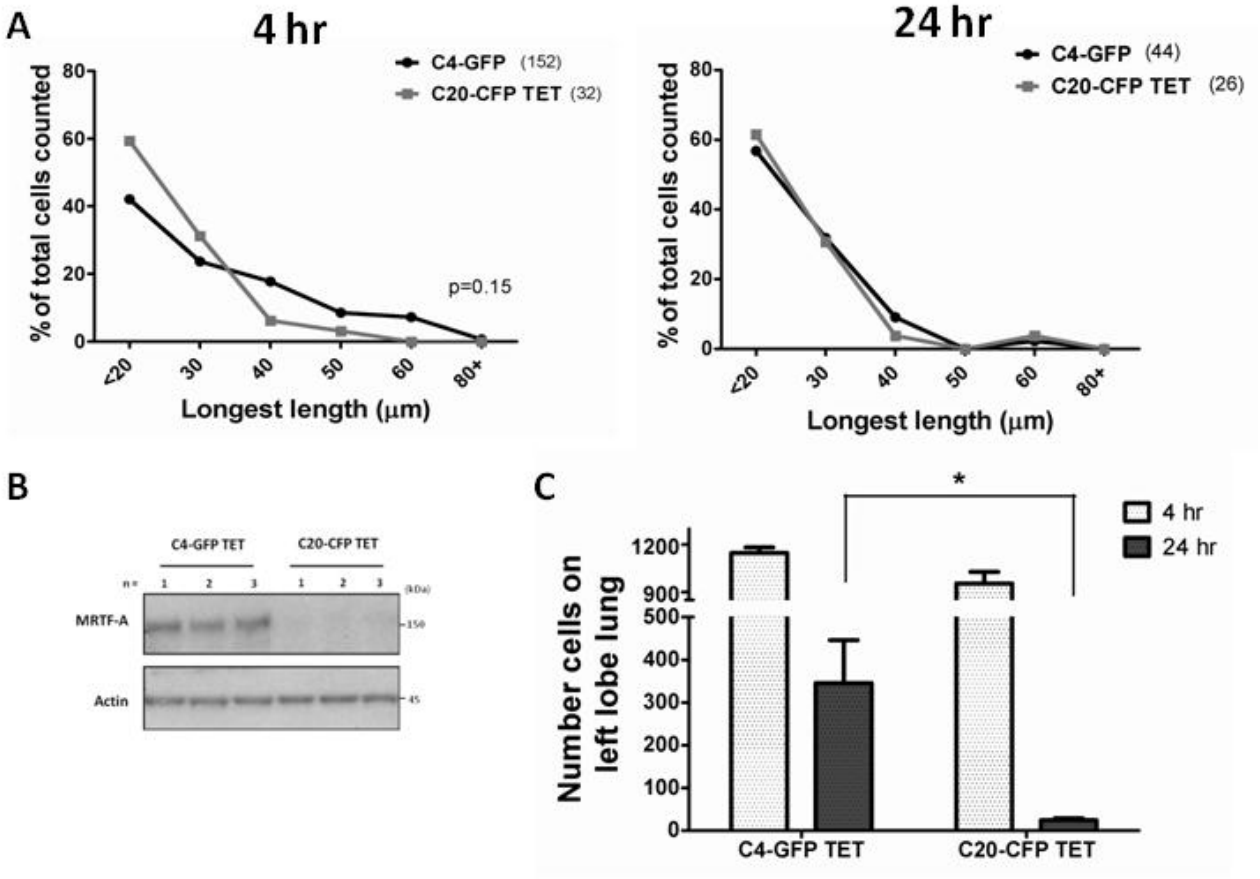

Figure 6.5 MRTF-A/B depleted cells show spreading defects *in vivo* and are cleared more efficiently from the lung during the first 24 hr after tail vein injection. SCID mice were injected with $3x10^5$ cells into the lateral tail vein, with lungs removed and counted 4 hr and 24 hr after injection and longest length measurements taken of cells within the lung vasculature. **A** Z-stack images were taken from tumour cells (number given in brackets) within the mouse lung from over 3 independent experiments, and longest length measured using the tool outlined in Section 6.3.2. At 4 hr post-injection the MRTF-A/B depleted C20-CFP TET cells exhibit shorter lengths, indicating less robust spreading compared to controls. No difference was seen in the cells remaining at 24 hr. Graphs show distribution of cells at different lengths, p value calculated using Chi squared test. **B** Uninjected cells were blotted to verify efficient MRTF-A depletion. **C** Much greater clearance was observed of MRTF-A/B depleted cells from the lung at 24 hr compared to control. Data is Mean +/- SEM n=3 unpaired t-test * $p<0.05$

As a control, C4-GFP cells were also pre-treated with tetracycline (C4-GFP TET). C4-GFP TET and C20-CFP TET cells were then injected into the tail vein of SCID mice and lungs removed and analysed as outlined in Section 6.3.1.2. There was little difference in cell retention at the early 4 hr time point; however, by 24 hr 97% of MRTF-A/B depleted cells had been cleared compared to only 70% of control cells (Figure 6.5C).

6.4 Results

6.4.1 Recombinant human TRAIL (rhTRAIL)

Before combination experiments could be performed, the efficacy of recombinant human TRAIL was tested alone. Tumour cells were injected into the tail vein of mice and the lungs removed at either 4 hr or 24 hr post-injection. To verify that rhTRAIL is effective in clearing circulating tumour cells, a subset of mice were given a single i.v. dose (5mg/kg) of rhTRAIL after 4 hr, with another subset receiving an equal volume of saline i.v. as a control. The single dose of TRAIL reduced the number of cells in the lungs of mice by 70% at 24 hr compared to untreated controls, whereas saline injection had little effect (Figure 6.6).

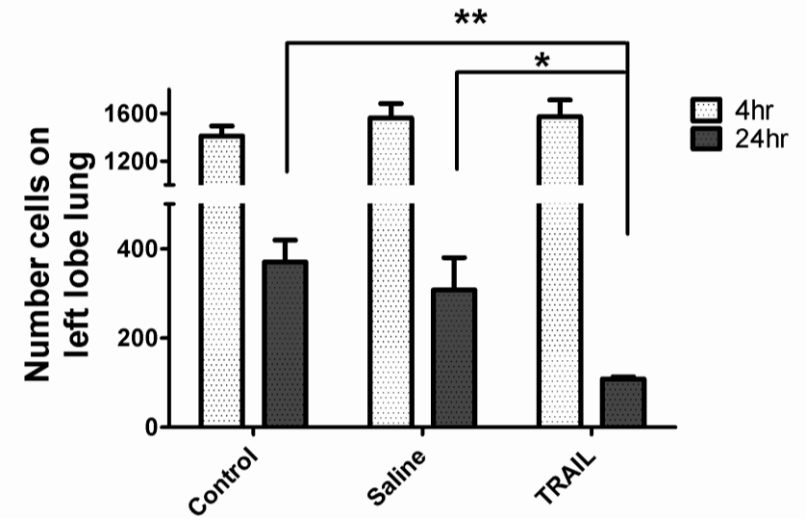

Figure 6.6 rhTRAIL is effective in clearing MDA-MB-231 cells from the lung. Mice were injected with GFP labelled MDA-MB-231 cells into the lateral tail vein. At 4 hr, the lungs were either harvested, or mice were injected i.v. with 100 µl of saline, or 100 µl rhTRAIL (5 mg/kg) and lungs harvested at 24 hr. TRAIL was effective in clearing circulating tumour cells from the lung over 24 hr. Mean +/- SEM n=8 ANOVA (Tukey post-test) * $p<0.05$ ** $p<0.01$

To ensure that rhTRAIL was reducing the number of cells in the lung by increased apoptosis, the number of TUNEL positive cells in the lung was measured.

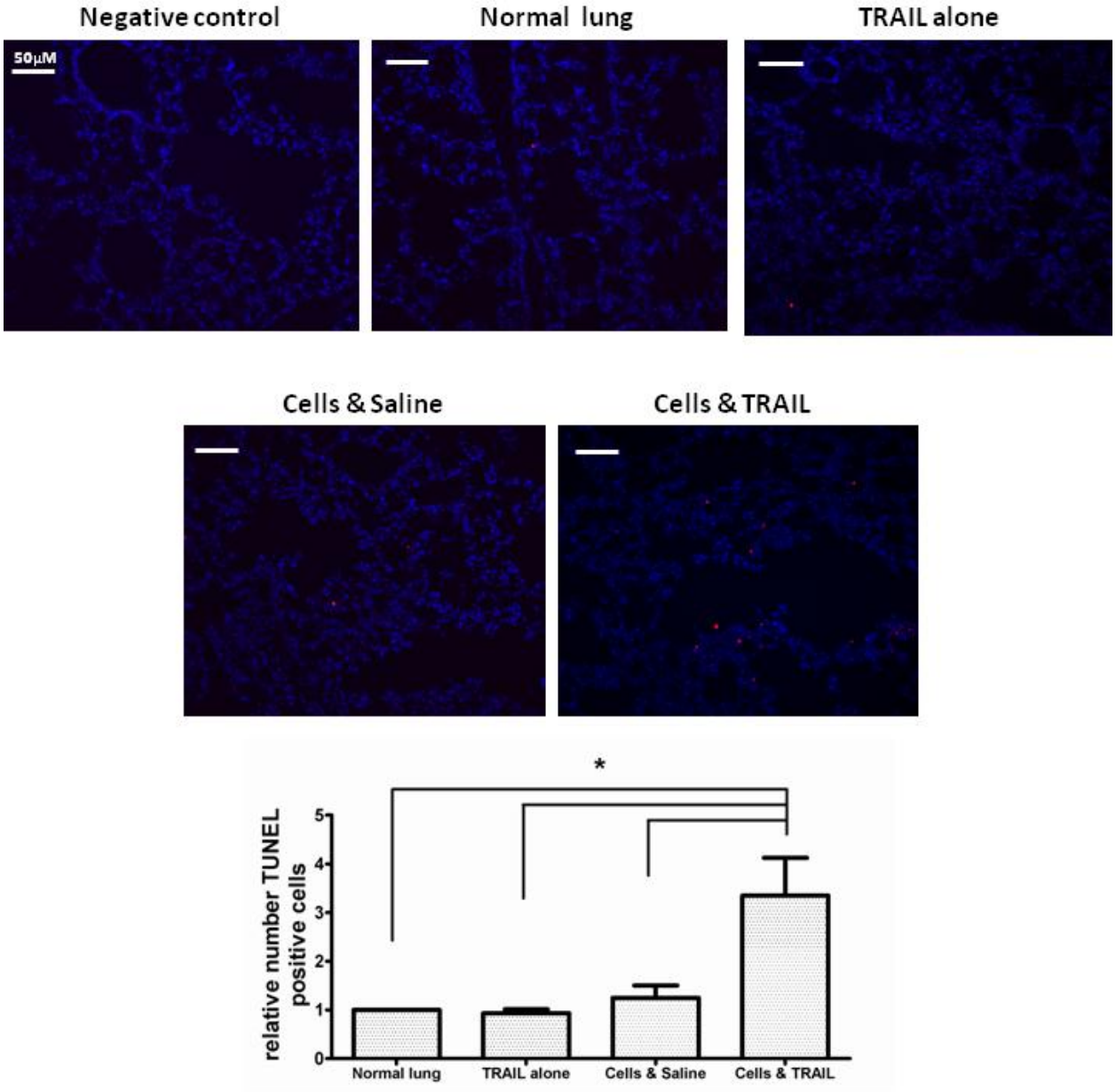

Figure 6.7 rhTRAIL clears MDA-MB-231 cells from the lung by apoptosis, without affecting the normal lung tissue. SCID mice were either uninjected (normal lung), injected with TRAIL (5 mg/kg) alone or injected with MDA-MB-231 tumour cells. At 4 hr after tumour cell injection, these mice were either injected with rhTRAIL or an equal volume of saline. **A** Lungs were isolated, 15 µm sections cut and stained with TUNEL (red) and nuclear Hoechst stain (blue). The active TdT enzyme was omitted from staining in the negative control sections. TUNEL stain was quantified using imageJ (outlined in section 2.7.1). Graph shows mean +/- SEM n=3 mice ANOVA *(Tukey post-test) * $p<0.05$

Lungs were taken from control untreated mice, mice injected with TRAIL alone for 4 hr, mice injected with tumour cells followed by saline, or those injected with tumour cells followed by TRAIL (Figure 6.7). Lungs were isolated, fixed, cut into sections and TUNEL stained. TRAIL treatment alone did not induce apoptosis in the mouse lung compared to the lung of untreated mice. Lungs containing tumour cells alone showed a 25% increase in TUNEL positive staining compared to control lungs, whereas tumour cell-injected lungs treated with TRAIL showed a 234% increase in TUNEL positive staining. This confirms that rhTRAIL treatment is inducing apoptosis specifically in the tumour cells in the mouse lung.

6.4.2 β1-blocking antibodies, PP2 and PF-573,228 in combination with rhTRAIL *in vivo*

The aim of the final part of this chapter is to investigate whether these inhibitors can sensitise MDA-MB-231 cells to rhTRAIL *in vivo*.

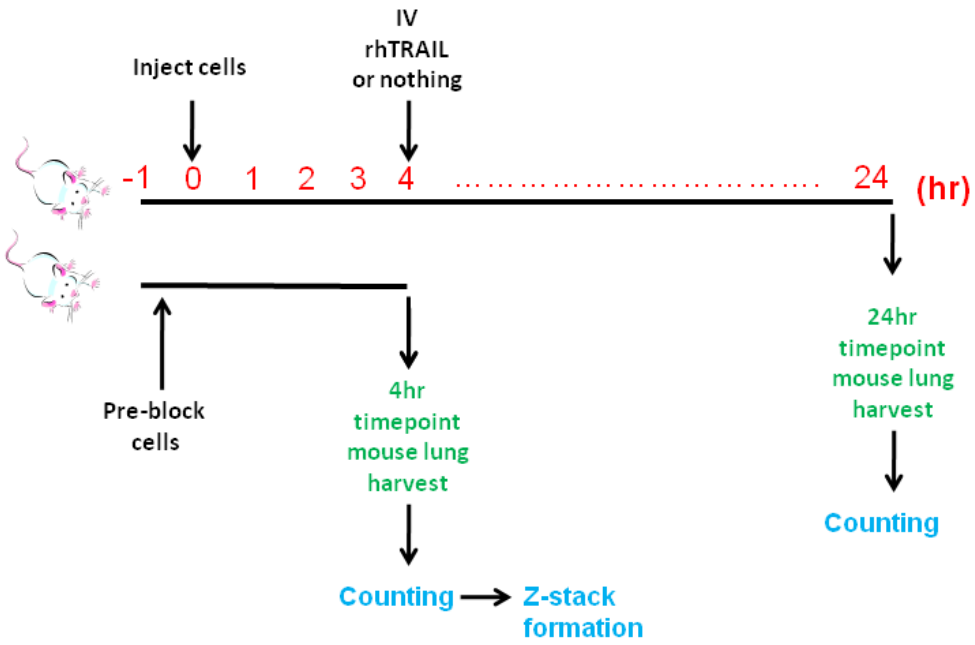

Figure 6.8 Schematic outlining the *in vivo* experimental schedule. A pair of mice were injected with MDA-MB-231 cells which had been pre-blocked for 30 min on ice with the appropriate inhibitor. At 4 hr after cell injection, the lungs of one mouse were harvested, cells on the lung surface counted using epifluorescent microscopy, and then z-stacks taken of individual cells using the confocal microscope. The remaining mouse was either left untreated, or injected intravenously with 5 mg/kg rhTRAIL, and lungs were harvested for counting after 24 hr.

Cells were pre-treated with the appropriate inhibitor 30 min prior to tail vein injection into mice. Mice were either uninjected or injected intravenously with 5 mg/kg rhTRAIL 4 hr after cell injection. Lungs were collected for analysis at 4 hr and 24 hr after injection (as outlined in figure 6.8).

6.4.2.1 PF-573,228 in combination with TRAIL

As shown in Section 5.3.4, the FAK inhibitor PF-228 increased TRAIL sensitivity in MDA-MB-231 cells by 23% *in vitro*. As PF-228 did not lead to marked cell spreading defects *in vitro*, the *in vivo* spreading was not measured. Mice were injected according to the schedule outlined above. The number of cells in the lung at 4 hr was the same in all conditions. By 24 hr, the number of cells in the lung was reduced by 31% in PF-228 treated cells compared to controls, suggesting the importance of FAK signalling in initial tumour cell retention in the lung (Figure 6.9). Following TRAIL treatment, the numbers of both control and PF-228 treated cells were significantly reduced; however, the clearance of PF-228 treated cells was 13% higher than control cells. Although this suggests that PF-228 does sensitise cells to TRAIL *in vivo*, this value did not reach significance.

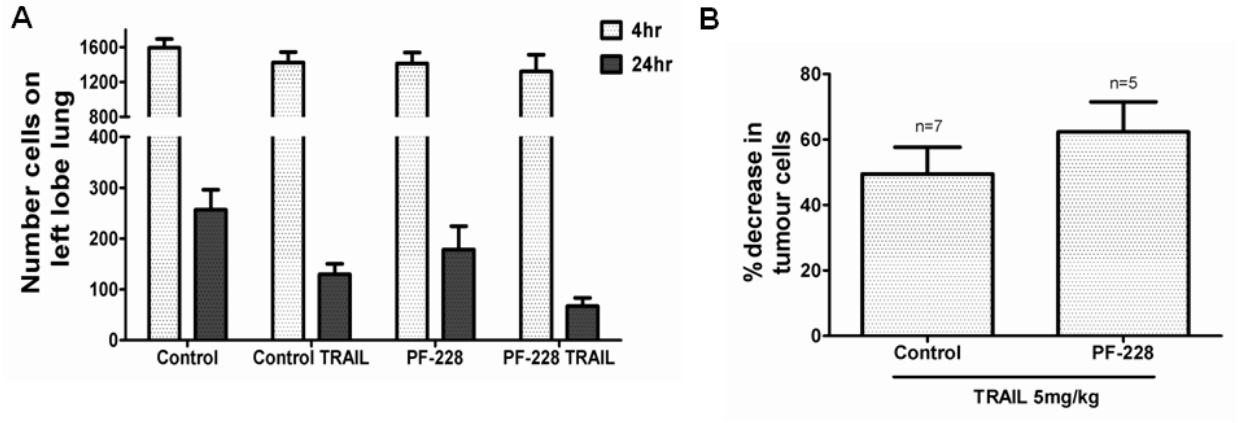

Figure 6.9 FAK inhibition using PF-228 leads to mild, but not significant TRAIL sensitisation *in vivo*. MDA-MB-231 cells were pre-blocked on ice for 30 min with 10 μM PF-228 prior to tail vein injection. Experiments were performed according to the schedule outlined in Figure 6.8 and analysis method outlined in Section 6.3.1 **A** Number of cells on the left lobe of the lung 4 hr or 24 hr after cell injection **B** Decrease of cells after TRAIL treatment compared to non-TRAIL treated controls expressed as a %. Mean +/- SEM (number of mice shown above graph).

6.4.2.2 PP2 in combination with TRAIL

Treating cells with the SFK inhibitor PP2 gave a large TRAIL sensitisation effect *in vitro* (Figure 5.11), with viability of MDA-MB-231 cells after TRAIL reduced by a further 19% compared to PP3 treated cells. PP2-treated cells also showed a 61% reduction in the ability to attach and spread on fibronectin compared to untreated control cells (Figure 5.9). To test whether this spreading defect could be seen *in vivo*, mice were injected with MDA-MB-231 cells which had been pre-treated with 10 μM PP2 for 30 min on ice. At 4 hr post-injection, lungs were scanned with a confocal microscope, cell images acquired, reconstructed and measured using the MATLAB tool outlined in Section 6.3.2. Compared to untreated cells, PP2 treated cells showed a much higher proportion of cells with a longest length of ≤20 μm (Figure 6.10A). Whereas only 20% of PP2 treated cells showed longest length measurements over 40 μm, 33% of control cells were longer than 40 μm. Therefore the spreading defects seen in PP2 treated cells *in vitro* can also be observed *in vivo*.

To investigate whether these defects could result in increased TRAIL sensitivity in vivo, mice were injected with PP2 pre-treated MDA-MB-231 cells followed by i.v. administration of rhTRAIL, as outlined in Figure 6.8. Unlike cells treated with PF-228, PP2 treatment did not alter lung retention at either 4 hr or 24 hr post-injection. However, after TRAIL treatment only an average of 48 cells remained in the left lobe of the mouse lung in PP2 treated cells compared to 130 in the lungs of mice injected with control cells (Figure 6.10B). This constituted a 32% reduction in tumour cell retention in PP2 treated cells compared to controls (Figure 6.10C). Therefore, SFK inhibition does act synergistically with TRAIL treatment to increase clearance of metastatic tumour cells from the mouse lung.

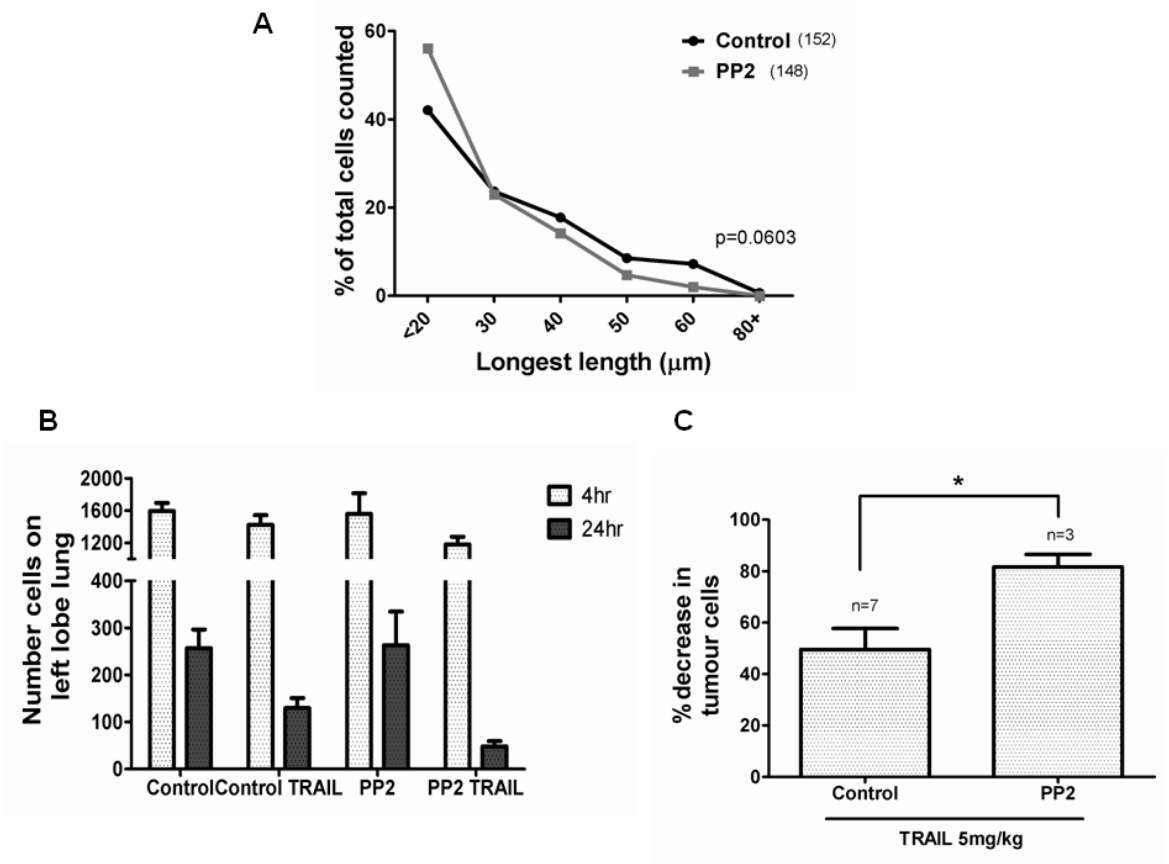

Figure 6.10 PP2 treatment of MDA-MB-231 cells decreases *in vivo* spreading and enhances TRAIL sensitisation. Mice were pre-treated with 10 μM PP2 on ice for 30 min prior to tail vein injection into SCID mice. Control data replotted for case of comparison. **A** At 4 hr after injection, lungs were harvested and cell images taken using confocal microscopy. Longest length measurements were taken for individual tumour cells and shown as a frequency plot. Although PP2 treated cells showed shorter lengths than control cells, this did not reach significance. Number of cells counted shown in brackets. P value determined by Chi squared test. **B** At 4 hr or 24 hr after injection, lungs were harvested and tumour cells counted using epifluorescent microscopy. PP2 treatment alone had no effect on lung retention, but in combination with TRAIL led to significant reductions. **C** Data expressed as a % decrease of cells at 24 hr after TRAIL treatment compared to non-TRAIL treated controls. Mean +/- SEM; number of mice shown above graph; unpaired t-test *p<0.05.

6.4.2.3. Integrin β1 blocking in combination with TRAIL

Blocking MDA-MB-231 cells *in vitro* with a β1 blocking antibody inhibited cell spreading by 85% on fibronectin, and TRAIL treatment led to a reduction in viability which was 19% greater than in control cells (Figures 5.2 & 5.3). To investigate whether the spreading defect in β1-blocked MDA-MB-231 cells is maintained *in vivo*, cells were pre-treated for 30 min with 20 μg/ml of integrin β1-blocking antibody, a

concentration previously used for *in vivo* blocking experiments (Carbonell et al., 2009). Lungs were removed, and analysed using the MATLAB tool. At 4 hr after injection this showed shorter cell lengths in β1-blocked cells compared to control cells, indicating a reduced capacity for spreading (Figure 6.11A).

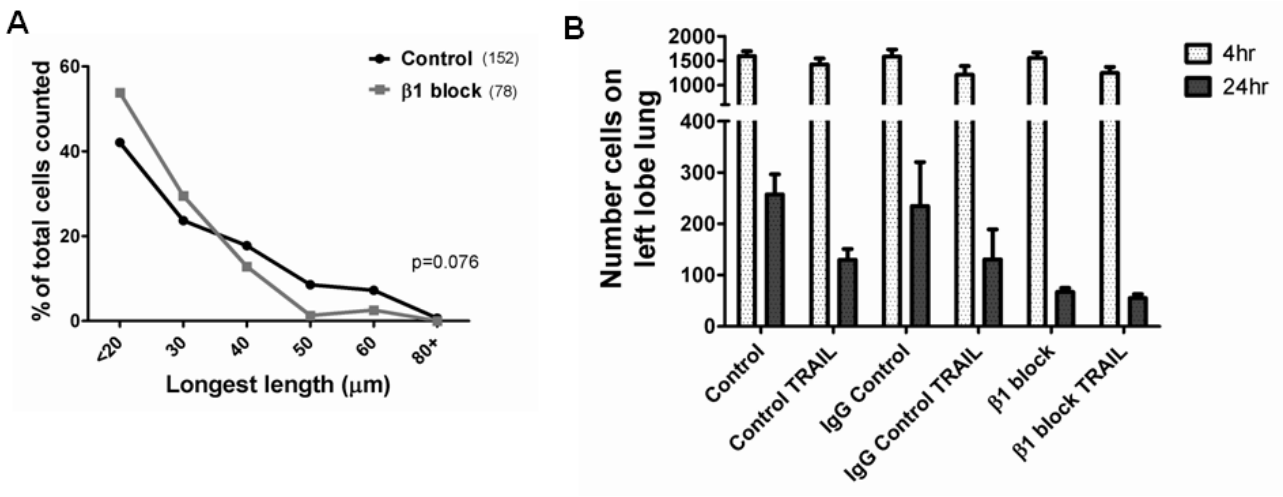

Figure 6.11 Integrin β1 blocking in MDA-MB-231 cells influences spreading and reduces lung retention *in vivo*. MDA-MB-231 cells were pre-treated with 10 μg/ml β1-blocking antibody or control IgG antibody for 30 min on ice before tail vein injection into SCID mice. Control data replotted for case of comparison. **A** Lungs were removed 4 hr post-injection and cell images taken by confocal microscopy. Cell lengths were determined using the MATLAB tool and show distribution differences between the two cell conditions, although these did not reach significance. Number of cells counted shown in brackets. P value determined by Chi squared test. **B** Cells were counted on the left lobe of mouse lungs 4 hr and 24 hr post-injection in all treatment conditions. B1 blocking resulted in large loss of cells from the lung by 24 hr hours. N=7 (β1-block control) n=5 (β1-block TRAIL) n=3 (IgG controls).

This difference was not robust enough to reach significance, but a difference in cell length distribution was evident between blocked and unblocked cells. Whereas 33% of control cells had a longest length measurement of over 40 μm, only 15% of β1-blocked MDA-MB-231 cells showed the same level of elongation.

None of the treatment conditions affected the number of cells in the lung at 4 hr after injection, and pre-treatment of cells with an IgG control antibody did not appear to alter lung retention compared to controls (Figure 6.11B). However, consistent with its characterised roles in the adhesion of cancer cells to the vasculature (Wang et al., 2004, Carbonell et al., 2009), blocking the β1 integrin subunit alone led to a

78% reduction in lung retention by 24hr compared to untreated controls. In combination with TRAIL, this value was not greatly reduced, suggesting that the majority of the TRAIL sensitive cells had already been cleared.

6.4.3 Investigation of an alternative experimental design to reduce variation

Despite increased *in vivo* TRAIL sensitivity in MDA-MB-231 cells pre-treated with PF-573,228 and PP2, only the PP2 treated cells showed a sensitivity increase which reached significance. The experimental design outlined in Figure 6.8 was used as it allowed concomitant analysis of both cell numbers and cell lengths in the same lung immediately following isolation. This enabled fewer mice to be used to obtain data, in line with the 3R's (reduction, refinement, replacement) of humane animal experimentation. However this meant that each lung had to be removed and immediately analysed, preventing more than two lungs from being isolated at the same time. For this reason experiments could not be performed using paired groups of animals, and this resulted in high variation between repeat animals. An alternative method would be to inject a set of mice with the same batch of tumour cells, with each mouse representing a different experimental arm (Figure 6.12). This should reduce the variation as the batch of cells, mice and TRAIL would all be the same, and would allow direct comparison between paired animals in different conditions. As large numbers of lungs would need to be harvested at the same time, this experimental design would prevent immediate analysis, instead requiring lungs to be fixed using PFA, cut into sections and mounted onto microscope slides. It would also mean that these lungs would not be amenable to confocal microscopy for cell length measurements. However, to investigate the potential of this alternative design to reduce error, a pilot experiment was performed. As the difference between control cells and IgG control-blocked cells (in Figure 6.11) showed the highest level of variation despite being expected to show no difference, these were the conditions used for the pilot experiment. Four mice were injected in the schedule outlined below. The 4 hr time point was discarded for this pilot experiment, as differences in the number of cell in the lung at this time point were not seen under any treatment condition.

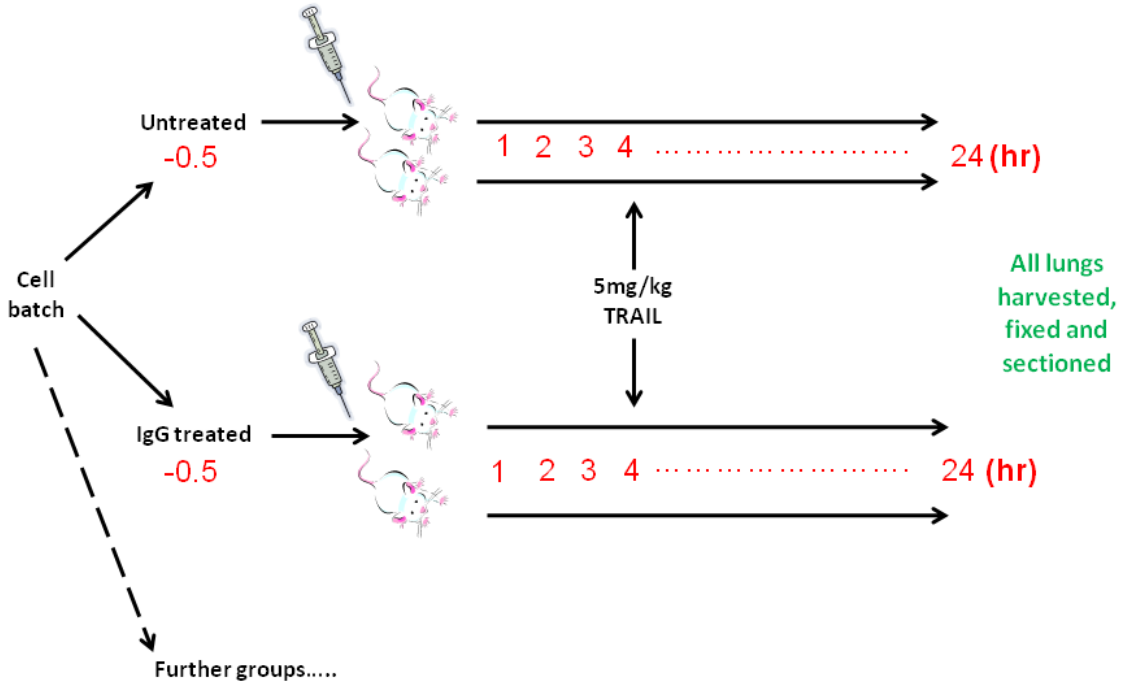

Figure 6.12 Proposal for new experimental scheme. To reduce variation between treatment conditions, large groups of mice could be injected simultaneously, with at least one mouse representing each experimental arm. At 24 hr, following all appropriate treatments, all lungs could be removed simultaneously and fixed to allow long term storage. Lungs could then be sectioned, and cells within the lung counted by microscopy. For this pilot experiment, cells were either untreated or treated for 30 min with IgG control antibody prior to injection. At 4 hr post-injection one mouse from each arm was injected with 5 mg/kg rhTRAIL. Within this experimental design, there is also scope to add further experimental arms.

Lungs were harvested following perfusion with the fixative PFA, and then sectioned into 15 µm thick sections. After mounting onto microscope slides, GFP positive tumour cells in these sections could be easily counted and analysed using epifluorescent microscopy (Figure 6.13A). Cells were counted from multiple lung sections, and showed little variation across sections. This experiment was performed twice, with two different batches of mice and the variation between the control and IgG-blocked mice was much lower than that seen in Figure 6.11B.

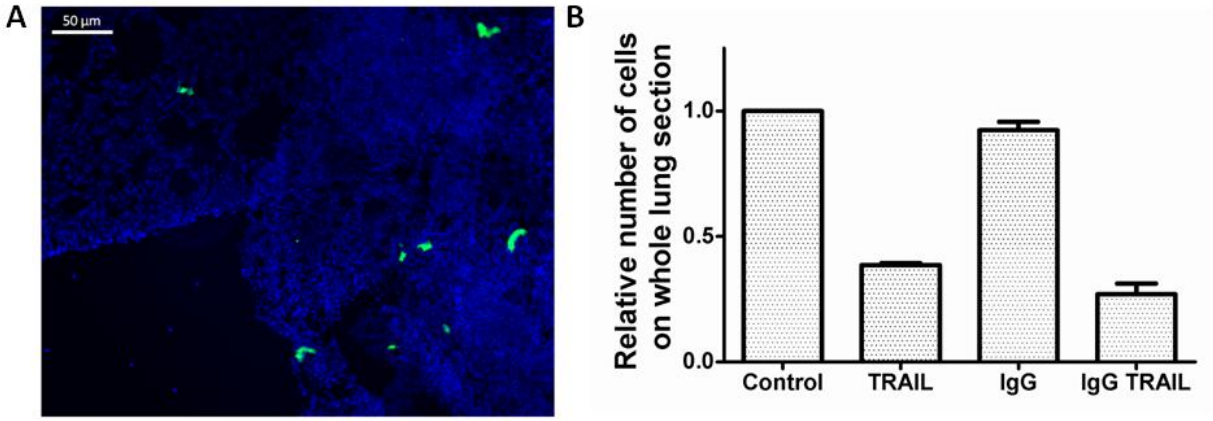

Figure 6.13 Pilot experiment using alternative experimental design shows lower variation. Two SCID mice were injected i.v. with unblocked MDA-MB-231 cells and two injected with IgG blocked cells (10 µg/ml for 30 min) cells from the same cell preparation. At 4 hr post-injection, one mouse from each treatment arm was given a 5 mg/kg i.v. dose of rhTRAIL. At 24 hr after cell injection, all lungs were removed simultaneously, fixed in PFA and stored for sectioning. **A** Lung sections at 10x magnification show easily detectable GFP positive MDA-MB-231 tumour cells within the mouse lung (Hoechst nuclear stain in blue). **B** The number of cells across a whole lung section was counted, and an average calculated from analysis of 6 sections from each lung. Mean +/- SD from two independent experiments.

Therefore this alternative experimental design allows more accurate and comparable data to be obtained, therefore may allow TRAIL sensitisation differences to be more easily detected.

6.5 Summary of Findings

•Software has been developed using MatLab, which allows the measurement of cell length of 3D tumour cells within the mouse lung vasculature.

•MDA-MB-231 cells which are MRTF-A/B depleted, PP2 treated, or treated with a β1 integrin blocking antibody show reductions in cell length *in vivo* in the mouse lung.

•Treatment of mice with rhTRAIL alone causes significant tumour cell apoptosis and clearance from the lung in an experimental metastasis model using MDA-MB-231 cells.

•MDA-MB-231 cells pretreated with PP2 in combination with rhTRAIL lead to a significantly greater increase in tumour cell clearance than rhTRAIL alone.

•Pretreatment with PF-228 leads to a mild enhancement of TRAIL-mediated tumour cell clearance from the lung.

•Pretreatment of cells with a β1 blocking antibody alone led to a large reduction in tumour cell retention in the lung at 24 hr, which could not be enhanced by rhTRAIL treatment.

•The experimental *in vivo* experimental design could be modified to reduce variation in future experiments.

6.6 Discussion

The first two aims of this chapter were to develop assays in which tumour cell number could be quantified in the lung, and cell shape could also be measured. Figures 6.1-6.5 present the method by which these assays were developed and tested in MRTF-A/B depleted and control cells. The MATLAB tool allows the measurement of the longest lengths of cells within the mouse vasculature, giving an indication of how elongated a cell is. This automated method prevents laborious manual measurements of tumour cell axis measurements, and allows analysis of axis length from 3D tumour cells rather than 2D lung sections. The requirement of the user to manually define the cell border before measurement may add error to the measurement value, however this was deemed less than the error from measuring cell morphology from 2D lung slices. One limitation of this model is that autofluorescent signals could lead to false positives during tumour cell analysis, however as signals with a length less than 15 µm were discarded as 'fragments', small noise signals are unlikely to have influenced the final results. Although differences in tumour cell length could be observed following MRTF-A/B depletion, PP2 treatment, and integrin blocking, none of these differences reached significance and the distribution of cell lengths *in vivo* no longer

followed a Gaussian distribution. This may reflect the complexity of the microenvironment *in vivo* compared to *in vitro* tissue culture. Cells are exposed to a variety of growth signals and extracellular matrix molecules within the microenvironment, all of which may influence their morphology. Similarly, tumour cells can become lodged in small blood vessels, therefore limiting their ability to elongate and spread. As shown in Chapter 4, MRTF-A/B depleted cells show characteristic cell spreading defects, and have been previously reported to have reduced colony forming ability in the lung over the first 24 hr following tail vein injection into mice (Medjkane et al., 2009). Therefore, they presented a good model in which to test the assays outlined in this chapter. The *in vitro* spreading defects in MRTF-A/B depleted cells were visible in the lung *in vivo* 4 hr after injection, suggesting that signals from the lung microenvironment cannot allow cells to overcome these defects. This difference at 4 hr did not reach significance, likely due to the small sample size for C20-CFP TET cells. In line with these previous *in vitro* and *in vivo* findings, MRTF-A/B depleted cells (C20-CFP TET) showed greater clearance from the lung 24 hr after tail vein injection compared to control (C4-GFP) cells (Figure 6.5C). There was no difference in cell number in the lung at 4 hr, also a common finding in the early studies of metastatic inefficiency. These studies showed that cells initially lodge in the lung irrespective of their metastatic ability (Fidler, 1970, Price et al., 1986) and that differences between cell lines only become apparent by 24 hr after injection. Interestingly, Medjkane did not attribute the loss of C20-CFP TET cells in the lung to increased apoptosis, as caspase-3 staining in the lung did not show any difference in control vs. MRTF-A/B depleted cells. However apoptotic cells are rapidly phagocytosed *in vivo*, there is likely to be a wide time range over which cells die, and this staining only picks up apoptotic cells at a specific point during the apoptosis process. Therefore staining for a particular stage of apoptosis at a single time point *in vivo* may not yield representative data in this case.

Recombinant human TRAIL was chosen as a method of therapeutic TRAIL delivery as it triggers apoptosis through both TRAIL receptors DR4 and DR5. For MDA-MB-231 cells, a single dose of 5 mg/kg rhTRAIL was

effective in reducing the number of cells in the lung at 24 hr by 65% (Figure 6.6). This is in line with previous studies showing that a single dose of rhTRAIL could induce apoptosis *in vivo* in a mouse xenograft model (Ashkenazi et al., 1999). In chimpanzees, the serum concentration of rhTRAIL after a 5 mg/kg dose was as high as 10 µg/ml after 1 hr (Kelley et al., 2001). This is 100 times higher than the concentrations shown to induce apoptosis *in vitro* in this thesis. In light of this fast-acting ability, and the short half life of rhTRAIL, mice were treated with a single dose 4 hr after cell injection. This corresponded to when the spreading defects were observed to be the greatest (Figure 6.5A). Interestingly, recent work has identified the DR5 agonistic antibody lexatumumab as having a greater effect than the DR4 agonistic antibody mapatumumab in a mouse model of triple negative breast cancer using MDA-MB-231 cells (Malin et al., 2011). Therefore, combining potential inhibitors with lexatumumab may give a greater therapeutic effect in studies using triple negative breast cancers.

TUNEL staining confirmed that rhTRAIL treatment cleared the tumour cells from the lung by apoptosis. Reassuringly, rhTRAIL administration alone did not enhance apoptosis in the mouse lung, in line with previous reports of its specificity for transformed cells (Wiley et al., 1995, Ashkenazi et al., 1999). Lungs containing tumour cells only showed a 25% increase in TUNEL staining, however as mentioned above, the natural kinetics of tumour cell apoptosis in the lung are likely to be much slower than that induced rapidly by TRAIL. Cells are likely to be lost continuously over a period of hours, depending on their interaction with apoptotic triggers such as NK cells within the lung microenvironment. This would mean that significant increases in TUNEL staining may be difficult to detect. Kim et al. showed that TUNEL staining 24 hr after injection could detect increased levels of apoptosis in non-metastatic compared to metastatic cell lines in the lung, suggesting that the time point used in this study may be too early to pick up apoptosis in non-TRAIL injected lungs (Kim et al., 2004). However for the TRAIL-treated mice, all the cells in the circulation were exposed to TRAIL at the same time, creating a robust and rapid increase in apoptosis which was readily detectable through this method.

Once the assays had been developed and tested, and the rhTRAIL treatment shown to be effective, combination experiments were performed with cells treated with PF-228, PP2 and β1-blocking antibody. The ability of PP2 and β1-blocking antibody treated MDA-MB-231 cells to prevent effective cell spreading *in vivo* was measured using the MATLAB tool, outlined in Section 6.3.2. This showed that both inhibitors prevented spreading in the vasculature 4 hr after injection compared to unblocked control cells. Furthermore, these experiments showed that pre-treatment of cells with PP2 could induce significant increases in TRAIL-mediated clearance from the lung over 24 hr, with PF-228 treated cells showing mild but non-significant increases. Interestingly, PP2 completely eliminated FAK activity *in vitro*, a finding also reported for the SRC inhibitor bosutinib *in vivo* (Jallal et al., 2007). Although this may contribute to the enhanced effect of PP2 *in vivo*, the downstream targets of each inhibitor and their ability to cross-inhibit other members was not thoroughly investigated in this work. Previous work has shown that PP2 can also sensitise human pancreatic cell lines to chemotherapy *in vitro* and *in vivo* (Duxbury et al., 2004b, Ischenko et al., 2008), further emphasising its potential role as an apoptosis enhancer. As hepatotoxicity has been reported previously with TRAIL treatments and TRAIL combination strategies (Ganten et al., 2006, Koschny et al., 2007), any novel combination strategy would have to be carefully tested for hepatotoxicity. *In vitro* experiments by De Toni et al. have shown that whilst combinations of TRAIL and PP2 induce high levels of apoptosis in hepatoma cancer cells, they do not enhance apoptosis of normal hepatocytes (De Toni et al., 2007). These data suggest that combination of a SFK inhibitor and a TRAIL therapy may have limited hepatotoxicity *in vivo*. It would be useful to investigate the effects of PF-228 and β integrin blocking on normal hepatocyte apoptosis *in vitro* too. A recent study has also shown that high SRC activity is associated with bone metastasis in breast cancer patients and can protect breast cancer cells from TRAIL-induced apoptosis within the bone microenvironment (Zhang et al., 2009a). By showing that SRC is involved in TRAIL resistance *in vivo*, this study further supports the findings of this thesis that targeting

integrin-mediated signalling pathways in combination with a TRAIL therapy could give beneficial effects on metastasis.

As β1 integrin blocking led to a large loss of cells from the lung after 24 hr, TRAIL treatment only reduced this by a further 20%, compared to 50% for control cells. This indicates that the majority of the TRAIL sensitive cells had already been lost from the lung vasculature. Pre-treating cells with PF-228 alone also led to a significant reduction in lung retention at 24 hr compared to control cells. This is likely to reflect the important roles for these proteins in mediating cell attachment and adhesion to the vasculature (Wang et al., 2004, Carbonell et al., 2009). As MDA-MB-231 cells rely mainly on β1 integrin-mediated adhesion, lacking β3 subunit expression (Figure 5.2), inhibition of this integrin may significantly inhibit sustained adhesion. However, as integrins have also been shown to mediate the protective interaction of tumour cells with platelets in the circulation during metastasis, inhibition of this interaction could make circulating tumour cells more susceptible to NK cell mediated attack. NK cells have been shown to kill circulating tumour cells through expression of perforin, FasL and TRAIL (Smyth et al., 1999, Kayagaki et al., 1999, Takeda et al., 2001), and work by Dr S Hino (Figure 3.2) has highlighted the importance of endogenous TRAIL in the regulation of lung metastasis. For this reason, it would be interesting to investigate whether FAK inhibition or β1 integrin-blocking alone increased the rate of apoptosis in the lung in the absence of the rhTRAIL treatment.

These *in vivo* experiments showed high variation, which could impair the observation of greater differences. This experimental design was chosen over PCR or batch isolation of lungs, as it allowed the sequential extraction of data on cell number and cell morphology, therefore reducing the potential number of mice needed. However, due to the time-consuming and technical method for isolating each lung in this manner, a maximum of only two lungs could be isolated at the same time, preventing multiple paired experiments from being performed. As the rhTRAIL was prone to precipitation 7 days after

purification, new aliquots of rhTRAIL needed to be purified weekly. Therefore mice were injected on different days, often with different batches of cells and different batches of TRAIL, adding large sources for error between repeats. The data presented in Figure 6.13 show that this variation can be reduced by modification of the experimental design, involving injection of large numbers of mice simultaneously, with each mouse representing a different experimental arm. Although this prevents cell shape analysis, it does show reduced variability and allows direct comparisons between paired animals. Further work should investigate the effects of PF-228 in combination with TRAIL using this experimental design, as the reduced variability may yield greater differences between untreated or PF-228 pre-treated cells.

Experimental metastasis models allow the consistent generation of large numbers of site specific metastasis. They also allow the rapid and controlled analysis of the later stages of the metastatic process. Therefore, this model provided a convenient and efficient method for the investigation of cancer cell survival within the vasculature. However, as these models bypass the early stages of cancer cell extravasation, they do not completely represent the physiological metastatic process. Equally, although pre-treating tumour cells with inhibitors *in vivo* allowed simple investigation into TRAIL sensitivity, again this does not represent a therapeutically viable strategy. To more closely approach the physiological situation, mice could be injected orthotopically with MDA-MB-231 cells into the mammary fat pad. Once the tumour had reached a certain size, mice could be treated systemically with both TRAIL therapy and an appropriate inhibitor. In an orthotopic mouse model using MDA-MB-231 cells in BALB/c *nu/nu* mice, daily treatment with bosutinib SRC inhibitor by oral gavage led to a reduction in primary tumour growth and a reduction in the number of metastatic foci (Jallal et al., 2007), therefore adding a TRAIL treatment step into this kind of experiment would not be difficult. Another advantage of measuring metastatic growth in this manner is that it is measured over a longer time period than 24 hr. The experiments outlined in this chapter investigated cell retention at this time because the first 24 hr were shown to be the most important for tumour cell survival in the vasculature (Fidler, 1970, Price et al., 1986, Wong et al., 2001,

Kim et al., 2004). However, no analysis was performed to determine whether there was a difference in proliferation rate or senescence in the cells remaining at 24 hr after each treatment. It is also possible that the cells co-treated with TRAIL and a cell adhesion/spreading inhibitor may continue to die more readily beyond the 24 hr time point. Therefore investigating the number of metastatic foci in a long-term experiment may show a more significant effect of the combination therapy. As endogenous TRAIL expression has been well characterised on NK cells in the liver, it would also be interesting to evaluate the effect of these combinations on liver, as well as lung metastasis.

In conclusion, this chapter presents a useful tool for the analysis of tumour cell morphology in the mouse lung *in vivo*. It also presents data showing that the SRC family kinase inhibitor PP2 can act synergistically with rhTRAIL to clear MDA-MB-231 breast cancer cells from the mouse lung, with a FAK inhibitor also showing promising results. Further work is needed to gain less variable data, and to investigate these sensitisation effects in other cell lines and other types of *in vivo* metastasis model.

Chapter 7: General discussion

The overall aim of this thesis was to investigate the hypothesis that inhibition of cell adhesion could sensitise tumour cells to TRAIL-induced apoptosis. TRAIL sensitivity was defined as an increase in TRAIL-induced apoptosis which was greater when TRAIL was used in combination with a secondary agent, than the apoptosis caused by each agent when used individually. This hypothesis was shown to be correct under the majority of circumstances tested *in vitro,* and outlined in the first three results chapters. This finding is in line with previous reports that detachment can control sensitivity to apoptosis induced by FasL and TNF-α *in vitro* (Shain et al., 2002, Rosen et al., 2002, Fornaro et al., 2003). The proteins targeted are outlined in Figure 7.1.

7.1 Adhesion-mediated TRAIL sensitivity

Chapter 3 presents proof of principle experiments whereby anoikis-resistant human breast cancer and melanoma cell lines were cultured on low attachment plates and shown to be significantly more sensitive to TRAIL-induced apoptosis. These findings confirmed a previous study that suggested a role for matrix adhesion in controlling TRAIL resistance in MCF7 breast cancer cells (Goldberg et al., 2001), and added further support to the hypothesis presented above. All three cell lines showed TRAIL sensitisation,

independent of their basal level of TRAIL resistance, and investigation into apoptosis protein expression changes in MDA-MB-231 cells showed increased expression of DR5 in cells in low attachment conditions.

To further investigate whether cell adhesion and spreading defects could alter TRAIL sensitivity, Chapter 4 utilised a cell model in which cytoskeletal gene expression in MDA-MB-231 cells could be reduced through inducible RNA silencing of the transcriptional coactivators MRTF-A and B.

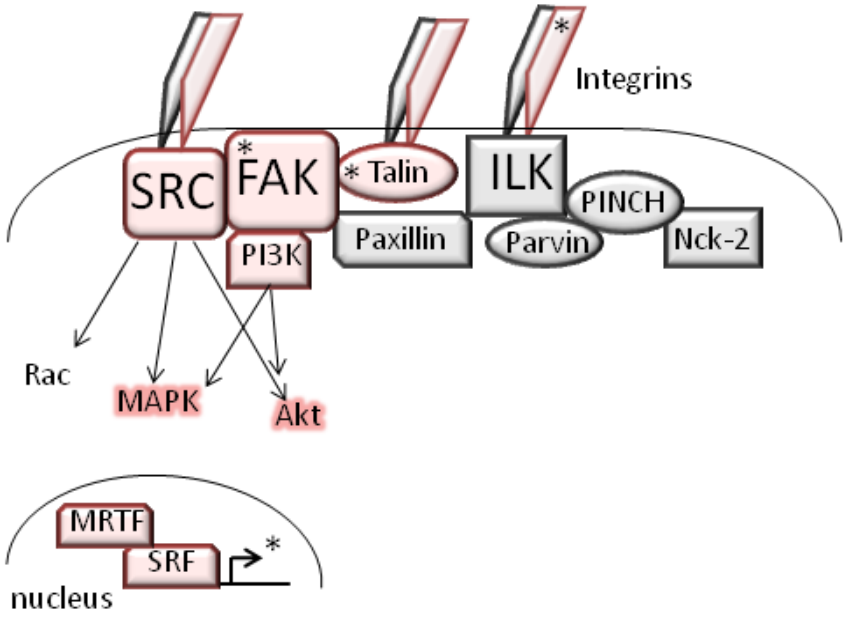

Figure 7.1 Schematic representation of the proteins targeted in this thesis. Red shading represents pathway members whose depletion leads to TRAIL sensitisation in this thesis. Grey boxes represent molecules which have either not been tested or do not sensitize to TRAIL in this thesis. * denotes either computationally predicted or known targets of SRF.

The work presented in that chapter confirmed reports of marked attachment and spreading defects in MRTF-A/B depleted cells, and showed sensitisation to both TNF-α and TRAIL-induced apoptosis (Medjkane et al., 2009). These cells also showed higher protein levels of both receptors DR4 and DR5, however only DR5 levels were increased at the surface and DR5 was shown to be more important for transducing the apoptotic signal. MRTF-A/B depleted cells also showed reductions in OPG transcription and secretion, however this was not at a concentration high enough to protect from TRAIL induced apoptosis. These cells

showed a reduction in signalling through ERK1/2, and showed variable alterations in the intrinsic apoptosis pathway components BCL-2 and HTRA2/Omi. To further support the presence of susceptibility in the intrinsic apoptosis pathway, MRTF-A/B depleted cells showed robust caspase-9 activation. This was the first report showing the ability of MRTF-A/B to control TRAIL sensitivity, and the first to show that human MRTF-A/B can control sensitivity to TNF-α, as previously shown with mouse mrtf-a (Sasazuki et al., 2002).

Chapter 5 then went on to look at the role of specific integrin signalling molecules in the control of TRAIL sensitivity in MDA-MB-231 and 1205Lu cells. This showed that targeting β1 and β3 integrin subunits, talin, SRC and FAK with siRNA or inhibitors leads to TRAIL sensitisation, however ILK knockdown did not. The SFK inhibitor PP2 was likely to sensitise cells to TRAIL through its inhibition of a number of survival signalling pathways, including AKT and ERK1/2. Interestingly, PP2 treated cells did not show receptor level changes, but did again show increased caspase-9 cleavage, indicative of intrinsic apoptosis pathway amplification.

7.2 TRAIL sensitivity mechanisms

The first 2 chapters of this thesis show the importance of death receptor expression in the control of TRAIL resistance following matrix detachment. DR5 expression levels were increased in MDA-MB-231 cells on low attachment plates and surface DR5 expression increased in MRTF-A/B depleted cells. For MRTF-A/B depleted cells this increase appeared to arise as a result of reduced degradation rather than increased transcription. In support of this finding, recent work has found detachment induced relocalisation of DR5 from the Golgi to the cell membrane in an oesophageal cancer cell line (Liu et al., 2009). Previous studies have also shown the importance of DR5 for controlling anoikis (Samara et al., 2007, Laguinge et al., 2008), suggesting that rhTRAIL or DR5 blocking monoclonal antibodies such as lexatumumab may have more therapeutic effect than a DR4 blocking antibody when used in combination studies.

Cell detachment has also been shown to increase cell surface levels of Fas (Aoudjit and Vuori, 2001, Kamarajan et al., 2010). Interestingly, although little differences in Fas expression were detected on the protein arrays, TNFR1 levels were substantially increased both in low attachment conditions and following MRTF-A/B depletion. This increase in TNFR expression in MRTF-A/B depleted cells could explain their enhanced sensitivity to TNF-α induced apoptosis, suggesting a switch from anti- to pro-apoptotic TNFR signalling. Although further work was not done to investigate this response to TNF-α, it would provide an interesting avenue for additional research.

Interestingly, PP2 treated cells did not show similar increases in death receptor levels at the whole cell protein level, further confirmed by other reports using PP2 (De Toni et al., 2007). Therefore although death receptor changes induced by cell detachment seem to be common in many cell lines, this effect may still be cell line dependent.

Both PP2 treated and MRTF-A/B depleted cells showed increased activation of the intrinsic apoptosis pathway through caspase-9. This is unlikely to be mediated through p53, as MDA-MB-231 cells have mutant p53 (Petitjean et al., 2007). In the case of MRTF-A/B depleted cells, increased expression of BID could result in increased BID cleavage following caspase-8 activation from the DISC. It is also possible that alterations in the levels of BCL-2 family proteins could allow increased caspase-9 activation, with mild reductions in BCL-2 expression shown in MRTF-A/B depleted cells. Although the work in this thesis does not characterise the exact mechanism behind this amplification, many studies have implicated intrinsic apoptosis pathway members such as BCL-2, BCL-X_L, BIM and BAX in the control of apoptosis following disruption of attachment or integrin signalling (Gilmore et al., 2000, Matter and Ruoslahti, 2001, Coll et al., 2002, Reginato et al., 2003, Galante et al., 2009). However, the control of apoptosis protein expression by attachment appears to be dependent not only on the cell line but on the matrix type and even the integrin subunit involved. For example, Fornaro and colleagues found that although attachment of PC3 cells to

fibronectin could increase survivin levels and protect from apoptosis, this response was not seen in LNCAP cells cultured on fibronectin. Similarly, after attachment of PC3 cells to laminin rather than fibronectin, BCL-2 expression was altered, with survivin levels unchanged (Fornaro et al., 2003).

Numerous studies have also implicated the importance of survival signalling pathways such as AKT, ERK1/2, NFκB and p38 in the control of apoptosis proteins downstream of cell attachment, but the dominating pathway appears to differ between cell lines and culture conditions (Sonoda et al., 2000, Lane et al., 2008, Grosse-Wilde et al., 2008). In this thesis, ERK1/2 inactivation was seen both in MRTF-A/B depleted and PP2 treated cells, and correlated with the onset of TRAIL sensitivity. AKT inactivation was also seen in PP2 treated cells, and the TRAIL sensitivity effect was likely to be mediated by a combination of the inhibition of the two, along with the disruption of NFκB and potentially other unidentified signalling pathways. Reduction in the activity of these survival signalling pathways may account for the increased activation of the intrinsic apoptosis pathway in these cells, as ERK, AKT and NFκB are known to regulate the expression of a number of proteins involved in the intrinsic apoptosis pathway (Sonoda et al., 2000, Gilmore et al., 2000, Aoudjit and Vuori, 2001, Reginato et al., 2003, Fornaro et al., 2003). A number of recent studies have implicated AKT signalling in the control of TRAIL resistance in ovarian, neuroblastoma and breast cancer lines both in general (Opel et al., 2011), and after disruption of adhesion (Lane et al., 2008, Lane et al., 2010). The authors of these studies suggest the potential for AKT inhibitors as a combination strategy with TRAIL therapy. However, MDA-MB-231 cells have been shown to express low levels of active AKT, with their anoikis resistance being mediated through ERK1/2 signalling (Eckert et al., 2004). Similarly, enhanced TRAIL sensitivity in detached mouse carcinoma cells was shown correlate with reductions in ERK1/2 and not AKT activity (Grosse-Wilde et al., 2008). The data presented in this thesis shows the importance of both ERK1/2 and AKT in the control of TRAIL sensitivity in both MDA-MB-231 and 1205Lu cells. By inhibiting ERK1/2 and AKT signalling, a combinatory increase in TRAIL sensitivity could be observed. Other survival pathways have also be implicated in the control of apoptosis following

detachment including reductions in NFκB and induction of p38 (Rosen et al., 2002), and the dependence of cells upon a particular pathway for survival is likely to be dependent on cell type and mutation status. Therefore targeting cell adhesion at a level which can control a number of survival signalling pathways, as exhibited using the SFK inhibitor PP2, would potentially sensitise a broader range of cell lines to TRAIL induced apoptosis. These cells would also be less likely to develop rapid resistance to the drug, as multiple signalling pathways would be inhibited.

One of the limitations of the work in this thesis is that it does not distinguish sensitisation effects resulting from altered integrin signalling following detachment from those resulting from alterations in cell shape. It is possible that in addition to altered survival signalling downstream of integrins, that changes in cell distension (as a direct result of cytoskeletal disruption and cell rounding) can also account for some of the apoptosis sensitivity (Franklin-Tong and Gourlay, 2008). Previous studies have implicated cell spreading as a factor in the control of apoptosis. Growing single cells on surfaces coated with differentially spaced matrix coated islands allowed cell distension to be altered, without affecting the surface area of contact (Chen et al., 1997). Cells which were more spread were shown to be more protected from spontaneous apoptosis than those which were less distended. Similarly, MCF10 cells could be sensitised to apoptosis through cytoskeletal disruption, independent of adhesion (Martin and Leder, 2001).Therefore the ability of many of the inhibitors used in this thesis to induce cell rounding or spreading defects may influence the apoptotic response through mechanisms which depend on cytoskeletal disruption as well as a reduction in integrin-mediated survival signals.

Recent work has also shown that the integrin binding protein CCN1 can influence TNF ligand induced apoptosis, but by promoting rather than suppressing it (Franzen et al., 2009). This contrasts with the work presented here, and by others, and suggests added complexity to the role of adhesion in the control of sensitivity to TNF ligands. This highlights the importance of testing the results of this thesis on a wide

range of ECM matrix proteins, and emphasizes the need to test these combination strategies thoroughly *in vivo*, where cells are in contact with a wide range of ECM proteins.

7.3 TRAIL sensitisation *in vivo*

The effect of combining rhTRAIL with PF228 or PP2 on the retention of MDA-MB-231 cells in the mouse lung gave promising results, with PP2 and rhTRAIL resulting in an 81 % decrease in lung metastasis only 24 hr after injection. However, due to the variability of the *in vivo* data, and the artificial nature of the metastasis model, further work needs to be done to investigate the effect of these combinations in long term metastasis assays and in orthotopic or spontaneous mouse models of metastasis.

However the striking anti-metastatic effect of β1 integrin blocking alone in MDA-MB-231 highlights the critical role for this signalling pathway in controlling metastasis. As inhibitors to SRC, FAK and β1 integrins have been shown to reduce metastasis through their inhibition of adhesion, migration and invasion, they also have significant anti-metastatic properties when used as single agents (Fujita et al., 1992, Trevino et al., 2006, Jallal et al., 2007). The work presented here suggests an added advantage of targeting this pathway in cancer therapy. Not only will cells have reduced ability to adhere to platelets or the vasculature during metastasis, but they will be more sensitive to death signals from the immune system or from combination with exogenous TRAIL therapies. Therefore targeting this pathway provides a two pronged attack for the elimination of circulating tumour cells.

As the targets for TRAIL sensitisation outlined in this thesis are currently targets for therapeutic cancer treatment, inhibitors already exist for the majority of them. There are also a range of SRC and FAK inhibitors in clinical trials, with dasatinib already approved for use in the clinic against chronic myeloid leukaemia (Das et al., 2006). Further work should combine these agents with rhTRAIL *in vitro* and *in vivo* at concentrations which are currently used safely in the clinic. Another interesting inhibitor to investigate

would be the Rho-inhibitor CCG-1423, shown to reduce SRF activity (Evelyn et al., 2007). As a recent study has shown greater efficacy of the DR5 agonistic antibody lexatumumab in triple negative breast cancers, it would also be interesting to test the inhibitors outlined in this thesis in combination lexatumumab *in vivo*, rather than rhTRAIL, to investigate whether this combination would show even greater synergy (Malin et al., 2011).

7.4 Findings in context

During the duration of this thesis work, more studies have emerged showing the importance of cell adhesion in controlling TRAIL resistance. Lane et al, found that detachment of ovarian cancer cell lines could sensitise them to TRAIL-induced apoptosis *in vitro* through a reduction in AKT activity (Lane et al., 2008) and that epithelial ovarian cancer ascites can provide ovarian cancer cells with protection from TRAIL-induced apoptosis through integrin activation of FAK and AKT and reduction in BID levels (Lane et al., 2010, Goncharenko-Khaider et al., 2010). Detachment was also shown to sensitise mouse squamous cell carcinoma cells to TRAIL-induced apoptosis through a reduction in ERK1/2 signalling (Grosse-Wilde et al., 2008) and to sensitise an oesophageal cell line to a DR5 agonistic antibody (Liu et al., 2009). Interestingly, in fetal colon and HT29 colon adenocarcinoma cell lines, detachment increased resistance to TRAIL through a process mediated by activation of FAK and AKT. Although this contrasts with other reports of detachment induced TRAIL sensitivity, it again highlights the potential of inhibitors targeting FAK and AKT in the control of TRAIL sensitivity (Kočí et al., 2011). Further highlighting a role for this TRAIL response *in vivo*, SRC was found to mediate the protection of metastatic breast cancer cells from TRAIL-induced apoptosis in the bone microenvironment (Zhang et al., 2009a).

Together with the data for melanoma and breast cell lines presented in this thesis, these findings suggest that adhesion is likely to be an important mechanism for TRAIL resistance in many cancer types. Anoikis-resistant cells may be able to prevent spontaneous apoptosis by alterations in the levels of their

intracellular apoptosis regulators. However, it seems apparent that these 'signalling blocks' are not strong enough to protect from exogenous application of death ligands such as TNF-α and TRAIL. Therefore targeting tumour cell adhesion in combination with a TRAIL therapy could provide an effective method of clearing even the most aggressive tumour cells from the circulation

The level of TRAIL sensitisation achieved through the mechanisms reported in this thesis are within the range of the sensitisation reported for other combination strategies such as proteasome inhibitors, histone deacetylase inhibitors and small molecule BCL-2 inhibitors (Hao et al., 2004, Khanbolooki et al., 2006, Voortman et al., 2007, Schüler et al., 2010). They are also greater than the levels of sensitivity induced by TRAIL in combination with gefinitib in bladder cancer cell lines (Shrader et al., 2007). A large number of studies have investigated the combination potential of proteasome inhibitors and HDACi with TRAIL therapies, and cells lines have been shown to vary greatly in their sensitivity to the combination effects. This is likely to be due to their mutation status, and their reliance on particular signalling pathways. For example, the leukaemia cell line K562, which does not signal through the intrinsic pathway of apoptosis is resistant to the sensitisation effects of BCL-2 inhibitors in combination with TRAIL (Hao et al., 2004). Therefore again, it will be useful to test the inhibitors in this thesis with a broader range of cancer cell lines, to fully investigate its potential as a therapeutic strategy.

The sensitisation effects reported in this thesis were not as high as those recently reported in two triple negative breast cancer cell lines (CRL2335 and MDA-MB-468) treated with TRAIL and cisplatin *in vitro* (Xu et al., 2011). However cisplatin in combination with TRAIL has also been shown to induce apoptosis in primary human hepatocytes and lymphocytes *in vitro* (Ganten et al., 2006, Meurette et al., 2006). Therefore to fully compare it to existing combination strategies, further work needs to investigate whether the inhibitors used in this thesis would have the advantage of not inducing hepatotoxicity when

used in combination with TRAIL. Work by De Toni has already purported to this, showing that PP2 and TRAIL do not exhibit hepatotoxicity *in vitro* (De Toni et al., 2007).

Whilst the work for this thesis was being done, a number of reports implicated the multi-kinase inhibitor sorafenib as a potential TRAIL sensitising agent, through its ability to down regulate the pro-apoptotic molecule MCL-1 (Ricci et al., 2007, Huang and Sinicrope, 2010). A phase I trial with sorafenib and the agonistic DR4 TRAIL receptor antibody is currently underway in patients with advanced hepatocellular carcinoma, with a phase II study currently recruiting. The results of these trials will be eagerly anticipated.

In conclusion, the work outlined in this thesis greatly supports a role for cell adhesion in controlling TRAIL sensitivity, and builds on the limited number of initial studies in this area. It presents a number of ways in which TRAIL sensitivity could be altered, and presents a potential new therapeutic target in combination with TRAIL therapies. It also opens up the field for further investigation into other signalling pathways involved in cell-cell or cell-matrix interactions, and their ability to influence TRAIL signalling. As metastasis is the main reason for cancer patient mortality, finding effective therapeutic strategies to prevent and reduce circulating tumour cells is essential to prolong the length and quality of life in cancer patients.

References

ADAMS, C., TOTPAL, K., LAWRENCE, D., MARSTERS, S., PITTI, R., YEE, S., ROSS, S., DEFORGE, L., KOEPPEN, H., SAGOLLA, M., COMPAAN, D., LOWMAN, H., HYMOWITZ, S. & ASHKENAZI, A. 2008. Structural and functional analysis of the interaction between the agonistic monoclonal antibody Apomab and the proapoptotic receptor DR5. *Cell Death Differ,* 15**,** 751-61.

AHMED, N., RILEY, C., OLIVA, K., STUTT, E., RICE, G. E. & QUINN, M. A. 2003. Integrin-linked kinase expression increases with ovarian tumour grade and is sustained by peritoneal tumour fluid. *J Pathol,* 201**,** 229-37.

AL-MEHDI, A. B., TOZAWA, K., FISHER, A. B., SHIENTAG, L., LEE, A. & MUSCHEL, R. J. 2000. Intravascular origin of metastasis from the proliferation of endothelium-attached tumor cells: a new model for metastasis. *Nat Med,* 6**,** 100-2.

ALBIGÈS-RIZO, C., FRACHET, P. & BLOCK, M. R. 1995. Down regulation of talin alters cell adhesion and the processing of the alpha 5 beta 1 integrin. *J Cell Sci,* 108 (Pt 10)**,** 3317-29.

ALMEIDA, E. A., ILIĆ, D., HAN, Q., HAUCK, C. R., JIN, F., KAWAKATSU, H., SCHLAEPFER, D. D. & DAMSKY, C. H. 2000. Matrix survival signaling: from fibronectin via focal adhesion kinase to c-Jun NH(2)-terminal kinase. *J Cell Biol,* 149**,** 741-54.

AOUDJIT, F. & VUORI, K. 2001. Matrix attachment regulates Fas-induced apoptosis in endothelial cells: a role for c-flip and implications for anoikis. *J Cell Biol,* 152**,** 633-43.

ARASE, H., ARASE, N. & SAITO, T. 1995. Fas-mediated cytotoxicity by freshly isolated natural killer cells. *J Exp Med,* 181**,** 1235-8.

ASHKENAZI, A. & DIXIT, V. 1998. Death receptors: signaling and modulation. *Science,* 281**,** 1305-8.

ASHKENAZI, A., PAI, R., FONG, S., LEUNG, S., LAWRENCE, D., MARSTERS, S., BLACKIE, C., CHANG, L., MCMURTREY, A., HEBERT, A., DEFORGE, L., KOUMENIS, I., LEWIS, D., HARRIS, L., BUSSIERE, J., KOEPPEN, H., SHAHROKH, Z. & SCHWALL, R. 1999. Safety and antitumor activity of recombinant soluble Apo2 ligand. *J Clin Invest,* 104**,** 155-62.

ATTWELL, S., MILLS, J., TROUSSARD, A., WU, C. & DEDHAR, S. 2003. Integration of cell attachment, cytoskeletal localization, and signaling by integrin-linked kinase (ILK), CH-ILKBP, and the tumor suppressor PTEN. *Mol Biol Cell,* 14**,** 4813-25.

ATTWELL, S., ROSKELLEY, C. & DEDHAR, S. 2000. The integrin-linked kinase (ILK) suppresses anoikis. *Oncogene,* 19**,** 3811-5.

BAE, S. I., CHERIYATH, V., JACOBS, B. S., REU, F. J. & BORDEN, E. C. 2008. Reversal of methylation silencing of Apo2L/TRAIL receptor 1 (DR4) expression overcomes resistance of SK-MEL-3 and SK-MEL-28 melanoma cells to interferons (IFNs) or Apo2L/TRAIL. *Oncogene,* 27**,** 490-8.

BAETU, T. M., KWON, H., SHARMA, S., GRANDVAUX, N. & HISCOTT, J. 2001. Disruption of NF-kappaB signaling reveals a novel role for NF-kappaB in the regulation of TNF-related apoptosis-inducing ligand expression. *J Immunol,* 167**,** 3164-73.

BARNHART, B. C., LEE, J. C., ALAPPAT, E. C. & PETER, M. E. 2003. The death effector domain protein family. *Oncogene,* 22**,** 8634-44.

BEIERLE, E., MA, X., TRUJILLO, A., KURENOVA, E., CANCE, W. & GOLUBOVSKAYA, V. 2009. Inhibition of focal adhesion kinase and src increases detachment and apoptosis in human neuroblastoma cell lines. *Mol Carcinog*.

BERGER, A. B., SEXTON, K. B. & BOGYO, M. 2006. Commonly used caspase inhibitors designed based on substrate specificity profiles lack selectivity. *Cell Res,* 16**,** 961-3.

BOATRIGHT, K., RENATUS, M., SCOTT, F., SPERANDIO, S., SHIN, H., PEDERSEN, I., RICCI, J., EDRIS, W., SUTHERLIN, D., GREEN, D. & SALVESEN, G. 2003. A unified model for apical caspase activation. *Mol Cell,* 11**,** 529-41.

BOATRIGHT, K. M., DEIS, C., DENAULT, J. B., SUTHERLIN, D. P. & SALVESEN, G. S. 2004. Activation of caspases-8 and -10 by FLIP(L). *Biochem J,* 382**,** 651-7.

BODMER, J. L., HOLLER, N., REYNARD, S., VINCIGUERRA, P., SCHNEIDER, P., JUO, P., BLENIS, J. & TSCHOPP, J. 2000. TRAIL receptor-2 signals apoptosis through FADD and caspase-8. *Nat Cell Biol,* 2**,** 241-3.

BOLDIN, M. P., GONCHAROV, T. M., GOLTSEV, Y. V. & WALLACH, D. 1996. Involvement of MACH, a novel MORT1/FADD-interacting protease, in Fas/APO-1- and TNF receptor-induced cell death. *Cell,* 85**,** 803-15.

BOLDIN, M. P., VARFOLOMEEV, E. E., PANCER, Z., METT, I. L., CAMONIS, J. H. & WALLACH, D. 1995. A novel protein that interacts with the death domain of Fas/APO1 contains a sequence motif related to the death domain. *J Biol Chem,* 270**,** 7795-8.

BONFOCO, E., CHEN, W., PAUL, R., CHERESH, D. & COOPER, N. 2000. beta1 integrin antagonism on adherent, differentiated human neuroblastoma cells triggers an apoptotic signaling pathway. *Neuroscience,* 101**,** 1145-52.

BOYER, B., BOURGEOIS, Y. & POUPON, M. 2002. Src kinase contributes to the metastatic spread of carcinoma cells. *Oncogene,* 21**,** 2347-56.

BRANDT, D. T., BAARLINK, C., KITZING, T. M., KREMMER, E., IVASKA, J., NOLLAU, P. & GROSSE, R. 2009. SCAI acts as a suppressor of cancer cell invasion through the transcriptional control of beta1-integrin. *Nat Cell Biol,* 11**,** 557-68.

BRATTON, S. B., MACFARLANE, M., CAIN, K. & COHEN, G. M. 2000. Protein complexes activate distinct caspase cascades in death receptor and stress-induced apoptosis. *Exp Cell Res,* 256**,** 27-33.

BRATTON, S. B., WALKER, G., SRINIVASULA, S. M., SUN, X. M., BUTTERWORTH, M., ALNEMRI, E. S. & COHEN, G. M. 2001. Recruitment, activation and retention of caspases-9 and -3 by Apaf-1 apoptosome and associated XIAP complexes. *EMBO J,* 20**,** 998-1009.

BRAUN, A., BORDOY, R., STANCHI, F., MOSER, M., KOSTKA G, G., EHLER, E., BRANDAU, O. & FÄSSLER, R. 2003. PINCH2 is a new five LIM domain protein, homologous to PINCHand localized to focal adhesions. *Exp Cell Res,* 284**,** 239-50.

BROOKS, P. C., CLARK, R. A. & CHERESH, D. A. 1994. Requirement of vascular integrin alpha v beta 3 for angiogenesis. *Science,* 264**,** 569-71.

BURRIDGE, K. & CONNELL, L. 1983. A new protein of adhesion plaques and ruffling membranes. *J Cell Biol,* 97**,** 359-67.

BURRIDGE, K. & MANGEAT, P. 1984. An interaction between vinculin and talin. *Nature,* 308**,** 744-6.

CAIN, K., BROWN, D. G., LANGLAIS, C. & COHEN, G. M. 1999. Caspase activation involves the formation of the aposome, a large (approximately 700 kDa) caspase-activating complex. *J Biol Chem,* 274**,** 22686-92.

CALDERWOOD, D. A., ZENT, R., GRANT, R., REES, D. J., HYNES, R. O. & GINSBERG, M. H. 1999. The Talin head domain binds to integrin beta subunit cytoplasmic tails and regulates integrin activation. *J Biol Chem,* 274**,** 28071-4.

CAMIDGE, D., HERBST, R., GORDON, M., ECKHARDT, S., KURZROC, R., DURBIN, B., ING, J., LING, J., SAGER, J. & MENDELSON, D. 2007. A phase I safety and pharmacokinetic study of apomab, a human DR5 agonist antibody, in patients with advanced cancer. Journal of Clinical Oncology.

CAMIDGE, D., HERBST, R., GORDON, M., ECKHARDT, S., KURZROCK, R., DURBIN, B., ING, J., TOHNYA, T., SAGER, J., ASHKENAZI, A., BRAY, G. & MENDELSON, D. 2010. A phase I safety and pharmacokinetic study of the death receptor 5 agonistic antibody PRO95780 in patients with advanced malignancies. *Clin Cancer Res,* 16**,** 1256-63.

CANCE, W. G., HARRIS, J. E., IACOCCA, M. V., ROCHE, E., YANG, X., CHANG, J., SIMKINS, S. & XU, L. 2000. Immunohistochemical analyses of focal adhesion kinase expression in benign and malignant human breast and colon tissues: correlation with preinvasive and invasive phenotypes. *Clin Cancer Res,* 6**,** 2417-23.

CAO, X. L., HU, X. M., HU, J. Q. & ZHENG, W. X. 2011. Myocardin-related transcription factor-A promoting neuronal survival against apoptosis induced by hypoxia/ischemia. *Brain Res,* 1385**,** 263-74.

CARBONELL, W., ANSORGE, O., SIBSON, N. & MUSCHEL, R. 2009. The vascular basement membrane as "soil" in brain metastasis. *PLoS One,* 4**,** e5857.

CARDONE, M. H., ROY, N., STENNICKE, H. R., SALVESEN, G. S., FRANKE, T. F., STANBRIDGE, E., FRISCH, S. & REED, J. C. 1998. Regulation of cell death protease caspase-9 by phosphorylation. *Science,* 282**,** 1318-21.

CHAN, F. K., CHUN, H. J., ZHENG, L., SIEGEL, R. M., BUI, K. L. & LENARDO, M. J. 2000. A domain in TNF receptors that mediates ligand-independent receptor assembly and signaling. *Science,* 288**,** 2351-4.

CHANG, D. W., XING, Z., PAN, Y., ALGECIRAS-SCHIMNICH, A., BARNHART, B. C., YAISH-OHAD, S., PETER, M. E. & YANG, X. 2002. c-FLIP(L) is a dual function regulator for caspase-8 activation and CD95-mediated apoptosis. *EMBO J,* 21**,** 3704-14.

CHELIKANI, P., FITA, I. & LOEWEN, P. 2004. Diversity of structures and properties among catalases. *Cell Mol Life Sci,* 61**,** 192-208.

CHEN, B., LIU, S., WANG, X., XU, W., LI, Y., ZHAO, W. & WU, J. 2009. TRAIL-R1 polymorphisms and cancer susceptibility: an evidence-based meta-analysis. *Eur J Cancer,* 45**,** 2598-605.

CHEN, C., EDELSTEIN, L. C. & GÉLINAS, C. 2000. The Rel/NF-kappaB family directly activates expression of the apoptosis inhibitor Bcl-x(L). *Mol Cell Biol,* 20**,** 2687-95.

CHEN, C. S., MRKSICH, M., HUANG, S., WHITESIDES, G. M. & INGBER, D. E. 1997. Geometric control of cell life and death. *Science,* 276**,** 1425-8.

CHEN, H. C., APPEDDU, P. A., ISODA, H. & GUAN, J. L. 1996. Phosphorylation of tyrosine 397 in focal adhesion kinase is required for binding phosphatidylinositol 3-kinase. *J Biol Chem,* 271**,** 26329-34.

CHEN, H. C., APPEDDU, P. A., PARSONS, J. T., HILDEBRAND, J. D., SCHALLER, M. D. & GUAN, J. L. 1995. Interaction of focal adhesion kinase with cytoskeletal protein talin. *J Biol Chem,* 270**,** 16995-9.

CHEN, Q., KINCH, M. S., LIN, T. H., BURRIDGE, K. & JULIANO, R. L. 1994. Integrin-mediated cell adhesion activates mitogen-activated protein kinases. *J Biol Chem,* 269**,** 26602-5.

CHEN, Z. Y., CAI, L., BIE, P., WANG, S. G., JIANG, Y., DONG, J. H. & LI, X. W. 2010. Roles of Fyn in pancreatic cancer metastasis. *J Gastroenterol Hepatol,* 25**,** 293-301.

CHICHEPORTICHE, Y., BOURDON, P. R., XU, H., HSU, Y. M., SCOTT, H., HESSION, C., GARCIA, I. & BROWNING, J. L. 1997. TWEAK, a new secreted ligand in the tumor necrosis factor family that weakly induces apoptosis. *J Biol Chem,* 272**,** 32401-10.

CHINNAIYAN, A. M., O'ROURKE, K., LANE, B. R. & DIXIT, V. M. 1997. Interaction of CED-4 with CED-3 and CED-9: a molecular framework for cell death. *Science,* 275**,** 1122-6.

CHINNAIYAN, A. M., O'ROURKE, K., TEWARI, M. & DIXIT, V. M. 1995. FADD, a novel death domain-containing protein, interacts with the death domain of Fas and initiates apoptosis. *Cell,* 81**,** 505-12.

CHIPUK, J. E. & GREEN, D. R. 2008. How do BCL-2 proteins induce mitochondrial outer membrane permeabilization? *Trends Cell Biol,* 18**,** 157-64.

CHOW, L. M., JARVIS, C., HU, Q., NYE, S. H., GERVAIS, F. G., VEILLETTE, A. & MATIS, L. A. 1994. Ntk: a Csk-related protein-tyrosine kinase expressed in brain and T lymphocytes. *Proc Natl Acad Sci U S A,* 91**,** 4975-9.

CLANCY, L., MRUK, K., ARCHER, K., WOELFEL, M., MONGKOLSAPAYA, J., SCREATON, G., LENARDO, M. J. & CHAN, F. K. 2005. Preligand assembly domain-mediated ligand-independent association between

TRAIL receptor 4 (TR4) and TR2 regulates TRAIL-induced apoptosis. *Proc Natl Acad Sci U S A,* 102**,** 18099-104.

COBB, B. S., SCHALLER, M. D., LEU, T. H. & PARSONS, J. T. 1994. Stable association of pp60src and pp59fyn with the focal adhesion-associated protein tyrosine kinase, pp125FAK. *Mol Cell Biol,* 14**,** 147-55.

COLL, M. L., ROSEN, K., LADEDA, V. & FILMUS, J. 2002. Increased Bcl-xL expression mediates v-Src-induced resistance to anoikis in intestinal epithelial cells. *Oncogene,* 21**,** 2908-13.

COLLETT, M., BRUGGE, J. & ERIKSON, R. 1978. Characterization of a normal avian cell protein related to the avian sarcoma virus transforming gene product. *Cell,* 15**,** 1363-9.

CORDES, N. 2004. Overexpression of hyperactive integrin-linked kinase leads to increased cellular radiosensitivity. *Cancer Res,* 64**,** 5683-92.

CORDES, N., SEIDLER, J., DURZOK, R., GEINITZ, H. & BRAKEBUSCH, C. 2006. beta1-integrin-mediated signaling essentially contributes to cell survival after radiation-induced genotoxic injury. *Oncogene,* 25**,** 1378-90.

CRETNEY, E., TAKEDA, K., YAGITA, H., GLACCUM, M., PESCHON, J. J. & SMYTH, M. J. 2002. Increased susceptibility to tumor initiation and metastasis in TNF-related apoptosis-inducing ligand-deficient mice. *J Immunol,* 168**,** 1356-61.

CZERNILOFSKY, A., LEVINSON, A., VARMUS, H., BISHOP, J., TISCHER, E. & GOODMAN, H. 1980. Nucleotide sequence of an avian sarcoma virus oncogene (src) and proposed amino acid sequence for gene product. *Nature,* 287**,** 198-203.

DAS, J., CHEN, P., NORRIS, D., PADMANABHA, R., LIN, J., MOQUIN, R. V., SHEN, Z., COOK, L. S., DOWEYKO, A. M., PITT, S., PANG, S., SHEN, D. R., FANG, Q., DE FEX, H. F., MCINTYRE, K. W., SHUSTER, D. J., GILLOOLY, K. M., BEHNIA, K., SCHIEVEN, G. L., WITYAK, J. & BARRISH, J. C. 2006. 2-aminothiazole as a novel kinase inhibitor template. Structure-activity relationship studies toward the discovery of N-(2-chloro-6-methylphenyl)-2-[[6-[4-(2-hydroxyethyl)-1- piperazinyl)]-2-methyl-4-pyrimidinyl]amino)]-1,3-thiazole-5-carboxamide (dasatinib, BMS-354825) as a potent pan-Src kinase inhibitor. *J Med Chem,* 49**,** 6819-32.

DATTA, S. R., DUDEK, H., TAO, X., MASTERS, S., FU, H., GOTOH, Y. & GREENBERG, M. E. 1997. Akt phosphorylation of BAD couples survival signals to the cell-intrinsic death machinery. *Cell,* 91**,** 231-41.

DE TONI, E. N., KUNTZEN, C., GERBES, A. L., THASLER, W. E., SONUC, N., MUCHA, S. R., CAMAJ, P., BRUNS, C., GÖKE, B. & EICHHORST, S. T. 2007. P60-c-src suppresses apoptosis through inhibition of caspase 8 activation in hepatoma cells, but not in primary hepatocytes. *J Hepatol,* 46**,** 682-91.

DE TONI, E. N., THIEME, S. E., HERBST, A., BEHRENS, A., STIEBER, P., JUNG, A., BLUM, H., GÖKE, B. & KOLLIGS, F. T. 2008. OPG is regulated by beta-catenin and mediates resistance to TRAIL-induced apoptosis in colon cancer. *Clin Cancer Res,* 14**,** 4713-8.

DEL BUFALO, D., BIROCCIO, A., LEONETTI, C. & ZUPI, G. 1997. Bcl-2 overexpression enhances the metastatic potential of a human breast cancer line. *FASEB J,* 11**,** 947-53.

DELCOMMENNE, M., TAN, C., GRAY, V., RUE, L., WOODGETT, J. & DEDHAR, S. 1998. Phosphoinositide-3-OH kinase-dependent regulation of glycogen synthase kinase 3 and protein kinase B/AKT by the integrin-linked kinase. *Proc Natl Acad Sci U S A,* 95**,** 11211-6.

DESGROSELLIER, J. S. & CHERESH, D. A. 2010. Integrins in cancer: biological implications and therapeutic opportunities. *Nat Rev Cancer,* 10**,** 9-22.

DEVERAUX, Q. L., ROY, N., STENNICKE, H. R., VAN ARSDALE, T., ZHOU, Q., SRINIVASULA, S. M., ALNEMRI, E. S., SALVESEN, G. S. & REED, J. C. 1998. IAPs block apoptotic events induced by caspase-8 and cytochrome c by direct inhibition of distinct caspases. *EMBO J,* 17**,** 2215-23.

DEVERAUX, Q. L., TAKAHASHI, R., SALVESEN, G. S. & REED, J. C. 1997. X-linked IAP is a direct inhibitor of cell-death proteases. *Nature,* 388**,** 300-4.

DOROTHÉE, G., VERGNON, I., MENEZ, J., ECHCHAKIR, H., GRUNENWALD, D., KUBIN, M., CHOUAIB, S. & MAMI-CHOUAIB, F. 2002. Tumor-infiltrating CD4+ T lymphocytes express APO2 ligand (APO2L)/TRAIL upon specific stimulation with autologous lung carcinoma cells: role of IFN-alpha on APO2L/TRAIL expression and -mediated cytotoxicity. *J Immunol,* 169**,** 809-17.

DU, C., FANG, M., LI, Y., LI, L. & WANG, X. 2000. Smac, a mitochondrial protein that promotes cytochrome c-dependent caspase activation by eliminating IAP inhibition. *Cell,* 102**,** 33-42.

DUXBURY, M. S., ITO, H., ZINNER, M. J., ASHLEY, S. W. & WHANG, E. E. 2004a. Focal adhesion kinase gene silencing promotes anoikis and suppresses metastasis of human pancreatic adenocarcinoma cells. *Surgery,* 135**,** 555-62.

DUXBURY, M. S., ITO, H., ZINNER, M. J., ASHLEY, S. W. & WHANG, E. E. 2004b. Inhibition of SRC tyrosine kinase impairs inherent and acquired gemcitabine resistance in human pancreatic adenocarcinoma cells. *Clin Cancer Res,* 10**,** 2307-18.

EARNSHAW, W. C., MARTINS, L. M. & KAUFMANN, S. H. 1999. Mammalian caspases: structure, activation, substrates, and functions during apoptosis. *Annu Rev Biochem,* 68**,** 383-424.

ECKERT, L. B., REPASKY, G. A., ULKÜ, A. S., MCFALL, A., ZHOU, H., SARTOR, C. I. & DER, C. J. 2004. Involvement of Ras activation in human breast cancer cell signaling, invasion, and anoikis. *Cancer Res,* 64**,** 4585-92.

EKE, I., HEHLGANS, S. & CORDES, N. 2009a. There's something about ILK. *Int J Radiat Biol,* 85**,** 929-36.

EKE, I., KOCH, U., HEHLGANS, S., SANDFORT, V., STANCHI, F., ZIPS, D., BAUMANN, M., SHEVCHENKO, A., PILARSKY, C., HAASE, M., BARETTON, G. B., CALLEJA, V., LARIJANI, B., FÄSSLER, R. & CORDES, N. 2010. PINCH1 regulates Akt1 activation and enhances radioresistance by inhibiting PP1alpha. *J Clin Invest,* 120**,** 2516-27.

EKE, I., LEONHARDT, F., STORCH, K., HEHLGANS, S. & CORDES, N. 2009b. The small molecule inhibitor QLT0267 Radiosensitizes squamous cell carcinoma cells of the head and neck. *PLoS One,* 4**,** e6434.

ELLIS, H. M. & HORVITZ, H. R. 1986. Genetic control of programmed cell death in the nematode C. elegans. *Cell,* 44**,** 817-29.

ELLIS, R. E., YUAN, J. Y. & HORVITZ, H. R. 1991. Mechanisms and functions of cell death. *Annu Rev Cell Biol,* 7**,** 663-98.

EMERY, J. G., MCDONNELL, P., BURKE, M. B., DEEN, K. C., LYN, S., SILVERMAN, C., DUL, E., APPELBAUM, E. R., EICHMAN, C., DIPRINZIO, R., DODDS, R. A., JAMES, I. E., ROSENBERG, M., LEE, J. C. & YOUNG, P. R. 1998. Osteoprotegerin is a receptor for the cytotoxic ligand TRAIL. *J Biol Chem,* 273**,** 14363-7.

EMI, M., FUJIWARA, Y., NAKAJIMA, T., TSUCHIYA, E., TSUDA, H., HIROHASHI, S., MAEDA, Y., TSURUTA, K., MIYAKI, M. & NAKAMURA, Y. 1992. Frequent loss of heterozygosity for loci on chromosome 8p in hepatocellular carcinoma, colorectal cancer, and lung cancer. *Cancer Res,* 52**,** 5368-72.

ESKES, R., DESAGHER, S., ANTONSSON, B. & MARTINOU, J. C. 2000. Bid induces the oligomerization and insertion of Bax into the outer mitochondrial membrane. *Mol Cell Biol,* 20**,** 929-35.

ESTRUGO, D., FISCHER, A., HESS, F., SCHERTHAN, H., BELKA, C. & CORDES, N. 2007. Ligand bound beta1 integrins inhibit procaspase-8 for mediating cell adhesion-mediated drug and radiation resistance in human leukemia cells. *PLoS One,* 2**,** e269.

EVELYN, C. R., WADE, S. M., WANG, Q., WU, M., IÑIGUEZ-LLUHÍ, J. A., MERAJVER, S. D. & NEUBIG, R. R. 2007. CCG-1423: a small-molecule inhibitor of RhoA transcriptional signaling. *Mol Cancer Ther,* 6**,** 2249-60.

FALSCHLEHNER, C., SCHAEFER, U. & WALCZAK, H. 2009. Following TRAIL's path in the immune system. *Immunology,* 127**,** 145-54.

FELDING-HABERMANN, B., O'TOOLE, T. E., SMITH, J. W., FRANSVEA, E., RUGGERI, Z. M., GINSBERG, M. H., HUGHES, P. E., PAMPORI, N., SHATTIL, S. J., SAVEN, A. & MUELLER, B. M. 2001. Integrin activation controls metastasis in human breast cancer. *Proc Natl Acad Sci U S A,* 98**,** 1853-8.

FIDLER, I. 1970. Metastasis: guantitative analysis of distribution and fate of tumor embolilabeled with 125 I-5-iodo-2'-deoxyuridine. *J Natl Cancer Inst,* 45**,** 773-82.

FINCHAM, V. & FRAME, M. 1998. The catalytic activity of Src is dispensable for translocation to focal adhesions but controls the turnover of these structures during cell motility. *EMBO J,* 17**,** 81-92.

FINCHAM, V. J., BRUNTON, V. G. & FRAME, M. C. 2000a. The SH3 domain directs acto-myosin-dependent targeting of v-Src to focal adhesions via phosphatidylinositol 3-kinase. *Mol Cell Biol,* 20**,** 6518-36.

FINCHAM, V. J., JAMES, M., FRAME, M. C. & WINDER, S. J. 2000b. Active ERK/MAP kinase is targeted to newly forming cell-matrix adhesions by integrin engagement and v-Src. *EMBO J,* 19**,** 2911-23.

FISCHER, U., STROH, C. & SCHULZE-OSTHOFF, K. 2006. Unique and overlapping substrate specificities of caspase-8 and caspase-10. *Oncogene,* 25**,** 152-9.

FORNARO, M., PLESCIA, J., CHHEANG, S., TALLINI, G., ZHU, Y. M., KING, M., ALTIERI, D. C. & LANGUINO, L. R. 2003. Fibronectin protects prostate cancer cells from tumor necrosis factor-alpha-induced apoptosis via the AKT/survivin pathway. *J Biol Chem,* 278**,** 50402-11.

FRANKLIN-TONG, V. E. & GOURLAY, C. W. 2008. A role for actin in regulating apoptosis/programmed cell death: evidence spanning yeast, plants and animals. *Biochem J,* 413**,** 389-404.

FRANZEN, C. A., CHEN, C. C., TODOROVIĆ, V., JURIC, V., MONZON, R. I. & LAU, L. F. 2009. Matrix protein CCN1 is critical for prostate carcinoma cell proliferation and TRAIL-induced apoptosis. *Mol Cancer Res,* 7**,** 1045-55.

FRISCH, S. & FRANCIS, H. 1994. Disruption of epithelial cell-matrix interactions induces apoptosis. *J Cell Biol,* 124**,** 619-26.

FRISCH, S., VUORI, K., RUOSLAHTI, E. & CHAN-HUI, P. 1996. Control of adhesion-dependent cell survival by focal adhesion kinase. *J Cell Biol,* 134**,** 793-9.

FUJITA, S., SUZUKI, H., KINOSHITA, M. & HIROHASHI, S. 1992. Inhibition of cell attachment, invasion and metastasis of human carcinoma cells by anti-integrin beta 1 subunit antibody. *Jpn J Cancer Res,* 83**,** 1317-26.

FUKAI, F., MASHIMO, M., AKIYAMA, K., GOTO, T., TANUMA, S. & KATAYAMA, T. 1998. Modulation of apoptotic cell death by extracellular matrix proteins and a fibronectin-derived antiadhesive peptide. *Exp Cell Res,* 242**,** 92-9.

GALANTE, J. M., MORTENSON, M. M., BOWLES, T. L., VIRUDACHALAM, S. & BOLD, R. J. 2009. ERK/BCL-2 pathway in the resistance of pancreatic cancer to anoikis. *J Surg Res,* 152**,** 18-25.

GANTEN, T. M., KOSCHNY, R., SYKORA, J., SCHULZE-BERGKAMEN, H., BÜCHLER, P., HAAS, T. L., SCHADER, M. B., UNTERGASSER, A., STREMMEL, W. & WALCZAK, H. 2006. Preclinical differentiation between apparently safe and potentially hepatotoxic applications of TRAIL either alone or in combination with chemotherapeutic drugs. *Clin Cancer Res,* 12**,** 2640-6.

GAO, J., ZHU, J., LI, H. Y., PAN, X. Y., JIANG, R. & CHEN, J. X. 2011. Small interfering RNA targeting integrin-linked kinase inhibited the growth and induced apoptosis in human bladder cancer cells. *Int J Biochem Cell Biol*.

GIBSON, S. B., OYER, R., SPALDING, A. C., ANDERSON, S. M. & JOHNSON, G. L. 2000. Increased expression of death receptors 4 and 5 synergizes the apoptosis response to combined treatment with etoposide and TRAIL. *Mol Cell Biol,* 20**,** 205-12.

GILMORE, A. P., METCALFE, A. D., ROMER, L. H. & STREULI, C. H. 2000. Integrin-mediated survival signals regulate the apoptotic function of Bax through its conformation and subcellular localization. *J Cell Biol,* 149**,** 431-46.

GINEITIS, D. & TREISMAN, R. 2001. Differential usage of signal transduction pathways defines two types of serum response factor target gene. *J Biol Chem,* 276**,** 24531-9.

GINGRICH, J. C., DAVIS, D. R. & NGUYEN, Q. 2000. Multiplex detection and quantitation of proteins on western blots using fluorescent probes. *Biotechniques,* 29**,** 636-42.

GLAVES, D., HUBEN, R. P. & WEISS, L. 1988. Haematogenous dissemination of cells from human renal adenocarcinomas. *Br J Cancer,* 57**,** 32-5.

GLINSKY, G., GLINSKY, V., IVANOVA, A. & HUESER, C. 1997. Apoptosis and metastasis: increased apoptosis resistance of metastatic cancer cells is associated with the profound deficiency of apoptosis execution mechanisms. *Cancer Lett,* 115**,** 185-93.

GOLDBERG, G., JIN, Z., ICHIKAWA, H., NAITO, A., OHKI, M., EL-DEIRY, W. & TSUDA, H. 2001. Global effects of anchorage on gene expression during mammary carcinoma cell growth reveal role of tumor necrosis factor-related apoptosis-inducing ligand in anoikis. *Cancer Res,* 61**,** 1334-7.

GOLUBOVSKAYA, V. M., FINCH, R. & CANCE, W. G. 2005. Direct interaction of the N-terminal domain of focal adhesion kinase with the N-terminal transactivation domain of p53. *J Biol Chem,* 280**,** 25008-21.

GONCHARENKO-KHAIDER, N., LANE, D., MATTE, I., RANCOURT, C. & PICHÉ, A. 2010. The inhibition of Bid expression by Akt leads to resistance to TRAIL-induced apoptosis in ovarian cancer cells. *Oncogene,* 29**,** 5523-36.

GRAFF, J. R., DEDDENS, J. A., KONICEK, B. W., COLLIGAN, B. M., HURST, B. M., CARTER, H. W. & CARTER, J. H. 2001. Integrin-linked kinase expression increases with prostate tumor grade. *Clin Cancer Res,* 7**,** 1987-91.

GRECO, F. A., BONOMI, P., CRAWFORD, J., KELLY, K., OH, Y., HALPERN, W., LO, L., GALLANT, G. & KLEIN, J. 2008. Phase 2 study of mapatumumab, a fully human agonistic monoclonal antibody which targets and activates the TRAIL receptor-1, in patients with advanced non-small cell lung cancer. *Lung Cancer,* 61**,** 82-90.

GREEN, T., FENNELL, M., WHITTAKER, R., CURWEN, J., JACOBS, V., ALLEN, J., LOGIE, A., HARGREAVES, J., HICKINSON, D., WILKINSON, R., ELVIN, P., BOYER, B., CARRAGHER, N., PLÉ, P., BERMINGHAM, A., HOLDGATE, G., WARD, W., HENNEQUIN, L., DAVIES, B. & COSTELLO, G. 2009. Preclinical anticancer activity of the potent, oral Src inhibitor AZD0530. *Mol Oncol*.

GRIFFITH, T. S., WILEY, S. R., KUBIN, M. Z., SEDGER, L. M., MALISZEWSKI, C. R. & FANGER, N. A. 1999. Monocyte-mediated tumoricidal activity via the tumor necrosis factor-related cytokine, TRAIL. *J Exp Med,* 189**,** 1343-54.

GROSSE-WILDE, A., VOLOSHANENKO, O., BAILEY, S., LONGTON, G., SCHAEFER, U., CSERNOK, A., SCHÜTZ, G., GREINER, E., KEMP, C. & WALCZAK, H. 2008. TRAIL-R deficiency in mice enhances lymph node metastasis without affecting primary tumor development. *J Clin Invest,* 118**,** 100-110.

GUETTLER, S., VARTIAINEN, M., MIRALLES, F., LARIJANI, B. & TREISMAN, R. 2008. RPEL motifs link the serum response factor cofactor MAL but not myocardin to Rho signaling via actin binding. *Mol Cell Biol,* 28**,** 732-42.

HAASE, M., GMACH, C. C., EKE, I., HEHLGANS, S., BARETTON, G. B. & CORDES, N. 2008. Expression of integrin-linked kinase is increased in differentiated cells. *J Histochem Cytochem,* 56**,** 819-29.

HAKEM, R., HAKEM, A., DUNCAN, G. S., HENDERSON, J. T., WOO, M., SOENGAS, M. S., ELIA, A., DE LA POMPA, J. L., KAGI, D., KHOO, W., POTTER, J., YOSHIDA, R., KAUFMAN, S. A., LOWE, S. W., PENNINGER, J. M. & MAK, T. W. 1998. Differential requirement for caspase 9 in apoptotic pathways in vivo. *Cell,* 94**,** 339-52.

HALL, C. L., YAO, M., HILL, L. L. & OWEN-SCHAUB, L. B. 2004. Essential role for hematopoietic Fas ligand (FasL) in the suppression of melanoma lung metastasis revealed in bone marrow chimeric mice. *Clin Exp Metastasis,* 21**,** 251-6.

HANAHAN, D. & WEINBERG, R. A. 2000. The hallmarks of cancer. *Cell,* 100**,** 57-70.

HANAHAN, D. & WEINBERG, R. A. 2011. Hallmarks of cancer: the next generation. *Cell,* 144**,** 646-74.

HANNIGAN, G. E., LEUNG-HAGESTEIJN, C., FITZ-GIBBON, L., COPPOLINO, M. G., RADEVA, G., FILMUS, J., BELL, J. C. & DEDHAR, S. 1996. Regulation of cell adhesion and anchorage-dependent growth by a new beta 1-integrin-linked protein kinase. *Nature,* 379**,** 91-6.

HANNIGAN, G. E., MCDONALD, P. C., WALSH, M. P. & DEDHAR, S. 2011. Integrin-linked kinase: Not so 'pseudo' after all. *Oncogene*.

HAO, J. H., YU, M., LIU, F. T., NEWLAND, A. C. & JIA, L. 2004. Bcl-2 inhibitors sensitize tumor necrosis factor-related apoptosis-inducing ligand-induced apoptosis by uncoupling of mitochondrial respiration in human leukemic CEM cells. *Cancer Res,* 64**,** 3607-16.

HAYNES, N. M., HAWKINS, E. D., LI, M., MCLAUGHLIN, N. M., HÄMMERLING, G. J., SCHWENDENER, R., WINOTO, A., WENSKY, A., YAGITA, H., TAKEDA, K., KERSHAW, M. H., DARCY, P. K. & SMYTH, M. J. 2010. CD11c+ dendritic cells and B cells contribute to the tumoricidal activity of anti-DR5 antibody therapy in established tumors. *J Immunol,* 185**,** 532-41.

HEGDE, R., SRINIVASULA, S. M., ZHANG, Z., WASSELL, R., MUKATTASH, R., CILENTI, L., DUBOIS, G., LAZEBNIK, Y., ZERVOS, A. S., FERNANDES-ALNEMRI, T. & ALNEMRI, E. S. 2002. Identification of Omi/HtrA2 as a mitochondrial apoptotic serine protease that disrupts inhibitor of apoptosis protein-caspase interaction. *J Biol Chem,* 277**,** 432-8.

HEHLGANS, T. & PFEFFER, K. 2005. The intriguing biology of the tumour necrosis factor/tumour necrosis factor receptor superfamily: players, rules and the games. *Immunology,* 115**,** 1-20.

HENGARTNER, M. O., ELLIS, R. E. & HORVITZ, H. R. 1992. Caenorhabditis elegans gene ced-9 protects cells from programmed cell death. *Nature,* 356**,** 494-9.

HERBST, R., ECKHARDT, S., KURZROCK, R., EBBINGHAUS, S., O'DWYER, P., GORDON, M., NOVOTNY, W., GOLDWASSER, M., TOHNYA, T., LUM, B., ASHKENAZI, A., JUBB, A. & MENDELSON, D. 2010. Phase I Dose-Escalation Study of Recombinant Human Apo2L/TRAIL, a Dual Proapoptotic Receptor Agonist, in Patients With Advanced Cancer. *J Clin Oncol*.

HESS, F., ESTRUGO, D., FISCHER, A., BELKA, C. & CORDES, N. 2007. Integrin-linked kinase interacts with caspase-9 and -8 in an adhesion-dependent manner for promoting radiation-induced apoptosis in human leukemia cells. *Oncogene,* 26**,** 1372-84.

HO, L. H., READ, S. H., DORSTYN, L., LAMBRUSCO, L. & KUMAR, S. 2008. Caspase-2 is required for cell death induced by cytoskeletal disruption. *Oncogene,* 27**,** 3393-404.

HOFMANN, K., BUCHER, P. & TSCHOPP, J. 1997. The CARD domain: a new apoptotic signalling motif. *Trends Biochem Sci,* 22**,** 155-6.

HOLEN, I., CROSS, S., NEVILLE-WEBBE, H., CROSS, N., BALASUBRAMANIAN, S., CROUCHER, P., EVANS, C., LIPPITT, J., COLEMAN, R. & EATON, C. 2005. Osteoprotegerin (OPG) expression by breast cancer cells in vitro and breast tumours in vivo--a role in tumour cell survival? *Breast Cancer Res Treat,* 92**,** 207-15.

HOLEN, I., CROUCHER, P. I., HAMDY, F. C. & EATON, C. L. 2002. Osteoprotegerin (OPG) is a survival factor for human prostate cancer cells. *Cancer Res,* 62**,** 1619-23.

HOLMSTRÖM, T. H., SCHMITZ, I., SÖDERSTRÖM, T. S., POUKKULA, M., JOHNSON, V. L., CHOW, S. C., KRAMMER, P. H. & ERIKSSON, J. E. 2000. MAPK/ERK signaling in activated T cells inhibits CD95/Fas-mediated apoptosis downstream of DISC assembly. *EMBO J,* 19**,** 5418-28.

HORAK, P., PILS, D., HALLER, G., PRIBILL, I., ROESSLER, M., TOMEK, S., HORVAT, R., ZEILLINGER, R., ZIELINSKI, C. & KRAINER, M. 2005. Contribution of epigenetic silencing of tumor necrosis factor-related apoptosis inducing ligand receptor 1 (DR4) to TRAIL resistance and ovarian cancer. *Mol Cancer Res,* 3**,** 335-43.

HORWITZ, A., DUGGAN, K., BUCK, C., BECKERLE, M. C. & BURRIDGE, K. 1986. Interaction of plasma membrane fibronectin receptor with talin--a transmembrane linkage. *Nature,* 320**,** 531-3.

HOTTE, S. J., HIRTE, H. W., CHEN, E. X., SIU, L. L., LE, L. H., COREY, A., IACOBUCCI, A., MACLEAN, M., LO, L., FOX, N. L. & OZA, A. M. 2008. A phase 1 study of mapatumumab (fully human monoclonal antibody to TRAIL-R1) in patients with advanced solid malignancies. *Clin Cancer Res,* 14**,** 3450-5.

HSU, H., SHU, H. B., PAN, M. G. & GOEDDEL, D. V. 1996. TRADD-TRAF2 and TRADD-FADD interactions define two distinct TNF receptor 1 signal transduction pathways. *Cell,* 84**,** 299-308.

HUANG, D. & AMERO, S. A. 1997. Measurement of antigen by enhanced chemiluminescent western blot. *Biotechniques,* 22**,** 454-6, 458.

HUANG, S. & SINICROPE, F. A. 2010. Sorafenib inhibits STAT3 activation to enhance TRAIL-mediated apoptosis in human pancreatic cancer cells. *Mol Cancer Ther,* 9**,** 742-50.

HUGHES, M. A., HARPER, N., BUTTERWORTH, M., CAIN, K., COHEN, G. M. & MACFARLANE, M. 2009. Reconstitution of the death-inducing signaling complex reveals a substrate switch that determines CD95-mediated death or survival. *Mol Cell,* 35**,** 265-79.

HUMPHRIES, J., BYRON, A. & HUMPHRIES, M. 2006. Integrin ligands at a glance. *J Cell Sci,* 119**,** 3901-3.

HYMOWITZ, S. G., CHRISTINGER, H. W., FUH, G., ULTSCH, M., O'CONNELL, M., KELLEY, R. F., ASHKENAZI, A. & DE VOS, A. M. 1999. Triggering cell death: the crystal structure of Apo2L/TRAIL in a complex with death receptor 5. *Mol Cell,* 4**,** 563-71.

ICHIKAWA, K., LIU, W., ZHAO, L., WANG, Z., LIU, D., OHTSUKA, T., ZHANG, H., MOUNTZ, J., KOOPMAN, W., KIMBERLY, R. & ZHOU, T. 2001. Tumoricidal activity of a novel anti-human DR5 monoclonal antibody without hepatocyte cytotoxicity. *Nat Med,* 7**,** 954-60.

ILIĆ, D., FURUTA, Y., KANAZAWA, S., TAKEDA, N., SOBUE, K., NAKATSUJI, N., NOMURA, S., FUJIMOTO, J., OKADA, M. & YAMAMOTO, T. 1995. Reduced cell motility and enhanced focal adhesion contact formation in cells from FAK-deficient mice. *Nature,* 377**,** 539-44.

IM, J. H., FU, W., WANG, H., BHATIA, S. K., HAMMER, D. A., KOWALSKA, M. A. & MUSCHEL, R. J. 2004. Coagulation facilitates tumor cell spreading in the pulmonary vasculature during early metastatic colony formation. *Cancer Res,* 64**,** 8613-9.

IRBY, R., MAO, W., COPPOLA, D., KANG, J., LOUBEAU, J., TRUDEAU, W., KARL, R., FUJITA, D., JOVE, R. & YEATMAN, T. 1999. Activating SRC mutation in a subset of advanced human colon cancers. *Nat Genet,* 21**,** 187-90.

IRBY, R. & YEATMAN, T. 2000. Role of Src expression and activation in human cancer. *Oncogene,* 19**,** 5636-42.

IRMLER, M., THOME, M., HAHNE, M., SCHNEIDER, P., HOFMANN, K., STEINER, V., BODMER, J. L., SCHRÖTER, M., BURNS, K., MATTMANN, C., RIMOLDI, D., FRENCH, L. E. & TSCHOPP, J. 1997. Inhibition of death receptor signals by cellular FLIP. *Nature,* 388**,** 190-5.

ISCHENKO, I., CAMAJ, P., SEELIGER, H., KLEESPIES, A., GUBA, M., DE TONI, E. N., SCHWARZ, B., GRAEB, C., EICHHORN, M. E., JAUCH, K. W. & BRUNS, C. J. 2008. Inhibition of Src tyrosine kinase reverts chemoresistance toward 5-fluorouracil in human pancreatic carcinoma cells: an involvement of epidermal growth factor receptor signaling. *Oncogene,* 27**,** 7212-22.

ISHIZAWAR, R. C., MIYAKE, T. & PARSONS, S. J. 2007. c-Src modulates ErbB2 and ErbB3 heterocomplex formation and function. *Oncogene,* 26**,** 3503-10.

JALLAL, H., VALENTINO, M. L., CHEN, G., BOSCHELLI, F., ALI, S. & RABBANI, S. A. 2007. A Src/Abl kinase inhibitor, SKI-606, blocks breast cancer invasion, growth, and metastasis in vitro and in vivo. *Cancer Res,* 67**,** 1580-8.

JANSSEN, E. M., DROIN, N. M., LEMMENS, E. E., PINKOSKI, M. J., BENSINGER, S. J., EHST, B. D., GRIFFITH, T. S., GREEN, D. R. & SCHOENBERGER, S. P. 2005. CD4+ T-cell help controls CD8+ T-cell memory via TRAIL-mediated activation-induced cell death. *Nature,* 434**,** 88-93.

JEMAL, A., BRAY, F., CENTER, M. M., FERLAY, J., WARD, E. & FORMAN, D. 2011. Global cancer statistics. *CA Cancer J Clin,* 61**,** 69-90.

JIN, Z., MCDONALD, E. R., DICKER, D. T. & EL-DEIRY, W. S. 2004. Deficient tumor necrosis factor-related apoptosis-inducing ligand (TRAIL) death receptor transport to the cell surface in human colon cancer cells selected for resistance to TRAIL-induced apoptosis. *J Biol Chem,* 279**,** 35829-39.

JO, M., KIM, T. H., SEOL, D. W., ESPLEN, J. E., DORKO, K., BILLIAR, T. R. & STROM, S. C. 2000. Apoptosis induced in normal human hepatocytes by tumor necrosis factor-related apoptosis-inducing ligand. *Nat Med,* 6**,** 564-7.

JOHANSEN, F. E. & PRYWES, R. 1995. Serum response factor: transcriptional regulation of genes induced by growth factors and differentiation. *Biochim Biophys Acta,* 1242**,** 1-10.

JOHNSEN, A. C., HAUX, J., STEINKJER, B., NONSTAD, U., EGEBERG, K., SUNDAN, A., ASHKENAZI, A. & ESPEVIK, T. 1999. Regulation of APO-2 ligand/trail expression in NK cells-involvement in NK cell-mediated cytotoxicity. *Cytokine,* 11**,** 664-72.

JOHNSTONE, R. W., FREW, A. J. & SMYTH, M. J. 2008. The TRAIL apoptotic pathway in cancer onset, progression and therapy. *Nat Rev Cancer,* 8**,** 782-98.

JONES, R. J., AVIZIENYTE, E., WYKE, A. W., OWENS, D. W., BRUNTON, V. G. & FRAME, M. C. 2002. Elevated c-Src is linked to altered cell-matrix adhesion rather than proliferation in KM12C human colorectal cancer cells. *Br J Cancer,* 87**,** 1128-35.

JUHASZ, I., ALBELDA, S., ELDER, D., MURPHY, G., ADACHI, K., HERLYN, D., VALYI-NAGY, I. & HERLYN, M. 1993. Growth and invasion of human melanomas in human skin grafted to immunodeficient mice. *Am J Pathol,* 143**,** 528-37.

KAKSONEN, M., TORET, C. P. & DRUBIN, D. G. 2006. Harnessing actin dynamics for clathrin-mediated endocytosis. *Nat Rev Mol Cell Biol,* 7**,** 404-14.

KAMARAJAN, P., BUNEK, J., LIN, Y., NUNEZ, G. & KAPILA, Y. L. 2010. Receptor-interacting protein shuttles between cell death and survival signaling pathways. *Mol Biol Cell,* 21**,** 481-8.

KANDASAMY, K. & SRIVASTAVA, R. 2002. Role of the phosphatidylinositol 3'-kinase/PTEN/Akt kinase pathway in tumor necrosis factor-related apoptosis-inducing ligand-induced apoptosis in non-small cell lung cancer cells. *Cancer Res,* 62**,** 4929-37.

KANNER, S. B., REYNOLDS, A. B., VINES, R. R. & PARSONS, J. T. 1990. Monoclonal antibodies to individual tyrosine-phosphorylated protein substrates of oncogene-encoded tyrosine kinases. *Proc Natl Acad Sci U S A,* 87**,** 3328-32.

KAPLAN, K. B., BIBBINS, K. B., SWEDLOW, J. R., ARNAUD, M., MORGAN, D. O. & VARMUS, H. E. 1994. Association of the amino-terminal half of c-Src with focal adhesions alters their properties and is regulated by phosphorylation of tyrosine 527. *EMBO J,* 13**,** 4745-56.

KAUFMANN, S. H., DESNOYERS, S., OTTAVIANO, Y., DAVIDSON, N. E. & POIRIER, G. G. 1993. Specific proteolytic cleavage of poly(ADP-ribose) polymerase: an early marker of chemotherapy-induced apoptosis. *Cancer Res,* 53**,** 3976-85.

KAYAGAKI, N., YAMAGUCHI, N., NAKAYAMA, M., TAKEDA, K., AKIBA, H., TSUTSUI, H., OKAMURA, H., NAKANISHI, K., OKUMURA, K. & YAGITA, H. 1999. Expression and function of TNF-related apoptosis-inducing ligand on murine activated NK cells. *J Immunol,* 163**,** 1906-13.

KELLEY, S. K., HARRIS, L. A., XIE, D., DEFORGE, L., TOTPAL, K., BUSSIERE, J. & FOX, J. A. 2001. Preclinical studies to predict the disposition of Apo2L/tumor necrosis factor-related apoptosis-inducing ligand in humans: characterization of in vivo efficacy, pharmacokinetics, and safety. *J Pharmacol Exp Ther,* 299**,** 31-8.

KERR, J., WYLLIE, A. & CURRIE, A. 1972. Apoptosis: a basic biological phenomenon with wide-ranging implications in tissue kinetics. *Br J Cancer,* 26**,** 239-57.

KHANBOLOOKI, S., NAWROCKI, S. T., ARUMUGAM, T., ANDTBACKA, R., PINO, M. S., KURZROCK, R., LOGSDON, C. D., ABBRUZZESE, J. L. & MCCONKEY, D. J. 2006. Nuclear factor-kappaB maintains TRAIL resistance in human pancreatic cancer cells. *Mol Cancer Ther,* 5**,** 2251-60.

KIETZMANN, T. & GÖRLACH, A. 2005. Reactive oxygen species in the control of hypoxia-inducible factor-mediated gene expression. *Semin Cell Dev Biol,* 16**,** 474-86.

KIM, J. W., WONG, C. W., GOLDSMITH, J. D., SONG, C., FU, W., ALLION, M. B., HERLYN, M., AL-MEHDI, A. B. & MUSCHEL, R. J. 2004. Rapid apoptosis in the pulmonary vasculature distinguishes non-metastatic from metastatic melanoma cells. *Cancer Lett,* 213**,** 203-12.

KIM, K., FISHER, M., XU, S. & EL-DEIRY, W. 2000. Molecular determinants of response to TRAIL in killing of normal and cancer cells. *Clin Cancer Res,* 6**,** 335-46.

KISCHKEL, F. C., HELLBARDT, S., BEHRMANN, I., GERMER, M., PAWLITA, M., KRAMMER, P. H. & PETER, M. E. 1995. Cytotoxicity-dependent APO-1 (Fas/CD95)-associated proteins form a death-inducing signaling complex (DISC) with the receptor. *EMBO J,* 14**,** 5579-88.

KISCHKEL, F. C., LAWRENCE, D. A., CHUNTHARAPAI, A., SCHOW, P., KIM, K. J. & ASHKENAZI, A. 2000. Apo2L/TRAIL-dependent recruitment of endogenous FADD and caspase-8 to death receptors 4 and 5. *Immunity,* 12**,** 611-20.

KLINGHOFFER, R. A., SACHSENMAIER, C., COOPER, J. A. & SORIANO, P. 1999. Src family kinases are required for integrin but not PDGFR signal transduction. *EMBO J,* 18**,** 2459-71.

KLUCK, R. M., BOSSY-WETZEL, E., GREEN, D. R. & NEWMEYER, D. D. 1997. The release of cytochrome c from mitochondria: a primary site for Bcl-2 regulation of apoptosis. *Science,* 275**,** 1132-6.

KOPF, E. & ZHARHARY, D. 2007. Antibody arrays--an emerging tool in cancer proteomics. *Int J Biochem Cell Biol,* 39**,** 1305-17.

KOPP, P. M., BATE, N., HANSEN, T. M., BRINDLE, N. P., PRAEKELT, U., DEBRAND, E., COLEMAN, S., MAZZEO, D., GOULT, B. T., GINGRAS, A. R., PRITCHARD, C. A., CRITCHLEY, D. R. & MONKLEY, S. J. 2010. Studies on the morphology and spreading of human endothelial cells define key inter- and intramolecular interactions for talin1. *Eur J Cell Biol,* 89**,** 661-73.

KOSCHNY, R., GANTEN, T. M., SYKORA, J., HAAS, T. L., SPRICK, M. R., KOLB, A., STREMMEL, W. & WALCZAK, H. 2007. TRAIL/bortezomib cotreatment is potentially hepatotoxic but induces cancer-specific apoptosis within a therapeutic window. *Hepatology,* 45**,** 649-58.

KOUL, D., SHEN, R., BERGH, S., LU, Y., DE GROOT, J. F., LIU, T. J., MILLS, G. B. & YUNG, W. K. 2005. Targeting integrin-linked kinase inhibits Akt signaling pathways and decreases tumor progression of human glioblastoma. *Mol Cancer Ther,* 4**,** 1681-8.

KOČÍ, L., HÝŽD'ALOVÁ, M., VACULOVÁ, A., HOFMANOVÁ, J. & KOZUBÍK, A. 2011. Detachment-mediated resistance to TRAIL-induced apoptosis is associated with stimulation of the PI3K/Akt pathway in fetal and adenocarcinoma epithelial colon cells. *Cytokine,* 55**,** 34-9.

KRICK, S., SHI, S., JU, W., FAUL, C., TSAI, S. Y., MUNDEL, P. & BÖTTINGER, E. P. 2008. Mpv17l protects against mitochondrial oxidative stress and apoptosis by activation of Omi/HtrA2 protease. *Proc Natl Acad Sci U S A,* 105**,** 14106-11.

KROEMER, G., GALLUZZI, L., VANDENABEELE, P., ABRAMS, J., ALNEMRI, E., BAEHRECKE, E., BLAGOSKLONNY, M., EL-DEIRY, W., GOLSTEIN, P., GREEN, D., HENGARTNER, M., KNIGHT, R., KUMAR, S., LIPTON, S., MALORNI, W., NUÑEZ, G., PETER, M., TSCHOPP, J., YUAN, J., PIACENTINI, M., ZHIVOTOVSKY, B., MELINO, G. & 2009, N. C. O. C. D. 2009. Classification of cell death: recommendations of the Nomenclature Committee on Cell Death 2009. *Cell Death Differ,* 16**,** 3-11.

KRUYT, F. 2008. TRAIL and cancer therapy. *Cancer Lett,* 263**,** 14-25.

KURENOVA, E., XU, L., YANG, X., BALDWIN, A. J., CRAVEN, R., HANKS, S., LIU, Z. & CANCE, W. 2004. Focal adhesion kinase suppresses apoptosis by binding to the death domain of receptor-interacting protein. *Mol Cell Biol,* 24**,** 4361-71.

KUWANA, T., BOUCHIER-HAYES, L., CHIPUK, J. E., BONZON, C., SULLIVAN, B. A., GREEN, D. R. & NEWMEYER, D. D. 2005. BH3 domains of BH3-only proteins differentially regulate Bax-mediated mitochondrial membrane permeabilization both directly and indirectly. *Mol Cell,* 17**,** 525-35.

LAGUINGE, L., SAMARA, R., WANG, W., EL-DEIRY, W., CORNER, G., AUGENLICHT, L., MISHRA, L. & JESSUP, J. 2008. DR5 receptor mediates anoikis in human colorectal carcinoma cell lines. *Cancer Res,* 68**,** 909-17.

LAGUINGE, L. M., LIN, S., SAMARA, R. N., SALESIOTIS, A. N. & JESSUP, J. M. 2004. Nitrosative stress in rotated three-dimensional colorectal carcinoma cell cultures induces microtubule depolymerization and apoptosis. *Cancer Res,* 64**,** 2643-8.

LAI, M. T., HUA, C. H., TSAI, M. H., WAN, L., LIN, Y. J., CHEN, C. M., CHIU, I. W., CHAN, C., TSAI, F. J. & JINN-CHYUAN SHEU, J. 2011. Talin-1 overexpression defines high risk for aggressive oral squamous cell carcinoma and promotes cancer metastasis. *J Pathol,* 224**,** 367-76.

LAMHAMEDI-CHERRADI, S. E., ZHENG, S. J., MAGUSCHAK, K. A., PESCHON, J. & CHEN, Y. H. 2003. Defective thymocyte apoptosis and accelerated autoimmune diseases in TRAIL-/- mice. *Nat Immunol,* 4**,** 255-60.

LANE, D., CARTIER, A., RANCOURT, C. & PICHÉ, A. 2008. Cell detachment modulates TRAIL resistance in ovarian cancer cells by downregulating the phosphatidylinositol 3-kinase/Akt pathway. *Int J Gynecol Cancer,* 18**,** 670-6.

LANE, D., GONCHARENKO-KHAIDER, N., RANCOURT, C. & PICHÉ, A. 2010. Ovarian cancer ascites protects from TRAIL-induced cell death through alphavbeta5 integrin-mediated focal adhesion kinase and Akt activation. *Oncogene,* 29**,** 3519-31.

LAWRENCE, D., SHAHROKH, Z., MARSTERS, S., ACHILLES, K., SHIH, D., MOUNHO, B., HILLAN, K., TOTPAL, K., DEFORGE, L., SCHOW, P., HOOLEY, J., SHERWOOD, S., PAI, R., LEUNG, S., KHAN, L., GLINIAK, B., BUSSIERE, J., SMITH, C. A., STROM, S. S., KELLEY, S., FOX, J. A., THOMAS, D. & ASHKENAZI, A. 2001. Differential hepatocyte toxicity of recombinant Apo2L/TRAIL versions. *Nat Med,* 7**,** 383-5.

LEONG, S., COHEN, R. B., GUSTAFSON, D. L., LANGER, C. J., CAMIDGE, D. R., PADAVIC, K., GORE, L., SMITH, M., CHOW, L. Q., VON MEHREN, M., O'BRYANT, C., HARIHARAN, S., DIAB, S., FOX, N. L., MICELI, R. & ECKHARDT, S. G. 2009. Mapatumumab, an antibody targeting TRAIL-R1, in combination with paclitaxel and carboplatin in patients with advanced solid malignancies: results of a phase I and pharmacokinetic study. *J Clin Oncol,* 27**,** 4413-21.

LEWIS, B. C., KLIMSTRA, D. S., SOCCI, N. D., XU, S., KOUTCHER, J. A. & VARMUS, H. E. 2005. The absence of p53 promotes metastasis in a novel somatic mouse model for hepatocellular carcinoma. *Mol Cell Biol,* 25**,** 1228-37.

LI, H., ZHU, H., XU, C. J. & YUAN, J. 1998. Cleavage of BID by caspase 8 mediates the mitochondrial damage in the Fas pathway of apoptosis. *Cell,* 94**,** 491-501.

LI, P., NIJHAWAN, D., BUDIHARDJO, I., SRINIVASULA, S. M., AHMAD, M., ALNEMRI, E. S. & WANG, X. 1997. Cytochrome c and dATP-dependent formation of Apaf-1/caspase-9 complex initiates an apoptotic protease cascade. *Cell,* 91**,** 479-89.

LI, S., CHANG, S., QI, X., RICHARDSON, J. A. & OLSON, E. N. 2006. Requirement of a myocardin-related transcription factor for development of mammary myoepithelial cells. *Mol Cell Biol,* 26**,** 5797-808.

LIPFERT, L., HAIMOVICH, B., SCHALLER, M. D., COBB, B. S., PARSONS, J. T. & BRUGGE, J. S. 1992. Integrin-dependent phosphorylation and activation of the protein tyrosine kinase pp125FAK in platelets. *J Cell Biol,* 119**,** 905-12.

LIPTON, A., ALI, S. M., LEITZEL, K., CHINCHILLI, V., WITTERS, L., ENGLE, L., HOLLOWAY, D., BEKKER, P. & DUNSTAN, C. R. 2002. Serum osteoprotegerin levels in healthy controls and cancer patients. *Clin Cancer Res,* 8**,** 2306-10.

LIU, G. C., ZHANG, J., LIU, S. G., GAO, R., LONG, Z. F., TAO, K. & MA, Y. F. 2009. Detachment of esophageal carcinoma cells from extracellular matrix causes relocalization of death receptor 5 and apoptosis. *World J Gastroenterol,* 15**,** 836-44.

LIU, J., COSTELLO, P. C., PHAM, N. A., PINTILLIE, M., JABALI, M., SANGHERA, J., TSAO, M. S. & JOHNSTON, M. R. 2006a. Integrin-linked kinase inhibitor KP-392 demonstrates clinical benefits in an orthotopic human non-small cell lung cancer model. *J Thorac Oncol,* 1**,** 771-9.

LIU, Z., LI, H., WU, X., YOO, B. H., YAN, S. R., STADNYK, A. W., SASAZUKI, T., SHIRASAWA, S., LACASSE, E. C., KORNELUK, R. G. & ROSEN, K. V. 2006b. Detachment-induced upregulation of XIAP and cIAP2 delays anoikis of intestinal epithelial cells. *Oncogene,* 25**,** 7680-90.

LU, Y., YU, Q., LIU, J. H., ZHANG, J., WANG, H., KOUL, D., MCMURRAY, J. S., FANG, X., YUNG, W. K., SIMINOVITCH, K. A. & MILLS, G. B. 2003. Src family protein-tyrosine kinases alter the function of PTEN to regulate phosphatidylinositol 3-kinase/AKT cascades. *J Biol Chem,* 278**,** 40057-66.

LUO, X., BUDIHARDJO, I., ZOU, H., SLAUGHTER, C. & WANG, X. 1998. Bid, a Bcl2 interacting protein, mediates cytochrome c release from mitochondria in response to activation of cell surface death receptors. *Cell,* 94**,** 481-90.

MA, Z., MORRIS, S. W., VALENTINE, V., LI, M., HERBRICK, J. A., CUI, X., BOUMAN, D., LI, Y., MEHTA, P. K., NIZETIC, D., KANEKO, Y., CHAN, G. C., CHAN, L. C., SQUIRE, J., SCHERER, S. W. & HITZLER, J. K. 2001. Fusion of two novel genes, RBM15 and MKL1, in the t(1;22)(p13;q13) of acute megakaryoblastic leukemia. *Nat Genet,* 28**,** 220-1.

MALIN, D., CHEN, F., SCHILLER, C., KOBLINSKI, J. E. & CRYNS, V. L. 2011. Enhanced Metastasis Suppression by Targeting TRAIL Receptor 2 in a Murine Model of Triple-Negative Breast Cancer. *Clin Cancer Res*.

MARAIS, R., WYNNE, J. & TREISMAN, R. 1993. The SRF accessory protein Elk-1 contains a growth factor-regulated transcriptional activation domain. *Cell,* 73**,** 381-93.

MARINI, P., DENZINGER, S., SCHILLER, D., KAUDER, S., WELZ, S., HUMPHREYS, R., DANIEL, P. T., JENDROSSEK, V., BUDACH, W. & BELKA, C. 2006. Combined treatment of colorectal tumours with agonistic TRAIL receptor antibodies HGS-ETR1 and HGS-ETR2 and radiotherapy: enhanced effects in vitro and dose-dependent growth delay in vivo. *Oncogene,* 25**,** 5145-54.

MARK J SMYTH, E. C., KAZUYOSHI TAKEDA, ROBERT H WILTROUT, LISA M SEDGER, NOBUHIKO KAYAGAKI, HIDEO YAGITA, KO OKUMURA 2001. Tumor Necrosis Factor-related Apoptosis-inducing Ligand (TRAIL) contributes to Interferon gamma-dependent Natural Killer Cell protection from Tumor Metastasis. *The Journal of Experimental Medicine,* 193**,** 9.

MAROTTA, A., TAN, C., GRAY, V., MALIK, S., GALLINGER, S., SANGHERA, J., DUPUIS, B., OWEN, D., DEDHAR, S. & SALH, B. 2001. Dysregulation of integrin-linked kinase (ILK) signaling in colonic polyposis. *Oncogene,* 20**,** 6250-7.

MARTIN, B. P., FREW, A. J., BOTS, M., FOX, S., LONG, F., TAKEDA, K., YAGITA, H., ATADJA, P., SMYTH, M. J. & JOHNSTONE, R. W. 2011. Antitumor activities and on-target toxicities mediated by a TRAIL receptor agonist following cotreatment with panobinostat. *Int J Cancer,* 128**,** 2735-47.

MARTIN, S. S. & LEDER, P. 2001. Human MCF10A mammary epithelial cells undergo apoptosis following actin depolymerization that is independent of attachment and rescued by Bcl-2. *Mol Cell Biol,* 21**,** 6529-36.

MATTER, M. & RUOSLAHTI, E. 2001. A signaling pathway from the alpha5beta1 and alpha(v)beta3 integrins that elevates bcl-2 transcription. *J Biol Chem,* 276**,** 27757-63.

MAWJI, I. A., SIMPSON, C. D., HURREN, R., GRONDA, M., WILLIAMS, M. A., FILMUS, J., JONKMAN, J., DA COSTA, R. S., WILSON, B. C., THOMAS, M. P., REED, J. C., GLINSKY, G. V. & SCHIMMER, A. D. 2007. Critical role for Fas-associated death domain-like interleukin-1-converting enzyme-like inhibitory protein in anoikis resistance and distant tumor formation. *J Natl Cancer Inst,* 99**,** 811-22.

MCCONKEY, D. J., GREENE, G. & PETTAWAY, C. A. 1996. Apoptosis resistance increases with metastatic potential in cells of the human LNCaP prostate carcinoma line. *Cancer Res,* 56**,** 5594-9.

MCKEE, C. M., YE, Y. & RICHBURG, J. H. 2006. Testicular germ cell sensitivity to TRAIL-induced apoptosis is dependent upon p53 expression and is synergistically enhanced by DR5 agonistic antibody treatment. *Apoptosis,* 11**,** 2237-50.

MEDJKANE, S., PEREZ-SANCHEZ, C., GAGGIOLI, C., SAHAI, E. & TREISMAN, R. 2009. Myocardin-related transcription factors and SRF are required for cytoskeletal dynamics and experimental metastasis. *Nat Cell Biol,* 11**,** 257-68.

MEHLEN, P. & PUISIEUX, A. 2006. Metastasis: a question of life or death. *Nat Rev Cancer,* 6**,** 449-58.

MERCHER, T., CONIAT, M. B., MONNI, R., MAUCHAUFFE, M., NGUYEN KHAC, F., GRESSIN, L., MUGNERET, F., LEBLANC, T., DASTUGUE, N., BERGER, R. & BERNARD, O. A. 2001. Involvement of a human gene related to the Drosophila spen gene in the recurrent t(1;22) translocation of acute megakaryocytic leukemia. *Proc Natl Acad Sci U S A,* 98**,** 5776-9.

MEURETTE, O., FONTAINE, A., REBILLARD, A., LE MOIGNE, G., LAMY, T., LAGADIC-GOSSMANN, D. & DIMANCHE-BOITREL, M. T. 2006. Cytotoxicity of TRAIL/anticancer drug combinations in human normal cells. *Ann N Y Acad Sci,* 1090**,** 209-16.

MIANO, J., LONG, X. & FUJIWARA, K. 2007. Serum response factor: master regulator of the actin cytoskeleton and contractile apparatus. *Am J Physiol Cell Physiol,* 292**,** C70-81.

MIANO, J. M. 2010. Role of serum response factor in the pathogenesis of disease. *Lab Invest,* 90**,** 1274-84.

MICHEAU, O., LENS, S., GAIDE, O., ALEVIZOPOULOS, K. & TSCHOPP, J. 2001. NF-kappaB signals induce the expression of c-FLIP. *Mol Cell Biol,* 21**,** 5299-305.

MICHEAU, O. & TSCHOPP, J. 2003. Induction of TNF receptor I-mediated apoptosis via two sequential signaling complexes. *Cell,* 114**,** 181-90.

MIRALLES, F., POSERN, G., ZAROMYTIDOU, A. I. & TREISMAN, R. 2003. Actin dynamics control SRF activity by regulation of its coactivator MAL. *Cell,* 113**,** 329-42.

MIRANTI, C. K. & BRUGGE, J. S. 2002. Sensing the environment: a historical perspective on integrin signal transduction. *Nat Cell Biol,* 4**,** E83-90.

MITA, M., KELLY, K. R., MITA, A., RICART, A. D., ROMERO, O., TOLCHER, A., HOOK, L., OKEREKE, C., KRIVELEVICH, I., ROSSIGNOL, D. P., GILES, F. J., ROWINSKY, E. K. & TAKIMOTO, C. 2011. Phase I study of E7820, an oral inhibitor of integrin {alpha}-2 expression with antiangiogenic properties, in patients with advanced malignancies. *Clin Cancer Res,* 17**,** 193-200.

MIYAMOTO, S., TERAMOTO, H., GUTKIND, J. S. & YAMADA, K. M. 1996. Integrins can collaborate with growth factors for phosphorylation of receptor tyrosine kinases and MAP kinase activation: roles of integrin aggregation and occupancy of receptors. *J Cell Biol,* 135**,** 1633-42.

MONKLEY, S. J., PRITCHARD, C. A. & CRITCHLEY, D. R. 2001. Analysis of the mammalian talin2 gene TLN2. *Biochem Biophys Res Commun,* 286**,** 880-5.

MORI, E., THOMAS, M., MOTOKI, K., NAKAZAWA, K., TAHARA, T., TOMIZUKA, K., ISHIDA, I. & KATAOKA, S. 2004. Human normal hepatocytes are susceptible to apoptosis signal mediated by both TRAIL-R1 and TRAIL-R2. *Cell Death Differ,* 11**,** 203-7.

MORITA, T., MAYANAGI, T. & SOBUE, K. 2007. Reorganization of the actin cytoskeleton via transcriptional regulation of cytoskeletal/focal adhesion genes by myocardin-related transcription factors (MRTFs/MAL/MKLs). *Exp Cell Res,* 313**,** 3432-45.

MORITZ, T., NIEDERLE, N., BAUMANN, J., MAY, D., KURSCHEL, E., OSIEKA, R., KEMPENI, J., SCHLICK, E. & SCHMIDT, C. 1989. Phase I study of recombinant human tumor necrosis factor alpha in advanced malignant disease. *Cancer Immunol Immunother,* 29**,** 144-50.

MORO, L., VENTURINO, M., BOZZO, C., SILENGO, L., ALTRUDA, F., BEGUINOT, L., TARONE, G. & DEFILIPPI, P. 1998. Integrins induce activation of EGF receptor: role in MAP kinase induction and adhesion-dependent cell survival. *EMBO J,* 17**,** 6622-32.

MOSER, M., LEGATE, K. R., ZENT, R. & FÄSSLER, R. 2009. The tail of integrins, talin, and kindlins. *Science,* 324**,** 895-9.

MUPPIDI, J. R., TSCHOPP, J. & SIEGEL, R. M. 2004. Life and death decisions: secondary complexes and lipid rafts in TNF receptor family signal transduction. *Immunity,* 21**,** 461-5.

MUZIO, M., CHINNAIYAN, A. M., KISCHKEL, F. C., O'ROURKE, K., SHEVCHENKO, A., NI, J., SCAFFIDI, C., BRETZ, J. D., ZHANG, M., GENTZ, R., MANN, M., KRAMMER, P. H., PETER, M. E. & DIXIT, V. M. 1996. FLICE, a novel FADD-homologous ICE/CED-3-like protease, is recruited to the CD95 (Fas/APO-1) death--inducing signaling complex. *Cell,* 85**,** 817-27.

MUZIO, M., SALVESEN, G. S. & DIXIT, V. M. 1997. FLICE induced apoptosis in a cell-free system. Cleavage of caspase zymogens. *J Biol Chem,* 272**,** 2952-6.

MUZIO, M., STOCKWELL, B. R., STENNICKE, H. R., SALVESEN, G. S. & DIXIT, V. M. 1998. An induced proximity model for caspase-8 activation. *J Biol Chem,* 273**,** 2926-30.

MÉHES, G., WITT, A., KUBISTA, E. & AMBROS, P. F. 2001. Circulating breast cancer cells are frequently apoptotic. *Am J Pathol,* 159**,** 17-20.

MÜHLETHALER-MOTTET, A., FLAHAUT, M., BOURLOUD, K. B., NARDOU, K., COULON, A., LIBERMAN, J., THOME, M. & GROSS, N. 2011. Individual caspase-10 isoforms play distinct and opposing roles in the initiation of death receptor-mediated tumour cell apoptosis. *Cell Death Dis,* 2**,** e125.

NAGAPRASHANTHA, L. D., VATSYAYAN, R., LELSANI, P. C., AWASTHI, S. & SINGHAL, S. S. 2011. The sensors and regulators of cell-matrix surveillance in anoikis resistance of tumors. *Int J Cancer,* 128**,** 743-52.

NAKANO, K. & VOUSDEN, K. H. 2001. PUMA, a novel proapoptotic gene, is induced by p53. *Mol Cell,* 7**,** 683-94.

NAM, S., KIM, D., CHENG, J. Q., ZHANG, S., LEE, J. H., BUETTNER, R., MIROSEVICH, J., LEE, F. Y. & JOVE, R. 2005. Action of the Src family kinase inhibitor, dasatinib (BMS-354825), on human prostate cancer cells. *Cancer Res,* 65**,** 9185-9.

NEVILLE-WEBBE, H., CROSS, N., EATON, C., NYAMBO, R., EVANS, C., COLEMAN, R. & HOLEN, I. 2004. Osteoprotegerin (OPG) produced by bone marrow stromal cells protects breast cancer cells from TRAIL-induced apoptosis. *Breast Cancer Res Treat,* 86**,** 269-79.

NIESWANDT, B., HAFNER, M., ECHTENACHER, B. & MÄNNEL, D. 1999. Lysis of tumor cells by natural killer cells in mice is impeded by platelets. *Cancer Res,* 59**,** 1295-300.

NIKOLOPOULOS, S. N. & TURNER, C. E. 2000. Actopaxin, a new focal adhesion protein that binds paxillin LD motifs and actin and regulates cell adhesion. *J Cell Biol,* 151**,** 1435-48.

NITSCH, R., BECHMANN, I., DEISZ, R. A., HAAS, D., LEHMANN, T. N., WENDLING, U. & ZIPP, F. 2000. Human brain-cell death induced by tumour-necrosis-factor-related apoptosis-inducing ligand (TRAIL). *Lancet,* 356**,** 827-8.

ODA, E., OHKI, R., MURASAWA, H., NEMOTO, J., SHIBUE, T., YAMASHITA, T., TOKINO, T., TANIGUCHI, T. & TANAKA, N. 2000. Noxa, a BH3-only member of the Bcl-2 family and candidate mediator of p53-induced apoptosis. *Science,* 288**,** 1053-8.

OGASAWARA, J., WATANABE-FUKUNAGA, R., ADACHI, M., MATSUZAWA, A., KASUGAI, T., KITAMURA, Y., ITOH, N., SUDA, T. & NAGATA, S. 1993. Lethal effect of the anti-Fas antibody in mice. *Nature,* 364**,** 806-9.

OKADA, M. & NAKAGAWA, H. 1989. A protein tyrosine kinase involved in regulation of pp60c-src function. *J Biol Chem,* 264**,** 20886-93.

OPEL, D., NAUMANN, I., SCHNEIDER, M., BERTELE, D., DEBATIN, K. M. & FULDA, S. 2011. Targeting aberrant PI3K/Akt activation by PI103 restores sensitivity to TRAIL-induced apoptosis in neuroblastoma. *Clin Cancer Res,* 17**,** 3233-47.

OTEY, C. A., PAVALKO, F. M. & BURRIDGE, K. 1990. An interaction between alpha-actinin and the beta 1 integrin subunit in vitro. *J Cell Biol,* 111**,** 721-9.

OVCHARENKO, D., KELNAR, K., JOHNSON, C., LENG, N. & BROWN, D. 2007. Genome-scale microRNA and small interfering RNA screens identify small RNA modulators of TRAIL-induced apoptosis pathway. *Cancer Res,* 67**,** 10782-8.

OWEN-SCHAUB, L. B., VAN GOLEN, K. L., HILL, L. L. & PRICE, J. E. 1998. Fas and Fas ligand interactions suppress melanoma lung metastasis. *J Exp Med,* 188**,** 1717-23.

PALUMBO, J., TALMAGE, K., MASSARI, J., LA JEUNESSE, C., FLICK, M., KOMBRINCK, K., JIROUSKOVÁ, M. & DEGEN, J. 2005. Platelets and fibrin(ogen) increase metastatic potential by impeding natural killer cell-mediated elimination of tumor cells. *Blood,* 105**,** 178-85.

PAN, G., NI, J., WEI, Y. F., YU, G., GENTZ, R. & DIXIT, V. M. 1997a. An antagonist decoy receptor and a death domain-containing receptor for TRAIL. *Science,* 277**,** 815-8.

PAN, G., NI, J., YU, G., WEI, Y. F. & DIXIT, V. M. 1998. TRUNDD, a new member of the TRAIL receptor family that antagonizes TRAIL signalling. *FEBS Lett,* 424**,** 41-5.

PAN, G., O'ROURKE, K., CHINNAIYAN, A. M., GENTZ, R., EBNER, R., NI, J. & DIXIT, V. M. 1997b. The receptor for the cytotoxic ligand TRAIL. *Science,* 276**,** 111-3.

PANKA, D. J., MANO, T., SUHARA, T., WALSH, K. & MIER, J. W. 2001. Phosphatidylinositol 3-kinase/Akt activity regulates c-FLIP expression in tumor cells. *J Biol Chem,* 276**,** 6893-6.

PARK, C. C., ZHANG, H., PALLAVICINI, M., GRAY, J. W., BAEHNER, F., PARK, C. J. & BISSELL, M. J. 2006. Beta1 integrin inhibitory antibody induces apoptosis of breast cancer cells, inhibits growth, and distinguishes malignant from normal phenotype in three dimensional cultures and in vivo. *Cancer Res,* 66**,** 1526-35.

PENNARUN, B., MEIJER, A., DE VRIES, E. G., KLEIBEUKER, J. H., KRUYT, F. & DE JONG, S. 2010. Playing the DISC: turning on TRAIL death receptor-mediated apoptosis in cancer. *Biochim Biophys Acta,* 1805**,** 123-40.

PETITJEAN, A., MATHE, E., KATO, S., ISHIOKA, C., TAVTIGIAN, S. V., HAINAUT, P. & OLIVIER, M. 2007. Impact of mutant p53 functional properties on TP53 mutation patterns and tumor phenotype: lessons from recent developments in the IARC TP53 database. *Hum Mutat,* 28**,** 622-9.

PITTI, R. M., MARSTERS, S. A., RUPPERT, S., DONAHUE, C. J., MOORE, A. & ASHKENAZI, A. 1996. Induction of apoptosis by Apo-2 ligand, a new member of the tumor necrosis factor cytokine family. *J Biol Chem,* 271**,** 12687-90.

PLUMMER, R., ATTARD, G., PACEY, S., LI, L., RAZAK, A., PERRETT, R., BARRETT, M., JUDSON, I., KAYE, S., FOX, N. L., HALPERN, W., COREY, A., CALVERT, H. & DE BONO, J. 2007. Phase 1 and pharmacokinetic study of lexatumumab in patients with advanced cancers. *Clin Cancer Res,* 13**,** 6187-94.

POSERN, G. & TREISMAN, R. 2006. Actin' together: serum response factor, its cofactors and the link to signal transduction. *Trends Cell Biol,* 16**,** 588-96.

PRICE, J. E., AUKERMAN, S. L. & FIDLER, I. J. 1986. Evidence that the process of murine melanoma metastasis is sequential and selective and contains stochastic elements. *Cancer Res,* 46**,** 5172-8.

PRIDDLE, H., HEMMINGS, L., MONKLEY, S., WOODS, A., PATEL, B., SUTTON, D., DUNN, G. A., ZICHA, D. & CRITCHLEY, D. R. 1998. Disruption of the talin gene compromises focal adhesion assembly in undifferentiated but not differentiated embryonic stem cells. *J Cell Biol,* 142**,** 1121-33.

PUKAC, L., KANAKARAJ, P., HUMPHREYS, R., ALDERSON, R., BLOOM, M., SUNG, C., RICCOBENE, T., JOHNSON, R., FISCELLA, M., MAHONEY, A., CARRELL, J., BOYD, E., YAO, X. T., ZHANG, L., ZHONG, L., VON KERCZEK, A., SHEPARD, L., VAUGHAN, T., EDWARDS, B., DOBSON, C., SALCEDO, T. & ALBERT, V. 2005. HGS-ETR1, a fully human TRAIL-receptor 1 monoclonal antibody, induces cell death in multiple tumour types in vitro and in vivo. *Br J Cancer,* 92**,** 1430-41.

PUTHALAKATH, H., O'REILLY, L. A., GUNN, P., LEE, L., KELLY, P. N., HUNTINGTON, N. D., HUGHES, P. D., MICHALAK, E. M., MCKIMM-BRESCHKIN, J., MOTOYAMA, N., GOTOH, T., AKIRA, S., BOUILLET, P. & STRASSER, A. 2007. ER stress triggers apoptosis by activating BH3-only protein Bim. *Cell,* 129**,** 1337-49.

PUTHALAKATH, H., VILLUNGER, A., O'REILLY, L. A., BEAUMONT, J. G., COULTAS, L., CHENEY, R. E., HUANG, D. C. & STRASSER, A. 2001. Bmf: a proapoptotic BH3-only protein regulated by interaction with the myosin V actin motor complex, activated by anoikis. *Science,* 293**,** 1829-32.

RAVI, R., JAIN, A. J., SCHULICK, R. D., PHAM, V., PROUSER, T. S., ALLEN, H., MAYER, E. G., YU, H., PARDOLL, D. M., ASHKENAZI, A. & BEDI, A. 2004. Elimination of hepatic metastases of colon cancer cells via p53-independent cross-talk between irinotecan and Apo2 ligand/TRAIL. *Cancer Res,* 64**,** 9105-14.

RAWSON, C., COSOLA-SMITH, C. & BARNES, D. 1990. Death of serum-free mouse embryo cells caused by epidermal growth factor deprivation is prevented by cycloheximide, 12-O-tetradecanoylphorbol-13-acetate, or vanadate. *Exp Cell Res,* 186**,** 177-81.

RAYNAUD, F. I., ECCLES, S., CLARKE, P. A., HAYES, A., NUTLEY, B., ALIX, S., HENLEY, A., DI-STEFANO, F., AHMAD, Z., GUILLARD, S., BJERKE, L. M., KELLAND, L., VALENTI, M., PATTERSON, L., GOWAN, S., DE HAVEN BRANDON, A., HAYAKAWA, M., KAIZAWA, H., KOIZUMI, T., OHISHI, T., PATEL, S., SAGHIR, N., PARKER, P., WATERFIELD, M. & WORKMAN, P. 2007. Pharmacologic characterization of a potent inhibitor of class I phosphatidylinositide 3-kinases. *Cancer Res,* 67**,** 5840-50.

REARDON, D. A., FINK, K. L., MIKKELSEN, T., CLOUGHESY, T. F., O'NEILL, A., PLOTKIN, S., GLANTZ, M., RAVIN, P., RAIZER, J. J., RICH, K. M., SCHIFF, D., SHAPIRO, W. R., BURDETTE-RADOUX, S., DROPCHO, E. J., WITTEMER, S. M., NIPPGEN, J., PICARD, M. & NABORS, L. B. 2008. Randomized phase II study of cilengitide, an integrin-targeting arginine-glycine-aspartic acid peptide, in recurrent glioblastoma multiforme. *J Clin Oncol,* 26**,** 5610-7.

REES, D. J., ADES, S. E., SINGER, S. J. & HYNES, R. O. 1990. Sequence and domain structure of talin. *Nature,* 347**,** 685-9.

REGINATO, M. J., MILLS, K. R., PAULUS, J. K., LYNCH, D. K., SGROI, D. C., DEBNATH, J., MUTHUSWAMY, S. K. & BRUGGE, J. S. 2003. Integrins and EGFR coordinately regulate the pro-apoptotic protein Bim to prevent anoikis. *Nat Cell Biol,* 5**,** 733-40.

REN, D., TU, H. C., KIM, H., WANG, G. X., BEAN, G. R., TAKEUCHI, O., JEFFERS, J. R., ZAMBETTI, G. P., HSIEH, J. J. & CHENG, E. H. 2010. BID, BIM, and PUMA are essential for activation of the BAX- and BAK-dependent cell death program. *Science,* 330**,** 1390-3.

RENSING-EHL, A., FREI, K., FLURY, R., MATIBA, B., MARIANI, S., WELLER, M., AEBISCHER, P., KRAMMER, P. & FONTANA, A. 1995. Local Fas/APO-1 (CD95) ligand-mediated tumor cell killing in vivo. *Eur J Immunol,* 25**,** 2253-8.

RICART, A. D., TOLCHER, A. W., LIU, G., HOLEN, K., SCHWARTZ, G., ALBERTINI, M., WEISS, G., YAZJI, S., NG, C. & WILDING, G. 2008. Volociximab, a chimeric monoclonal antibody that specifically binds alpha5beta1 integrin: a phase I, pharmacokinetic, and biological correlative study. *Clin Cancer Res,* 14**,** 7924-9.

RICCI, M. S., KIM, S. H., OGI, K., PLASTARAS, J. P., LING, J., WANG, W., JIN, Z., LIU, Y. Y., DICKER, D. T., CHIAO, P. J., FLAHERTY, K. T., SMITH, C. D. & EL-DEIRY, W. S. 2007. Reduction of TRAIL-induced Mcl-1 and cIAP2 by c-Myc or sorafenib sensitizes resistant human cancer cells to TRAIL-induced death. *Cancer Cell,* 12**,** 66-80.

RICHARDSON, A., MALIK, R., HILDEBRAND, J. & PARSONS, J. 1997. Inhibition of cell spreading by expression of the C-terminal domain of focal adhesion kinase (FAK) is rescued by coexpression of Src or catalytically inactive FAK: a role for paxillin tyrosine phosphorylation. *Mol Cell Biol,* 17**,** 6906-14.

ROBERTS, W. G., UNG, E., WHALEN, P., COOPER, B., HULFORD, C., AUTRY, C., RICHTER, D., EMERSON, E., LIN, J., KATH, J., COLEMAN, K., YAO, L., MARTINEZ-ALSINA, L., LORENZEN, M., BERLINER, M., LUZZIO, M., PATEL, N., SCHMITT, E., LAGRECA, S., JANI, J., WESSEL, M., MARR, E., GRIFFOR, M. & VAJDOS, F. 2008. Antitumor activity and pharmacology of a selective focal adhesion kinase inhibitor, PF-562,271. *Cancer Res,* 68**,** 1935-44.

ROSEN, K., SHI, W., CALABRETTA, B. & FILMUS, J. 2002. Cell detachment triggers p38 mitogen-activated protein kinase-dependent overexpression of Fas ligand. A novel mechanism of Anoikis of intestinal epithelial cells. *J Biol Chem,* 277**,** 46123-30.

ROUS, P. 1911. A SARCOMA OF THE FOWL TRANSMISSIBLE BY AN AGENT SEPARABLE FROM THE TUMOR CELLS. *J Exp Med,* 13**,** 397-411.

RYTÖMAA, M., MARTINS, L. M. & DOWNWARD, J. 1999. Involvement of FADD and caspase-8 signalling in detachment-induced apoptosis. *Curr Biol,* 9**,** 1043-6.

SAFA, A. R., DAY, T. W. & WU, C. H. 2008. Cellular FLICE-like inhibitory protein (C-FLIP): a novel target for cancer therapy. *Curr Cancer Drug Targets,* 8**,** 37-46.

SAHAI, E. 2007. Illuminating the metastatic process. *Nat Rev Cancer,* 7**,** 737-49.

SAKAMOTO, S., MCCANN, R., DHIR, R. & KYPRIANOU, N. 2010. Talin1 promotes tumor invasion and metastasis via focal adhesion signaling and anoikis resistance. *Cancer Res,* 70**,** 1885-95.

SAKUMA, Y., TAKEUCHI, T., NAKAMURA, Y., YOSHIHARA, M., MATSUKUMA, S., NAKAYAMA, H., OHGANE, N., YOKOSE, T., KAMEDA, Y., TSUCHIYA, E. & MIYAGI, Y. 2009. Lung adenocarcinoma cells floating in lymphatic vessels resist anoikis by expressing phosphorylated Src. *J Pathol*.

SALVESEN, G. S. & DIXIT, V. M. 1999. Caspase activation: the induced-proximity model. *Proc Natl Acad Sci U S A,* 96**,** 10964-7.

SAMARA, R. N., LAGUINGE, L. M. & JESSUP, J. M. 2007. Carcinoembryonic antigen inhibits anoikis in colorectal carcinoma cells by interfering with TRAIL-R2 (DR5) signaling. *Cancer Res,* 67**,** 4774-82.

SANCHEZ-CARBAYO, M., SOCCI, N. D., LOZANO, J. J., HAAB, B. B. & CORDON-CARDO, C. 2006. Profiling bladder cancer using targeted antibody arrays. *Am J Pathol,* 168**,** 93-103.

SASAZUKI, T., SAWADA, T., SAKON, S., KITAMURA, T., KISHI, T., OKAZAKI, T., KATANO, M., TANAKA, M., WATANABE, M., YAGITA, H., OKUMURA, K. & NAKANO, H. 2002. Identification of a novel transcriptional activator, BSAC, by a functional cloning to inhibit tumor necrosis factor-induced cell death. *J Biol Chem,* 277**,** 28853-60.

SATYAMOORTHY, K., DEJESUS, E., LINNENBACH, A., KRAJ, B., KORNREICH, D., RENDLE, S., ELDER, D. & HERLYN, M. 1997. Melanoma cell lines from different stages of progression and their biological and molecular analyses. *Melanoma Res,* 7 Suppl 2**,** S35-42.

SCAFFIDI, C., FULDA, S., SRINIVASAN, A., FRIESEN, C., LI, F., TOMASELLI, K. J., DEBATIN, K. M., KRAMMER, P. H. & PETER, M. E. 1998. Two CD95 (APO-1/Fas) signaling pathways. *EMBO J,* 17**,** 1675-87.

SCAFFIDI, C., SCHMITZ, I., KRAMMER, P. H. & PETER, M. E. 1999. The role of c-FLIP in modulation of CD95-induced apoptosis. *J Biol Chem,* 274**,** 1541-8.

SCHALLER, M. D., BORGMAN, C. A., COBB, B. S., VINES, R. R., REYNOLDS, A. B. & PARSONS, J. T. 1992. pp125FAK a structurally distinctive protein-tyrosine kinase associated with focal adhesions. *Proc Natl Acad Sci U S A,* 89**,** 5192-6.

SCHALLER, M. D., HILDEBRAND, J. D., SHANNON, J. D., FOX, J. W., VINES, R. R. & PARSONS, J. T. 1994. Autophosphorylation of the focal adhesion kinase, pp125FAK, directs SH2-dependent binding of pp60src. *Mol Cell Biol,* 14**,** 1680-8.

SCHARENBERG, M. A., CHIQUET-EHRISMANN, R. & ASPARUHOVA, M. B. 2010. Megakaryoblastic leukemia protein-1 (MKL1): Increasing evidence for an involvement in cancer progression and metastasis. *Int J Biochem Cell Biol,* 42**,** 1911-4.

SCHEIDEREIT, C. 2006. IkappaB kinase complexes: gateways to NF-kappaB activation and transcription. *Oncogene,* 25**,** 6685-705.

SCHLAEPFER, D. D., HANKS, S. K., HUNTER, T. & VAN DER GEER, P. 1994. Integrin-mediated signal transduction linked to Ras pathway by GRB2 binding to focal adhesion kinase. *Nature,* 372**,** 786-91.

SCHLAEPFER, D. D. & HUNTER, T. 1997. Focal adhesion kinase overexpression enhances ras-dependent integrin signaling to ERK2/mitogen-activated protein kinase through interactions with and activation of c-Src. *J Biol Chem,* 272**,** 13189-95.

SCHNEIDER, P., OLSON, D., TARDIVEL, A., BROWNING, B., LUGOVSKOY, A., GONG, D., DOBLES, M., HERTIG, S., HOFMANN, K., VAN VLIJMEN, H., HSU, Y. M., BURKLY, L. C., TSCHOPP, J. & ZHENG, T. S. 2003. Identification of a new murine tumor necrosis factor receptor locus that contains two novel murine receptors for tumor necrosis factor-related apoptosis-inducing ligand (TRAIL). *J Biol Chem,* 278**,** 5444-54.

SCHNEIDER, P., THOME, M., BURNS, K., BODMER, J. L., HOFMANN, K., KATAOKA, T., HOLLER, N. & TSCHOPP, J. 1997. TRAIL receptors 1 (DR4) and 2 (DR5) signal FADD-dependent apoptosis and activate NF-kappaB. *Immunity,* 7**,** 831-6.

SCHNEIDER, T., OSL, F., FRIESS, T., STOCKINGER, H. & SCHEUER, W. 2002. Quantification of human Alu sequences by real-time PCR--an improved method to measure therapeutic efficacy of anti-metastatic drugs in human xenotransplants. *Clin Exp Metastasis,* 19**,** 571-82.

SCHRATT, G., PHILIPPAR, U., HOCKEMEYER, D., SCHWARZ, H., ALBERTI, S. & NORDHEIM, A. 2004. SRF regulates Bcl-2 expression and promotes cell survival during murine embryonic development. *EMBO J,* 23**,** 1834-44.

SCHUTZ-GESCHWENDER, A., ZHANG, Y., HOLT, T., MCDERMITT, D. & MICHAEL OLIVEL, D. 2004. Quantitative, two-color western blot detection with infrared fluorescence. LI-COR Biosciences.

SCHÜLER, S., FRITSCHE, P., DIERSCH, S., ARLT, A., SCHMID, R. M., SAUR, D. & SCHNEIDER, G. 2010. HDAC2 attenuates TRAIL-induced apoptosis of pancreatic cancer cells. *Mol Cancer,* 9**,** 80.

SCREPANTI, V., WALLIN, R., LJUNGGREN, H. & GRANDIEN, A. 2001. A central role for death receptor-mediated apoptosis in the rejection of tumors by NK cells. *J Immunol,* 167**,** 2068-73.

SECCHIERO, P., GONELLI, A., CARNEVALE, E., MILANI, D., PANDOLFI, A., ZELLA, D. & ZAULI, G. 2003. TRAIL promotes the survival and proliferation of primary human vascular endothelial cells by activating the Akt and ERK pathways. *Circulation,* 107**,** 2250-6.

SECCHIERO, P., GONELLI, A., MIRANDOLA, P., MELLONI, E., ZAMAI, L., CELEGHINI, C., MILANI, D. & ZAULI, G. 2002. Tumor necrosis factor-related apoptosis-inducing ligand induces monocytic maturation of leukemic and normal myeloid precursors through a caspase-dependent pathway. *Blood,* 100**,** 2421-9.

SEKI, N., HAYAKAWA, Y., BROOKS, A. D., WINE, J., WILTROUT, R. H., YAGITA, H., TANNER, J. E., SMYTH, M. J. & SAYERS, T. J. 2003. Tumor necrosis factor-related apoptosis-inducing ligand-mediated apoptosis is an important endogenous mechanism for resistance to liver metastases in murine renal cancer. *Cancer Res,* 63**,** 207-13.

SENETAR, M. A. & MCCANN, R. O. 2005. Gene duplication and functional divergence during evolution of the cytoskeletal linker protein talin. *Gene,* 362**,** 141-52.

SETHI, T., RINTOUL, R. C., MOORE, S. M., MACKINNON, A. C., SALTER, D., CHOO, C., CHILVERS, E. R., DRANSFIELD, I., DONNELLY, S. C., STRIETER, R. & HASLETT, C. 1999. Extracellular matrix proteins protect small cell lung cancer cells against apoptosis: a mechanism for small cell lung cancer growth and drug resistance in vivo. *Nat Med,* 5**,** 662-8.

SHAH, D., NACIRI, M., CLEE, P. & AL-RUBEAI, M. 2006. NucleoCounter-An efficient technique for the determination of cell number and viability in animal cell culture processes. *Cytotechnology,* 51**,** 39-44.

SHAIN, K. H., LANDOWSKI, T. H. & DALTON, W. S. 2002. Adhesion-mediated intracellular redistribution of c-Fas-associated death domain-like IL-1-converting enzyme-like inhibitory protein-long confers resistance to CD95-induced apoptosis in hematopoietic cancer cell lines. *J Immunol,* 168**,** 2544-53.

SHAW, P. E., SCHRÖTER, H. & NORDHEIM, A. 1989. The ability of a ternary complex to form over the serum response element correlates with serum inducibility of the human c-fos promoter. *Cell,* 56**,** 563-72.

SHERIDAN, J. P., MARSTERS, S. A., PITTI, R. M., GURNEY, A., SKUBATCH, M., BALDWIN, D., RAMAKRISHNAN, L., GRAY, C. L., BAKER, K., WOOD, W. I., GODDARD, A. D., GODOWSKI, P. & ASHKENAZI, A. 1997. Control of TRAIL-induced apoptosis by a family of signaling and decoy receptors. *Science,* 277**,** 818-21.

SHIN, M. S., KIM, H. S., LEE, S. H., PARK, W. S., KIM, S. Y., PARK, J. Y., LEE, J. H., LEE, S. K., LEE, S. N., JUNG, S. S., HAN, J. Y., KIM, H., LEE, J. Y. & YOO, N. J. 2001. Mutations of tumor necrosis factor-related

apoptosis-inducing ligand receptor 1 (TRAIL-R1) and receptor 2 (TRAIL-R2) genes in metastatic breast cancers. *Cancer Res,* 61**,** 4942-6.

SHIVAPURKAR, N., TOYOOKA, S., TOYOOKA, K. O., REDDY, J., MIYAJIMA, K., SUZUKI, M., SHIGEMATSU, H., TAKAHASHI, T., PARIKH, G., PASS, H. I., CHAUDHARY, P. M. & GAZDAR, A. F. 2004. Aberrant methylation of trail decoy receptor genes is frequent in multiple tumor types. *Int J Cancer,* 109**,** 786-92.

SHRADER, M., PINO, M., LASHINGER, L., BAR-ELI, M., ADAM, L., DINNEY, C. & MCCONKEY, D. 2007. Gefitinib reverses TRAIL resistance in human bladder cancer cell lines via inhibition of AKT-mediated X-linked inhibitor of apoptosis protein expression. *Cancer Res,* 67**,** 1430-5.

SIEG, D. J., HAUCK, C. R., ILIC, D., KLINGBEIL, C. K., SCHAEFER, E., DAMSKY, C. H. & SCHLAEPFER, D. D. 2000. FAK integrates growth-factor and integrin signals to promote cell migration. *Nat Cell Biol,* 2**,** 249-56.

SIMPSON, C. D., ANYIWE, K. & SCHIMMER, A. D. 2008. Anoikis resistance and tumor metastasis. *Cancer Lett,* 272**,** 177-85.

SLACK-DAVIS, J. K., MARTIN, K. H., TILGHMAN, R. W., IWANICKI, M., UNG, E. J., AUTRY, C., LUZZIO, M. J., COOPER, B., KATH, J. C., ROBERTS, W. G. & PARSONS, J. T. 2007. Cellular characterization of a novel focal adhesion kinase inhibitor. *J Biol Chem,* 282**,** 14845-52.

SMYTH, M. J., THIA, K. Y., CRETNEY, E., KELLY, J. M., SNOOK, M. B., FORBES, C. A. & SCALZO, A. A. 1999. Perforin is a major contributor to NK cell control of tumor metastasis. *J Immunol,* 162**,** 6658-62.

SOHN, D., TOTZKE, G., ESSMANN, F., SCHULZE-OSTHOFF, K., LEVKAU, B. & JÄNICKE, R. U. 2006. The proteasome is required for rapid initiation of death receptor-induced apoptosis. *Mol Cell Biol,* 26**,** 1967-78.

SONG, J. H., TSE, M. C., BELLAIL, A., PHUPHANICH, S., KHURI, F., KNETEMAN, N. M. & HAO, C. 2007. Lipid rafts and nonrafts mediate tumor necrosis factor related apoptosis-inducing ligand induced apoptotic and nonapoptotic signals in non small cell lung carcinoma cells. *Cancer Res,* 67**,** 6946-55.

SONODA, Y., MATSUMOTO, Y., FUNAKOSHI, M., YAMAMOTO, D., HANKS, S. K. & KASAHARA, T. 2000. Anti-apoptotic role of focal adhesion kinase (FAK). Induction of inhibitor-of-apoptosis proteins and apoptosis suppression by the overexpression of FAK in a human leukemic cell line, HL-60. *J Biol Chem,* 275**,** 16309-15.

SORIA, J. C., SMIT, E., KHAYAT, D., BESSE, B., YANG, X., HSU, C. P., REESE, D., WIEZOREK, J. & BLACKHALL, F. 2010. Phase 1b study of dulanermin (recombinant human Apo2L/TRAIL) in combination with paclitaxel, carboplatin, and bevacizumab in patients with advanced non-squamous non-small-cell lung cancer. *J Clin Oncol,* 28**,** 1527-33.

SOTIROPOULOS, A., GINEITIS, D., COPELAND, J. & TREISMAN, R. 1999. Signal-regulated activation of serum response factor is mediated by changes in actin dynamics. *Cell,* 98**,** 159-69.

SOUNG, Y. H., LEE, J. W., KIM, S. Y., NAM, S. W., PARK, W. S., KIM, S. H., LEE, J. Y., YOO, N. J. & LEE, S. H. 2004. Mutation of FADD gene is rare in human colon and stomach cancers. *APMIS,* 112**,** 595-7.

SPIERINGS, D. C., DE VRIES, E. G., VELLENGA, E., VAN DEN HEUVEL, F. A., KOORNSTRA, J. J., WESSELING, J., HOLLEMA, H. & DE JONG, S. 2004. Tissue distribution of the death ligand TRAIL and its receptors. *J Histochem Cytochem,* 52**,** 821-31.

SPRICK, M. R., WEIGAND, M. A., RIESER, E., RAUCH, C. T., JUO, P., BLENIS, J., KRAMMER, P. H. & WALCZAK, H. 2000. FADD/MORT1 and caspase-8 are recruited to TRAIL receptors 1 and 2 and are essential for apoptosis mediated by TRAIL receptor 2. *Immunity,* 12**,** 599-609.

SRINIVASULA, S. M. & ASHWELL, J. D. 2008. IAPs: what's in a name? *Mol Cell,* 30**,** 123-35.

SRIVASTAVA, R. K., KURZROCK, R. & SHANKAR, S. 2010. MS-275 sensitizes TRAIL-resistant breast cancer cells, inhibits angiogenesis and metastasis, and reverses epithelial-mesenchymal transition in vivo. *Mol Cancer Ther,* 9**,** 3254-66.

STENNICKE, H. R., DEVERAUX, Q. L., HUMKE, E. W., REED, J. C., DIXIT, V. M. & SALVESEN, G. S. 1999. Caspase-9 can be activated without proteolytic processing. *J Biol Chem,* 274**,** 8359-62.

STENNICKE, H. R., JÜRGENSMEIER, J. M., SHIN, H., DEVERAUX, Q., WOLF, B. B., YANG, X., ZHOU, Q., ELLERBY, H. M., ELLERBY, L. M., BREDESEN, D., GREEN, D. R., REED, J. C., FROELICH, C. J. & SALVESEN, G. S. 1998. Pro-caspase-3 is a major physiologic target of caspase-8. *J Biol Chem,* 273**,** 27084-90.

STUPACK, D., PUENTE, X., BOUTSABOUALOY, S., STORGARD, C. & CHERESH, D. 2001. Apoptosis of adherent cells by recruitment of caspase-8 to unligated integrins. *J Cell Biol,* 155**,** 459-70.

STUPACK, D. G., TEITZ, T., POTTER, M. D., MIKOLON, D., HOUGHTON, P. J., KIDD, V. J., LAHTI, J. M. & CHERESH, D. A. 2006. Potentiation of neuroblastoma metastasis by loss of caspase-8. *Nature,* 439**,** 95-9.

SUN, Q., CHEN, G., STREB, J., LONG, X., YANG, Y., STOECKERT, C. J. & MIANO, J. 2006. Defining the mammalian CArGome. *Genome Res,* 16**,** 197-207.

SWANN, J. B. & SMYTH, M. J. 2007. Immune surveillance of tumors. *J Clin Invest,* 117**,** 1137-46.

TACHIBANA, K., URANO, T., FUJITA, H., OHASHI, Y., KAMIGUCHI, K., IWATA, S., HIRAI, H. & MORIMOTO, C. 1997. Tyrosine phosphorylation of Crk-associated substrates by focal adhesion kinase. A putative mechanism for the integrin-mediated tyrosine phosphorylation of Crk-associated substrates. *J Biol Chem,* 272**,** 29083-90.

TADOKORO, S., SHATTIL, S. J., ETO, K., TAI, V., LIDDINGTON, R. C., DE PEREDA, J. M., GINSBERG, M. H. & CALDERWOOD, D. A. 2003. Talin binding to integrin beta tails: a final common step in integrin activation. *Science,* 302**,** 103-6.

TAIT, S. W. & GREEN, D. R. 2010. Mitochondria and cell death: outer membrane permeabilization and beyond. *Nat Rev Mol Cell Biol,* 11**,** 621-32.

TAKEDA, K., HAYAKAWA, Y., SMYTH, M. J., KAYAGAKI, N., YAMAGUCHI, N., KAKUTA, S., IWAKURA, Y., YAGITA, H. & OKUMURA, K. 2001. Involvement of tumor necrosis factor-related apoptosis-inducing ligand in surveillance of tumor metastasis by liver natural killer cells. *Nat Med,* 7**,** 94-100.

TAKEDA, K., SMYTH, M. J., CRETNEY, E., HAYAKAWA, Y., KAYAGAKI, N., YAGITA, H. & OKUMURA, K. 2002. Critical role for tumor necrosis factor-related apoptosis-inducing ligand in immune surveillance against tumor development. *J Exp Med,* 195**,** 161-9.

TAKEDA, K., YAMAGUCHI, N., AKIBA, H., KOJIMA, Y., HAYAKAWA, Y., TANNER, J. E., SAYERS, T. J., SEKI, N., OKUMURA, K., YAGITA, H. & SMYTH, M. J. 2004. Induction of tumor-specific T cell immunity by anti-DR5 antibody therapy. *J Exp Med,* 199**,** 437-48.

TAMAGIKU, Y., SONODA, Y., KUNISAWA, M., ICHIKAWA, D., MURAKAMI, Y., AIZU-YOKOTA, E. & KASAHARA, T. 2004. Down-regulation of procaspase-8 expression by focal adhesion kinase protects HL-60 cells from TRAIL-induced apoptosis. *Biochem Biophys Res Commun,* 323**,** 445-52.

TAMKUN, J. W., DESIMONE, D. W., FONDA, D., PATEL, R. S., BUCK, C., HORWITZ, A. F. & HYNES, R. O. 1986. Structure of integrin, a glycoprotein involved in the transmembrane linkage between fibronectin and actin. *Cell,* 46**,** 271-82.

TANNAPFEL, A., ANHALT, K., HÄUSERMANN, P., SOMMERER, F., BENICKE, M., UHLMANN, D., WITZIGMANN, H., HAUSS, J. & WITTEKIND, C. 2003. Identification of novel proteins associated with hepatocellular carcinomas using protein microarrays. *J Pathol,* 201**,** 238-49.

TAYLOR, R., CULLEN, S. & MARTIN, S. 2008. Apoptosis: controlled demolition at the cellular level. *Nat Rev Mol Cell Biol,* 9**,** 231-41.

THOMAS, S. & BRUGGE, J. 1997. Cellular functions regulated by Src family kinases. *Annu Rev Cell Dev Biol,* 13**,** 513-609.

THORNBERRY, N. A. & LAZEBNIK, Y. 1998. Caspases: enemies within. *Science,* 281**,** 1312-6.

TICE, D., BISCARDI, J., NICKLES, A. & PARSONS, S. 1999. Mechanism of biological synergy between cellular Src and epidermal growth factor receptor. *Proc Natl Acad Sci U S A,* 96**,** 1415-20.

TOILLON, R. A., DESCAMPS, S., ADRIAENSSENS, E., RICORT, J. M., BERNARD, D., BOILLY, B. & LE BOURHIS, X. 2002. Normal breast epithelial cells induce apoptosis of breast cancer cells via Fas signaling. *Exp Cell Res,* 275**,** 31-43.

TRARBACH, T., MOEHLER, M., HEINEMANN, V., KÖHNE, C., PRZYBOREK, M., SCHULZ, C., SNELLER, V., GALLANT, G. & KANZLER, S. 2010. Phase II trial of mapatumumab, a fully human agonistic monoclonal antibody that targets and activates the tumour necrosis factor apoptosis-inducing ligand receptor-1 (TRAIL-R1), in patients with refractory colorectal cancer. *Br J Cancer*.

TREVINO, J. G., SUMMY, J. M., LESSLIE, D. P., PARIKH, N. U., HONG, D. S., LEE, F. Y., DONATO, N. J., ABBRUZZESE, J. L., BAKER, C. H. & GALLICK, G. E. 2006. Inhibition of SRC expression and activity inhibits tumor progression and metastasis of human pancreatic adenocarcinoma cells in an orthotopic nude mouse model. *Am J Pathol,* 168**,** 962-72.

TROUSSARD, A. A., MCDONALD, P. C., WEDERELL, E. D., MAWJI, N. M., FILIPENKO, N. R., GELMON, K. A., KUCAB, J. E., DUNN, S. E., EMERMAN, J. T., BALLY, M. B. & DEDHAR, S. 2006. Preferential dependence of breast cancer cells versus normal cells on integrin-linked kinase for protein kinase B/Akt activation and cell survival. *Cancer Res,* 66**,** 393-403.

TU, Y., HUANG, Y., ZHANG, Y., HUA, Y. & WU, C. 2001. A new focal adhesion protein that interacts with integrin-linked kinase and regulates cell adhesion and spreading. *J Cell Biol,* 153**,** 585-98.

TU, Y., LI, F., GOICOECHEA, S. & WU, C. 1999. The LIM-only protein PINCH directly interacts with integrin-linked kinase and is recruited to integrin-rich sites in spreading cells. *Mol Cell Biol,* 19**,** 2425-34.

VARFOLOMEEV, E., MAECKER, H., SHARP, D., LAWRENCE, D., RENZ, M., VUCIC, D. & ASHKENAZI, A. 2005. Molecular determinants of kinase pathway activation by Apo2 ligand/tumor necrosis factor-related apoptosis-inducing ligand. *J Biol Chem,* 280**,** 40599-608.

VARTIAINEN, M., GUETTLER, S., LARIJANI, B. & TREISMAN, R. 2007. Nuclear actin regulates dynamic subcellular localization and activity of the SRF cofactor MAL. *Science,* 316**,** 1749-52.

VAUX, D. L. & SILKE, J. 2003. HtrA2/Omi, a sheep in wolf's clothing. *Cell,* 115**,** 251-3.

VAZQUEZ-MARTIN, A., COLOMER, R. & MENENDEZ, J. A. 2007. Protein array technology to detect HER2 (erbB-2)-induced 'cytokine signature' in breast cancer. *Eur J Cancer,* 43**,** 1117-24.

VOORTMAN, J., RESENDE, T. P., ABOU EL HASSAN, M. A., GIACCONE, G. & KRUYT, F. A. 2007. TRAIL therapy in non-small cell lung cancer cells: sensitization to death receptor-mediated apoptosis by proteasome inhibitor bortezomib. *Mol Cancer Ther,* 6**,** 2103-12.

WAGNER, K. W., PUNNOOSE, E. A., JANUARIO, T., LAWRENCE, D. A., PITTI, R. M., LANCASTER, K., LEE, D., VON GOETZ, M., YEE, S. F., TOTPAL, K., HUW, L., KATTA, V., CAVET, G., HYMOWITZ, S. G., AMLER, L. & ASHKENAZI, A. 2007. Death-receptor O-glycosylation controls tumor-cell sensitivity to the proapoptotic ligand Apo2L/TRAIL. *Nat Med,* 13**,** 1070-7.

WALCZAK, H., MILLER, R. E., ARIAIL, K., GLINIAK, B., GRIFFITH, T. S., KUBIN, M., CHIN, W., JONES, J., WOODWARD, A., LE, T., SMITH, C., SMOLAK, P., GOODWIN, R. G., RAUCH, C. T., SCHUH, J. C. & LYNCH, D. H. 1999. Tumoricidal activity of tumor necrosis factor-related apoptosis-inducing ligand in vivo. *Nat Med,* 5**,** 157-63.

WANG, C. Y., MAYO, M. W., KORNELUK, R. G., GOEDDEL, D. V. & BALDWIN, A. S. 1998. NF-kappaB antiapoptosis: induction of TRAF1 and TRAF2 and c-IAP1 and c-IAP2 to suppress caspase-8 activation. *Science,* 281**,** 1680-3.

WANG, D., CHANG, P. S., WANG, Z., SUTHERLAND, L., RICHARDSON, J. A., SMALL, E., KRIEG, P. A. & OLSON, E. N. 2001. Activation of cardiac gene expression by myocardin, a transcriptional cofactor for serum response factor. *Cell,* 105**,** 851-62.

WANG, D. Z., LI, S., HOCKEMEYER, D., SUTHERLAND, L., WANG, Z., SCHRATT, G., RICHARDSON, J. A., NORDHEIM, A. & OLSON, E. N. 2002. Potentiation of serum response factor activity by a family of myocardin-related transcription factors. *Proc Natl Acad Sci U S A,* 99**,** 14855-60.

WANG, H., FU, W., IM, J. H., ZHOU, Z., SANTORO, S. A., IYER, V., DIPERSIO, C. M., YU, Q. C., QUARANTA, V., AL-MEHDI, A. & MUSCHEL, R. J. 2004. Tumor cell alpha3beta1 integrin and vascular laminin-5 mediate pulmonary arrest and metastasis. *J Cell Biol,* 164**,** 935-41.

WANG, J., ZHENG, L., LOBITO, A., CHAN, F. K., DALE, J., SNELLER, M., YAO, X., PUCK, J. M., STRAUS, S. E. & LENARDO, M. J. 1999. Inherited human Caspase 10 mutations underlie defective lymphocyte and dendritic cell apoptosis in autoimmune lymphoproliferative syndrome type II. *Cell,* 98**,** 47-58.

WANG, S. & EL-DEIRY, W. S. 2003. TRAIL and apoptosis induction by TNF-family death receptors. *Oncogene,* 22**,** 8628-33.

WANG, Y. V., WADE, M., WONG, E., LI, Y. C., RODEWALD, L. W. & WAHL, G. M. 2007. Quantitative analyses reveal the importance of regulated Hdmx degradation for p53 activation. *Proc Natl Acad Sci U S A,* 104**,** 12365-70.

WEBB, D. J., DONAIS, K., WHITMORE, L. A., THOMAS, S. M., TURNER, C. E., PARSONS, J. T. & HORWITZ, A. F. 2004. FAK-Src signalling through paxillin, ERK and MLCK regulates adhesion disassembly. *Nat Cell Biol,* 6**,** 154-61.

WEI, K., CHE, N. & CHEN, F. 2007. Myocardin-related transcription factor B is required for normal mouse vascular development and smooth muscle gene expression. *Dev Dyn,* 236**,** 416-25.

WEI, M. C., ZONG, W. X., CHENG, E. H., LINDSTEN, T., PANOUTSAKOPOULOU, V., ROSS, A. J., ROTH, K. A., MACGREGOR, G. R., THOMPSON, C. B. & KORSMEYER, S. J. 2001. Proapoptotic BAX and BAK: a requisite gateway to mitochondrial dysfunction and death. *Science,* 292**,** 727-30.

WEINER, T. M., LIU, E. T., CRAVEN, R. J. & CANCE, W. G. 1993. Expression of focal adhesion kinase gene and invasive cancer. *Lancet,* 342**,** 1024-5.

WEISS, L., ELKIN, G. & BARBERA-GUILLEM, E. 1993. The differential resistance of B16 wild-type and F10 cells to mechanical trauma in vitro. *Invasion Metastasis,* 13**,** 92-101.

WHITE, D., KURPIOS, N., ZUO, D., HASSELL, J., BLAESS, S., MUELLER, U. & MULLER, W. 2004. Targeted disruption of beta1-integrin in a transgenic mouse model of human breast cancer reveals an essential role in mammary tumor induction. *Cancer Cell,* 6**,** 159-70.

WHITE, D. E., CARDIFF, R. D., DEDHAR, S. & MULLER, W. J. 2001. Mammary epithelial-specific expression of the integrin-linked kinase (ILK) results in the induction of mammary gland hyperplasias and tumors in transgenic mice. *Oncogene,* 20**,** 7064-72.

WILEY, S. R., SCHOOLEY, K., SMOLAK, P. J., DIN, W. S., HUANG, C. P., NICHOLL, J. K., SUTHERLAND, G. R., SMITH, T. D., RAUCH, C., SMITH, C. A. & ET AL. 1995. Identification and characterization of a new member of the TNF family that induces apoptosis. *Immunity,* 3**,** 673-82.

WILLIS, S. N., CHEN, L., DEWSON, G., WEI, A., NAIK, E., FLETCHER, J. I., ADAMS, J. M. & HUANG, D. C. 2005. Proapoptotic Bak is sequestered by Mcl-1 and Bcl-xL, but not Bcl-2, until displaced by BH3-only proteins. *Genes Dev,* 19**,** 1294-305.

WILLIS, S. N., FLETCHER, J. I., KAUFMANN, T., VAN DELFT, M. F., CHEN, L., CZABOTAR, P. E., IERINO, H., LEE, E. F., FAIRLIE, W. D., BOUILLET, P., STRASSER, A., KLUCK, R. M., ADAMS, J. M. & HUANG, D. C. 2007. Apoptosis initiated when BH3 ligands engage multiple Bcl-2 homologs, not Bax or Bak. *Science,* 315**,** 856-9.

WONG, C. W., LEE, A., SHIENTAG, L., YU, J., DONG, Y., KAO, G., AL-MEHDI, A. B., BERNHARD, E. J. & MUSCHEL, R. J. 2001. Apoptosis: an early event in metastatic inefficiency. *Cancer Res,* 61**,** 333-8.

WONG, C. W., SONG, C., GRIMES, M. M., FU, W., DEWHIRST, M. W., MUSCHEL, R. J. & AL-MEHDI, A. B. 2002. Intravascular location of breast cancer cells after spontaneous metastasis to the lung. *Am J Pathol,* 161**,** 749-53.

WOODS, N. T., YAMAGUCHI, H., LEE, F. Y., BHALLA, K. N. & WANG, H. G. 2007. Anoikis, initiated by Mcl-1 degradation and Bim induction, is deregulated during oncogenesis. *Cancer Res,* 67**,** 10744-52.

WU, C. 2005. PINCH, N(i)ck and the ILK: network wiring at cell-matrix adhesions. *Trends Cell Biol,* 15**,** 460-6.

WU, G. 2009. TRAIL as a target in anti-cancer therapy. *Cancer Lett,* 285**,** 1-5.

WU, G. S., BURNS, T. F., ZHAN, Y., ALNEMRI, E. S. & EL-DEIRY, W. S. 1999. Molecular cloning and functional analysis of the mouse homologue of the KILLER/DR5 tumor necrosis factor-related apoptosis-inducing ligand (TRAIL) death receptor. *Cancer Res,* 59**,** 2770-5.

XU, J., ZHOU, J., WEI, W. & WU, G. 2010. Activation of the Akt survival pathway contributes to TRAIL resistance in cancer cells. *PLoS One,* 5**,** e10226.

XU, L., YIN, S., BANERJEE, S., SARKAR, F. & REDDY, K. B. 2011. Enhanced anticancer effect of the combination of cisplatin and TRAIL in triple-negative breast tumor cells. *Mol Cancer Ther,* 10**,** 550-7.

XU, L. H., YANG, X., BRADHAM, C. A., BRENNER, D. A., BALDWIN, A. S., CRAVEN, R. J. & CANCE, W. G. 2000. The focal adhesion kinase suppresses transformation-associated, anchorage-independent apoptosis in human breast cancer cells. Involvement of death receptor-related signaling pathways. *J Biol Chem,* 275**,** 30597-604.

YAMAJI, S., SUZUKI, A., SUGIYAMA, Y., KOIDE , Y., YOSHIDA, M., KANAMORI, H., MOHRI, H., OHNO, S. & ISHIGATSUBO, Y. 2001. A novel integrin-linked kinase-binding protein, affixin, is involved in the early stage of cell-substrate interaction. *J Cell Biol,* 153**,** 1251-64.

YANG, E., ZHA, J., JOCKEL, J., BOISE, L. H., THOMPSON, C. B. & KORSMEYER, S. J. 1995. Bad, a heterodimeric partner for Bcl-XL and Bcl-2, displaces Bax and promotes cell death. *Cell,* 80**,** 285-91.

YANG, J., LIU, X., BHALLA, K., KIM, C. N., IBRADO, A. M., CAI, J., PENG, T. I., JONES, D. P. & WANG, X. 1997. Prevention of apoptosis by Bcl-2: release of cytochrome c from mitochondria blocked. *Science,* 275**,** 1129-32.

YANG, X., CHANG, H. Y. & BALTIMORE, D. 1998. Autoproteolytic activation of pro-caspases by oligomerization. *Mol Cell,* 1**,** 319-25.

YAO, E. S., ZHANG, H., CHEN, Y. Y., LEE, B., CHEW, K., MOORE, D. & PARK, C. 2007. Increased beta1 integrin is associated with decreased survival in invasive breast cancer. *Cancer Res,* 67**,** 659-64.

YAREMKO, M. L., RECANT, W. M. & WESTBROOK, C. A. 1995. Loss of heterozygosity from the short arm of chromosome 8 is an early event in breast cancers. *Genes Chromosomes Cancer,* 13**,** 186-91.

YEH, J. H., HSU, S. C., HAN, S. H. & LAI, M. Z. 1998. Mitogen-activated protein kinase kinase antagonized fas-associated death domain protein-mediated apoptosis by induced FLICE-inhibitory protein expression. *J Exp Med,* 188**,** 1795-802.

YIN, X. M., WANG, K., GROSS, A., ZHAO, Y., ZINKEL, S., KLOCKE, B., ROTH, K. A. & KORSMEYER, S. J. 1999. Bid-deficient mice are resistant to Fas-induced hepatocellular apoptosis. *Nature,* 400**,** 886-91.

YOULE, R. J. & STRASSER, A. 2008. The BCL-2 protein family: opposing activities that mediate cell death. *Nat Rev Mol Cell Biol,* 9**,** 47-59.

YU, W., ISRAEL, K., LIAO, Q. Y., ALDAZ, C. M., SANDERS, B. G. & KLINE, K. 1999. Vitamin E succinate (VES) induces Fas sensitivity in human breast cancer cells: role for Mr 43,000 Fas in VES-triggered apoptosis. *Cancer Res,* 59**,** 953-61.

YUAN, J., SHAHAM, S., LEDOUX, S., ELLIS, H. M. & HORVITZ, H. R. 1993. The C. elegans cell death gene ced-3 encodes a protein similar to mammalian interleukin-1 beta-converting enzyme. *Cell,* 75**,** 641-52.

YUE, H. H., DIEHL, G. E. & WINOTO, A. 2005. Loss of TRAIL-R does not affect thymic or intestinal tumor development in p53 and adenomatous polyposis coli mutant mice. *Cell Death Differ,* 12**,** 94-7.

ZAMAI, L., PONTI, C., MIRANDOLA, P., GOBBI, G., PAPA, S., GALEOTTI, L., COCCO, L. & VITALE, M. 2007. NK cells and cancer. *J Immunol,* 178**,** 4011-6.

ZAMAI, L., SECCHIERO, P., PIERPAOLI, S., BASSINI, A., PAPA, S., ALNEMRI, E. S., GUIDOTTI, L., VITALE, M. & ZAULI, G. 2000. TNF-related apoptosis-inducing ligand (TRAIL) as a negative regulator of normal human erythropoiesis. *Blood,* 95**,** 3716-24.

ZERAFA, N., WESTWOOD, J. A., CRETNEY, E., MITCHELL, S., WARING, P., IEZZI, M. & SMYTH, M. J. 2005. Cutting edge: TRAIL deficiency accelerates hematological malignancies. *J Immunol,* 175**,** 5586-90.

ZHANG, X., BORROW, J., ZHANG, X., NGUYEN, T. & HERSEY, P. 2003a. Activation of ERK1/2 protects melanoma cells from TRAIL-induced apoptosis by inhibiting Smac/DIABLO release from mitochondria. *Oncogene,* 22**,** 2869-81.

ZHANG, X., JIANG, G., CAI, Y., MONKLEY, S., CRITCHLEY, D. & SHEETZ, M. 2008. Talin depletion reveals independence of initial cell spreading from integrin activation and traction. *Nat Cell Biol,* 10**,** 1062-8.

ZHANG, X., WANG, Q., GERALD, W., HUDIS, C., NORTON, L., SMID, M., FOEKENS, J. & MASSAGUÉ, J. 2009a. Latent bone metastasis in breast cancer tied to Src-dependent survival signals. *Cancer Cell,* 16**,** 67-78.

ZHANG, X., ZHANG, X., GRAY, C., NGUYEN, T. & HERSEY, P. 2001. Tumor necrosis factor-related apoptosis-inducing ligand-induced apoptosis of human melanoma is regulated by smac/DIABLO release from mitochondria. *Cancer Res,* 61**,** 7339-48.

ZHANG, X. D., FRANCO, A., MYERS, K., GRAY, C., NGUYEN, T. & HERSEY, P. 1999. Relation of TNF-related apoptosis-inducing ligand (TRAIL) receptor and FLICE-inhibitory protein expression to TRAIL-induced apoptosis of melanoma. *Cancer Res,* 59**,** 2747-53.

ZHANG, X. R., ZHANG, L. Y., DEVADAS, S., LI, L., KEEGAN, A. D. & SHI, Y. F. 2003b. Reciprocal expression of TRAIL and CD95L in Th1 and Th2 cells: role of apoptosis in T helper subset differentiation. *Cell Death Differ,* 10**,** 203-10.

ZHANG, Y., YOSHIDA, T. & ZHANG, B. 2009b. TRAIL induces endocytosis of its death receptors in MDA-MB-231 breast cancer cells. *Cancer Biol Ther,* 8**,** 917-22.

ZHANG, Y. & ZHANG, B. 2008. TRAIL resistance of breast cancer cells is associated with constitutive endocytosis of death receptors 4 and 5. *Mol Cancer Res,* 6**,** 1861-71.

ZHAO, J. & GUAN, J. L. 2009. Signal transduction by focal adhesion kinase in cancer. *Cancer Metastasis Rev,* 28**,** 35-49.

ZHUANG, L., LEE, C., SCOLYER, R., MCCARTHY, S., ZHANG, X., THOMPSON, J., SCREATON, G. & HERSEY, P. 2006. Progression in melanoma is associated with decreased expression of death receptors for tumor necrosis factor-related apoptosis-inducing ligand. *Hum Pathol,* 37**,** 1286-94.

ZINONOS, I., LABRINIDIS, A., LEE, M., LIAPIS, V., HAY, S., PONOMAREV, V., DIAMOND, P., FINDLAY, D. M., ZANNETTINO, A. C. & EVDOKIOU, A. 2011. Anticancer efficacy of Apo2L/TRAIL is retained in the presence of high and biologically active concentrations of osteoprotegerin in vivo. *J Bone Miner Res,* 26**,** 630-43.

ZOU, H., HENZEL, W. J., LIU, X., LUTSCHG, A. & WANG, X. 1997. Apaf-1, a human protein homologous to C. elegans CED-4, participates in cytochrome c-dependent activation of caspase-3. *Cell,* 90**,** 405-13.

Supplementary data

Supplementary Chapter S1 : Apoptosis array optimization……224

Supplementary Chapter 1: Apoptosis Array Optimisation

S1. Introduction

Protein arrays are becoming an increasingly popular tool for investigating protein expression changes within entire signalling pathways (Kopf and Zharhary, 2007). This high-throughput method of protein analysis allows sensitive, simultaneous investigations to be performed, highlighting potential targets of interest much more rapidly than conventional Western blotting. These arrays can be used with a variety of sample types including whole cell lysates, tissue samples and conditioned media, giving them a wide scope of application in the proteomics field. The ability to investigate global protein changes is essential for our understanding of disease changes, drug responses, and to aid the identification of therapeutic biomarkers (Tannapfel et al., 2003, Sanchez-Carbayo et al., 2006, Vazquez-Martin et al., 2007).

Protein arrays such as the Proteome Profiler™ Arrays from R&D Systems allow the investigation of protein expression changes within a number of important biological pathways including the apoptosis pathway. They are created by the spotting of duplicate spots of capture antibody onto a nitrocellulose membrane. The incubation of biological samples with these membranes results in the binding of sample proteins to the relevant capture antibodies. The more protein present in the sample, the greater the amount will bind to the capture antibody, allowing the determination of protein levels within samples. A cocktail of biotinylated detection antibodies are used to detect the presence of protein bound to each spot, and this

signal is amplified using HRP-conjugated streptavidin. The HRP tag allows the imaging of the arrays using conventional chemiluminescence substrates and development onto X-ray film (Huang and Amero, 1997).

S1.1 Chemiluminescence/film data acquisition

Although chemiluminescence allows relatively rapid detection using X-ray film and reasonable sensitivity, there are two main limitations: noise and dynamic range. As well as the inherent noise caused by the grain of the film, both the film development and subsequent scanning create opportunities for dust and scratches to become introduced from the physical handling of the film. An example of noise in a film image can be seen in figure S1A.

For this application, the dynamic range of film is relatively poor meaning that adequate exposure of the weaker spots results in overexposure of the stronger spots. Figure S1B shows a 10 sec and 1 min exposure of the same protein array to film. Spots that appear missing in the 10 sec exposure become visible in the 1 min exposure but at the expense of over exposing the stronger spots.

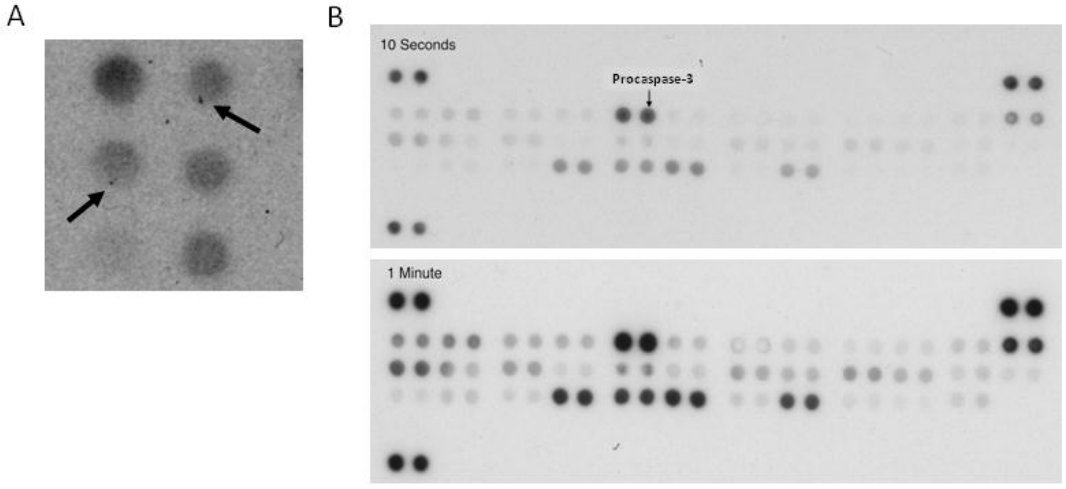

Figure S1. Noise and dynamic range limitations of array images on film. A Enlarged portion of an R&D Systems Proteome Profiler™ Array imaged using chemiluminescence/film illustrating noise due to film grain and dust (indicated by arrows).**B** 350 µg of MDA-MB-231 whole cell lysate incubated with the array and developed using ECL + reagent with a 10 sec or 1 min exposure. Some of the weaker spots in the 1 min exposure are missing in the 10 sec exposure, whilst the stronger spots are over exposed in the 1 min exposure.

Figure S2A shows the spatial intensity distribution for the second of the procaspase-3 spots (labelled in figure S1B) resulting from a 10 sec and 1 min exposure. The flat top of the distribution for the 1 min exposure suggests saturation. Plotting the average intensity of each of the protein spot pairs for the 10 sec exposure against those of the 1 min exposure gives a curve which flattens at high values. The consequence of this saturation effect is that multiple exposures are necessary to acquire intensity values for all of the protein pairs that are free from saturation.

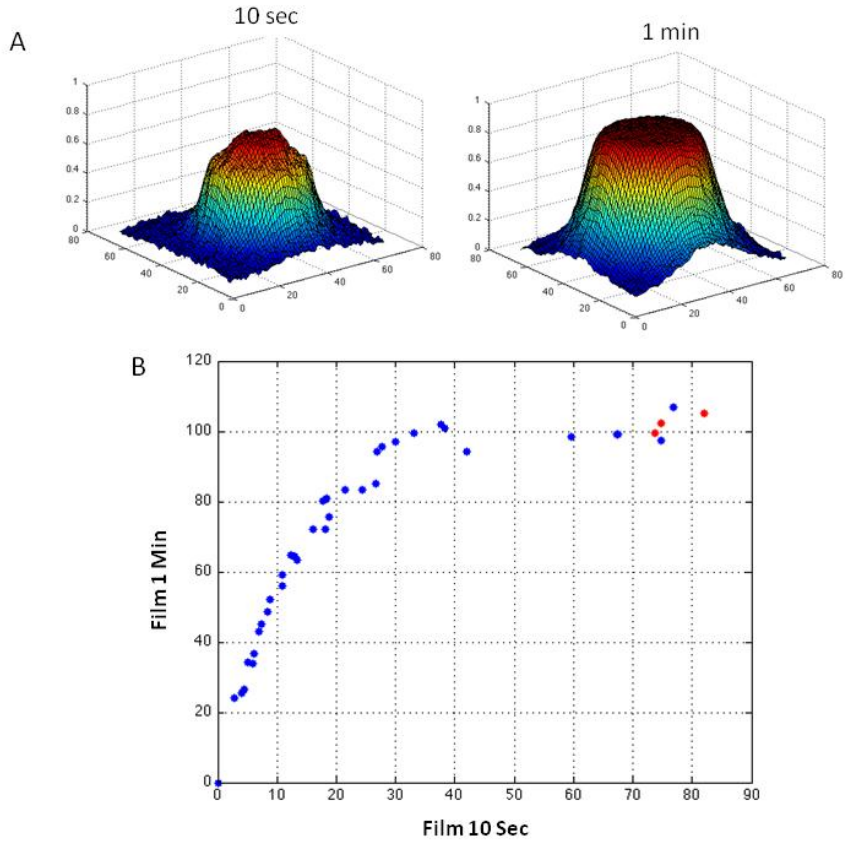

Figure S2. Evidence of signal saturation on film images of arrays. A The light intensity distribution for the second procaspase-3 spot (see figure S1) for a 10 sec and 1 min exposure. The flat top of the distribution for the 1 min exposure suggests saturation. **B** Plot of the averaged spot pair values for the 10 sec and 1 min exposures. The points in red correspond to the 3 pairs of control spots. The flattening of the curve for high values suggests saturation in the 1 min exposure.

Another possible method of chemiluminescence detection is the In Vivo Imaging System (IVIS® 200) from Caliper Life Sciences. This machine is designed for non-invasive *in vivo* imaging, as it can detect fluorescence and bioluminescence with a high sensitivity. However the IVIS is susceptible to background noise resulting from cosmic ray strikes, giving a much worse signal to noise ratio than film images. To overcome this, multiple exposures would need to be taken which were beyond the capacity of the software. For these reasons, imaging arrays on the IVIS was ruled out as an impractical means of data acquisition. Although chemiluminescence has long been the conventional method of Western blot and protein array detection, fluorescence based detection methods are becoming an appealing alternative.

S1.2 Fluorescence data acquisition

The use of fluorescent detection techniques gives the opportunity for multiplexed analysis using fluorophores emitting at different wavelengths and eliminates the reliance on variable enzymatic reaction steps. However previous studies have shown that fluorescent probes within the visible light range have lower sensitivity than chemiluminescence due to the tendency of the biological membranes to auto fluoresce (Gingrich et al., 2000). The use of fluorophores which can be excited in the infrared detection range eliminates this problem of autofluorescence, greatly increasing the sensitivity and application of fluorophore-based detection.

The Proteome Profiler™ Array Human Apoptosis Array protocol can be adjusted to replace streptavidin-HRP with a streptavidin conjugated fluorophore (Alexa-700). This emits light only when excited at the appropriate wavelength, using equipment such as the Odyssey® Infrared Imager from LI-COR® Biosciences (figure S3).

Figure S3. Array image acquired using infrared detection using Licor® Odyssey.

There are distinct advantages of using infrared fluorescence over chemiluminescence for array data acquisition. Firstly, acquiring protein array data using infrared fluorescence allows the direct digitization of array read-outs, reducing the opportunity for the incorporation of noise into images. Secondly, as the signal from the conjugated fluorophore is only emitted following excitation, there is the possibility of re-scanning arrays after the initial experiment was performed. A third distinct advantage of using infrared detection techniques is that they have a much higher sensitivity, detecting proteins over a much greater linear range than chemiluminescence techniques (Schutz-Geschwender et al., 2004, Wang et al., 2007).

S1.3 Semi-quantitation of arrays

Both chemiluminescence and fluorescence detection methods result in an array image in which spot intensity relates to protein level. The next challenge is to quantitate the spot intensity, allowing more meaningful comparisons between conditions. Without the ability to fully or semi-quantitate protein expression levels, conclusions must be drawn on relative protein expression levels using the limitations of the human eye. The instructions for semi-quantitation of arrays provided with the R&D Systems apoptosis array are greatly subject to interpretation and suggest a laborious process of manually planting a region of interest over each spot using software such as ImageJ to derive average intensity values for each spot. For large arrays, this can be an arduous and inaccurate process.

S2. Aims

The primary aim of this chapter is to develop an automatic software tool to allow rapid and accurate semi-quantitation of data from the R&D Systems human apoptosis arrays used in this thesis. For the work in this thesis, chemiluminescent data acquisition methods were used to obtain array images. However, once developed, this tool was tested on arrays developed using different data acquisition techniques. This led to the development of a general tool which could be adapted to different array types and on array images acquired using both chemiluminescent and fluorescent techniques.

The second aim was to use the tool to investigate the potential merits and/or limitations of chemiluminescence and infrared data acquisition techniques.

This work was performed in collaboration with Dr P D Allen of the GIROB Imaging Core, Gray Institute of Radiation Oncology and Biology, Oxford.

S3. Materials & Methods

To develop an automatic method of protein level semi-quantification, the Proteome Profiler™ Human Apoptosis Array Kit was used (#ARY009) from R&D Systems. Each array membrane contains 35 apoptosis proteins, spotted in duplicate adjacent spots, along with negative and positive control spots (see Figure S4).

Each kit contained four individual arrays: two were prepared using the chemiluminescence method (Film A and Film B) and the remaining two prepared using the infrared method (Licor A and Licor B). All four were prepared using the same biological sample so that intra- and inter-method variability could be investigated. Image analysis software was designed by Dr P D Allen using MATLAB® (Mathworks®).

A

B

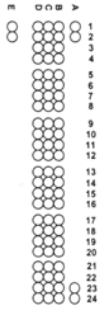

C

Coordinate	Target/Control	Coordinate	Target/Control
A1, A2	Positive Control	C13, C14	HO-2/HMOX2
A23, A24	Positive Control	C15, C16	HSP27
B1, B2	Bad	C17, C18	HSP60
B3, B4	Bax	C19, C20	HSP70
B5, B6	Bcl-2	C21, C22	HTRA2/Omi
B7, B8	Bcl-x	C23, C24	Livin
B9, B10	Pro-Caspase-3	D1, D2	PON2
B11, B12	Cleaved Caspase-3	D3, D4	p21/CIP1/CDNK1A
B13, B14	Catalase	D5, D6	p27/Kip1
B15, B16	cIAP-1	D7, D8	Phospho-p53 (S15)
B17, B18	cIAP-2	D9, D10	Phospho-p53 (S46)
B19, B20	Claspin	D11, D12	Phospho-p53 (S392)
B21, B22	Clusterin	D13, D14	Phospho-Rad17 (S635)
B23, B24	Cytochrome c	D15, D16	SMAC/Diablo
C1, C2	TRAIL R1/DR4	D17, D18	Survivin
C3, C4	TRAIL R2/DR5	D19, D20	TNF RI/TNFRSF1A
C5, C6	FADD	D21, D22	XIAP
C7, C8	Fas/TNFSF6	D23, D24	PBS (Negative Control)
C9, C10	HIF-1α	E1, E2	Positive Control
C11, C12	HO-1/HMOX1/HSP32		

Figure S4 R&D System Proteome Profiler™ human apoptosis array. A An example of a human apoptosis array generated using 350 µg of MDA-MB-231 whole cell lysate and developed onto film using chemiluminescence. **B** Overlay outlining which spots pairs correspond to which apoptosis protein, outlined in the table in **C**.

S3.1 Chemiluminescence detection

MDA-MB-231 cells were lysed using the lysis buffer provided in the array kit. Protein concentration was measured using a BCA assay (Thermoscientific). The array membranes were prepared as outlined in Chapter 2, Section 2.5 and developed using X-ray development as described in Chapter 2, Section 2.3.6.

S3.2 Infrared detection

For the analysis of membranes using infrared detection techniques, the protocol for membrane preparation required alteration. Whole cell lysates were prepared as outlined above. Prior to blocking, the numbers printed on the top of the membranes were cut off and the membrane marked in pencil. This was

necessary to prevent autofluorescence of the ink used to print the numbers (see figure S5). Instead of Streptavidin-HRP solution, membranes were incubated with a 1/7500 dilution of Streptavidin Alexa-Fluor 700 (Invitrogen) for 30 min at room temperature in the dark. After the final wash, membranes were read using the Odyssey® Infrared Imager from LI-COR® Biosciences. Images were acquired using the 685 nm laser, with a resolution of 84 µm, illumination setting of L1.5 and quality set to `highest' (i.e. no image compression).

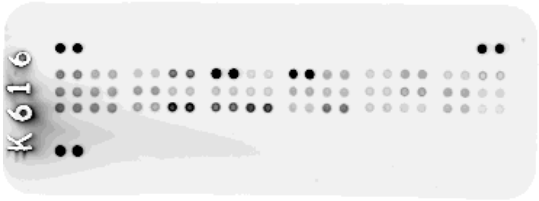

Figure S5. A LI-COR image of a membrane showing autofluorescent contamination from the ink in the serial number. The serial number must be removed *prior* to preparation.

S3.3 Image Analysis

The image analysis outlined in this section was performed using MATLAB® software by Dr P D Allen.

S3.3.1 Template creation

R&D Systems produce a range of protein arrays investigating specific biological pathways, each using a different spatial arrangement of spots. For automatic analysis of the arrays, a template was created for each array type, containing the relative coordinates and protein label of each spot. This template could then be fitted automatically to array images using a rigid registration. This rigid template is only a starting point for further image analysis because, as shown in Figure S6, manufacturing inconsistencies mean that the array spots are never exactly aligned to the rigid template created by the transparency overlay.

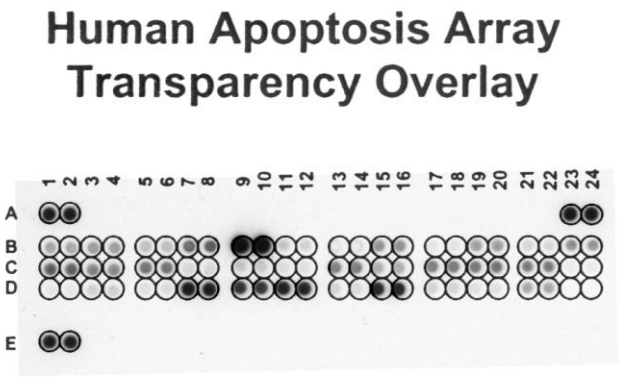

Figure S6. Example of a processed protein array aligned with a transparency overlay image. The two furthest reference spots E1 and A24 were aligned in this overlay. However, fluctuations in precise spot position make perfect alignment impossible.

S3.3.2 Spot centre location

Due to these inconsistencies in array manufacture, the rigid registration of the protein array template to the two extreme reference spots must then be refined through a local search for the true spot centres. However, from looking at the spot profiles, it is clearly evident that the intensity pattern of the spots varies depending on the data acquisition type (Figure S7). Therefore different search strategies must be designed to find the centres of the spots imaged by film and Licor®. For example, Figure S7A shows that in film images the spots mainly appear as diffuse 'blobs', whereas they appear as sharply defined annuli in Licor® images (Figure S7B).

An explanation for this difference is likely to be that although the manufacturing protocol prints the antibody on the membrane with an annuli shape, the placing of film onto the membrane allows light to hit the film in all directions. This will result in the creation of a blurred image which appears as a diffuse spot. This also suggests that in film images, the diameter of the spot may appear to widen with protein intensity, as light is scattered over a further distance.

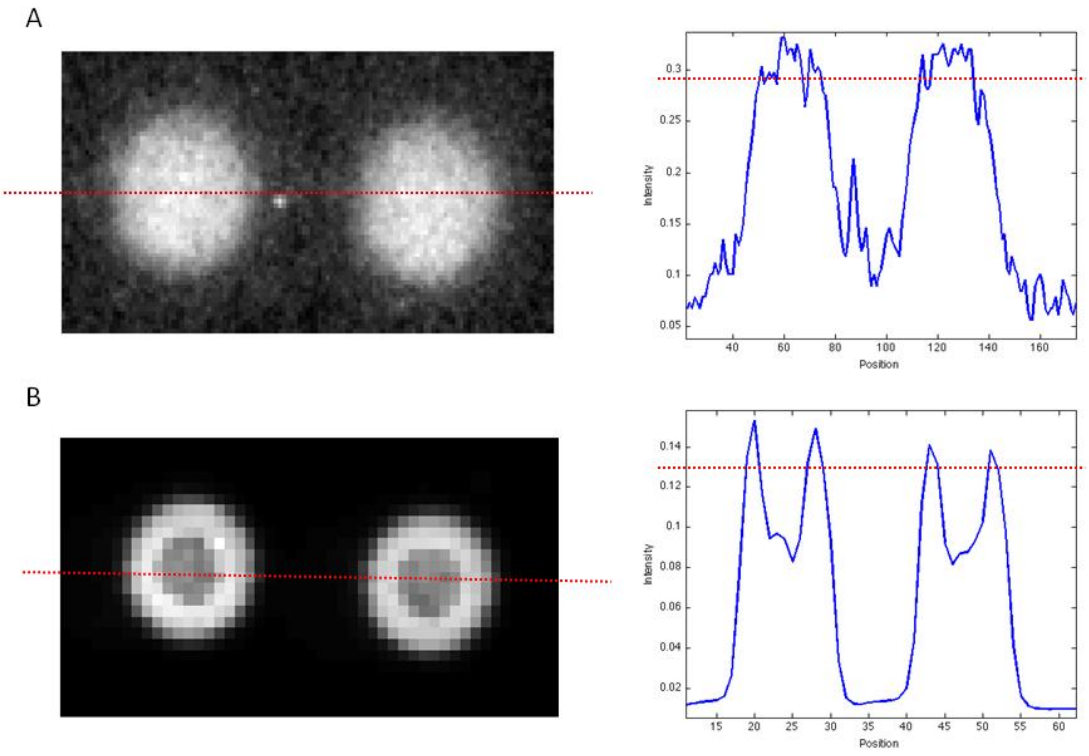

Figure S7. Difference in appearance of corresponding spot pair from arrays processed using film (A) and Licor® (B). Licor® images shown clearly defined annuli shape, compared to the diffuse appearance of film spots. Red line indicates the cross section through the spot pairs which is represented graphically (right).

When the array is scanned using the Licor® Odyssey, only the area under the scan head is illuminated at one time. This prevents the light scattering effect seen on the film, therefore resulting in an image which more genuinely represents the true spot signal. This difference in spot pattern must be taken into account when designing a spot centering method.

An appropriate template was created and a local template matching search was used to find the spot centre. The film template defined the spot centre as the location from which radial profiles in all directions would be most similar. For the Licor®, an annulus template match was used to find the spot centre.

S3.3.3 Quantification of spot intensity

For film, although spot intensity can be measured from the central region of the spot using the method outlined above, the size of the spots in the images appear to increase with intensity. In fact, the spots are all the same radius and so this is an artefact of the imaging process caused by light being emitted obliquely from the spot edge. Therefore, as the intensity of the spot increases, the apparent spot radius also increases. As the real spot radius is known, it would seem sensible to define spot intensity as the average value obtained from a region centered on the spot of radius R, and given that there may be small errors in spot centre location, taking a fraction of R would ensure that a value was taken from within the border of the `real' spot.

However, when the central part of the spot has reached saturation, the peripheral light intensity outside the spot may still be below saturation and so the spot will still appear to grow in size as a function of protein density. Therefore, the total intensity was measured over an area which was larger than the known genuine spot radius, but less half the distance between spots (to prevent measuring signal from an adjacent spot). This method helped to overcome some of the saturation problems outlined in Section S1.1. Figure S8 shows the results of testing this hypothesis on the same images used for figure S2B. This plot still deviates from linearity for the highest values, but allows the extraction of more useful data as fewer spots have reached saturation.

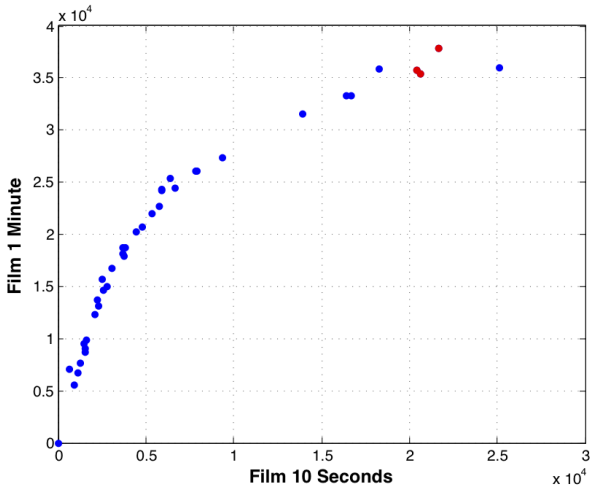

Figure S8. Comparison of a 1 min and 10 sec exposure to film, using an analysis tool which takes into account the increasing spot diameter. Measuring film spot intensity over a larger area overcomes some of the saturation problems seen in Figure S2B.

Figure S9 shows spot pair profiles obtained from Licor® images. In each figure two arrays are compared: A and B, two arrays from the same kit prepared using the same biological sample. Theoretically, the protein levels and hence spot intensities should be the same on both arrays. Looking closely at the profiles, it is the `rim' of the spots that gives the consistent values with the centres varying significantly.

Thus when processing Licor® images, the intensity value for each spot is simply the average of the pixel positions given by the annulus template. This means that spot centering and data extraction can be combined in the same computational step.

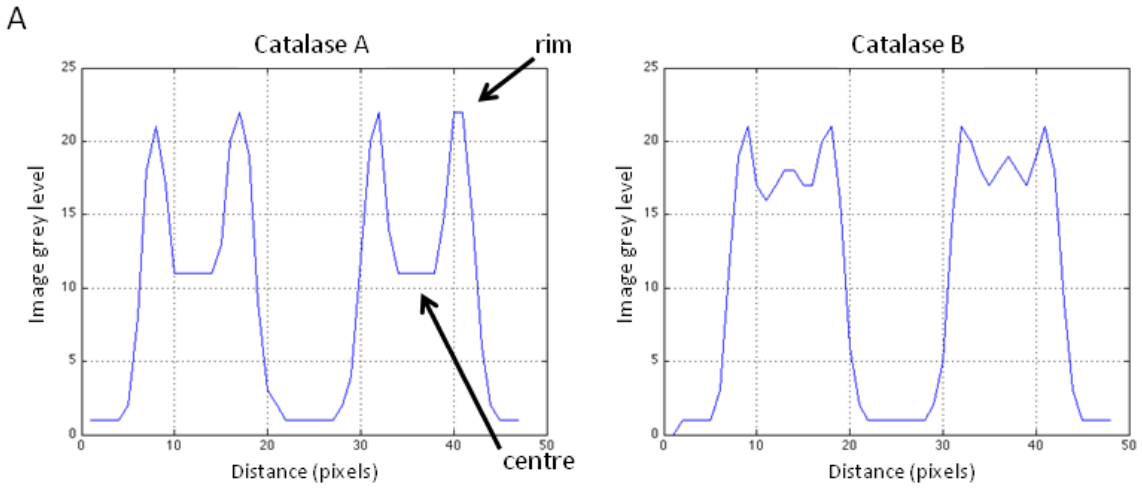

Figure S9. Spot profiles for the catalase protein pairs from two Licor® repeats. Data from two array repeats (A and B) performed with the same MDA-MB-231 sample showing the outer rim values to be more consistent than the centre values.

S3.3.4 Semi-quantitation of protein levels

Once a numerical value has been assigned to each spot using the methods outlined above, these are converted into a value which represents relative protein level. This is done by taking the average of the two duplicate spots which represent each individual protein. To account for background signals, an average value is taken from two negative control spots and this is subtracted from the average protein value.

The MatLab program is designed to give 3 outputs to the user

1. A plot of relative protein levels.

2. A spreadsheet which lists the protein names, individual values for each replicate, mean value for each spot pair, and the difference between each spot pair value.

3. A spread sheet which lists all the spot values in the order they appear in the template.

S4.Testing the templates: comparison of chemiluminescence vs infrared data acquisition techniques

Using the newly developed MatLab tool described above to extract relative protein values from the Proteome Profiler™ Arrays, the relative merits of chemiluminescence (using film development) and infrared (using Licor®) detection techniques were compared.

S4.1 Catalase spot detection

As described earlier, the same biological sample was used on 4 apoptosis protein array membranes; 2 developed onto film and 2 analysed using the Licor® Odyssey. When comparing these two detection techniques, there is one stark and consistent difference between the results from the two acquisition techniques. The catalase spot is completely absent in arrays developed onto film (Figure S10A) whereas it can clearly be seen in Licor® images of the same sample (Figure S10B).

Catalase is an enzyme responsible for the breakdown of hydrogen peroxide into water and oxygen (Chelikani et al., 2004). Hydrogen peroxide is essential for the chemiluminescence reaction which generates the light needed for acquisition by film. Therefore it seems probable that where lysates express high levels of catalase, this protein bound to the membrane can interfere with the luminescence reaction, preventing light being emitted from the catalase spot. This would suggest that infrared detection using the Licor® may be the only accurate method for analysing catalase protein levels from these apoptosis arrays. Whatever the reason for this discrepancy, it is a marked and consistent observation which must be kept in mind when deciding which data acquisition method to use.

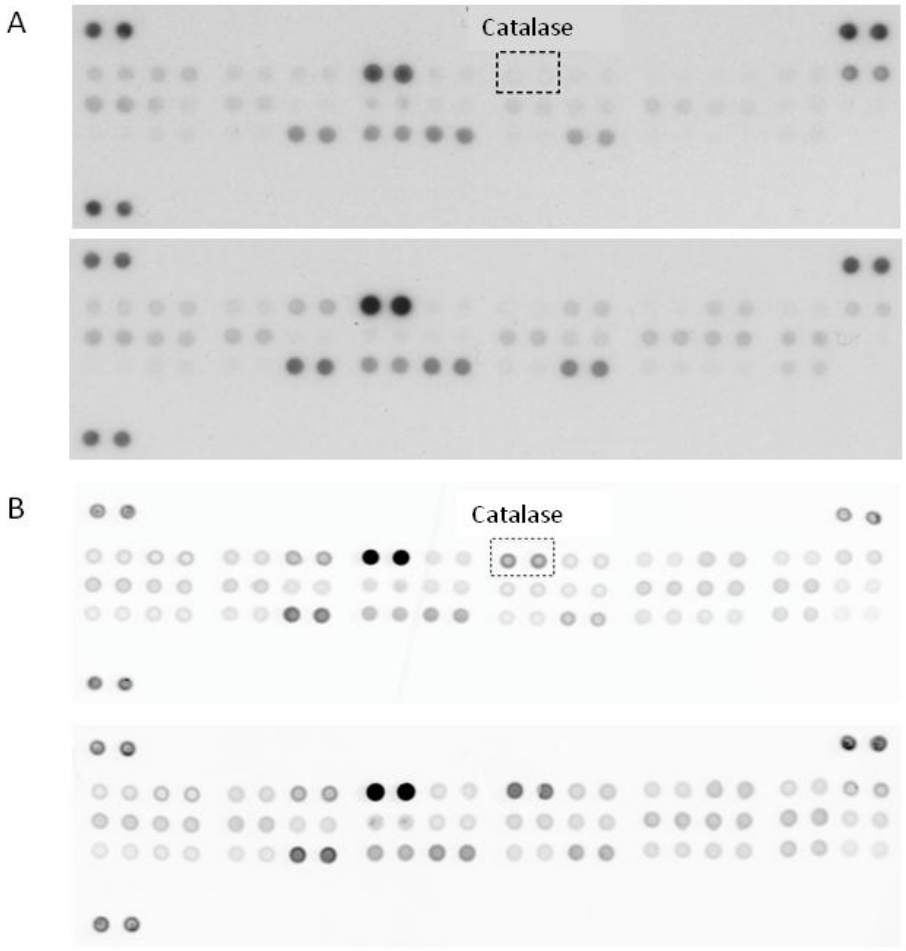

Figure S10. Film images consistently lack catalase protein signal. Four protein array repeats using the same MDA-MB-231 whole cell sample; two developed onto film and two using the Licor® Odyssey. **A** Shows duplicates developed onto film, both lacking a detectable catalase spot. **B** Shows duplicates acquired using the Licor® Odyssey which show strong catalase signal.

S4.2 Repeatability

To investigate the repeatability of the film and Licor® methods the correlation between the protein values obtained from each method was calculated. The Pearson correlation can be distorted by particularly strong signals, such as the strong procaspase-3 signals. Therefore the Spearman correlation was calculated

as this determines the correlation based on ranking the data and therefore is less influenced by large, isolated data values.

Looking at the images in figure S10, the Licor® repeats appear to be more consistent than the film repeats, where some large film discrepancies can be seen by eye. This observation is supported by the correlations in Table S1, showing that the Spearman correlation value is lower for film repeats than for Licor® repeats.

Comparison	Spearman
Licor® A vs Licor® B	0.9316
Film A vs Film B	0.7439
Mean film vs Mean Licor®	0.9013

Table S1. Inter and intra variability of the protein levels obtained by film and LICOR® Odyssey. Spearman rank correlation values from values obtained from repeats using the same biological sample. Due to the large catalase signal differences between film and Licor®, catalase values were excluded from the correlation calculation to prevent distortion of the values.

The correlation between film and Licor® is no worse than the correlation between film A and film B, suggesting that the results obtained by Licor® are consistent with those obtained with film.

To verify that the annulus is the most consistent portion of the spot signal, variation between corresponding spots was compared for two Licor® repeats using the same sample. The values for each corresponding spot should be the same across repeats; however some small difference were often seen. The mean of this difference ($\overline{Diff}$) was calculated for all spot pairs on the array, representing the mean magnitude of the differences between the repeats. It was also calculated for a subset of highly expressed proteins. $\overline{Diff}$ values were calculated from data extracted using spot templates which measured the

whole spot, only annulus region, or only the core spot region. As shown in Table S2, the template measuring spot intensity from the annulus gave consistently lower $\overline{Diff}$ between repeats, illustrating that the values from the annulus region are more consistent than the inner core. For highly expressed proteins, $\overline{Diff}$ from the core was twice the value of that calculated from the annulus region and this could reach over four times higher for certain individual spot pairs.

	$\overline{Diff}$ **(all data spots)**	$\overline{Diff}$ **(strong spots only)**
Whole spot template	0.6633	1.1002
Annulus only template	0.6074	0.8811
Core only template	0.8816	2.0185

Table S2. $\overline{Diff}$ values confirm the improved reliability of Licor® data semi-quantified using the annulus template.

This confirms that the annulus template should be used for more accurate spot intensity extraction when analysing images from the Licor® Odyssey.

S5. Discussion

The main aim of this work was to develop an automatic tool for semi-quantitation of human apoptosis arrays. In this chapter, a method is presented allowing the semi-quantitation of protein array spots using data acquired both from chemiluminescence and infrared data collection techniques.

Due to the differences in spot appearance which result from using these two data acquisition techniques, two different analysis methods had to be designed. In the case of film, the optimum method measures a value calculated from the entire protein spot, whereas images acquired from the Licor® required a method which measures only from the outer 'annulus' region.

Although the software for analysing arrays developed onto film can be altered to integrate the size of the spot in order to overcome some saturation problems, the use of infrared greatly reduces the problem of saturation and the need for multiple exposures. Although this tool is not fully quantitative, as it does not use a standard concentration curve to determine that absolute amount of each protein in each sample, it allows the comparison of relative amounts of proteins across different samples.

This software was then used to compare the relative merits of chemiluminescence and infrared fluorescence as array detection techniques. Film development of chemiluminescence gave a wide dynamic range, posing some practical problems for data analysis. To ensure that none of the data points are saturated, multiple exposures must be taken, and data analysed from an exposure in which the signal is great enough for detection but not yet saturated. Development onto film also gave opportunity for the incorporation of noise into the array images, capable of creating artificial signals within the array spots. Chemiluminescence detection using the IVIS®200 proved to be very impractical due to very large levels of background noise and limitations of the software. In comparison, infrared data acquisition using the Licor® Odyssey gave data with higher sensitivity, much lower levels of background noise, and the potential to re-scan at later times. By comparing array repeats with the two methods, this data shows that the repeatability of data acquired using infrared fluorescence is higher than with film, suggesting that it is a more reliable method of protein array detection. In addition to this, the most reliable data is extracted from infrared array images using the software which measured intensity only from the annulus region. It also became apparent that the catalase spot could only be measured using infrared detection techniques, possibly because the catalase protein bound to these arrays can interfere with the chemiluminescence reaction.

In conclusion, this data presents an accurate and time-efficient tool for analysing protein arrays. This tool was used to confirm the superiority of infrared data acquisition over chemiluminescence. Although the

chemiluminescence technique was used to collect experimental data for this thesis, it was the results from these early experiments that led to the realisation of the need for a more efficient analysis method. The software tools developed and outlined in this optimisation chapter are now currently being used by other scientists within the department in order to gain more reliable and reproducible protein array results.